DOKUZ EYLÜL UNIVERSITY

GRADUATE SCHOOL OF NATURAL AND APPLIED SCIENCES

BUCKLING OF ECONOMICAL COMPOSITE BARS

by

Yeliz PEKBEY

September, 2005

İZMİR

BUCKLING OF ECONOMICAL COMPOSITE BARS

A Thesis Submitted to the
Graduate School of Natural and Applied Sciences of Dokuz Eylül University
In Partial Fulfillment of the Requirements for the Degree of Doctor of Philosophy in
Mechanical Engineering, Mechanics Program

by
Yeliz PEKBEY

September, 2005
İZMİR

We have read the thesis entitled **"BUCKLING OF ECONIMICAL COMPOSITE BARS"** completed by **Yeliz PEKBEY** under supervision of **Prof. Dr. Onur SAYMAN** and we certify that in our opinion it is fully adequate, in scope and in quality, as a thesis for the degree of Doctor of Philosophy.

Prof. Dr. Onur SAYMAN

Supervisor

Prof. Dr. Ramazan KARAKUZU   Assoc. Prof. Dr. Aydoğan OZDAMAR

Thesis Committee Member   Thesis Committee Member

Prof. Dr. Mahmut ÖZBAY   Assist. Prof. Dr. K. Turgut GURSEL

Examining Committee Member   Examining Committee Member

Prof. Dr. Cahit HELVACI
Director
Graduate School of Natural and Applied Sciences

ACKNOWLEDGMENTS

BUCKLING OF ECONOMICAL COMPOSITE BARS

ABSTRACT

Tadjbakhsk & Keller (1962) and Olhoff & Rasmussen (1977)-Masur (1984) obtained different solutions with respect to critical buckling load and optimum form for clamped-clamped ends of columns, which have variable cross-section, subjected to compressive force. Myers & Spillers (1986) and Barnes (1988) encouraged Tadjbaksh & Keller's solution. In 1977, Olhoff & Rasmussen claimed that the optimal solutions given by Tadjbaksh & Keller were incorrect for clamped-clamped ends and they obtained optimum solution through application of a numeric method in solving the differential equation. Seyranian (1983, 1984), Masur (1984), Overton (1991), Cox & Overton (1992), Seyranian, Lund & Olhoff (1994) and Seyranian & Privalova also encouraged Olhoff & Rasmussen's solution with clamped ends of columns.

The critical buckling load results of Tadjbaksh & Keller, Olhoff & Rasmussen (1977)-Masur (1984) are very closer with each other for clamped-clamped ends. However, the difference is originated from optimum shape of the column, especially in points of minimum thickness. Tadjbaksh & Keller determined unimodal optimal solution, namely, possessing a single buckling mode for columns with clamped ends. They found the points of vanishing cross-section to be placed at $x=0,25$ and $x=0,75$ where the column ends $x=0$ and $x=L$ are assumed to be clamped-clamped ends while Olhoff & Rasmussen (1977)-Masur (1984) obtained nonzero cross-section in these points with bimodal optimum solution.

In this Ph. D. thesis, it was also proved that the solutions of Tadjbakhsk & Keller (1962) and Olhoff & Rasmussen (1977)-Masur (1984) were not optimum for columns with clamped ends. True solution then was obtained with both bimodal

solution and crushing criteria. In analytic solution, Masur's bimodal solution was used for clamped-clamped case. Both experiments and numeric studies were carried out to verify new optimum proposed solution. In this Ph. D. thesis, in order to test the accuracy of new optimized composite column with clamped ends, it was used materials such as sapele, oak, cedar and manufactured composite materials including, glass-epoxy, glass vinylester and glass-polyester with 0, 45 and 90 degree of fiber orientation angle with circle cross-sections. The critical buckling load and column's volume obtained from new optimum proposed solution were compared with results found by Tadjbakhsh & Keller (1962) and Olhoff & Rasmussen (1977)-Masur (1984). New proposed optimum model's results were in agreement with results obtained by numerical analysis and by experiments.

Keywords: Buckling, optimum shape design; maximum critical buckling load, bimodal solution; unimodal solution; crush strength.

EKONOMİK KOMPOZİT ÇUBUKLARIN BURKULMASI

ÖZ

Basmaya zorlanan değişken enine kesitli ankastre-ankastre yataklı çubukların kritik burkulma kuvvetleri ve optimum formları Tadjbakhsk & Keller (1962) ve Olhoff & Rasmussen (1977)-Masur (1984) tarafından farklı verilmiştir. Tadjbakhsk & Keller (1962)' in sonuçlarını Myers & Spillers (1986) ve Barnes (1988) desteklemiştir. Olhoff-Rasmussen, 1977 yılında yapmış olduğu çalışmasında, Tadjbakhsk-Keller'in ankastre-ankastre yataklama durumu için bulmuş olduğu sonuçların yanlış olduğunu iddia etmiş ve bu durum için problemin optimum çözümünü nümerik olarak yapmıştır. Tadjbakhsk & Keller'in ankastre-ankastre yataklama durumu için bulmuş olduğu sonuçların yanlış olduğu iddiası, Seyranian (1983, 1984), Masur (1984), Overton (1991), Cox & Overton (1992), Seyranian, Lund & Olhoff (1994) and Seyranian & Privalova (2003) tarafından da kabul görmüştür.

Ankastre-ankastre yataklama durumu için, Tadjbaksh & Keller, Olhoff & Rasmussen (1977)-Masur (1984)'un bulmuş olduğu kritik burkulma kuvvetleri, birbirine oldukça yakın değerlerdir. Ancak farklılık, optimum formdan, özellikle kesitin minimum olduğu noktalardan kaynaklanmaktadır. Tadjbakhsh & Keller (1962) unimodal çözüm ile, çubuğun ankastre olarak yataklandığı noktalar $x=0$ ve $x=L$ olmak üzere, $x=0,25$ ve $x=0,75$ noktalarında kesiti sıfır olarak bulurken, Olhoff & Rasmussen (1977)-Masur (1984) bimodal çözüm ile bu noktalarda sıfırdan farklı kesit alanları elde etmişlerdir.

Bu çalışmada, öncelikle değişken enine kesitli optimum çubuklarda kabul gören Tadjbakhsh & Keller (1962) ve Olhoff & Rasmussen (1977)-Masur (1984) tarafından verilen çözümlerin yanlış olduğu gösterilmiş, ardından da Masur'un

analitik çözümüne ezilme kriteri eklenerek doğru çözüm verilmiştir. Çalışmada verilen çözüme uygun ankastre-ankastre çubuklar deneysel ve nümerik yöntemlerle incelenmiştir. Bu incelemede; daire enine kesitine sahip 0, 45 ve 90° fiber oryantasyon açısına sahip glass-epoxy, glass-vinylester ve glass-polyester ile doğal kompozit olan sapele, cedar ve meşe çubuklar örnek olarak alınmıştır. Çalışma kapsamında yeni çözümle elde edilen kritik kuvvetler ve çubuk hacimleri, Tadjbakhsh & Keller (1962) ve Olhoff & Rasmussen (1977)-Masur (1984) tarafından verilenler ile karşılaştırılmıştır. Yeni çözümle elde edilen optimum çubukların deneysel ve nümerik yöntemle bulunan kritik burkulma kuvvetleri örtüşmektedir.

Anahtar sözcükler: Burkulma, optimum enine kesit değişimi, maksimum kritik burkulma kuvveti, bimodal çözüm, unimodal çözüm, ezilme dayanımı.

CONTENTS

CHAPTER ONE
INTRODUCTION

1.1   Problem Statement

Structural members with variable cross-section are commonly used in mechanical, civil and aeronautics engineering to optimize the distribution of weight and strength. Especially, it is increasingly used composites in the design of lightweight thin flexible structures. However, the design of such structures gives serious challenges arising from the problem of structural stability. It is required the stability analysis the determination of their practical carrying capacity. In recent years, it has been concentrated stability of structure. Many structural elements are becoming thinner and more slender by using high strength materials. The design of slender members is often governed by stability considerations because of their slenderness. It is very important that the structural members have an enough safety against the loss of stability.

One form of the loss of stability is the lateral buckling of columns. The buckling of elastic structures is one of the most crucial problems in engineering. Mechanical buckling is the forthcoming or instantaneous collapse of a structure because of internal and/or external loads, which, however, would not be sufficiently intense to cause mechanical yield of the material in the structure. Lateral instability that occurs while the material is stressed below the yield point means as elastic buckling. On the analysis of stress, it has to be considered that the stresses in a beam system do not exceed the ultimate strength of materials given. Nevertheless, on the problem of stability, the critical load that causes a column to buckle is aimed. Although the stresses that occur in the material of a loaded column remain in allowable limits, the equilibrium of this column can become unstable under the same critical compressive load, which leads the whole system to collapse.

Buckling plays a very important role in the design of slender columns. Linear buckling of column structures is an important design constraint, especially where weight is chief concern. It plays important roles eigenvalues of symmetric matrices in many different areas of applied mathematics. For example, it may desirable to minimize the largest eigenvalue in a control application, because the size of the largest eigenvalue describes system stability. However, it may desirable to maximize the smallest eigenvalue in a structure analysis application, because the smallest eigenvalue defines a buckling load. It might have an optimization objective in other applications, which does not involve eigenvalues, but cover constraints on eigenvalues (Overton, 1991).

Optimum design of structures against buckling may be accomplished by finding the minimum weight design of a structure, which satisfies the prescribed buckling load constraint. On the other hand, it can be maximized the fundamental buckling load for a structure while keeping its weight or volume constant. Alternatively, it may be to maximize the buckling load for a structure with a given volume, mass, or weight. It may be included as well other performance criteria, such as strength and stiffness. The designer is often urged to reduce structural mass and/or increase buckling load. Additionally, it is maintained safety margins, comfort and aerodynamic performance at acceptable levels.

On optimization problems involving eigenvalues, it is considered the problem of determining the shape of the strongest column having a given length and volume, as other words, maximization of minimum eigenvalue. The model problem is exactly useful to many applications. Mathematically, this problem is the least eigenvalue of a self-adjoint fourth–order differential operator. The meaning of the least eigenvalue of differential equation is that it corresponds to the critical buckling load in model of the column. It is to increase the lowest buckling eigenvalue during the optimization procedure. It is required Lagrange's problem the maximization of this least eigenvalue, over all possible functions defining the cross-sectional area of the column. In other words, it is expressed finding the shape of the domain that minimizes the least eigenvalue of the Laplacian.

It has been widely discussed in the literature the behavior of axially compressed columns with varying cross-section. Columns having variable cross-section are widely used in complex structures to accomplish a better distribution of strength and weight and sometimes to satisfy architectural and functional requirements. In the analysis of such structures, non-linearity may arise due to large deformations and material properties. The obtaining of the elastic curve of a column is necessary. Because it is required that not only the stresses induced in the column should not exceed allowable stress but also the maximum deflection of the column should not be greater than a certain predetermined value depending on the operating conditions of the column (Anonymous, 2005a).

The problem, especially clamped-clamped case, is a controversial alone which mathematicians and structural engineers have addressed. The optimum shape of the clamped-clamped column compressed at its ends a given length and volume was first dealt with by Tadjbakhsh & Keller (1962). The unimodal solutions obtained by Tadjbakhsh & Keller are not optimal because the column buckles by the modes with discontinuities of the slope corresponding to the lower critical load. This leads to necessity of the bimodal formulation of the optimization problem.

Olhoff & Rasmussen (1977) discovered that the optimum design should be bimodal and the critical load is governed by a repeated eigenvalue. They also first displayed that the solution by Tadjbakhsh & Keller for clamped ends is not optimum due to a buckling mode that becomes critical at a lower value of the axial load than the mode considered in the analytical solution of Tadjbakhsh & Keller optimality equations.

This Ph. D. thesis deals with shape design of the strongest column with maximum buckling load. It was considered the well-known problem of maximizing the critical buckling load of an elastic column of variable cross-sectional area and prescribed length and volume. The aim was to determine the composite column of least volume that has the same critical load. It may be defined the buckling design problem as

finding the minimum weight structure that satisfies a prescribed buckling load. The initial of a composite column was the design objective. Furthermore it was reinvestigated the optimization problem of the clamped-clamped column under buckling load, which was previously dealt with by Tadjbakhsh & Keller and Olhoff & Rasmussen. The unimodal and bimodal solutions were analyzed for several of boundary conditions and it was shown that for nonzero support stiffness they are not optimal. The proposed model of the problem according to bimodal solution obtained by Masur was set up. An important limit case of a clamped-clamped supported column that has caused debate in many publications is analyzed.

Consequently, in this Ph. D. Thesis, the problem of determining the optimum shape of an elastic clamped column of given length and volume such that the fundamental buckling loads was a maximum was reinvestigated.

1.2   Objectives of Present Research

This thesis have purposed the problem of finding the shape of the strongest column which has the largest fundamental buckling load with equal length and volume for the clamped–clamped ends. In particular, it is revised the result hitherto considered to be optimum solution for unconstrained column with clamped ends. It is also reformulated and extended the problem which finding the shape of the strongest column with clamped-clamped ends.

This thesis also shows a comparison of the optimal shapes of columns investigated in literature. The optimum column cross-sectional area function is chosen design parameter. The solution depends on this cross-sectional area function. The column cross-sections are assumed to be geometrically similar and a minimum value is specified for the cross-sectional area taking into consideration both buckling and stability criterion in the points of the minimum thickness. Thus, in order to determine the strongest column of given length and volume such that the fundamental buckling load is a maximum, it is necessary to take into account both buckling and crushing criteria in the points of the minimum thickness. The

achievable savings of materials as well as of weight of constructions will found in comparison to the systems of columns with constant cross-section.

1.3   Research Methodology

The optimization problem consists in determining the column shape that maximizes the fundamental buckling load for given length and volume. This thesis can be divided in three main groups:

- Analytical methods,
- Numerical methods and
- Experimental investigation.

The results of the analytical model were verified by the experimental data and numerical methods. It was used both numerical and experimental methods for new solution which based on buckling and crushing criteria. A comparison between obtained analytical, experimental and numerical results was accomplished. The experimental results were found to be consistent with the experimental data and finite element models. Experiments were carried out to determine the effect of the fiber orientation angle in different natural and manufactured composite materials including, cedar, oak, sapele; glass-epoxy, glass-vinylester and glass-polyester. The composite column specimens were designed and manufactured according to uniform cross-sections and variable cross-sections.

The proposed model of the composite column, which offered this Ph. D. thesis, was determined using Masur's solution. Shape design of the strongest column had been developed taking into consideration the effect of the crushing in points of minimum thickness. The performance of shape design was validated through experimental results. The optimum eigenvalues and the corresponding eigenfunctions with respect to the minimum constraint of cross-sectional area were obtained. The buckling characteristics of columns with uniform and variable cross-section were investigated for wood composite materials and manufactured composite materials,

which consisted of glass-epoxy, glass-polyester and glass-vinylester with different fiber orientation angle: 0, 45 and 90 degree of fiber orientation angle. The critical buckling load analysis was also performed by the finite element method. Finite element models were constructed with different composite columns with variable cross-section. Experiments were conducted to verify and validate the analytical and finite element results. The proposed design models were found to produce better results.

1.4 Literature Review

1.4.1 A review of the Optimization Problem for Columns Subjected to Buckling

The buckling of elastic columns is a fundamental topic in structural mechanics. Optimization of columns against buckling is essential to enhance by decreasing the possibility of reaching an unstable equilibrium position under any contemplated loading. A large number of publications have appeared eigenvalue optimization algorithms. Timoshenko & Gere (1961) and Smittses (1976) wrote the most relevant books on the stability of columns.

Euler (1744) determined critical buckling loads affecting columns with constant cross-section and with four different bearing types. However, the cross-section of the column should be variable, if economical as well as lighter constructions must be designed. Hence, Ratzersdorfer (1936) executed the first examination for columns hinged at both ends, in order to solve the stability problem more extensively for obtaining economical as well as lighter constructions. In his study, circular and rectangular cross-sections were treated. Furthermore, Keller (1960) was determined the shape of the strongest column with simply supported ends. Later, Tadjbaksh & Keller (1962) presented the optimum shape for the strongest column of a given length and volume with for different support ends "clamped/clamped, clamped/free and clamped/slide-hinged case". Taylor (1967) studied direct and concise energy method than that developed by Tadjbakhsh & Keller. Smitses (1973) was the first

person to use in finite element analysis and iterative procedure to optimize the shape of the columns.

Bauld & Tzeng (1984) presented a Vlasov type theory for thin-walled beams with open cross sections made from midplane symmetric, fiber-reinforced laminates. A linear theory suitable for stress and deflection determination was presented first, followed by a nonlinear theory that was suitable for bifurcation and limit point stability analyses of the global buckling modes of beams under different applied loads and boundary conditions at end cross sections.

Szyskowski & Watson (1998) optimized single buckling mode columns and frames of a given volume to find the highest resistance against buckling. ANSYS program was used to solve the eigenvalue problem.

Vaziri & Xie (1992) proposed a new numerical model for analyzing the buckling of columns with variable distributed axial loads. The presented method was transformed the traditional eigenvalue problem into an initial boundary value problem which could be solved by numerical integrations.

Qiusheng, Hong & Guiqing (1994) found the exact solutions for the stability analysis of a one-step bar of varying cross-section subjected to concentrate and distributed axial loads first. Then the exact solution of that bar was used to derive the eigenvalue equation of a multi-step bar of varying cross-section subjected to loads that are more complicated by using transition matrices. All of the exact solutions were expressed in terms of Bessel's functions and super-geometric series.

Ishidaet & Sugiyama (1995) dealt with the proposal of a new genetic algorithm based optimization algorithm and its application to the discrete shape design of the strongest column with maximum buckling load of the first mode under constraint of constant weight. The buckling load analysis was performed by the finite element method. Qiusheng, Hong & Guiqing (1995) demonstrated the exact solutions for stability analysis of bars with varying cross sections subjected to simple or

complicated loads, including concentrated and variable distributed axial loads. The distribution of flexural stiffness of the bar and axial loads acting on the bar were expressed as power functions or exponential functions; also, the extracted exact solutions are expressed in terms of Bessel functions and super geometric series. Tada & Wang (1995) reinvestigated the optimization problem of the clamped-clamped column under buckling load, which was previously dealt with by Tadjbakhsh & Keller. Both numerical and analytical methods based on the single and bimodal formulations were used in investigating the behavior of the optimum eigenvalues and the corresponding eigenfunctions with respect to the minimum constraint of cross-sectional area. The conditional optimum column under the single modal formulation was determined. The optimum column together with two mutually symmetrical eigenfunctions under bimodal formulation was obtained.

Coello, Christiansen & Farrera (1996) studied the optimum design of axially loaded non-prismatic steel columns, in which the objective was to minimize their volume under a given load by changing their shape, and assuming that were subjected to buckling and strength constraints. They used a genetic algorithm to move through the search space of possible column designs, and choose the best one. Both floating point and binary representation were used and compared to a more traditional optimization technique based on the generalized reduced gradient method. Lin, Polyzois & Shah (1996) studied buckling problem of thin-walled composite structural members by finite element method. A finite element having seven degrees of freedom at each node was developed to study the stability problem of thin-walled fiber-reinforced plastic (FRP) structural members. The influence of the in plane shear strain on the stability of the members was considered. The shape functions for the rotation and unit length rotation induced by warping were derived. The static and geometric stiffness matrices of a general beam element were established based on the developed shape functions. The bifurcation-buckling problem of thin-walled pultruded open-sections subjected to various loading and boundary conditions was examined through a number of examples. It was shown that the influence of the shear strain on the buckling capacity of the fiber-reinforced plastic structural members was significant and must be taken into account in the design of such members.

In 1999, Khong presented a multi objective optimal design for uniaxially loaded laminated composite panels. The fuzzy theory was utilized in the formulation of the multi-objective optimization scheme. The strategy was engaged in different-weight age fuzzy membership functions, which was efficient in handling relative importance of objectives. Langthjem & Sugiyama (1999) concerned with optimization of a damped column subjected to a follower load. Sequential linear programming solved the optimization problem. By only including a constraint on the flutter load in the volume minimization, a very large volume reduction was possible but the static buckling load became very small. Consequently, the volume was minimized with constraints on both the flutter load and the static buckling load.

Vinogradov & Derrick (2000) examined the effects of material composition and properties on the non-linear buckling response of asymmetric laminated structures. The problem was studied through the analysis of asymmetric laminated columns composed of an arbitrary number of different material layers. The non-linear buckling behavior of the columns subjected to combine compression and bending was examined depending on parameters such as the number, orientation and stacking sequence. Arpakci (2000) considered the case "one end slide-clamped and the other sliding".

Later on, Fridman & Zyczkowski (2001) considered optimal design of columns under concentrated axial force subject to corrosive environment. The initial volume of a column was the design objective whereas the constraint refers to elastic buckling at a certain prescribed lifetime with corrosive wear of this column taken into account. Plane-tapered and uniformly spatially tapered columns were optimized under the conditions of plane or spatial corrosion. Variation treatment was led to fourth order Euler-Lagrange equations. Final optimal shapes of the columns were shown both corrosive wear corresponding to the prescribed lifetime. Elishakoff (2001) presented several closed-form solutions for the buckling eigenvalue problem of the columns with variable flexural rigidity along the axis. They examined the cases "one end sliding and the other hinged or clamped" by using the simplest fourth order

polynomial that satisfies boundary conditions. Rong, Xie & Yang (2001) proposed for maximizing the critical buckling load of a structure of constant weight, an improved for evolutionary structural optimization against buckling. They derived the sensivity numbers of the first eigenvalue or the first multiple eigenvalues by performing a variation operation.

Maalawi (2002) presented a novel approach of the optimization of flexible columns against buckling. The model formulation was considered columns that could be practically made of uniform segments with the true design variables defined to be the cross-sectional area, radius of gyration and length of each segment. Exact structural analysis was performed, ensuring the attainment of the absolute maximum critical buckling load for any number of segments, type of cross section and type of boundary conditions. Detailed results were presented and discussed for clamped columns having either solid or tubular cross-sectional configurations, where useful design trends had been recommended for optimum patterns with two, three and more segments. It was shown that the developed optimization model, which was not restricted to specific properties of the cross section, could give higher values of the critical load than those obtained from constrained-continuous shape optimization. In fact, the model had achieved in arriving at the global optimal column designs having the absolute maximum buckling load without violating the economic feasibility requirements.

Lee, Oh & Li (2002) defined the strongest column as the elastic column of given both length and volume, which can carry the highest axial load without buckling. A numerical method was developed for calculating the buckling loads of tapered columns of regular polygon cross-section with constant volume and both clamped ends. Pekbey & Ozdamar (2002) calculated variation of cross section with the length of the bar and critical buckling loads square, circle and equilateral cross sections for the case "one end slide-clamped and the other clamped". The difference between the uniform cross section and the variable cross section solution was compared in terms of material saving.

Drazumeric & Kosel (2003) considered elastic bar with a changeable cross-sectional area by using the small-displacement theory. An optimum geometry was obtained using the calculus of variation based on a mathematical model of buckling, which considered the geometric and boundary conditions. Ying, Li & Teng (2003) established based on the geometrically non-linear theory of axially extensible elastic rods, the governing equations of post buckling of a clamped-free rod with variable cross-sections, subjected to a combined load. The strong non-linear boundary value problems were numerically solved by using shooting method. The secondary equilibrium paths and the post-buckling configurations of the rod with linearly varied cross-sections were presented. Adali, Fene, Duvaut & Chiaruttini (2003) presented optimal design of composite laminates under buckling load uncertainty. The problem of stacking sequence design of a symmetrically laminated plate was solved for maximum buckling load under uncertain biaxial loads which belong to a given domain and the optimal stacking sequences were computed for a continuous fiber orientation using only 0^0, 45^0 and 90^0 ply angle combinations.

Atanackovic (2004) determined the shape of the lightest compressed rotating rod by using Pontryagin's maximum principle. It was shown that the cross-sectional area function was determined from the solution of a linear boundary value problem. The optimal shape of a rod was determined by numerical integration.

As seen above, there are several reports in the literature dealing with this topic, both from theoretical and experimental standpoints

1.4.2 A review the Optimization Problem for Debatable Case (Clamped-Clamped Case)

Euler (1744) determined critical buckling loads affecting columns with constant cross-section and with four different bearing types. However, the cross-section of the column should be variable, if economical as well as lighter constructions must be designed.

The minimization of structural weight and the maximization of critical buckling load are problems that have been addressed many times.

Tadjbakhsh & Keller (1962) examined the optimal longitudinal cross-sections of column under critical buckling loads for different support ends "clamped-clamped, clamped-free and clamped-slide-hinged case". They determined the optimal solution of buckling problem for columns with clamped ends analytically, which was unimodal, namely, possessing a single buckling mode as the solutions of the other cases. They obtained that the column cross-section vanished along with the bending moment at the two points. The points of vanishing cross-section and bending moment were found to be placed at *x=0,25* and *x=0,75* where the column ends *x=0* and *x=L* are assumed to be clamped-clamped. Tadjbakhsh & Keller obtained optimal design that exhibits hinges at the quarter points and symmetric buckling mode. The buckling load of the column was also noticed to be 52,638; which was 32,795% higher than the buckling load of a corresponding uniform column and exceeded by one third the dimensionless buckling load for a uniform column.

The results obtained by Tadjbaksh & Keller were not optimal in as much as the second buckling mode crossed the first and became critical at a lower load level. The true optimal design is bimodal, i.e., the critical load is governed by a repeated eigenvalue. It buckles into a single mode optimal statically determinate columns while clamped-clamped ends columns may exhibit a dual buckling mode. This phenomenon has been remarked first by Olhoff & Rasmussen (1977).

Olhoff & Rasmussen (1977) demonstrated that the unimodal solution obtained by Tadjbakhsh and Keller for clamped-clamped ends is incorrect. Olhoff & Rasmussen showed that the optimal solution for columns with clamped ends should be bimodal, that is to say, possessing two linearly independent buckling modes. Olhoff & Rasmussen introduced a "bimodal solution" of the problem of Lagrange, i.e. one that would accommodate double eigenvalues. They reformulated and extended the problem, including the possibility of the optimum fundamental buckling load being a double eigenvalue taking into account a prescribed minimum allowable value for the

column cross-sectional area. Their analytical development was based on a functional form as the bimodal potential energy of the column in its buckled configuration and the bimodal optimization problem was represented through this function. The governing equations for the problem were produced by variation analysis. They also found that geometrically unconstrained optimum column has finite cross-section throughout. It was performed a numerical solution by a finite difference method, allowing for possible jumps in the slope and in the shear force at two interior points of zero bending moment. Note that the solution found by Olhoff & Rasmussen exhibits no hinges. The buckling load of the column was also noticed to be 52,3563; which was 32,62% higher than the buckling load of a corresponding uniform column.

Myers & Spillers (1986) and Barnes (1988) encouraged Tadjbaksh & Keller's solution. They claimed that the optimal shapes given previously Tadjbaksh & Keller were mathematically correct. It was showed that there was no solution within the class of shapes for which the mathematical eigenvalue problems was given an adequate description of the physical buckling problem. They reported that these alternative designs obtained by Olhoff & Rasmussen had come closer and closer in both shape and buckling load to the original Tadjbaksh & Keller's solution.

The optimum bimodal buckling load obtained for the clamped-clamped case was later proved correct by many researchers. Researchers have obtained similar results for bimodal optimization solutions.

Masur (1984) derived the bimodal optimality conditions for the clamped-clamped case and stated an extension to multiple eigenvalues. Optimality was reached with the double eigenvalue solution. In addition, previously established by Olhoff & Rasmussen double eigenvalue solutions were reinvestigated in the light of singularity conditions. It was derived specific necessary and sufficient conditions for local and global optimality and explicit optimality criteria were created for double eigenvalues, including a geometric interpretation. It was also developed an analytical closed

solution for the case of the optimal design of clamped-clamped column. The results obtained by Masur were in good agreement with that by Olhoff & Rasmussen.

Szyszkowski, Watson & Fietkiewicz (1989) presented a more general method for the optimization of frames using the variation calculus and Lagrangian multipliers. A bimodal iterative procedure for optimizing frames of constant volume for maximum stability was discussed. The procedure was used the finite element technique and allowed treatment of the optimized structure as a potentially bimodal one. For a single mode, optimal design for the influence of the second mode was automatically eliminated by the iterative procedure. The numerical examples were presented to illustrate the convergence of the procedure for frames with both single mode and bimodal buckling failures.

Overton (1991) reported the optimal design of columns against buckling with extensive with the new algorithm. The problem was discretized, approximating by a piecewise constant function. Optimality conditions were derived for an important eigenvalue optimization model problem, emphasizing the representation of the generalized gradient in terms of dual matrix and given a practical algorithm for solving large-scale problems. The most feature of his algorithms was that it was computed the optimal dual matrix, which was the key to the verification of optimality and to sensivity analysis of the solution.

Cox & Overton (1992) gave the first proof of existence of a solution to the clamped-clamped problem. They offered the first systematic numerical results using direct optimization techniques that take into account the possibility of a multiple eigenvalue. Cox & Overton (1992) derived necessary conditions and constructed an algorithm for the maximization of a column's Euler buckling load under a variety of boundary conditions over a general class of admissible designs. They proved that symmetric clamped-clamped columns possess a positive first eigenfunction and introduced a symmetric rearrangement that was not decreased the columns buckling load. Their necessary conditions expressed in the language of Clarke's generalized gradient. Their main contribution to the problem of Lagrange was essentially two

hold. It was applied the generalized gradient of Clarke in i) a rigorous derivation of the necessary conditions ii) the construction of an efficient algorithm to solve the associated finite dimensional optimization problem. They focused on the clamped-clamped case. Their results for optimum columns are in good agreement with the results obtained by Olhoff & Rasmussen.

Szyazkowski (1992) derived a multimodal optimality criterion and used for numerical optimization of elastic structures with respect to buckling. It was tried to obtain optimum designs for clamped-clamped column using the optimality criteria method based on the finite element analysis.

Seyranian, Lund & Olhoff (1994) discussed characteristic features and inherent difficulties pertaining to the lack of usual differentiability properties in problems of sensivity analysis and optimum structural design with respect to multiple eigenvalues. They presented sensivity analysis of multiple eigenvalues based on the perturbation technique both multiple eigenvalues and corresponding eigenvectors. They considered the case where only a single design parameter was altered and then presented a method for efficient calculation of design sensivities of simple and multiple eigenvalues when all design parameters were changed simultaneously.

Lewis & Overton (1996) reinvestigated optimization of eigenvalues. They supported optimal solution obtained by Olhoff & Rasmussen. Various applications that had been especially influential, from structural analysis to combinatorial optimization were discussed and algorithmic developments were surveyed. They also investigated optimization of convex functions of eigenvalues of symmetric matrices subject to linear constraints. They derived a complete mathematical theory and presented some apparently new variation results about eigenvalues of nonsymmetrical matrices.

Manickarajah, Xie & Steven (2000) presented a simple method using the finite element analysis for the optimum design of columns and frames to enhance the elastic buckling resistance of structures. They also demonstrated the efficiency and

effectiveness of the proposed method for the optimum design of columns, frames with single modal, bimodal, and trimodal buckling failures.

Kanno & Ohsaki (2001) derived the necessary and sufficient conditions for global optimality for an eigenvalue optimization problem. They considered the problem of minimizing the structural volume under constraints on the lowest eigenvalue of the generalized eigenvalue problem with real symmetric matrices that was linear functions of design variables. The optimization problem was formulated as a semi definite programming problem.

Seyranian & Privalova (2003) dedicated to the optimization and post-buckling behavior of columns elastically supported at both ends. They proved that the unimodal solutions were not optimal and then the bimodal formulation of the problem was set up. They studied the initial post-buckling behavior of the bimodal optimal column. It was shown that the initial post-buckling behavior was governed by four supercritical solutions emanating from the trivial equilibrium state at the critical load. The stability of the new equilibrium states was investigated by using the second variation of the total potential energy.

Karaa (2003) investigated properties of the first eigenfuctions of the clamped column equation. It was mathematically showed that the clamped column equation might not possess a positive first eigenfunction.

Kruzelecki & Smas (2004) investigated the problem of the optimal design of simply supported columns under loadings controlled by displacements. It was searched for cross-sectional area, varying along the axis of the column that leaded to the maximal axial displacement caused by compression before the structure buckled. The optimal solutions for different constraints of minimal and maximal cross-sectional area and various elastic foundations were presented and considered the unimodal and bimodal problems.

Egorov (2004) proposed a new approach for the study of the classical Lagrange problem on the optimal form of a column with clamped-clamped ends and fixed volume. It was proved that there exists a column with the maximal possible value of the eigenvalue and that such a column is unique.

1.5   Thesis Outline

The thesis has six main chapters covering all the aspects of this work including the underlying theory upon which it is based.

The thesis begins with an introduction optimization problem followed by need and objectives of the present investigation. It is also reviewed the relevant literature in this chapter.

In Chapter 2, theoretical development of buckling for uniform cross-sections is given. Theoretical buckling equation for composite materials is also presented according to classical buckling theory and the first shear deformation theory. Properties of composite materials that used in this study are also explained. Especially properties of fiber and matrix were given.

Chapter 3 explains theoretical development of buckling for variable cross-sections. In this chapter, three approaches with respect to variable cross-section suggested by Tadjbakhsh & Keller (1962), Olhoff & Rasmussen (1977) and Masur (1984) are presented for optimized column against buckling for clamped-clamped ends. These approaches are described for six different sets of boundary conditions and three different variable cross sections including cross-sectional of circular shape, square shaped cross-sections and isosceles triangle cross-sections. In addition, in this chapter, new optimum solution is given considering both buckling and crushing criteria for clamped-clamped case. An example for glass-epoxy with 0 degree of fiber orientation angle is also given to explain new proposed optimum solution, and MATLAB program is presented for this example.

To verify new proposed optimum solution, it is carried out both experimental and numeric study for debatable clamped-clamped case.

In Chapter 4, the details of experimental test set-up, manufacturing and processing of composite materials, details of composite columns with variable and uniform cross-sections, and loading conditions are given. In Chapter 5, the results of finite element analysis are compared with the experimental data for debatable clamped-clamped case. ANSYS package program is used to obtain numeric analysis.

Finally, the results and conclusions are presented in Chapter 6.

CHAPTER TWO
THEORETICAL DEVELOPMENT OF BUCKLING FOR
UNIFORM CROSS-SECTIONS

2.1 Buckling : General Concepts

2.1.1   General

The selection of structural elements is depended on strength, stiffness and stability. It is used to strength to determine failure, while presuming that the elements will always be in static equilibrium. However, when certain structural members are subjected to compressive loads, they may fail due to lateral deflection or the compressive stress exceeding the yield strength. It is not alone sufficient the consideration of material strength and stiffness to predict the behavior of a structure. The stability considerations could be major in some applications. Lightweight structural members have been extensively used in many industrial fields such as in civil, mechanical and aerospace engineering. For that reason the stability problems of such structural members are of increasing importance.

The stability of the structure is ability to support a given load without experiencing a sudden change in its configuration. Stability of equilibrium means response of the structure due to a small disturbance from its equilibrium configuration.

If a beam element is under a compressive load and its length is called as a column. Columns must be designed for strength and stability. Buckling of a structure defines failure due to excessive displacements, and/or loss of stability of an equilibrium configuration of the structure. In recent years, buckling has become more of a problem because the use of high strength material requires less material for load support structures and components have become more slender. Buckling failures can

be sudden and catastrophic. Consequently, it must be given primary attention design of the column so that they can safely support the loads (Anonymous, 2005b, c, d, e).

Buckling is a geometric instability and mode of failure. Buckling is occurred about the principal axis having the least moment of inertia, namely it will buckle in the direction of smaller *(I)*. Load carrying ability increases as the moment of inertia increases, as elastic modulus increases but at length decreases. As a result, it will have very low tendency to buckle for short columns made of stiff material. Buckling is an important design constrain in the design of many structural systems. A method of understanding buckling is to create a safety design whereby applied design load is always much less than the theoretical buckling loads. Because the theoretical buckling load is determined based on ideal column with assumptions, it must be placed a large safety margin between the design load and the calculated critical buckling load (Anonymous, 2005f, g, h, i).

The critical buckling load depends on modulus of elasticity *(E)*, the moment of inertia *(I)* and the column's length *(L)*. There is no advantage of using high strength materials for columns subjected to buckling because the critical buckling load is independent of the material strength. Columns having higher flexural rigidity *(EI)* will be able to resist buckling better than columns with small flexural rigidity.

The stability of structure is its ability to support a given load without experiencing sudden change in its configuration. P_{CR}, critical or maximum axial load on the column just before it begins to buckle. It will be observed that if its equilibrium is disturbed, the system will be returned to its original equilibrium position. The system is said to be stable. Nevertheless, if $P > P_{CR}$, the system will move away from its original position and settle in a new position of equilibrium. In the second case, it is said to be unstable. As a result of, the system is stable for $P < P_{CR}$, namely, for values of the load smaller than the critical value, and unstable for $P > P_{CR}$.

The event of mechanical buckling of columns and beams has been studied extensively, with various models attempting to account for the vast number physical conditions that determine the behavior of the system. Several classical problems have been dealt with in the existing literature such as the Euler's column. Euler presented the first accurate stability analysis of a column in 1744. The classical buckling analysis is based on the so-called small deflection theory, yielding an eigenvalue problem. It is found the eigenvalues together with the eigenvectors, namely the mode shapes. The amplitudes of these eigenvectors are not determined. The smallest eigenvalue is called the critical buckling load. The critical buckling load for a column is dependent on its rigidity and its length.

The effect of shear deformation on critical buckling load is generally small, except for short columns. Euler-Bernoulli column theory neglects the effect of transverse shear deformation. Shear deformation effect reduces the buckling capacities of columns. Timoshenko column theory takes into account shear deformation on the buckling capacity of the column under compressive loads.

Two types of column failure modes are well known. Local (flange) buckling dominates the behavior of stubby columns. Global (Euler) buckling controls the behavior of slender columns. Buckling is typically associated with long slender column. The Euler mode involves a sudden lateral deflection without deformation of the cross section.

2.1.2   Stability Analysis

Energy approach is one method of analyses in stability. For an elastic system subjected to conservative forces, it can be expressed the total potential energy of the system as a function of a set of generalized displacements and the external applied forces. Conservative forces are known whose potential energy is dependent only on the final values of deflection, not the specific paths to reach these final values.

To obtain the equilibrium equation of the structure, the stationary point of the potential energy needs to be found. If the system is in equilibrium, its total potential energy must be stationary. Therefore, it generalized displacement equal to zero by setting the first derivative of the total potential energy function with respect to the each. If first derivative of the total potential energy function equal to zero, it is called as equilibrium conditions of the system.

Now, it is used potential energy for determining stability of structural systems. It can be examined the stability of an equilibrium position for any system by examining the terms of a Taylor series expansion for the potential energy V at the equilibrium position. For a one degree of freedom system:

$$V(Q+\delta) = V(Q) + \left.\frac{dV}{dQ}\right|_Q \delta + \frac{1}{2!}\left.\frac{d^2V}{dQ^2}\right|_Q \delta^2 + ... + \frac{1}{n!}\left.\frac{d^nV}{dQ^n}\right|_Q \delta^n + ... \qquad (2.1)$$

It is defined equilibrium and stability for a structural system in terms of total potential energy (Wadee, 2004):

- It is necessary and sufficient a stationary value of the potential energy with respect to the degrees of freedom for the equilibrium of the system.
- It is necessary and sufficient a complete relative minimum of the total potential energy with respect to the degrees of freedom for the stability of an equilibrium state.

First rule expresses that

$$\left.\frac{dV}{dQ}\right|_Q = 0 \qquad (2.2)$$

and so the change in V is

$$V(Q+\delta)-V(Q)=\frac{1}{2!}\frac{d^2V}{dQ^2}\bigg|_Q \delta^2 + \frac{1}{3!}\frac{d^3V}{dQ^3}\bigg|_Q \delta^3 + \frac{1}{4!}\frac{d^4V}{dQ^4}\bigg|_Q \delta^4 +$$

$$\frac{1}{5!}\frac{d^5V}{dQ^5}\bigg|_Q \delta^5 +...+\frac{1}{n!}\frac{d^nV}{dQ^n}\bigg|_Q \delta^n +... \qquad (2.3)$$

This series in Equation (2.3) has to be positive for any small perturbation δ for $V\,(Q)$ to be minimum namely stable. So, the following observations can be made:

- The first nonzero term must be positive for any δ for a stable system. It must be cover an even power of δ with a positive differential coefficient.
- If the series is zero, all derivates must be zero. This definition means neural stability.
- All other combinations are unstable.

For example if:

$$\frac{d^2V}{dQ^2}\bigg|_Q = 0, \text{but } \frac{d^3V}{dQ^3}\bigg|_Q \rangle 0 \qquad (2.4)$$

V is neither maximum nor minimum. However, it also becomes negative which implies instability for the negative δ the dominant term in the series. Linearizing deflections would only allow the determination of singular points. It would not allow analysis of their stability.

A way of visualizing why energy minima implies stable equilibrium is to cause a ball on a physical surface in static equilibrium as shown in three examples in Figure 2.1. It is displayed in Case (1) a ball on a local minimum with perturbing the ball away from its position by a small distance causes the ball to roll around about its original position, implying that the original position was stable. Case (2) shows a ball on a local maximum with perturbing the ball away from the top brings about the ball permanently to leave its original position, implying that the original position was

unstable. Case (3) shows a ball where one side rises and the other side falls away, namely a point of infection. Because this is called a position of neutral stability, it is actually unstable, as small perturbations would make it behave identically to case (2).

a) Potential energy profile   *b) Ball on a profiled surface*
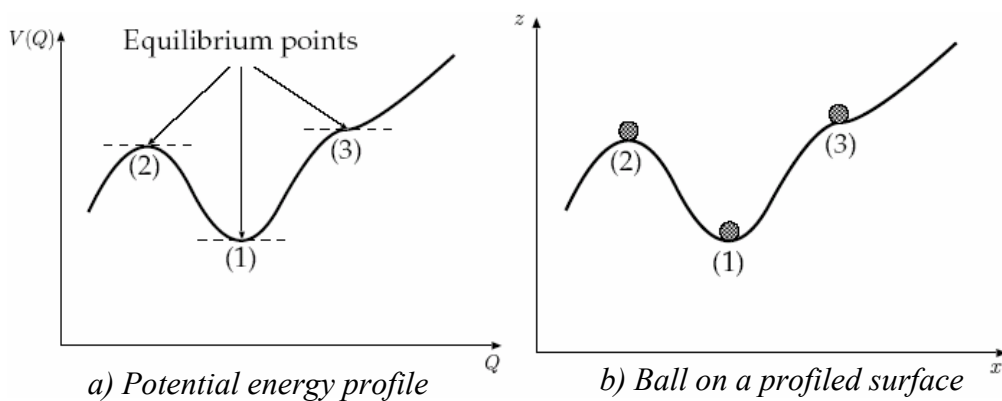
Figure 2.1 The rolling ball analogy for stability for single degree of freedom systems (Wadee, 2004)

For systems of n degrees of freedom, the potential energy profile becomes an $n+1$ dimensional surface. It is illustrated systems with two degrees of freedom have the stability possibilities in Figure 2.2. Cases (1) and (2) are fundamentally the same as for the single degree of freedom case. For systems with two degrees of freedom and more, however, it may have a surface in which one direction is a minimum but one of the other directions is a maximum; this is a saddle point, it is essentially unstable and is shown as case (3) for a two degree of freedom system (Wadee, 2004).

Case (1) Local minimum   *Case (2) Local maximum*   *Case (3) Saddle point*
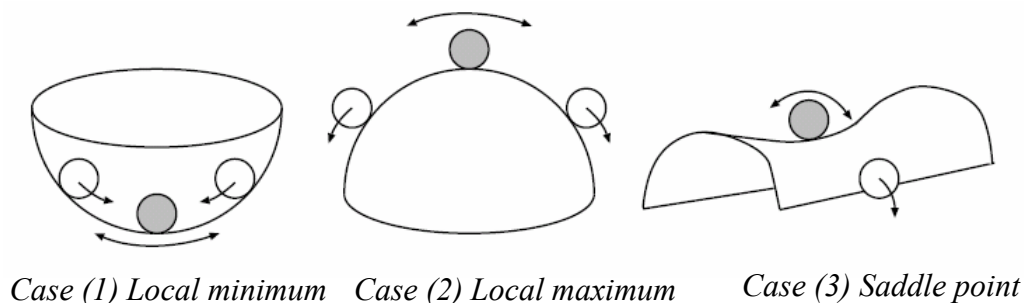
Figure 2.2 The rolling ball analogy for stability for more than one degree of freedom (Wadee, 2004)

It can be similarly considered the compressed bar. When a perfect column is subjected to a compressive axial force, the only deformation that occurred is a shortening of the column. For small value of force, if the column are to be deflected laterally by a force perpendicular to the column. Thereafter the lateral force removed, the column will return to its straight. This case means condition of stability. A small disturbance causes small magnitude of the displacement in the response. If the load is increased, when the lateral load is removed, the column will remain in the deformed shape and fail from a structural standpoint. A small disturbance causes large displacement (Figure 2.3). The structures become unstable. This condition is referred to as buckling. Structural instability failures are very hazardous. The critical load means the load at which the column starts buckling.
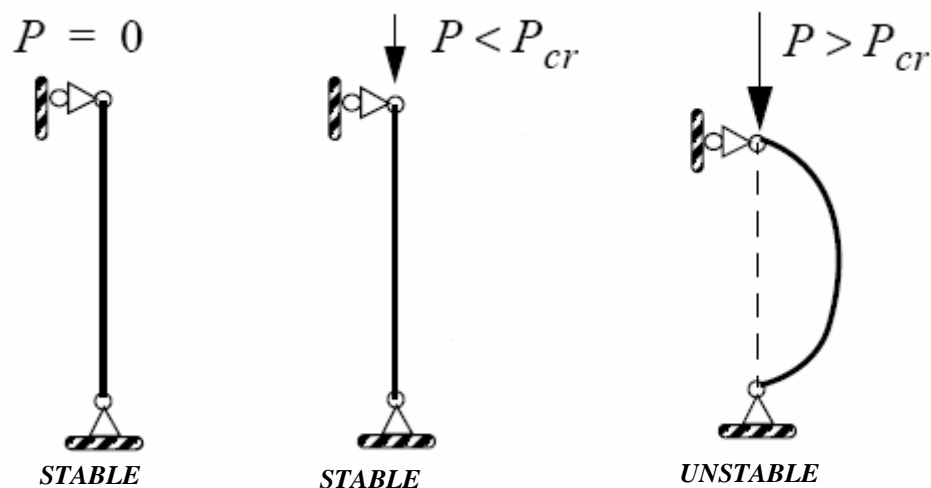
Figure 2.3 Equilibrium of a compressed column

The critical buckling load for a column is dependent on its rigidity and column's length. As expected, the critical load decreases as the column's length increases, eventually lateral buckling becomes more noticeable. This phenomenon can be mathematically modeled by means of finite element methods. When the compressive load attains the critical buckling load of the structural element, its total stiffness matrix becomes singular. At this point, the structural stiffness matrix has a nonempty null space, which means that it could statically undergo infinite displacement through the application of any nonzero lateral force. This implies an unstable equilibrium

points. It is determined the shape of the buckled beam by the vectors included within the null space of the total stiffness matrix. As the axial load increases beyond the critical buckling load, the dimension of the null space increases, and more buckling modes occur (Chase & Yim, 1999).

2.1.3   The Euler Formula for Columns

Euler (1744) computed the critical buckling loads for columns with the assumption of uniform cross-section for four different support types. Euler accepted that a column that is originally perfect column remains straight from the onset of loading. The load should reach a critical value for producing a small deflection of the column. It would suffer no deflection below this critical value.

The basic equations for analysis of column can be derived by considering the column. Consider a simply supported column, with length L and flexural rigidity EI loaded axially with a force P (Figure 2.4).
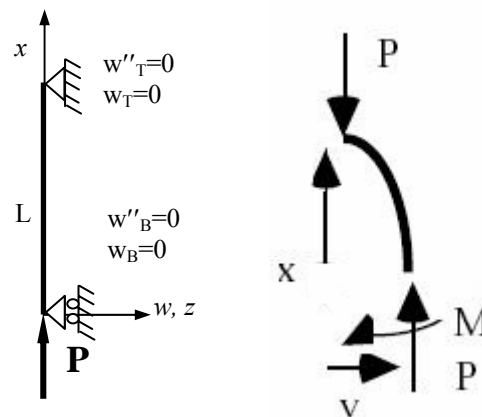
Figure 2.4 Column with pinned ends and free body diagram of upper part of the column

Equation moments at the cut end:

$$\sum M = Pw - M(x) = 0 \Rightarrow M(x) = Pw \tag{2.5}$$

where w is the lateral deflection at that point and x is the distance of the point from any given end. The deflection of the beam is related with its bending moment distribution. Bending theory states: $M=-EIw''$ curvature, which from linear bending theory can be written:

$$M = -EI\frac{d^2w}{dx^2}$$

(2.6)

and the governing equation for the buckling of column is then:

$$-EI\frac{d^2w}{dx^2} = Pw \Rightarrow EI\frac{d^2w}{dx^2} + Pw = 0$$

(2.7)

which simplifies to,

$$\frac{d^2w}{dx^2} + (\frac{P}{EI})w = 0 \Rightarrow k^2 = \frac{P}{EI}$$

(2.8)

This expression is in the form of a second order differential equation of the following type:

$$\frac{d^2w}{dx^2} + k^2w = 0$$

(2.9)

The solution of this equation is:

$$w = ACos(kx) + BSin(kx)$$

(2.10)

where A and B are constants, it can be determined using the column's kinematics boundary condition. It is given boundary condition for both pin-ended columns;

$$\begin{aligned} &\text{For } x=0 \Rightarrow w=0 \quad A+0=0 \text{ giving that } A=0 \\ &\text{For } x=L \Rightarrow w=0 \quad\quad BSin(kL)=0 \end{aligned}$$

(2.11)

If $B=0$, bending moment does not exist, so the only logical solution is for;

$$Sin(kL)=0 \tag{2.12}$$

and the only way that this can happen is if :

$$kL=n\pi, \ (n=1,2,3,......) \tag{2.13}$$

since $k^2 = \dfrac{P}{EI} = (\dfrac{n\pi}{L})^2$

then it is written buckling load as :

$$P = n^2 \dfrac{\pi^2 EI}{L^2} \tag{2.14}$$

where n define as the buckling mode shapes, as in Figure 2.5.
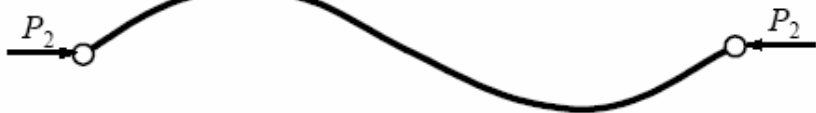
First mode of buckling	Buckling loads
P_1 ⟶⟵ P_1	$P_1 = \dfrac{\pi^2 EI}{L^2}$
Second mode of buckling	
P_2 ⟶⟵ P_2	$P_2 = \dfrac{4\pi^2 EI}{L^2}$
Third mode of buckling	
P_3 ⟶⟵ P_3	$P_3 = \dfrac{9\pi^2 EI}{L^2}$

Figure 2.5 First three modes of buckling loads of the column

The column buckles at P_1 because $P_1 < P_2 < P_3$ and never gets to P_2 or P_3 unless bracing is placed at the points where $w=0$ to preclude buckling at lower loads. Therefore, it is written as the critical buckling load for a pin-ended column:

$$P = n^2 \frac{\pi^2 EI}{L^2} = Pcr \qquad (2.15)$$

where, I least second moment of area, E, Young's modulus of elasticity, L, length of the column and Pcr, critical or maximum axial load on the column just before it begins to buckle. When $n=1$, it is obtained the smallest value of P so that the critical buckling load for the column is:

$$Pcr = \frac{\pi^2 EI}{L^2} \qquad (2.16)$$

This equation is known as Euler buckling load. When the load reaches the Euler buckling load, buckling suddenly occurs without any further load increase. The critical Euler buckling load clearly limits the column's safe load capacity. Higher orders of n may satisfy equilibrium, non-trivial solution and boundary conditions. These load levels can be reached, the column has lost it stability of the equilibrium state. It will not be capable of carrying on any further loads anymore. The non-trivial solution is called the buckling mode. It describes the pattern of the deflection immediately after buckling has occurred. The buckling mode shape is valid only for small deflections, where the material is still within its elastic limit. The Euler equation changes for columns with different end conditions. It is possible to set up the differential equation with suitable boundary conditions to obtain the Euler buckling.

Euler's formula can be given a general form for an elastic column,

$$P_{CR} = \frac{\pi^2 EI}{(KL)^2}$$
(2.17)

where *KL* represents the effective length of the column due to the end conditions and following:

- *K*=2 for fixed-free
- *K*=0,5 for fixed-fixed
- *K*=0,7 for pinned-fixed.

The effective length is shown in Figure 2.6 for various end conditions of column.
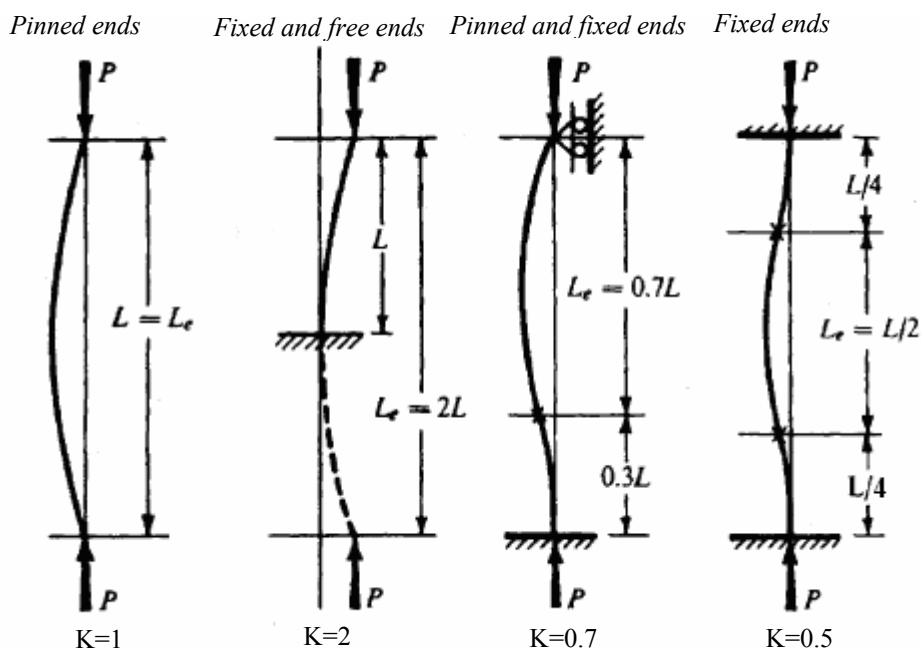
Figure 2.6 Effective lengths for various end conditions

2.1.4   Slenderness Ratio for Columns

It is very important subject end restraint and its effect on the load carrying capacity of columns. A thin-walled structure is made from a material whose thickness is much less than other structural dimensions. Buckling of thin walled structures may occur at stress well below the elastic limit. Critical buckling load depicts the ultimate capacity for a straight column in the engineering applications. There is a greater possibility for failure to occur, as members become more slender or thinner. The critical load because of buckling is less than maximum load needed for compressive yielding if the column is slender. The limiting value of the slenderness ratio is fundamentally a measure of the column's flexibility. The slenderness of a column is a function of effective length and the least radius of gyration. It is more useful to express the critical loading condition in terms of stress for purposes of design. It is given the following equation:

$$P_{CR} = \pi \sqrt{\frac{E}{\sigma_{yield}}} \tag{2.18}$$

into the case with both ends pinned, yielding the (Anonymous, 2005j):

$$\frac{L_e}{\rho} = \pi \sqrt{\frac{E}{\sigma_{yield}}} \text{ and } \rho = \sqrt{\frac{I}{A}} \tag{2.19}$$

where

ρ : *Radius of gyration calculated from the smallest moment of inertia*

E   : *Young's modulus*

I   : *Smallest moment of inertia of the column*

σ_{yield} : *Yield stress of the column*

A   : *Cross-sectional area of the column*

Le   : *Effective length*

The term, L_e/ρ is known as the slenderness ratio and contains information about the length and the cross-section. Figure 2.6 also shown the effective length for various end conditions of column. According to last equation, it can be seen that buckling will always happen about the column axis having the largest slenderness ratio, because a large slenderness ratio will give a small critical load.

It can be illustrated transition by plotting between stress and slenderness ratio, as shown in Figure 2.7. There is no sharply divided transition among the yielding and buckling in reality. The curve can be divided into three regions (Figure 2.8). It is the short column region in which yielding occurs when $\sigma=\sigma_{yield}$ in region A. Region B is an intermediate column region in which the column may yield or may buckle and empirical relations are used to approximate the resulting curve. It is for long columns in Region C. Buckling will occur in this region.
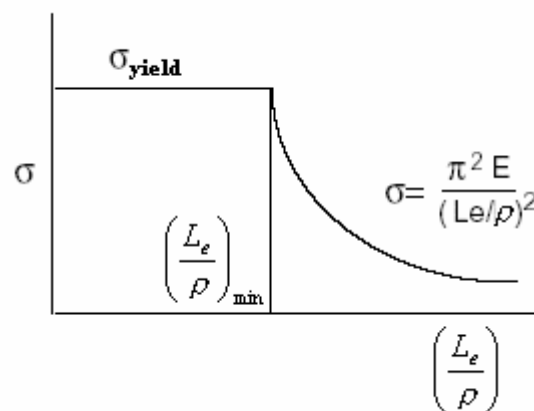
Figure 2.7 The relation between stress and slenderness ratio (Anonymous, 2005j)

It is valid $\sigma = \sigma_{yield}$ in region A, and $\sigma_{CR} = \pi^2 E / (L_e/k)^2$ in region C. Region C depends material, geometry and loading. It is often used empirical relations such as

parabolic approximation in region C. It is to fit a parabola to the σ - (L_e/ρ) curve from $\sigma = \sigma_{yield}$ to $\sigma = \sigma_{yield}/2$ such that.

For

$$0 \le \left(\frac{L_e}{\rho}\right) \le \left(\frac{L_e}{\rho}\right)_{min} \Rightarrow \sigma = \sigma_{yield}\left[1 - \frac{\left(\frac{L_e}{\rho}\right)^2}{\left(\frac{2L_e}{\rho}\right)^2_{min}}\right] \qquad (2.20)$$

For

$$\left(\frac{L_e}{\rho}\right) \rangle \left(\frac{L_e}{\rho}\right)_{min} \Rightarrow \sigma = \frac{\pi^2 E}{\left(\frac{L_e}{\rho}\right)^2} \qquad (2.21)$$
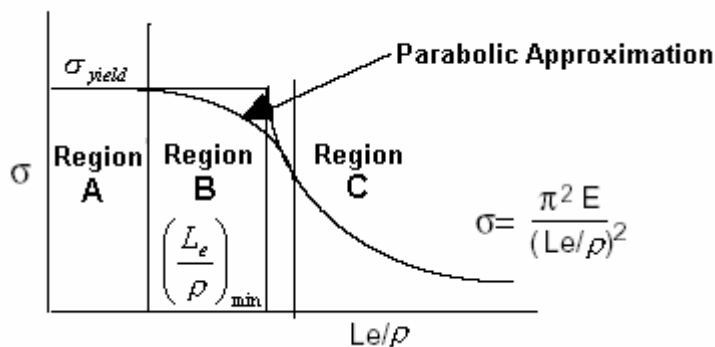
Figure 2.8 The relation between stress and slenderness ratio with parabolic approximation (Anonymous, 2005j)

Consequently, the buckling loads and stresses depend on stiffness of material, length of the column, cross-section dimensions, cross-sectional shape and end conditions (Mahfouz, 1999).

2.2 Buckling in Composite Materials

2.2.1   Introduction of Composite Materials

There has been a considerable increase in the use of advanced composite materials in various industries in recent years. The reason for this increase can be attributed to the great improvement of the stiffness-to-weight ratio and strength-to-weight ratio in composite materials. The development of composite materials with reduced weight and increased strength relative to the conventional metals or alloys, has played a critical role in achieving higher operating performance, long-life and reduced costs.

It can be divided structural elements into four main categories:

- *metals,*
- *ceramics,*
- *polymers and*
- *composites.*

The composite material is defined as composing of at least two substances in heterogeneous mix. It is combined two or more materials on a macroscopic scale in a specific way to accomplish desired mechanical properties. Modern technologies desire materials with combination of properties that cannot be met by the conventional metal alloys, ceramics and polymeric materials. To produce unique characteristics such as stiffness, toughness and high temperature strength, it can be combined metals, ceramics, glasses, polymers and cement.

Composites have become popular in a number of applications such as aerospace, marine applications, chemical industries and sporting goods and other industries. Military and commercial aircraft is the major structural applications for composites. Because in this field, weight reduction is critical for attaining higher speeds and increased payloads. There has been an enormous interest in the composite materials

in recent years. It is also selected composites for the purpose of weight saving, which in turn increases the fuel economy and payload capacity. It is used composites in wing skins, flaps, stabilizers and tail-boxes of advanced aircraft. It is made of composites rotor blades in helicopters not only for weight saving but also for better control of the twisting frequencies in the blades. It is also used composites the manipulator arms, tubes for mid-fuselage truss structure of space shuttles, exterior body component of automotive vehicles such as the hoods, door panels, rear leaf springs, drive shafts and sporting good industry such as bicycles, canoes racket-ball rackets, golf club shafts, racket-ball rackets, fishing rods snow and water skis, arrows, archery bows, hockey sticks and marine applications in structures such as boat hulls, decks, bulkheads, frames, masts and spars (Hassan, 1998).

Composite materials are used for high-performance applications because of desirable properties. Composite materials have been confirmed superior to metals such as robotics that used for various tasks. It can be improved strength, stiffness, weight reduction, thermal properties, fatigue life, corrosion resistance and wear resistance by forming a composite material. The behavior of composite materials also depends on many parameters that can be changed

Composite materials are composed of just two phases; one is termed the matrix, which is continuous and surrounds the other phase, often called the dispersed phase another is termed fiber. The composite is designed to show a combination of the best characteristics of each of the component materials. The commonly used composite materials are made of high-strength and high-stiffness fibers and held together by a matrix.

The performances of the composites depend on the mechanical properties, orientation, length, shape and composition of the fibers; the mechanical properties of the resin, the bond between the fibers and the matrix. Ease of fabrication, high fracture energy and potential for low cost are main features of composites materials

It is used a reinforcement phase and a binder phase, in many cases with more rigid and higher-strength fibers in a more compliant matrix. It was started firstly with glass fibers, followed by the more recent high-performance fibers. Continuous fibers such as glass, aramid and carbon embedded in a thermoset resin matrix (polyester, vinyl ester, or epoxy), which holds the fibers together and transfers the load between them. A typical example carbon fiber is broadly introduced into aerospace and sporting goods applications (Anonymous, 2005k).

There are both natural and manufactured composite materials. Bone, wood, bamboo is examples of cellular composites that exist in nature. Muscle tissue is a multidirectional fibrous laminate. Wood is the most common natural composite material. Wood is a fibrous composite, cellulose fiber in a lignin matrix. The lignin matrix joins the fibers and furnishes the stiffness. It is another example bone a natural composite that supports the weight of various members of the body. In addition to these naturally occurring composites, there are manufactured composite materials that have been in use for a very long time. The fiberglass-reinforced plastic used in household goods and in many applications is the most common example of a composite material. The plastic alone is relatively weak and has a low elastic modulus. However, it is very stable chemically and constitutes an excellent matrix for the composite. The glass fibers supply the strength and stiffness; their modulus of elasticity may be 50 times greater than that of the plastic (Anonymous, 2005k). Because the glass fibers can resist a much higher tensile stress before strain or yielding happens, they take most of the load when the composite is stressed.

Because fiber has quite different strength and stiffness properties in many cases, it must be thought that the fiber will be utilized in conjunction with a matrix. For example, the matrix has almost negligible strength and stiffness in comparison to the fiber with polymeric matrices. Since volume of fiber in the total composite volume (the fiber-volume fraction) will be approximately, say, 60%, the strength and stiffness will be diluted by a similar percentage, namely, a 40% loss of stiffness and strength will occur. In addition, if the loads are not strictly in one direction, some fraction of the fibers will have to be aligned in other than the principal load direction.

This further reduces the strength and stiffness in anyone direction. However, experience has indicated that meaningful structural advantages can still be acquired. Currently, composite applications in aircraft often deliver about 30% weight reduction (Anonymous, 2005k).

Composite materials are categorized into three types:

- *Fibrous composites*,
- *Particulate composites* and
- *Laminated composites*.

Fibrous composites consist of fibers of one material in a matrix material of another. Particulate composites consist of macro size particles of one material in matrix of another. Laminated composites composed of layers of different materials including composites of the first two types (Reddy, 1997).

Generally, the modeling of composite materials can be investigated from distinct levels: *macro mechanical* and *micro mechanical* scales. The macro mechanical approach is concerned with the contributions of each ply to the overall properties. Based on the known properties of the individual layers, the macro mechanical modeling involves investigation of the interaction of the individual layers of the laminate and their effect on the overall response of the laminate. For a given stacking sequence, the stress-strain relations of a composite laminate can be derived, and the various coupling mechanisms between in plane and out of plane deformation modes of a composite laminate can be explored. The micromechanical approach assumes that the complex microstructure of the composite can be replaced by a representative volume element or unit cell. The representative volume element has a regularly spaced any of parallel cylindrical fibers embedded in the homogeneous matrix material of infinite dimensions so that it can be isolated from the whole structure of the composite. The representative volume element has the same fiber volume fraction as the composite laminate and the respective properties of the fiber and matrix can be characterized individually. The individual constituents can then be

used together in the representative volume element model such that the overall response of the composite can be predicted.

2.2.1.1 Manufactured Composite Materials

2.2.1.1.1 Fiber Properties

Fibers are the principal component in composite material. It is fundamental load-bearing components in composite material. It has the largest volume fraction. Proper selection of the type, amount and orientation of fibers is very important because of influencing the characteristic of composite materials, such as specific gravity, tensile strength and modulus, compressive strength and modulus, fatigue strength, electrical, thermal conductivities and cost (Mallick, 1993).

Fibers are grouped into three different classifications based on diameter and character:

a) *whiskers,*
b) *fibers* and
c) *wires*.

It is whiskers very thin single crystals that have extremely large length-to-diameter ratios. Because of their small size, it has a high degree of crystalline perfection and is virtually flaw free, which accounts for their exceptionally high strengths. Whiskers are not used extensively as a reinforcement medium in spite of these high strengths. Because it is extraordinarily expensive. Further, it is difficult and often impractical to incorporate whiskers into a matrix. It is included whisker materials graphite, silicon carbide, silicon nitride and aluminum oxide.

Fibers are either polycrystalline or amorphous. Fibrous materials have small diameters. It is generally fibrous materials either polymers or ceramics (e.g., the polymer aramids, glass, carbon, boron, aluminum oxide and silicon carbide). Generally, the fibers are unidirectional or woven.

Fine wires have comparatively large diameters; typical materials include steel, molybdenum and tungsten. It is utilized as a radial steel reinforcement in automobile tires, in filament wound rocket casings and in wire wound high-pressure hoses (Anonymous, 2005k).

It is commercially available a number of fibers. The various types of fibers currently in use are glass-fiber, kevlar-fiber, carbon fiber, boron-fiber, silicon carbide-fiber and other fibers. They displayed a wide range of structural properties, including strength, stiffness and durability.

Among all the fiber materials, glass fibers are the most widely used reinforcement for composites. This is because their specific characteristics are relatively well known and they can be produced at relatively low cost. Glass fiber with polymeric matrices has been used in various commercial products such as piping, tanks, boats, and sporting goods. Due to the combination of low cost, corrosion resistance, and in many cases efficient manufacturing potential, glass is by far the most extensively used fiber. Glass fiber composites show low stiffness, high elongation, and moderate strength and weight, and generally lower cost relative to other composites. It has been used widely where corrosion resistance is important, such as in piping for the chemical industry and in marine applications. It is used as a continuous fiber in textile forms such as cloth and as a chopped fiber in less critical applications. It is commonly utilized the two types of glass fibers in the industry: E-glass and S-glass. Another type, known as C-glass, is used in chemical applications requiring greater corrosion resistance to acids than is supplied by E-glass (Anonymous, 2005k and Mallick, 1993).

Kevlar fibers have the lowest specific gravity and the highest tensile strength-to-weight ratio among the current reinforcing fibers. Both glass-fiber and kevlar-fiber composites display good toughness in impact environments. It is used in many marine and aerospace applications where lightweight, high tensile strength and resistance to impact damage are important. Kevlar fibers have high tensile strength but lower compressive strength. Kevlar is inclined to respond under impact in a ductile manner, as opposed to carbon fiber, which tends to fail in a more brittle manner (Anonymous, 2005k and Mallick, 1993).

Carbon fibers are widely used in aerospace and some applications of sporting goods, taking advantage of the relatively high stiffness-to-weight and high strength-to weight ratios of these fibers. The high stiffness and strength combined with low density and intermediate cost have made carbon fiber second only to glass fiber in use. It is ranged the tensile modulus from 207 GPa on the low side to 1035 GPa on the high side (Mallick, 1993). Carbon fibers vary in strength and stiffness with the processing variables, so that different grades are available such as high modulus or intermediate modulus, with the trade-off being between high modulus and high strength.

The tensile strength of carbon fiber differs with the specific type being considered. Although a typical range of values is on the order of 3,1 to 5,5 GPa (450 to 800 ksi) for fiber tensile strength, and stiffness on the order of 240 GPa (35 Msi), combined with a specific gravity of 1,7. Therefore the fiber itself is stronger than 7075 T6 aluminum by a factor of 5 to 10, and stiffer by a factor of 3,5 at approximately 60% of the weight. It is obvious the potential for advantages in mechanical design of high-performance structures (Anonymous, 2005k).

Even though lower-cost carbon fibers have showed on the market, current costs for carbon fibers are several times to an order of magnitude or more higher than aluminum. The cost differential implies that composite materials will be used in demanding applications, where rises in performance justify the higher material cost. Nevertheless, the material cost is only part of the story as manufacturing cost also

must be bear in mind. It has been possible to form parts of composites with a significantly fewer number of individual components compared to metallic structures and thus leading to an overall lower-cost structure. On the other hand, it may require fiber composite components a meaningful amount of hand labor, and thus have high manufacturing costs (Anonymous, 2005k).

Boron fibers show high stiffness-to-weight ratio, and good compressive strength, but also at very high cost. Tensile strength of boron fibers ranges of 379-414 GPa. Boron was one of the earliest fibers to be introduced into an aerospace application. However, whereas the prices of carbon fibers have dropped steadily since the introduction in the late 1960s, boron fibers have stayed expensive. Boron fibers have a relatively large diameter, typically approximately 200 microns. These fibers have been used in specialized applications both in aluminum and in polymeric matrices. Boron fibers also provide excellent resistance to buckling, which in turn contributes to high compressive strength for boron-fiber –reinforced composites (Mallick, 1993).

It is a number of other fibers under development for use with ceramic matrices to get very high-temperature applications such as for engine components. For example, it is given silicon carbide fiber, used in whisker form. These fibers may confirm to be significant in high temperature applications. It is obvious that their present use is a very small fraction of the use of glass, carbon, and Kevlar fibers (Anonymous, 2005k).

Silicon carbide fibers are utilized primarily in high temperature metal and ceramic matrix composites due to their excellent oxidation resistance and high temperature strength retention. It is about the same as those of boron at room temperature the strength and stiffness of silicon carbide fibers. Silicon carbide whisker reinforced metals are also receiving considerable attention as alternatives to unreinforced metals and continuous fiber reinforced metals. Silicon carbide whiskers are very small and so that standard metal forming processes such as extrusion, rolling and forging can be easily used, it is 8-20μ in (20-51nm) in diameter and about 0,03 mm long (Gibson, 1994).

Properties of some commercially used fibers are listed in the following table (Hassan, 1998):

Table 2.1 Properties of commonly used fibers (Hassan, 1998)

Fiber Type	Specific Gravity	Tensile Modulus (GPa)	Tensile Strength (MPa)	Strain to Failure (%)
E-glass	2,54	72,4	3450	4,8
S-glass	2,49	86,9	4300	5,0
Carbon	1,86	380	2700	0,7
Aramid (Kevlar-49)	1,45	131	3620	2,8
Boron	2,7	393	3100	0,8

2.2.1.1.2 Matrix Properties

The matrix in composite transfers stresses between the fibers, provides a barrier against an adverse environment, and preserves the surface of the fibers from mechanical abrasion. It plays a minor role in the tensile load-carrying capacity of a composite structure. However, it has a major influence selection of a matrix on the interlaminar shear as well as in-plane shear properties of the composite material. The matrix yields lateral support against the possibility of fiber buckling under compressive loading, therefore influencing to some extent the compressive strength of the composite material (Mallick, 1993).

The matrix phase binds the fibers together and acts as the medium by which an externally applied stress is transmitted and distributed to the fibers; only a very small proportion of an applied load is sustained by the matrix phase. It is essential that the matrix material should be ductile. Additionally, the elastic modulus of the fiber should be much higher than that of the matrix. It is protected the individual fibers from surface damage because of mechanical abrasion or chemical reactions with the environment. Further, it is separated the fibers and by virtue of its relative softness

and plasticity. The matrix is prevented the propagation of brittle cracks from fiber to fiber, which could result in disastrous failure. It is obvious that adhesive bonding forces between fiber and matrix be high. Adequate bonding is fundamental to maximize the stress transmittance from the weak matrix to the strong fibers. Consequently, the matrix holds the fibers together in a structural unit and preserves them from external damage, transfers and delivers the applied loads to the fibers, and in many cases provides some needed property such as ductility, toughness, or electrical insulation (Anonymous, 2005k and Gibson, 1994).

It have been used the thermoset polymers and a large amount of characterization data are accessible for these materials. The most common matrix material is resin, which includes polymers and epoxies.

Epoxy resins have a wide variety of properties because a larger number of starting materials curing agents and modifiers are available. In general, epoxy resins have high mechanical properties and excellent adhesion to the fibers. The epoxy resins are extensively used thermosets that propose superior performance, but are more costly relative to the polyesters. There is a wide range of epoxy resins available commercially. It must be consulted manufacturer's literature be to select the proper range of properties needed and the cost required to achieve these objectives. It is typical cure temperatures for the epoxies in the range of 121 to 177°C (250 to 350°F). However, some ambient temperature products are available. Consequently, epoxy matrix has many advantages such as, wide variety of properties, absence of volatile matters during cure, low shrinkage during cure, excellent resistance to chemicals and solvents, excellent adhesion to a wide variety to a wide variety of fillers, fibers and other substrates. However, it is the principal disadvantages relatively high cost and long cure time. Because of higher viscosity than other resins, epoxy resins are relatively expensive. For this reason, their usage became limited in some manufacturing processes like pultrusion that requires large quantities of resin (Mallick, 1993, Anonymous, 2005k and Hassan, 1998).

It is considered variables the inter laminar shear strength, which is a laminate property related to the shear strength of the matrix, the brittleness or toughness of the matrix, moisture and environmental resistance, and the range of elevated temperature properties if that is part of the product requirement. It is emphasized early aerospace epoxies used in prepregs resistance to hot, wet conditions, and while performing these objectives tended to be brittle and subject to damage from accidental impact. It has been more recent developments the high toughness epoxies, available at higher cost. Finally, it is listed followed the main characteristics of the property-cured product (Homam, 2000):

- excellent chemical resistance;
- very low shrinkage on cure
- outstanding adhesion to a variety of substrates, especially metals and concrete
- high tensile, compressive, and flexural strength
- excellent electrical insulation properties
- corrosion resistance
- ability to cure over a wide temperature range

It is typically limited the epoxies to 150^0C or less, depending on the specific material. It is available higher-temperature polymers such as bismalimides and polymers. However, they typically demonstrate increased brittleness. They are being used in applications such as cowlings and ducts for jet engines.

It can be formulated polyester resins in a variety of properties ranging from hard, brittle to soft, and flexible. Polyester resins advantages are low viscosity, fast cure time and low cost. However, its properties are generally lower than those for epoxies. Because of their lower viscosity and faster cure time, their processing is easier than most epoxy resins. Polyesters are used in the highest volume because of low cost and have adequate mechanical properties and environmental durability. Their high volumetric shrinkage is disadvantage as it might cause surface defects upon curing. Polyester composites are utilized pipes and tanks, shower stalls and bathtubs, boats and automobile components (Mallick, 1997 and Hassan, 1998).

Mechanical properties of vinylester resins are between those of epoxy and polyester resins. Vinylester resins have higher fracture toughness and better wet-out properties than epoxies and better adhesion to glass fibers than polyesters. They are also more flexible. Vinylester resins have good characteristics of epoxy resins, such as excellent chemical resistance and tensile strength, and of unsaturated polyester resins, such as low viscosity and fast curing. However, the volumetric shrinkage of vinylester resins is in the range of 5-10%, which is higher than that of the parent epoxy resins. It is also exhibited only moderate adhesive strengths compared with epoxy resins. It is lower-cost materials polyester and vinylester with similar but somewhat improved mechanical properties and developed solvent resistance. It gives a higher failure strain than typical polyesters, which in turn gives vinylester laminates superior mechanical properties, impact damage resistance and fatigue life (Mallick, 1993 and 1997).

It is known phenolics because of their good fire resistance. Due to the introduction of more stringent, their usage has increased fire, smoke and toxicity regulations. They still find many applications. Their main disadvantage is their highly brittle nature because of their low cost and good balance of properties (Hassan, 1998).

Metal matrix composites are being used for higher-temperature use than that available with polymeric matrices. It has been utilized aluminum with boron and carbon fibers. It is a successful application is that of a metal matrix piston manufactured by Toyota in Japan, used for increased wear resistance and high thermal conductivity. It has been manufactured over one million of these. Ceramic matrix materials are under development for still higher temperature ranges (Anonymous, 2005k).

2.2.1.1.3 Composite Properties

The need of lightweight, good-strength-characteristics and resistance to thermal effects in areas such as aircraft design, robotics, automobile industry and smart control have increased interest in composite materials.

Because of producing unique characteristics such as stiffness, toughness and high temperature strength, it can be combined metals, ceramics, glasses, polymers and cement in composite materials. Figure 2.9 makes a comparison between aluminum, steel and composite materials (Chawla, 2001).
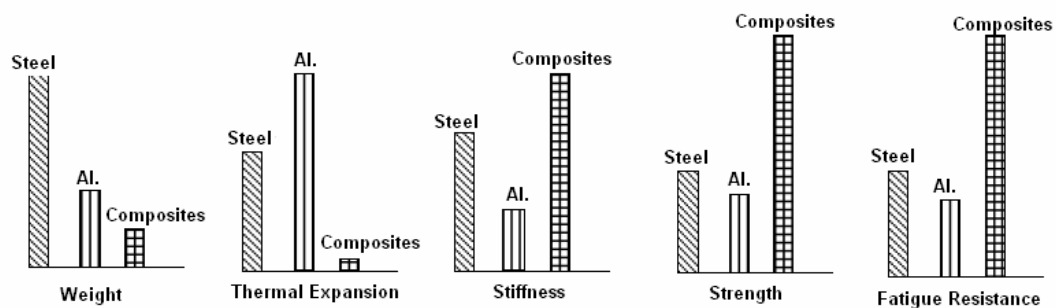
Figure 2.9 Comparison between materials and composite materials (Chawla, 2001)

The advantages of composite material are listed followed (Homam, 2000):

- They can be made with high strength and high specific strength (ratio of strength to specific weight)
- They can be made with high stiffness and high specific stiffness (ratio of
- stiffness to specific weight)
- Density is generally low
- Strength can be high at elevated temperature
- Impact and thermal shock resistance are good.
- Fatigue strength is good, often better than the metals
- Oxidation and corrosion resistance are particularly good

- Thermal expansion is low and can be controlled
- Thermal conductivity and electrical conductivity can be controlled
- Stress-rupture life is better relative to many metals
- Predetermined properties can be produced to meet individual needs
- Fabrication of large components can often carried out at lower cost than for metals

It has an important influence the arrangement or orientation of the fibers relative to one another, the fiber concentration and the distribution on the strength and other properties of fiber-reinforced composites.

2.2.1.2 Natural Composite Materials (Wood Properties)

Wood can be considered one of nature's complex composite materials. It is completely used as a material for many structures, furniture, tools, and decorative objects. This material has much utilization in the civil infrastructure and other important applications (Tabiei & Wu, 2000).

For comprehension of the mechanical properties, the individual structure characteristic of each tree has to be taken into consideration (Reiterer, Burgert, Sinn & Tschegg, 2002). Variability, or variation in properties, is common to wood materials. Because wood is a natural material and the tree is subject to many constantly changing influences (such as moisture, soil conditions, and growing space), wood properties vary considerably, even in clear material (Green, 1999).

Investigation of wood can be occurred on many different scales, i.e. structural timber level, fiber level, fibril level or cellulose chain level (Poulsen, Moran, Shilr & Byskov, 1997). Wood properties exhibit wide variability due to its natural origin. These variations are in part the result of the growth conditions of wood brought about by environmental factors such as climate, soil, water supply, and available nutrients. Wood is assumed to have three mutually perpendicular axes of symmetry with respect to its properties: longitudinal, radial, and tangential with reference to the

cylindrical bole of a tree (Tabarsa, 1999). Wood is a complex fiber-reinforced composite because of the orientation of the wood fibers and the manner in which a tree increases in diameter as it grows, properties vary along three mutually perpendicular axes: longitudinal, radial and tangential.

The longitudinal axis is parallel to the fiber (grain) direction, the radial axis is perpendicular to the grain direction and normal to the growth rings, and the tangential axis is perpendicular to the grain direction and tangent to the growth rings (Reiterer, Burgert, Sinn & Tshchegg, 2001). Although most wood properties differ in each of these three axis directions, differences between the radial and tangential axes are relatively minor when compared to differences between the radial or tangential axis and the longitudinal axis (Winandy, 1994). Hard woods are fine-grained and have a higher compressive strength than softwoods. Wood is unique in that it has two compressive strengths; one when loaded parallel to the grain and another when loaded perpendicular to the grain. When a wood column crushes the fibers of the wood actually split apart. In every case, crushing is a strength failure and does not depend upon the shape of the section (Anonymus, 1996l).

2.2.2 Determination of Mechanical Properties of Composite Materials
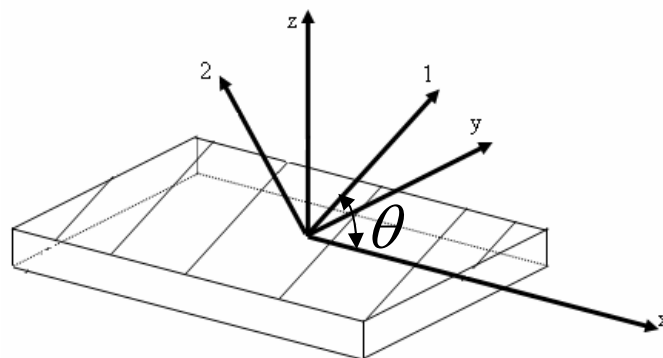
Figure 2.10 Definition of principal axes and loading axes for composite material (Mallick, 1993)

Let us consider a thin lamina in which fibers are positioned parallel to each other in a matrix, as shown in Figure 2.10. The material coordinate axis (1) is taken to be

parallel to the fiber, the axis (2) transverse to the fiber direction in the plane of the composite. It is made following assumptions determining the engineering constants:

- It exists perfect bonding between fibers and matrix
- Fibers are parallel and uniformly distributed throughout
- It is isotropic both fibers and matrix
- It is valid Hooke's law both fibers and matrix
- The applied loads are either parallel or perpendicular to the fiber direction
- Both fibers and matrix behave as linearly elastic material.

It is calculated from followed equations elastic properties of a unidirectional continuous fiber 0^0 lamina (Mallick, 1993):

$$Longitudinal\ modulus \Rightarrow E_{11} = E_f V_f + E_m V_m \tag{2.22a}$$

where V_f and V_m are fiber volume fraction and matrix volume fraction, respectively. Equation (2.22a) is written also Equation (2.22b):

$$E_{11} = E_f \frac{A_f}{A} + E_m \frac{A_m}{A} . \tag{2.22b}$$

It also defined E_f and E_m as modulus of the fiber and modulus of the matrix, respectively.

$$Transverse\ modulus \Rightarrow E_{22} = \frac{E_f E_m}{E_f V_m + E_m V_f} \tag{2.23}$$

While it is direction to the fibers young modulus of E_{11}, young modulus of the direction transverse to the fibers is E_{22}.

It expresses shear modulus as G_{12}, and Poisson's ratio is v_{12} :

$$Shear\ modulus \Rightarrow G_{12} = \frac{G_f G_m}{G_f V_m + G_m V_f} \tag{2.24}$$

$$Poisson's\ ratio \Rightarrow v_{21} = \frac{E_{22}}{E_{11}} v_{12} \tag{2.25}$$

It is calculated from followed equations elastic properties of an angle ply lamina in which continuous fibers are aligned at an angle θ with the positive x and y direction:

$$\frac{1}{E_{xx}} = \frac{\cos^4 \theta}{E_{11}} + \frac{\sin^4 \theta}{E_{22}} + \frac{1}{4}\left(\frac{1}{G_{12}} - \frac{2v_{12}}{E_{11}}\right)\sin^2 2\theta \tag{2.26}$$

$$\frac{1}{E_{yy}} = \frac{\sin^4 \theta}{E_{11}} + \frac{\cos^4 \theta}{E_{22}} + \frac{1}{4}\left(\frac{1}{G_{12}} - \frac{2v_{12}}{E_{11}}\right)\sin^2 2\theta \tag{2.27}$$

$$\frac{1}{G_{xy}} = \frac{1}{E_{11}} + \frac{2v_{12}}{E_{22}} + \frac{1}{E_{22}} - \left(\frac{1}{E_{11}} + \frac{2v_{12}}{E_{22}} + \frac{1}{E_{22}} - \frac{1}{G_{12}}\right)\cos^2 2\theta \tag{2.28}$$

$$v_{xy} = E_{xx}\left[\frac{v_{12}}{E_{11}} - \frac{1}{4}\left(\frac{1}{E_{11}} + \frac{2v_{12}}{E_{11}} + \frac{1}{E_{22}} - \frac{1}{G_{12}}\right)\right]\sin^2 2\theta \tag{2.29}$$

$$v_{yx} = \frac{E_{yy}}{E_{xx}} v_{xy} \tag{2.30}$$

where E_{11}, E_{22}, v_{12} and G_{12} are calculated Equations (2.22) through (2.25).

The three-dimensional stress-strain relation in reference to the local fiber coordinates1, 2 and 3 for a single layer is shown in Equation (2.31) (Mallick, 1993):

$$
\begin{pmatrix} \sigma_{11} \\ \sigma_{22} \\ \sigma_{33} \\ \sigma_{23} \\ \sigma_{13} \\ \sigma_{12} \end{pmatrix} = \begin{bmatrix} C_{11} & C_{12} & C_{13} & 0 & 0 & 0 \\ C_{12} & C_{22} & C_{23} & 0 & 0 & 0 \\ C_{13} & C_{23} & C_{33} & 0 & 0 & 0 \\ 0 & 0 & 0 & C_{44} & 0 & 0 \\ 0 & 0 & 0 & 0 & C_{55} & 0 \\ 0 & 0 & 0 & 0 & 0 & C_{66} \end{bmatrix} \begin{pmatrix} \varepsilon_{11} \\ \varepsilon_{22} \\ \varepsilon_{33} \\ 2\varepsilon_{23} \\ 2\varepsilon_{13} \\ 2\varepsilon_{12} \end{pmatrix}
\tag{2.31}
$$

where $\sigma_{11}, \sigma_{22}, \sigma_{33}$ and $\varepsilon_{11}, \varepsilon_{22}, \varepsilon_{33}$ are stresses and strains in the local material axes1, 2 and 3 respectively. $\sigma_{12}, \sigma_{13}, \sigma_{23}$ and $\varepsilon_{12}, \varepsilon_{13}, \varepsilon_{23}$ are shear stresses and strains, respectively, in the local material axes 1, 2 and 3. It is found below equations the stiffness constants (C_{ij}) from the engineering properties:

$$C_{11} = E_{11}(1 - v_{23}v_{32})/(1 - v_{12}v_{21} - v_{23}v_{32} - v_{13}v_{31} - 2v_{13}v_{21}v_{32})$$

$$C_{22} = E_{22}(1 - v_{13}v_{31})/(1 - v_{12}v_{21} - v_{23}v_{32} - v_{13}v_{31} - 2v_{13}v_{21}v_{32})$$

$$C_{33} = E_{33}(1 - v_{12}v_{21})/(1 - v_{12}v_{21} - v_{23}v_{32} - v_{13}v_{31} - 2v_{13}v_{21}v_{32})$$

$$C_{12} = E_{11}(v_{21} + v_{23}v_{31})/(1 - v_{12}v_{21} - v_{23}v_{32} - v_{13}v_{31} - 2v_{13}v_{21}v_{32})$$

$$C_{13} = E_{11}(v_{31} + v_{21}v_{32})/(1 - v_{12}v_{21} - v_{23}v_{32} - v_{13}v_{31} - 2v_{13}v_{21}v_{32})$$

$$C_{23} = E_{11}(v_{32} - v_{12}v_{31})/(1 - v_{12}v_{21} - v_{23}v_{32} - v_{13}v_{31} - 2v_{13}v_{21}v_{32})$$

$$C_{44} = G_{23}$$

$$C_{55} = G_{13}$$

$$C_{66} = G_{12} \tag{2.32}$$

It is applicable Equation (2.32) for general 3-D composite materials. It can be set to zero G_{13}, G_{23}, G_{33}, v_{13} and v_{23} for plain stress thin composite plates. The coordinate system 1-2-3 is offset by an angle θ relative to the global coordinate x-y-z as shown in Figure (2.10). Therefore, in order to transfer stresses and the strains to the global coordinate system, a transformation matrix should be used as follows (Reddy, 1997):

$$\{\bar{\sigma}\} = [T]^{-1}\{\sigma\} \text{ and } \{\bar{\varepsilon}\} = [T]^{-1}\{\varepsilon\} \tag{2.33}$$

where

$$[T] = \begin{bmatrix} \cos^2\theta & \sin^2\theta & 0 & & & -\sin 2\theta \\ \sin^2\theta & \cos^2\theta & 0 & & & \sin 2\theta \\ 0 & 0 & 1 & & & \\ 0 & 0 & & \cos\theta & \sin\theta & \\ 0 & 0 & & -\sin\theta & \cos\theta & \\ \cos\theta\sin\theta & -\cos\theta\sin\theta & & & & \cos^2\theta - \sin^2\theta \end{bmatrix} \tag{2.34}$$

It is expressed by substituting Equations (2.33) in (2.32) as follows:

$$\{\bar{\sigma}\} = [\bar{C}]\{\bar{\varepsilon}\}, [\bar{C}] = [T]^{-t}[T]^{-1}[C] \tag{2.35}$$
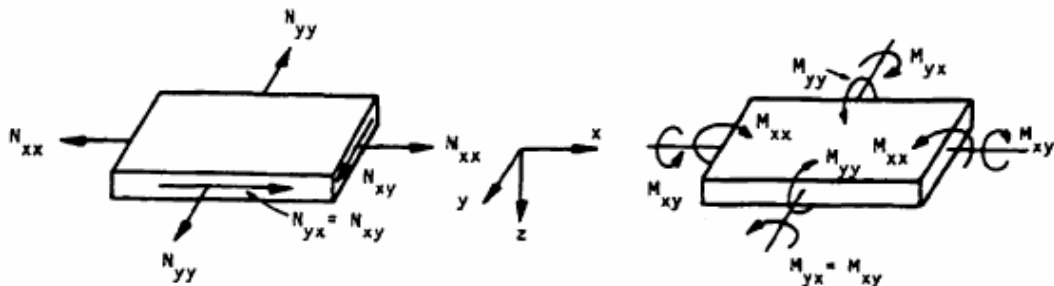

Figure 2.11 Moments and forces on the laminated plate according to the classical laminated theory (Mallick, 1993)

In advanced composite materials, several layers are stacked on each other, each of which may have different mechanical properties in different directions. Therefore, a laminated plate can be reinforced in more than one direction. The relation between the forces acting on a laminated plate, and the resulting strains can be found by integrating the stiffness coefficients of Equation (2.35), layer by layer, along the whole thickness of the laminate. Equation (2.36) shows global force-strain relationship of a laminate (Hassan, 1998).

$$
\begin{pmatrix} N_{xx} \\ N_{yy} \\ N_{xy} \\ M_{xx} \\ M_{yy} \\ M_{xy} \end{pmatrix} = \begin{bmatrix} A_{11} & A_{12} & A_{16} & B_{11} & B_{12} & B_{16} \\ A_{21} & A_{22} & A_{26} & B_{21} & B_{22} & B_{26} \\ A_{61} & A_{62} & A_{66} & B_{61} & B_{62} & B_{66} \\ B_{11} & B_{12} & B_{16} & D_{11} & D_{12} & D_{16} \\ B_{21} & B_{22} & B_{26} & D_{21} & D_{22} & D_{26} \\ B_{61} & B_{62} & B_{66} & D_{61} & D_{62} & D_{66} \end{bmatrix} \begin{pmatrix} \varepsilon_{xx}^{0} \\ \varepsilon_{yy}^{0} \\ \gamma_{xy}^{0} \\ \kappa_{xx} \\ \kappa_{yy} \\ \kappa_{xy} \end{pmatrix}
\tag{2.36}
$$

where

$$
(A_{ij}, B_{ij}, D_{ij}) = \int_{-h/2}^{h/2} \overline{C}_{ij}(1, z, z^2) dz
\tag{2.37}
$$

[A]=Extensional stiffness matrix for the laminate

[B]=Coupling stiffness matrix for the laminate

[D]=Bending stiffness matrix for the laminate

z = Distance from the midplane in the thickness direction

A_{ij} terms, form extensional stiffness matrix for the laminate, generate the in-plane extensional and the shearing deformations, ε_{ij}, when a laminate is subjected to in-plane forces N_{ij}. B_{ij} terms, form the extension-bending coupling stiffness matrix, generate the curvatures, κ_{ij}, when a laminate is subjected to the in-plane forces N_{ij} and the bending moments M_{ij}. Dij terms, the bending stiffness matrix generate the curvatures, κ_{ij}, when a laminate is subjected to the bending moments M_{ij}. The axial stiffness terms A_{16} and A_{26} if they exist in a laminate's stiffness matrix, produce in-

plane shear strain, γ_{xy}, when the laminate is subjected only to axial force. The bending stiffness terms D_{16} and D_{26} if they exist in a laminate's stiffness matrix, produce twisting curvature κ_{ij}, when the laminate is subjected to a bending moment (Hassan, 1998).

The strains shown in Equations (2.36) and (2.37) are the strains at the mid-plane of a laminate. However, the mid-plane strains of each layer are found from Equations (2.38).

$$\varepsilon_{xx} = \varepsilon_{xx}{}^0 + zk_{xx}$$

$$\varepsilon_{yy} = \varepsilon_{yy}{}^0 + zk_{yy} \qquad (2.38)$$

$$\gamma_{xy} = \gamma_{xy}{}^0 + zk_{xy}$$

2.2.3 Theoretical Buckling Equation for Composite Materials

A beam subjected to axial compressive load remains straight however shortens as the load increases from zero to a certain magnitude. The beam is said to be stable if a small axial or lateral disturbance applied to the beam keeps it in equilibrium. If the small additional disturbance results in a large response and the beam does not return to its original equilibrium configuration, namely, the beam is said to be unstable. It is called as buckling the onset of instability. It is termed as the critical buckling load the magnitude of the compressive axial load which the beam unstable. If the load is raised beyond this critical buckling load, the large deflection is occurred and beam tries another equilibrium configuration. Therefore, the load is of practical importance in the design of structural elements. It is measured buckling deflection onset of buckling (Reddy, 1997).

In the following section, it is investigated the critical buckling load according to both classical and first-order shear deformation theories.

2.2.3.1 Classical Buckling Theory

In the absence of in-plane forces, as the transverse deflection function *w,* the classical laminated theory constitutive equations for symmetric laminates are given by (Reddy, 1997),

$$
\left\{ \begin{matrix} M_{xx} \\ M_{yy} \\ M_{xy} \end{matrix} \right\} = \begin{bmatrix} D_{11} & D_{12} & D_{16} \\ D_{12} & D_{22} & D_{26} \\ D_{16} & D_{26} & D_{66} \end{bmatrix} \left\{ \begin{matrix} \dfrac{\partial^2 w}{\partial x^2} \\ \dfrac{\partial^2 w}{\partial y^2} \\ 2\dfrac{\partial^2 w}{\partial x \partial y} \end{matrix} \right\}
\tag{2.39}
$$

or inverse form, it has

$$
\left\{ \begin{matrix} \dfrac{\partial^2 w}{\partial x^2} \\ \dfrac{\partial^2 w}{\partial y^2} \\ 2\dfrac{\partial^2 w}{\partial x \partial y} \end{matrix} \right\} = - \begin{bmatrix} D^*_{11} & D^*_{12} & D^*_{16} \\ D^*_{12} & D^*_{22} & D^*_{26} \\ D^*_{16} & D^*_{26} & D^*_{66} \end{bmatrix} \left\{ \begin{matrix} M_{xx} \\ M_{yy} \\ M_{xy} \end{matrix} \right\}
\tag{2.40}
$$

$$
\frac{\partial^2 w}{\partial x^2} = -D^*_{11} M_{xx}, \frac{\partial^2 w}{\partial y^2} = -D^*_{12} M_{xx}, 2\frac{\partial^2 w}{\partial x \partial y} = -D^*_{16} M_{xx}
\tag{2.41}
$$

where *w* indicates the buckling deflection and D^*_{ij} (*i, j=1,2,6*) denote the elements of inverse matrix of D_{ij}.

While D^*_{ij} ($i, j=1, 2, 6$) is defined with Equation (2.34), Equation (2.35) is described D_{ij} matrix depending on plane-stress reduced stiffness Q_{ij}.

$$D^*_{11} = (D_{22}D_{66} - D_{26}D_{26})/D^*$$

$$D^*_{12} = (D_{16}D_{26} - D_{12}D_{66})/D^*$$

$$D^*_{16} = (D_{12}D_{26} - D_{22}D_{16})/D^*$$

$$D^* = D_{11}D_1 + D_{12}D_2 + D_{16}D_3$$

$$D_1 = D_{22}D_{66} - D_{26}D_{26}$$

$$D_2 = D_{16}D_{26} - D_{12}D_{66}$$

$$D_3 = D_{12}D_{26} - D_{22}D_{16}$$

(2.42)

$$D_{ij} = \frac{\bar{Q}_{ij} h^3}{12}$$

(2.43)

$\bar{Q}_{ij}$ is defined following equations:

$$\bar{Q}_{11} = Q_{11} \cos^4 \theta + 2(Q_{12} + 2Q_{66})\sin^2 \theta \cos^2 \theta + Q_{22} \sin^4 \theta$$

$$\bar{Q}_{12} = (Q_{11} + Q_{22} - 4Q_{66})\sin^2 \theta \cos^2 \theta + Q_{12}(\sin^4 \theta + \cos^4 \theta)$$

$$\bar{Q}_{22} = Q_{11} \sin^4 \theta + 2(Q_{12} + 2Q_{66})\sin^2 \theta \cos^2 \theta + Q_{22} \cos^4 \theta$$

(2.44)

$$\bar{Q}_{16} = (Q_{11} - Q_{12} - 2Q_{66})\sin \theta \cos^3 \theta + (Q_{12} - Q_{22} + 2Q_{66})\sin^3 \theta \cos \theta$$

$$\bar{Q}_{26} = (Q_{11} - Q_{12} - 2Q_{66})\sin^3 \theta \cos \theta + (Q_{12} - Q_{22} + 2Q_{66})\sin \theta \cos^3 \theta$$

$$\bar{Q}_{66} = (Q_{11} + Q_{22} - 2Q_{12} - 2Q_{66})\sin^2\theta\cos^2\theta + Q_{66}(\sin^4\theta + \cos^4\theta)$$

$$\bar{Q}_{44} = Q_{44}\cos^2\theta + Q_{55}\sin^2\theta$$

$$\bar{Q}_{45} = (Q_{55} - Q_{44})\cos\theta\sin\theta$$

$$\bar{Q}_{55} = Q_{55}\cos^2\theta + Q_{44}\sin^2\theta$$

In these equations, it is defined angle ply lamina in which continuous fibers are aligned at an angle θ with the positive x direction, as shown in Figure 2.10.

The plane-stress reduced stiffness Q_{ij}, is specified with Equation (2.45).

$$Q_{11} = \frac{E_{11}}{1 - v_{12}v_{21}}$$

$$Q_{12} = \frac{v_{12}E_{22}}{1 - v_{12}v_{21}}$$

$$Q_{22} = \frac{E_{22}}{1 - v_{12}v_{21}}$$ (2.45)

$$Q_{66} = G_{12}$$

$$Q_{44} = G_{23}$$

$$Q_{55} = G_{13}$$

Equation (2.41) displays that the transverse deflection function w, can be dependent of the coordinate y due to Poisson effect (D^*_{12}) and anisotropic shear coupling (D^*_{16}). These effects can be neglected only for long beams, namely, when the length-to-width ratio is large. It is a function of lamination scheme the length-to-width ratio for which the transverse deflection can be assumed independent of y (Reddy, 1997).
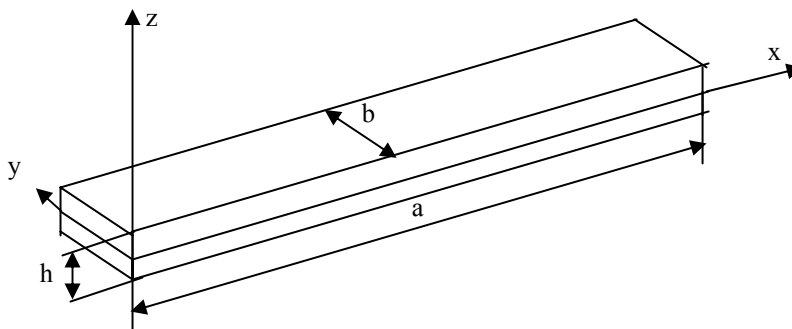
Figure 2.11 Geometry of beam (Reddy, 1997)

It is also written followed equation:

$$Q_x = \frac{\partial M_{xx}}{\partial x}, \frac{\partial^2 w}{\partial x^2} = -\frac{M}{E_{xx}^{\ b} I_{yy}} \ or \ \ M(x) = -E_{xx}^{\ b} I_{yy} \frac{\partial^2 w}{\partial x^2} \tag{2.46}$$

where b is the width and h is the total thickness of the beam, as shown in Figure 2.11.

It can be written followed the equation of motion of symmetrically long beams (Figure 2.12),
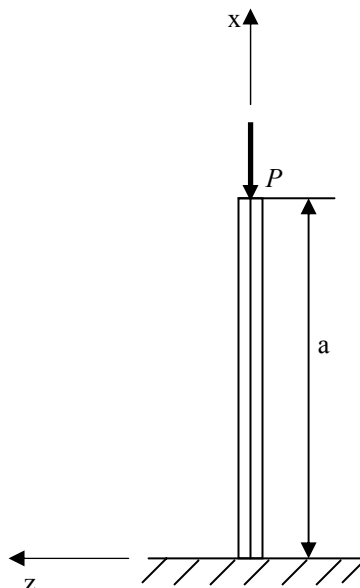
Figure 2.12 Geometry of beams subject to buckling under clamped-free edge conditions (Reddy, 1997)

Using Equation (2.46), the differential equation is obtained following equation:

$$\frac{-d^2}{dx^2}(E_{xx}{}^b I_{yy} \frac{d^2 w_0}{dx^2}) + bP \frac{d^2 w_0}{dx^2} = 0.$$

(2.47)

Equation (2.47) is differentiated according to x, it is found Equation (2.48) with Equation (2.49).

$$\frac{d^4 w}{dx^4} + \frac{bP}{E_{xx}{}^b I_{yy}} \frac{d^2 w}{dx^2} = 0$$

(2.48)

$$E_{xx}{}^b = \frac{12}{h^3 D_{11}{}^*} = \frac{b}{I_{yy} D_{11}{}^*}, I_{yy} = \frac{bh^3}{12}$$

(2.49)

If it is integrated, Equation (2.48) twice with respect to x, it is obtained Equation (2.50)

$$\frac{d^2 w}{dx^2} + \frac{bP}{E_{xx}{}^b I_{yy}} w = K_1 x + K_2$$

(2.50)

The general solution of Equation (2.48) gives Equation (2.51):

$$w(x) = c_1 \sin \lambda_b x + c_2 \cos \lambda_b x + c_3 x + c_4$$

(2.51)

where,

$$\lambda_b = \sqrt{\frac{bP}{E_{xx}{}^b I_{yy}}}, c_3 = \frac{K_1}{\lambda_b^2}, c_4 = \frac{K_2}{\lambda_b^2}.$$

(2.52)

The constants c_1 and c_2 can be detected using the boundary conditions of the beam. It is interested in obtaining the values of λ_b for which there exists a nonzero solution $w(x)$, namely, when beam experiences deflection. Once such a λ_b is noticed, it is determine the buckling load from Equation (2.52).

$$P = (\frac{E_{xx}{}^b I_{yy}}{b})\lambda_b{}^2 \tag{2.53}$$

The critical buckling load is the smallest value of P, which is given by the smallest value of λ_b. It is given by $w(x)$ the buckling shape or buckling mode. In the following, to determine λ_b and the critical buckling load for each of beam it is considered beams with different boundary conditions (Reddy, 1997).

2.2.3.1.1 Simply Supported Beam

For a simply supported beam, the boundary conditions are written following equations (Reddy, 1997):

$$w_0(0) = 0, w_0(a) = 0, \tag{2.54a}$$

$$M_{xx}(0) = \frac{d^2w}{dx^2}(0) = 0, M_{xx}(a) = \frac{d^2w}{dx^2}(a) = 0. \tag{2.54b}$$

When boundary conditions for simply supported beam are written Equation (2.51), it is obtained following equations:

$$w(0) = 0 \Rightarrow c_2 + c_4 = 0$$

$$w''(0) = 0 \Rightarrow -c_2\lambda_b{}^2 = 0 \Rightarrow c_2 = 0, c_4 = 0$$

$$w(a) = 0 \Rightarrow c_1 \sin \lambda_b a + c_3 a = 0$$

$$w''(a) = 0 \Rightarrow c_1 \sin \lambda_b a = 0 \Rightarrow c_3 = 0. \tag{2.55}$$

For a nontrivial solution, the condition is

$$c_1 \sin \lambda_b a = 0 \Rightarrow \lambda_b a = n\pi, n = 1,2,\ldots . \qquad (2.56)$$

And the buckling load is written by Equation (2.57):

$$bP = E_{xx}{}^b I_{yy} (\frac{n\pi}{a})^2 . \qquad (2.57)$$

The buckling mode is

$$w(x) = c_1 \sin \frac{n\pi x}{a}, c_1 \neq 0 . \qquad (2.58)$$

When $n=1$, the critical buckling load becomes

$$P_{cr} = \left(\frac{\pi}{a}\right)^2 \frac{E_{xx}{}^b I_{yy}}{b} = \frac{\pi^2}{12} \frac{E_{xx}{}^b h^3}{a^2} \qquad (2.59)$$

and the buckling mode or eigenfunction associated with it is

$$w(x) = c_1 \sin \frac{\pi x}{a} \qquad (2.60)$$

2.2.3.1.1 Clamped Beam

When the beam is fixed at both ends, the boundary conditions are (Reddy, 1997) written following equations:

$$w_0(0) = 0, w_0(a) = 0, \frac{dw}{dx}(0) = 0, \frac{dw}{dx}(a) = 0 . \qquad (2.61)$$

When boundary conditions for clamped beam are written in Equation (2.51), it is obtained following equations:

$$w(0) = 0 \Rightarrow c_2 + c_4 = 0$$

$$w'(0) = 0 \Rightarrow c_1 \lambda_b + c_3 = 0$$

$$w(a) = 0 \Rightarrow c_1 \sin \lambda_b a + c_2 \cos \lambda_b a + c_3 a + c_4 = 0$$

$$w'(a) = 0 \Rightarrow c_1 \lambda_b \cos \lambda_b a - c_2 \lambda_b \sin \lambda_b a + c_3 = 0 \tag{2.62}$$

It is obtained using Equations (2.62),

$$c_1 (\sin \lambda_b a - \lambda_b a) + c_2 (\cos \lambda_b a - 1) = 0 \tag{2.63}$$

$$c_1 (\cos \lambda_b a - 1) - c_2 \sin \lambda_b a = 0. \tag{2.64}$$

For a nontrivial solution, it must be zero the determinant of the coefficient matrix of the above two equations,

$$\begin{vmatrix} \sin \lambda_b a - \lambda_b a & \cos \lambda_b a - 1 \\ \cos \lambda_b a - 1 & -\sin \lambda_b a \end{vmatrix} = 0$$

It is obtained following equation if it is calculated above determinant:

$$\lambda_b a \sin \lambda_b a + 2 \cos \lambda_b a - 2 = 0. \tag{2.65}$$

The solution of the Equation (2.65), known as the characteristic equation, gives the eigenvalues $\lambda_b a$ and the buckling load is calculated from Equation (2.52). The critical buckling load is obtained followed (Reddy, 1997):

$$P_{cr} = \left(\frac{2\pi}{a}\right)^2 \frac{E_{xx}{}^b I_{yy}}{b} = \left(\frac{\pi^2}{3}\right) \frac{E_{xx}{}^b h^3}{a^2} \tag{2.66}$$

2.2.3.1.1 Clamped-Free Beam

When the beam is clamped-free, the boundary conditions are written following equations (Reddy, 1997):

$$w_0(0) = 0, Q_x(a) = 0, \frac{dw}{dx}(0) = 0, \frac{d^2w}{dx^2}(a) = 0 .$$ (2.67)

When boundary conditions for clamped-free beam are written in Equation (2.51), it is obtained following equations:

$$\frac{d^3w}{dx^3} + \lambda_b^2 \frac{dw}{dx} = 0 \Rightarrow x = a$$ (2.68)

The critical buckling load is also obtained followed equation:

$$P_{cr} = \left(\frac{\pi}{2a}\right)^2 \frac{E_{xx}^b I_{yy}}{b} = \left(\frac{\pi^2}{48}\right) \frac{E_{xx}^b h^3}{a^2} .$$ (2.69)

Table 2.1 The constants and eigenvalues for buckling of laminated composite beams with various boundary conditions (Reddy, 1997)

End Conditions at $x=0$ and $x=a$	Constants $w(x) = c_1 \sin \lambda_b x + c_2 \cos \lambda_b x + c_3 x + c_4$	Characteristic Equation
Hinged-Hinged	$c_1 \neq 0, c_2 = c_3 = c_4 = 0$	$\sin \lambda_n a = 0 \Rightarrow \lambda_n a = n\pi$
Fixed-Fixed	$c_1 = \dfrac{1}{(\sin \lambda_n a - \lambda_n a)}, c_3 = \dfrac{-1}{\lambda_n}$ $c_2 = -c_4 = \dfrac{1}{(\cos \lambda_n a - 1)}$	$\lambda_n a \sin(\lambda_n a) = 2(1 - \cos \lambda_n a)$ $\lambda_n a = 2\pi; 8,987; 4\pi, ...$
Fixed-Free	$c_1 = c_3 = 0$ $c_2 = -c_4 \neq 0$	$\cos \lambda_n a = 0$ $\lambda_n a = \dfrac{(2n-1)\pi}{2}$
Free-Free	$c_1 = c_3 = 0$ $c_2 \neq 0, c_4 \neq 0$	$\sin \lambda_n a = 0$ $\lambda_n a = n\pi$
Hinged-Fixed	$c_1 = \dfrac{1}{\lambda_n a \cos(\lambda_n a)}, c_3 = -1$ $c_2 = c_4 = 0$	$\tan \lambda_n a = \lambda_n a$ $\lambda_n a = 4,493; 7,725, ...$

It is contained governing equations in Table 2.1 for various boundary conditions. In addition, from this table, it is calculated critical buckling load for different end conditions.

2.2.3.2 First –Order Shear Deformation Theory

The first shear deformation theory known as Timoshenko beam theory. In the absence of in-plane forces, the first shear deformation theory constitutive equations for symmetric laminates are presented by (Reddy, 1997):

$$\begin{Bmatrix} M_{xx} \\ M_{yy} \\ M_{xy} \end{Bmatrix} = \begin{bmatrix} D_{11} & D_{12} & D_{16} \\ D_{12} & D_{22} & D_{26} \\ D_{16} & D_{26} & D_{66} \end{bmatrix} \begin{Bmatrix} \dfrac{\partial \phi_x}{\partial x} \\ \dfrac{\partial \phi_y}{\partial y} \\ \dfrac{\partial \phi_x}{\partial y} + \dfrac{\partial \phi_y}{\partial x} \end{Bmatrix}. \tag{2.70}$$

$$\begin{Bmatrix} Q_y \\ Q_x \end{Bmatrix} = K \begin{bmatrix} A_{44} & A_{45} \\ A_{45} & A_{55} \end{bmatrix} \begin{Bmatrix} \dfrac{\partial w}{\partial y} + \phi_y \\ \dfrac{\partial w}{\partial x} + \phi_x \end{Bmatrix} \tag{2.71}$$

or inverse form, it is written Equation (2.72):

$$\begin{Bmatrix} \dfrac{\partial \phi_x}{\partial x} \\ \dfrac{\partial \phi_y}{\partial y} \\ \dfrac{\partial \phi_x}{\partial y} + \dfrac{\partial \phi_y}{\partial x} \end{Bmatrix} = \begin{bmatrix} D^*_{11} & D^*_{12} & D^*_{16} \\ D^*_{12} & D^*_{22} & D^*_{26} \\ D^*_{16} & D^*_{26} & D^*_{66} \end{bmatrix} \begin{Bmatrix} M_{xx} \\ M_{yy} \\ M_{xy} \end{Bmatrix}. \tag{2.72}$$

It is also written Q_x, Q_y transverse force resultants following equation with Equation (2.74):

$$\begin{Bmatrix} \dfrac{\partial w}{\partial y} + \phi_y \\ \dfrac{\partial w}{\partial x} + \phi_x \end{Bmatrix} = \dfrac{1}{K} \begin{bmatrix} A^*_{44} & A^*_{45} \\ A^*_{45} & A^*_{55} \end{bmatrix} \begin{Bmatrix} Q_x \\ Q_y \end{Bmatrix} \tag{2.73}$$

where K is the shear correction coefficient, A^*_{ij} (i, j=4,5) express elements of the inverse of matrix of A, ϕ_x and ϕ_y are the rotation functions.

$$A^*_{44} = \frac{A_{55}}{A}, A^*_{55} = \frac{A_{44}}{A}, A^*_{45} = -\frac{A_{45}}{A}, A = A_{44}A_{55} - A_{45}A_{45} \qquad (2.74)$$

$$A_{ij} = \bar{Q}_{ij} h, \ A_{44} = G_{23}, A_{55} = G_{13} \qquad (2.75)$$

It is also written following equation for rotation functions:

$$\frac{\partial \phi_x}{\partial x} = D^*_{11}M_{xx}, \frac{\partial w}{\partial x} + \phi_x = \frac{A^*_{55}}{K}Q_x \qquad (2.76$$

It is obtained Equations (2.77) and (2.78) from Equation (2.71) and (2.72):

$$M(x) = E_{xx}^b I_{yy} \frac{\partial \phi_x}{\partial x}, M(x) = bM_{xx}, E_{xx}^b = \frac{12}{D^*_{11}h^3} \qquad (2.77)$$

$$Q(x) = KG_{xz}^b bh(\frac{\partial w}{\partial x} + \phi_x), Q(x) = bQ_x, G_{xz}^b = \frac{1}{A^*_{55}h}. \qquad (2.78)$$

According to first order shear deformation theory, the governing equations of buckling under compressive loads P are written Equations (2.79) and (2.80) (Reddy, 1997):

$$KG_{xz}^b bh(\frac{d^2w}{dx^2} + \frac{d\aleph}{dx}) + bP\frac{d^2w}{dx^2} = 0 \qquad (2.79)$$

$$E_{xx}^b I_{yy} \frac{d^2\aleph}{dx^2} - KG_{xz}^b bh(\frac{dw}{dx} + \aleph) = 0$$

$$\qquad (2.80)$$

$$\left(M_{xx} = \frac{d^2w}{dx^2} = \frac{d\aleph}{dx} \right)$$

If it is solved Equation (2.79) it is obtained Equation (2.81):

$$KG_{xz}{}^{b}bh\frac{d\aleph}{dx} = -(KG_{xz}{}^{b}bh - bP)\frac{d^2w}{dx^2}. \tag{2.81}$$

When Equation (2.81) integrated according to x it is obtained Equations (2.87) with Equations (2.83), (2.84), (2.85) and (2.86):

$$KG_{xz}{}^{b}bh\aleph(x) = -(KG_{xz}{}^{b}bh - bP)\frac{dw}{dx} + K_1 \tag{2.82}$$

$$\frac{d^2w}{dx^2} + \lambda^2 w + \frac{\lambda^2}{bP}(K_1 x + K_2) = 0 \tag{2.83}$$

$$E_{xx}{}^{b}I_{yy}\frac{d^3\aleph}{dx^3} - KG_{xz}{}^{b}bh(\frac{d^2w}{dx^2} + \frac{d\aleph}{dx}) = 0. \tag{2.84}$$

$$-E_{xx}{}^{b}I_{yy}\frac{d^2}{dx^2}\left[\left(1 - \frac{bP}{KG_{xz}{}^{b}bh}\right)\frac{d^2w}{dx^2}\right] \tag{2.85}$$

$$-KG_{xz}{}^{b}bh\left[\frac{d^2w}{dx^2} - \left(1 - \frac{bP}{KG_{xz}{}^{b}bh}\right)\frac{d^2w}{dx^2}\right] = 0 \tag{2.86}$$

$$E_{xx}{}^{b}I_{yy}(1 - \frac{bP}{KG_{xz}{}^{b}bh})\frac{d^4w}{dx^4} + bP\frac{d^2w}{dx^2} = 0 \tag{2.87}$$

The general solution of Equation (2.87) is obtained following equation with Equation (2.89):

$$w(x) = c_1 \sin \lambda x + c_2 \cos \lambda x + c_3 x + c_4 \qquad (2.88)$$

and

$$c_3 = -\frac{1}{bP}K_1, c_4 = -\frac{1}{bP}K_2 \qquad (2.89)$$

where

$$\lambda^2 = \frac{bP}{\left(1 - \dfrac{bP}{KG_{xz}{}^b bh}\right)E_{xx}{}^b I_{yy}} \; or \; bP = \frac{\lambda^2 E_{xx}{}^b I_{yy}}{\left(1 - \dfrac{\lambda^2 E_{xx}{}^b I_{yy}}{KG_{xz}{}^b bh}\right)} \qquad (2.90)$$

The constants c_1 and c_4 can be detected using the boundary conditions of the beam. The critical buckling load is obtained with Equation (2.90).

2.2.3.2.1 Simply Supported Beam

For a simply supported beam, the boundary conditions are expressed the following equations (Reddy, 1997):

$$w(0) = 0, w(a) = 0,$$

$$M_{xx}(0) = \frac{d^2 w}{dx^2}(0) = \frac{d\aleph}{dx}(0) = 0, M_{xx}(a) = \frac{d^2 w}{dx^2}(a) = \frac{d\aleph}{dx}(a) = 0 \;.$$

$$(2.91)$$

When boundary conditions for simply supported beam are written in Equation (2.88), it is obtained following equations:

$$w(0) = 0 \Rightarrow c_2 + c_4 = 0$$

$$w''(0) = 0 \Rightarrow -c_2\lambda^2 = 0 \Rightarrow c_2 = 0, c_4 = 0$$

$$w(a) = 0 \Rightarrow c_1 \sin \lambda a + c_3 a = 0$$

$$w''(a) = 0 \Rightarrow c_1 \sin \lambda a = 0 \Rightarrow c_3 = 0 \tag{2.92}$$

It is obtained $c_2=c_3=c_4=0$ and $c_1 \neq 0$ from Equation (2.92). For this reason, it is obtained Equation (2.93):

$$c_1 \neq 0 \Rightarrow \sin \lambda a = 0 \Rightarrow \lambda a = n\pi . \tag{2.93}$$

The critical buckling load is obtained followed equation:

$$\lambda^2 = \frac{bP}{\left(1 - \dfrac{bP}{KG_{xz}{}^b bh}\right) E_{xx}{}^b I_{yy}}$$

From this equation, it is written bP following equations:

$$bP = \lambda^2 E_{xx}{}^b I_{yy}\left(1 - \frac{bP}{KG_{xz}{}^b bh}\right) \Rightarrow bP\left(1 - \frac{\lambda^2 E_{xx}{}^b I_{yy}}{KG_{xz}{}^b bh}\right) = \lambda^2 E_{xx}{}^b I_{yy}$$

$$\tag{2.94}$$

$$bP = \frac{\lambda^2 E_{xx}{}^b I_{yy}}{\left(1 - \dfrac{\lambda^2 E_{xx}{}^b I_{yy}}{KG_{xz}{}^b bh}\right)} \tag{2.95}$$

When Equation (2.95) is rearranged, it is obtained Equation (2.98)

$$bP = \frac{\left(\lambda^2 E_{xx}{}^b I_{yy}\right)\left(KG_{xz}{}^b bh\right)}{\left(KG_{xz}{}^b bh - \lambda^2 E_{xx}{}^b I_{yy}\right)} \tag{2.96}$$

$$bP = \left(\frac{n\pi}{a}\right)^2 E_{xx}{}^b I_{yy} \frac{KG_{xz}{}^b bh}{\left(KG_{xz}{}^b bh - \left(\frac{n\pi}{a}\right)^2 E_{xx}{}^b I_{yy}\right)} \tag{2.97}$$

$$bP = \left(\frac{n\pi}{a}\right)^2 E_{xx}{}^b I_{yy}\left[1 - \frac{\left(\frac{n\pi}{a}\right)^2 E_{xx}{}^b I_{yy}}{KG_{xz}{}^b bh + \left(\frac{n\pi}{a}\right)^2 E_{xx}{}^b I_{yy}}\right] \tag{2.98}$$

The critical buckling load is given for $n=1$. It is obtained Equation (2.100) using Equations (2.98) and (2.99) for $n=1$:

$$bP_{cr} = \left(\frac{\pi}{a}\right)^2 E_{xx}{}^b I_{yy}\left[1 - \frac{\left(\frac{\pi}{a}\right)^2 E_{xx}{}^b I_{yy}}{KG_{xz}{}^b bh + \left(\frac{\pi}{a}\right)^2 E_{xx}{}^b I_{yy}}\right] \tag{2.99}$$

$$P_{cr} = \left(\frac{\pi}{a}\right)^2 E_{xx}{}^b \frac{I_{yy}}{b}\left[1 - \frac{\left(\frac{\pi}{a}\right)^2 E_{xx}{}^b I_{yy}}{KG_{xz}{}^b bh + \left(\frac{\pi}{a}\right)^2 E_{xx}{}^b I_{yy}}\right]. \tag{2.100}$$

As shown in results, it is obvious that shear deformation has the effect of decreasing the buckling load.

2.2.3.2.2 Clamped Beam

When the beam is fixed at both ends, the boundary conditions are written as follows:

$$w(0) = 0, w(a) = 0, \frac{dw}{dx}(0) = \aleph(0) = 0, \frac{dw}{dx}(a) = \aleph(a) = 0 \,. \tag{2.101}$$

When boundary conditions for clamped beam are written in Equation (2.88), it is obtained following equations:

$$w(0) = 0 \Rightarrow c_2 + c_4 = 0$$

$$w(a) = 0 \Rightarrow c_1 \sin \lambda a + c_2 \cos \lambda a + c_3 a + c_4 = 0$$

$$KG_{xz}{}^b bh \aleph(0) = -(KG_{xz}{}^b bh - bP)\frac{dw}{dx} + K_1 \Rightarrow K_1 = -c_3(bP)$$

$$\left(KG_{xz}{}^b bh - bP\right)(c_1\lambda + c_3) = -c_3 bP$$

$$(KG_{xz}{}^b bh - bP)c_1\lambda + (KG_{xz}{}^b bh - bP)c_3 + c_3 bP = 0$$

$$(KG_{xz}{}^b bh - bP)c_1\lambda + (KG_{xz}{}^b bh - bP + bP)c_3 = 0$$

$$c_3 + c_1\lambda \frac{(KG_{xz}{}^b bh - bP)}{KG_{xz}{}^b bh} = 0$$

$$c_3 + c_1\lambda \left[1 - \frac{bP}{KG_{xz}{}^b bh}\right] = 0$$

$$c_3 + \left(1 - \frac{bP}{KG_{xz}{}^b bh}\right)(\lambda c_1 \cos \lambda a - \lambda c_2 \sin \lambda a) = 0$$

$$2(\cos \lambda a - 1)\left(1 + \frac{\lambda^2 E_{xx}{}^b I_{yy}}{KG_{xz}{}^b bh}\right) + \lambda a \sin \lambda a = 0 \qquad (2.102)$$

Because the value of λa is obtained by solving the non-linear equation (2.102), it is readily determined the critical buckling load from Equation (2.89) (Reddy, 1997).

CHAPTER THREE

THEORETICAL DEVELOPMENT OF BUCKLING FOR VARIABLE CROSS-SECTIONS

3.1 Buckling Optimization

3.1.1 General

Structural use of composite materials have always been extensively used in the aeronautical industry, civil engineering appliations because of their strength-to-weigth and stiffness-to-weight ratios, incresingly low fabrication costs and an efficient behaviour under environmental conditions. Consequently, the structural use of composite materials are developing in areas where weight saving is most benefical. On the other hand, when the thin-walled composite material is subjected to in-plane compressive forces, the study of structural instability becomes essential for a safely design. In this case, the buckling strength could be main factor for the optimum design of composites

Structural optimization produces a significantly superior design than the conventional trial and error approach according to today's timing and budget constraints. It can be categorized structural optimization problems: Sizing/shape optimization and topology optimization. Topology optimization does not need an initial design as input. Given a specified region, loads and boundary conditions, the most structurally efficient material layout is detected. The traditional structural optimization mainly deals with geometry optimization problems. However, topology optimization has drawn more and more attentions recently (Gea & Luo, 2001).

It is called the objective function as the property of the structure to be minimized or maximized (weigth, cost, stiffness, strength, etc.).The objective function depends on a number of parameters called design variables, such as dimensional parameters and material properties; each design variable is defined within a particular range. All

these ranges bound a region of all possible designs; the design space. The structure to be optimized is typically subjected to some constraints, such as maximum weight, minimum stiffness, etc. The constraints set boundaries to the design space, thus specifying the feasible space, a space of all possible designs, which do not violate the constraints.

Many optimization techniques have been proposed to analyze problems ranging from structural to financial. Each technique has its advantages and disadvantages. There is no general rule to determine whether a particular technique is best suited to a given class of problems. It is the designer's task to select a method or a combination of methods based on experience, common sense and the characteristics of the problem. Moreover, the way the constraint requirements are treated is often decisive to the optimization procedure.

3.1.2   Formulation of Optimization Problem

A typical procedure in the search for the optimal design begins with the selection of an initial design; this is arbitrary but must be within the design space. Then, it is specified a search direction starting from this design and the minimum of the objective function in this direction is sought; such a minimizing point is called an intermediate design. This process is repeated until a minimum of the objective function is found (Filho, 1997).

The design of composite structures is complicated by the wide variety of matrix and fibre reinforcement materials available, the potential of stress concentrations, thermal residual stresses from the manufacturing process, the choice of ply thicknesses and number of plies and the spatial variation of ply orientation. Other design variables related to the structure topology and geometry are also often considered. In the design of structural components, a compromise between cost, performance and suitability is sought while satisfying prescribed requirements such as strength, maximum displacements allowed in certain regions, stress, strain limits, critical buckling load, size and esthetics. Whenever several feasible designs are available, a comparison between them must be carried out in order to determine

which one is the best. The comparison procedure is referred to as optimization; it is computationally expensive and time consuming, hence it requires the use of efficient methods and heavy computer processing (Faria 2000).

Optimum design of structures against buckling may be achieved by finding the minimum weight structure that satisfies a buckling load constraint. Alternatively, it may be to maximise the fundamental buckling load for a structure with a given volume or weight. In the proposed method, buckling load factor is maximised for constant structural weight. During the optimisation process, the main task is to raise the lowest buckling eigenvalue.

It is rapidly structural optimization becoming an integral part of the product design process. Optimization problems are formulated as the maximization of the smallest eigenvalue, which is single or multiple, subject to a global constraint of given total volume of material of the structure. Multiple eigenvalues in the form of buckling loads often happen in complex structures. For example, stiffner-reinforced thin walled plate and shell structures have a dense spectrum of eigenvalues and it is taken part multiple eigenvalues. Symmetry of structural systems may also lead to the apperance of several linearly independent buckling modes (Seyranian, Lund & Olhoff, 1994).

It is more difficult optimisation for maximum stability when the lowest buckling eigenvalue of the problem is inherently either multimodal or it becomes multimodal because of the optimisation process. During optimisation, it is often seen that while the first eigenvalue is increasing, the subsequent eigenvalues are decreasing and gradually the first two or more eigenvalues converge to each other, although the corresponding eigenvectors may remain totaly different. One of the main problems related to repeat eigenvalues is that they are not continuously differentiable. In this reason, the eigenvectors corresponding to the repeated eigenvalues are not unique.It is constituted diffuculties in finding sensivities of repeated eigenvalues with respect to design changes and derivation of necessary optimality condition in optimisation (Manickarajah, Xie & Steven, 2000).

The main duty is to raise the lowest the buckling eigenvalue during optimisation. Because of optimisation process, the second eigenvalue may become equal to the first eigenvalue for some structures. This means a bimodal buckling situation (Manickarajah, Xie & Steven, 2000).

Structural eigenvalue problem is followed:

$$K\phi_j = \lambda_j M\phi_j, j = 1,2,........n, \tag{3.1}$$

where K and M are symmetric positive definite matrices, λ_j is the eigenvalue and ϕ_j is the corresponding eigenvector. n is the dimension of the problem, hence has n solutions composed of eigenvalues λ_j and corresponding eigenvectors ϕ_j. It is real all eigenvalues and can be ordered in the following manner:

$$0\langle\lambda_1 \le \lambda_2 \le .... \le \lambda_j \le ... \le \lambda_n \tag{3.2}$$

K and M are also smooth functions of the design variables a_i, i=1, 2,....,I.

The optimization problems are written as follows:

$$\max_{a1,...aI} \min_{j=1,2,...n} \lambda_j \tag{3.3}$$

under the constraint

$$F(a_1,...a_I)=0 \tag{3.4}$$

where F is a smooth scalar fuction of the design variables a_i, i=1,2,....I.

3.1.2.1 Single Optimum Fundamental Eigenvalue

If the optimum is acquired at the simple lowest eigenvalue λ_1 with $\lambda_1 \langle \lambda_2 \leq \lambda_3 \leq ...$ then the necessary optimality condition implies linear independence of the gradient vectors of λ_1 and F

$$\nabla \lambda_1 - \gamma_0 f_0 = 0 \tag{3.5}$$

where

$$\nabla \lambda_1 = (\phi_1^T (\frac{\partial K}{\partial a_1} - \lambda_1 \frac{\partial M}{\partial a_1})\phi_1, ..., \phi_1^T (\frac{\partial K}{\partial a_1} - \lambda_1 \frac{\partial M}{\partial a_1})\phi_1),$$

$$f_0 = \nabla F = (\frac{\partial F}{\partial a_1}, ... \frac{\partial F}{\partial a_I}), \tag{3.6}$$

Moreover, γ_0 is a Lagrangian multiplier to be determined from Equation (3.4) (Seyranian, Lund & Olhoff, 1994).

3.1.2.2 Double Optimum Fundamental Eigenvalue

When the optimum is obtained at the double lowest eigenvalue $\lambda_1 = \lambda_2$, where $\lambda_1 = \lambda_2 \langle \lambda_3 \leq ...$ this is the non-differentiable case and it must be used directional derivatives.

When the first eigenvalue becomes close to the subsequent eigenvalues, there will be interference between the first and subsequent eigenvectors. Thus, the effect on the fundamental eigenvalue due to all eigenvectors needs to be included. An eigenvalue multiplicity parameter ε is described and the multimodality of the structure is determined by the number of eigenvalues within a ε distance of the lowest

eigenvalue. If for example the distance between λ_1 and λ_2, is within a certain limit, say $\varepsilon = 5\%$ and the distance between λ_1 and λ_3 is greater than $\varepsilon = 5\%$, it may be assumed that the structure has now become bimodal (Manickarajah, Xie & Steven, 2000).

Taking the vector of varied design variables in the form $a + \varepsilon e, \|e\| = 1$, it is achieved the directional derivatives μ_1 and μ_2 from (Seyranian, Lund & Olhoff, 1994)

$$\det\begin{bmatrix} f_{11}{}^T e - \mu & f_{12}{}^T e \\ f_{12}{}^T e & f_{22}{}^T e - \mu \end{bmatrix} = 0 . \tag{3.7}$$

This is a quadratic equation in μ. It is obtained for any direction e by solving quadratic equation in μ.

$$\mu_{12} = \frac{f_{11}{}^T e + f_{11}{}^T e \pm \sqrt{(f_{11}{}^T e - f_{22}{}^T e)^2 + 4(f_{12}{}^T e)^2}}{2} \tag{3.8}$$

The necessary optimality condition for a maximum is $\min(\mu_1, \mu_2) \le 0$, for any direction e satisfying the condition $f_0{}^T e = 0$. From Equation (3.7), it is seen that if it is taken the direction as –**e**, then both μ_1 and μ_2 will change their signs to the opposite ones. This implied that if for some direction **e** both derivatives μ_1, μ_2 are negative, then the design point is not a maximum, because a change in sign of the direction e leads to $\mu_1 \rangle 0$ and $\mu_2 \rangle 0$, namely a better design. This expresses that the necessary optimality condition in the bimodal case is

$$\mu_1 \mu_2 \le 0 \tag{3.9}$$

for any admissible variation e, i.e. a variaiton tat satisfies the condition

$$f_0{}^T e = 0 . \tag{3.10}$$

It is stated using Equations (3.7) and (3.8) the necessary optimality condition of Eqution (3.9) in the form

$$(f_{11}{}^T e)(f_{22}{}^T e) - (f_{12}{}^T e)^2 \leq 0 \tag{3.11}$$

for any arbitrary direction e satisfying the condition in Equation (3.10) (Seyranian, Lund & Olhoff, 1994).

The nondimensional optimization problem composes of determining the cross-sectional area function $A(x)$, which for a given value of the foundation modulus maximizes the smallest eigenvalue,

$$\max{}_{A(x)} \min{}_{j=1,2,\dots n} \lambda_j \tag{3.12}$$

subject to the condition of given column volume,

$$\int_0^1 A(x)dx = 1 \tag{3.13}$$

If the maximized smallest eigenvalue λ_1 is simple, i.e. $\lambda_1 \langle \lambda_2 \leq \lambda_3 \leq \dots$, then the necessary optimality condition takes the form Equation (3.1) with

$$\nabla \lambda_1 = 2 A(x)(w_1{}''(x))^2 , f_0 = 1 \tag{3.14}$$

where w is the lateral deflection function. The positive real constant γ_0 in Equation (3.1) is a Lagrangian multiplier to be determined by the dimensionless volume constraint that expresses Equation (3.13).

Let us consider the bimodal case where the smallest eigenvalue $\lambda_1 = \lambda_2 \langle \lambda_3 \leq \ldots$ is associated with two linearly independent eigenfunctions the appropriate boundary conditions. If it is considered a varied cross-sectional area function in the form $A(x) + \varepsilon e(x)$, then the double eigenvalue $\lambda_1 = \lambda_2 = \tilde{\lambda}$ associated with $A(x)$ will generally split into two distinct ones,

$$\lambda_j = \tilde{\lambda} + \varepsilon \mu_j, j = 1,2 \tag{3.15}$$

It is derived the following equation for determining the two directional derivatives $\mu = \mu_1 = \Delta\lambda_1 / \Delta\varepsilon$ and $\mu = \mu_2 = \Delta\lambda_2 / \Delta\varepsilon$ of the double eigenvalue,

$$\det\left[2\int_0^1 A(x)w_s^{''}(x)w_k^{''}(x)e(x)dx - \mu\delta_{sk} \right] = 0; s, k = 1,2. \tag{3.16}$$

The boundary conditions and design function $A(x)$ are symetric, $A(x) = A(1-x)$, it is useful to inquire symetric and antisymetric eigenfunctions $w_1(x) = w_1(1-x)$ and $w_2(x) = -w_2(1-x)$ in Equation (3.16). Because the arbitrary direction function $e(x)$ must be symetric along with $A(x)$, it is seen that the mixed term in Equation (3.16) vanishes:

$$2\int_0^1 A(x)w_1^{''}(x)w_2^{''}(x)e(x)dx = 0 \tag{3.17}$$

because integrang will be antisymetric for any arbitrary admissible function $e(x)$. The following equation is simple expressions for the directional derivatives of the double eigenvalue:

$$\mu_1 = 2\int_0^1 A(x)\left[w_1''(x)\right]^2 e(x)dx \tag{3.18}$$

$$\mu_2 = 2\int_0^1 A(x)\left[w_2''(x)\right]^2 e(x)dx \tag{3.19}$$

These expressions hold when the double eigenvalue can be treated as an intersection of two differentiable functionals, and are identical to those resulting from purely single modal formulations. However, in the general case of non-symetric boundary conditions and designs, the mixed term in Equation (3.17) does not vanish (Seyranian, Lund & Olhoff, 1994).

3.2 Tadjbaksh & Keller's Solution

Herein, the optimization problem for columns with clamped ends is represented according to Tadjbakhsh & Keller (1962).

Let us consider a thin, straight and elastic column with variable cross sections defined by the area $A(x)$ and the moment of inertia $I(x)$. As shown in Figure 3.1, the section of a given column is deflected under compressive load. The equilibrium of moments is arranged, with bending moment $M_y(x)$, deflection $w(x)$ and compressive load P parallel to the x-axis, as follows:
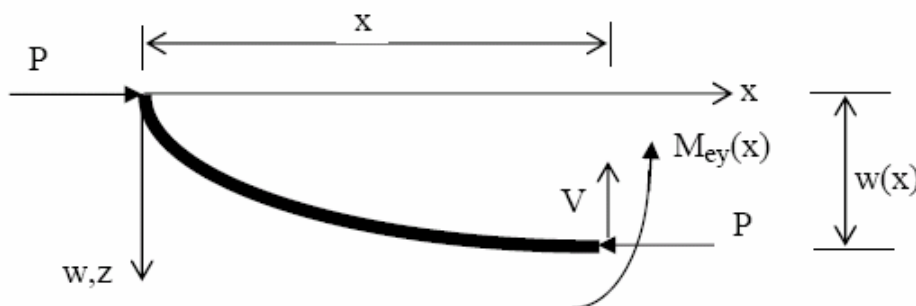
$$M_y(x) = Pw(x)\,. \tag{3.20}$$

Figure 3.1 Cross-section of the column under compressive load

With the minimum moment of inertia $I(x)$ of the cross-section and with the second derivative of the deflection function $w''(x)$, the bending moment follows from the equation of the elastic curve to:

$$M_y(x) = - EI(x)w''(x) .$$ (3.21)

If the Equations (3.20) and (3.21) are equated to each other and differentiated twice according to x, the generally valid differential equation of the problem is obtained as follows:

$$[-EI(x)w''(x)]'' - Pw''(x) = 0 .$$ (3.22)

It will be assumed that the cross-section planes of the column cannot be deformed. Consequently, the following relationship between the area moments of inertia and the areas yields according to Tadjbakhsh and Keller (1962):

$$I(x) = \alpha A^2(x) .$$ (3.23)

In Equation (3.23) the proportionality factor of the cross-section (α) depends on the cross-section form. Table 3.1 gives the three different cross-section forms.

Table 3.1 Form coefficient values of different cross-sections

Cross-section Form α	Square shaped cross-sections	Cross-sectional of circular shape	Isosceles triangle cross-sections
Form coefficient c	$\dfrac{1}{12}$	$\dfrac{1}{4\pi}$	$\dfrac{\sqrt{3}}{18}$

As *w(x)* expresses the lateral deflection from its straight position, the equation of equilibrium is followed equation:

$$- M_{xx} + P w_{xx} = 0$$

If the expression (3.23) is put into the differential Equation (3.22), it is obtained following equations:

$$-\left[- E\alpha A^2(x) w_{xx}\right]'' + P w_{xx} = 0 \tag{3.24}$$

$$E\alpha\left[A^2(x) w''(x)\right]'' + P w''(x) = 0 \tag{3.25}$$

It is introduced the following variables ς and the new independent function $\phi(\xi)$ as well as the abbreviation λ to solve differential equations:

$$\varsigma = x/L, \tag{3.26}$$

$$\phi(\varsigma) = L^2 A^2(\xi L) w''(\varsigma L), \tag{3.27}$$

$$\lambda = \frac{PL^2}{E\alpha}, \tag{3.28}$$

Equation (3.25) is obtained with variable transformation, in which the differentiated terms $\dot{\phi}$ and $\ddot{\phi}$ denote $\dot{\phi}(\varsigma) = \dfrac{d\phi}{d\varsigma}$ and $\ddot{\phi}(\varsigma) = \dfrac{d^2\phi}{d\varsigma^2}$, respectively:

$$E\alpha\left[\frac{\phi(\varsigma)}{L^2}\right]'' + P\frac{\phi(\varsigma)}{L^2 A^2(\varsigma L)} = 0$$

$$\frac{E\alpha}{L^2}\left[\phi(\varsigma)\right]'' + \frac{P}{L^2 A^2(\varsigma L)}\phi(\varsigma) = 0$$

It is written following equations, if it is made transformation of variation such as, $x = \varsigma L \Rightarrow \dfrac{d\varsigma}{dx} = \dfrac{1}{L}$:

$$\frac{E\alpha}{L^2}\left[\frac{d\phi(\varsigma)}{dx}\right]' + P\frac{\phi(\varsigma)}{L^2 A^2(\varsigma L)} = 0$$

$$\frac{E\alpha}{L^2}\left[\frac{d\phi}{d\varsigma}\frac{d\varsigma}{dx}\right]' + \frac{P\phi(\varsigma)}{L^2 A^2(\varsigma L)} = 0 \, ,$$

$$\frac{E\alpha}{L^2}\left[\frac{d\phi}{d\varsigma}\frac{1}{L}\right]' + \frac{P\phi(\varsigma)}{L^2 A^2(\varsigma L)} = 0 \, ,$$

$$\frac{E\alpha}{L^2}\frac{1}{L}\frac{d}{dx}(\frac{d\phi}{d\varsigma}) + \frac{P\phi(\varsigma)}{L^2 A^2(\varsigma L)} = 0 \, ,$$

$$\frac{E\alpha}{L^2}\frac{1}{L}\frac{d}{d\varsigma}\frac{d\varsigma}{dx}(\frac{d\phi}{d\varsigma}) + \frac{P\phi(\varsigma)}{L^2 A^2(\varsigma L)} = 0$$

$$\frac{E\alpha}{L^2}\frac{1}{L}\frac{1}{L}\frac{d}{d\varsigma}(\frac{d\phi}{d\varsigma}) + \frac{P\phi(\varsigma)}{L^2 A^2(\varsigma L)} = 0$$

$$\frac{E\alpha}{L^4}\frac{d^2\phi}{d\varsigma^2} + \frac{P}{L^2 A^2(\varsigma L)}\phi(\varsigma) = 0$$

$$\frac{d^2\phi}{d\varsigma^2} + \frac{P}{L^2 A^2(\varsigma L)}\frac{L^4}{E\alpha}\phi(\varsigma) = 0$$

$$\frac{d^2\phi}{d\varsigma^2} + \frac{\lambda}{A^2(\varsigma L)}\phi(\varsigma) = 0\,.$$

Consequently, it is obtained Equation (3.29):

$$\phi_{\varsigma\varsigma}(\varsigma) + \lambda A^{-2}\phi(\varsigma) = 0\,. \qquad (3.29)$$

The problem is now that of solving above equation, i.e. Equation (3.29), for ϕ subject to boundary conditions. This problem will have a nontrivial solution only if λ is an eigenvalue (Tadjbaksh & Keller, 1962).

It is rewritten Equation (3.29) using Equation (3.27):

$$\phi(\varsigma) = L^2 A^2(\varsigma L)w''(\varsigma L) \Rightarrow \phi(\varsigma)A^{-2}(\varsigma L) = L^2 w''(\varsigma L) \qquad (3.30)$$

$$\phi_{\varsigma\varsigma}(\varsigma) + \lambda A^{-2}\phi(\varsigma) = 0 \Rightarrow \phi_{\varsigma\varsigma}(\varsigma) + \lambda L^2 w''(\varsigma L) \qquad (3.31)$$

It is taken infinitesimal elements to obtain conditions with respect to different supported types. The free body diagram of the infinitesimal element of lenght *ds* is shown in Figure 3.2.
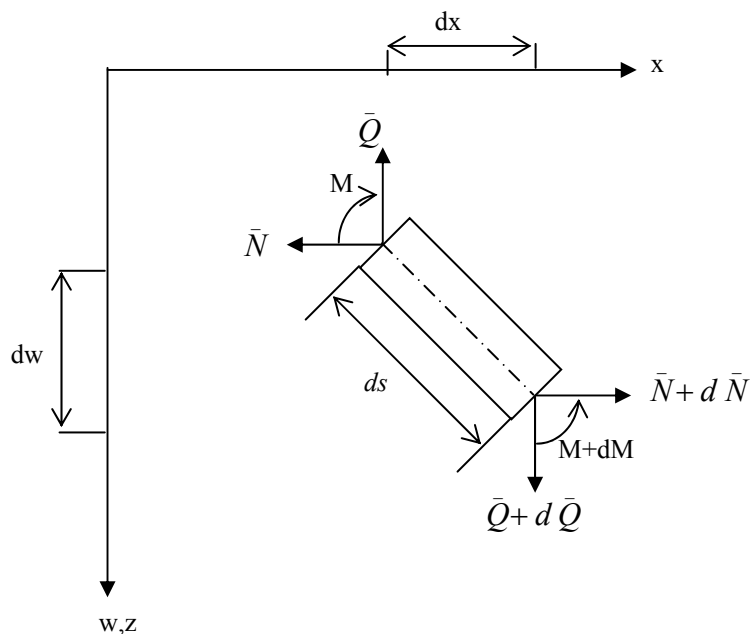

Figure 3.2 Free-body diagram of infinitesimal element

Accordingly, by equilibrium, it is written following equations:

$$\sum F_x = 0 \Rightarrow \bar{N} + d\bar{N} - \bar{N} = 0 \Rightarrow d\bar{N} = 0 \Rightarrow N = c_1$$

$$\sum F_z = 0 \Rightarrow \bar{Q} + d\bar{Q} - \bar{Q} = 0 \Rightarrow d\bar{Q} = 0 \Rightarrow \bar{Q} = c_2$$

$$\sum M = 0 \Rightarrow M + dM - M + \bar{N}.dw - \bar{Q}.dx = 0$$

$$\frac{dM}{dx} + \bar{N}\frac{dw}{dx} - \bar{Q} = 0 \Rightarrow \bar{Q} = \frac{dM}{dx} + \bar{N}\frac{dw}{dx}.$$

In this way, it is obtained Equation (3.32) for $Q(x)$:

$$\bar{Q} \approx Q(x) = \frac{dM}{dx} - P\frac{dw}{dx}.$$

(3.32)

Using Equation (3.23) in Equation (3.32), it yields,

$$Q(x) = -\left[EI'(x)w''(x) + EI(x)w'''(x) + Pw'(x)\right].$$

(3.33)

Using Equation (3.25) in Equation (3.27), it is written,

$$A^{-2}\phi = L^2 w_{xx}(\varsigma L)$$

$$w_{xx}(\varsigma L) = \frac{-1}{\lambda L^2}\phi_{\varsigma\varsigma}.$$

(3.34)

It is also derived Equation (3.35) from Equation (3.34) to obtain third derivative of the deflection function, $w'''(\varsigma)$.

$$w'''(\varsigma) = \frac{-1}{L^2 A_0^{\frac{1}{2}}} \frac{\cos\theta(\varsigma)}{\sin^2\theta(\varsigma)} \frac{d\theta}{d\varsigma}$$

(3.35)

It is now integrated Equation (3.35) once with respect to ς from:

$$\int_0^x w_{xx}(\varsigma L)dx = \frac{-1}{\lambda L^2}\int_0^x \phi_{\varsigma\varsigma}dx.$$

If it is made transformation of variation ($\varsigma = x/L$) in this integral, it is obtained following equations:

$$\int_0^\varsigma w_{xx}(\varsigma L)Ld\varsigma = \frac{-1}{\lambda L^2}\int_0^\varsigma \phi_{\varsigma\varsigma}Ld\varsigma$$

This integral is equal to Equation (3.36):

$$w_x(\varsigma L)\mid_{\varsigma=0}^\varsigma = \frac{-1}{\lambda L^2}L(\phi_\varsigma\mid_{\varsigma=0}^\varsigma)$$

$$w_x(\varsigma L) - w_x(0) = (\lambda L)^{-1}\left[\phi_\varsigma(0) - \phi_\varsigma(\varsigma)\right]. \tag{3.36}$$

For clamped-clamped, clamped-hinged and clamped-free cases, it is $w_x(x=0)=0$ at the end $x=0$. From this, the solution of differential equation,

$$w_x(\varsigma L) = (\lambda L)^{-1}\left[\phi_\varsigma(0) - \phi_\varsigma(\varsigma)\right]. \tag{3.37}$$

It is integrated Equation (3.37) with respect to ς from $\varsigma = 0$.

$$\int_{\varsigma=0}^\varsigma w_x(\varsigma L)d\varsigma = (\lambda L)^{-1}\int_{\varsigma=0}^\varsigma \left[\phi_\varsigma(0) - \phi_\varsigma(\varsigma)\right]d\varsigma$$

$$\int_{\varsigma=0}^\varsigma \left[\frac{d\phi(0)}{d\varsigma} - \frac{d\phi(\varsigma)}{d\varsigma}\right]d\varsigma = \phi_\varsigma\varsigma - \phi(\varsigma)\mid_{\varsigma=0}^\varsigma$$

$$w(\varsigma L) - w(0) = (\lambda)^{-1}\left[\phi_\varsigma\varsigma - \phi(\varsigma) + \phi(0)\right]. \tag{3.38}$$

It is $w_x(x=L)=0$ for clamped-clamped case at the other end $x=L$,

$$w(\varsigma L) = (\lambda)^{-1}\left[\phi_\varsigma(0)\varsigma - \phi(\varsigma) + \phi(0)\right] \tag{3.39}$$

The determination of the strongest column is now deriving with following general problem. It is investigated that $A(\varsigma)$ which maximizes the smallest eigenvalue. It is searched that function $A(x)$ which maximizes the buckling load among all functions satisfying following equation:

$$\int_0^L A(x)dx = V \Rightarrow \int_0^1 A(\varsigma)d\varsigma = \frac{V}{L} \tag{3.40}$$

3.2.1 An Essential Condition for Maximum Eigenvalue of Second-Order Systems

In this section, it is considered an essential condition for maximum eigenvalue of second-order systems. This analysis is based upon the fourth-order homogeneous differential equation with homogeneous boundary conditions which expresses the equilibrium of an elastic rod in the buckled state.

Numerous systems in structural dynamics are self-adjoint with distinct eigenvalues. This expresses that such systems have symmetric properties. A self-adjoint system has real eigenvalues and eigenfuctions. In addition the eigenfunctions are orthogonal to each other. However structural systems which continue aerodynamics forces, friction forces may lose their symmetries and beceme non-self adjoint. In this reason it is no longer applicable to the self-adjoint systems orthogonal relations and the expansion theorem which have been developed on the bases of self-adjoint properties (Jung & Feeny, 2002).

With a suitable change of variables this equation is reduced to a second-order self-adjoint equation with homogeneous boundary conditions. And then it is applied variational techniques to make the first buckling load and optimum shape of the column, and it is proved that the stationary eigenvalues determined are actually maximal (Tadjbaksh & Keller, 1962).

Let $\phi(x)$ be a solution of the equation

$$\phi_{xx} + \lambda\rho(x)\phi = 0 \,, 0 \le x \le L \tag{3.41}$$

and the homogeneous boundary conditions

$$\alpha_1\phi(0) + \alpha_2\phi_x(L) + \alpha_3\phi(L) = 0 \tag{3.42}$$

$$\alpha_1\phi(L) - \alpha_2\phi_x(0) + \alpha_4\phi(0) = 0 \,. \tag{3.43}$$

It is self-adjoint system for the Equations (3.41)-(3.43), hence all the eigenvalues are real. It is searched for $\rho(x)$ which maximizes the lowest eigenvalue subject to the condition (Tadjbaksh & Keller, 1962)

$$\int_0^L \rho^n(x)dx = k \,. \tag{3.44}$$

Here n and k are given constants. For $n = \dfrac{-1}{2}, k = V$ and $\rho = A^{-2}$, it is rewritten Equation (3.44):

$$\int_0^L \rho^n(x)dx = k \Rightarrow \int_0^L A(x)dx = V \tag{3.45}$$

Let us suppose that there exists a function $\rho_0(x)$, which maximizes the lowest eigenvalue. It is presented a family of functions $\rho(x,\varepsilon)$ which depend smoothly on ε and such that $\rho(x,0) = \rho_0(x)$. Then, λ and ϕ, the lowest eigenvalue and ccorresponding eigenfunction Equations (3.41)-(3.43) with $\rho = \rho(x,\varepsilon)$ depend smoothly on ε. Therefore, it may differentiate Equations (3.41)-(3.43) with respect to ε to get,

$$\phi'_{xx} + \lambda\rho\phi' = -\rho'\lambda\phi - \lambda'\rho\phi = 0 \tag{3.46}$$

$$\alpha_1\phi'(0) + \alpha_2\phi_x^{'}(L) + \alpha_3\phi'(L) = 0 \tag{3.47}$$

$$\alpha_1\phi'(L) - \alpha_2\phi_x^{'}(0) + \alpha_4\phi'(0) = 0 \tag{3.48}$$

$$\int_0^L \rho'\rho^{n-1}dx = 0 \,. \tag{3.49}$$

Equations (3.46) and (3.48) are an inhomogeneous system for ϕ'. The correponding homogeneous system is Equations (3.41)-(3.43) which has the solution ϕ. Hence because ϕ' exists, the rigth side of Equation (3.46) must be orthogonal ϕ. At $\varepsilon = 0$, when $\lambda' = 0$ and $\rho = \rho_0$ by assumption, this orthogonality condition is

$$\lambda\int_0^L \rho'\phi^2 dx = 0 \tag{3.50}$$

If $\lambda \neq 0$, Equation (3.50) shows that ϕ^2 is orthogonal to every functon ρ' that is orthogonal to ρ^{n-1}, according to Equation (3.49). Therefore ϕ^2 must be proportional to ρ^{n-1}. Because ϕ is the solution of a homogeneous problem it may be multiplied by a constant which makes the proportionality factor become unity (Tadjbaksh & Keller, 1962). Consequently, it is followed as a necessary condition for a maximum, the relation

$$\phi^2 = \rho^{n-1} \tag{3.51}$$

when $n = \dfrac{-1}{2}$ and $\rho = A^{-2}$ this relation get $\phi^2 = A^3$.

To obtain ϕ, ρ and λ satisfiying Equations (3.41)-(3.44) and Equation (3.51) it is proceeded by using Equation (3.51) to eliminate ρ from Equation (3.41). Then Equation (3.41) becomes,

$$\phi_{xx} + \lambda \phi^{1+(2/ n-1)} = 0 \tag{3.52}$$

Upon multiplying Equation (3.52) by ϕ_x and integrating, it is obtained:

$$2\frac{d^2\phi}{dx^2}\frac{d\phi}{dx} + 2\lambda\phi^{1+\frac{2}{n-1}}\frac{d\phi}{dx} = 0$$

$$2\int \frac{d^2\phi}{dx^2}\frac{d\phi}{dx}dx + 2\lambda\int \phi^{1+\frac{2}{n-1}}\frac{d\phi}{dx}dx = 0$$

$$\left(\frac{d\phi}{dx}\right)^2 + 2\lambda\left[\frac{\phi^{\frac{2n}{n-1}}}{\frac{2n}{n-1}} + C_0\right] = 0 \Rightarrow \left(\frac{d\phi}{dx}\right)^2 + \frac{\lambda(n-1)}{n}\left[\phi^{\frac{2n}{n-1}} + C_0\right] = 0$$

$$\left(\frac{d\phi}{dx}\right)^2 + \frac{\lambda(n-1)}{n}\phi^{\frac{2n}{n-1}} = \frac{\lambda(n-1)}{n}\phi_0^{\frac{2n}{n-1}}$$

$$\phi_x^2 + \frac{\lambda(n-1)}{n}\phi^{2n/n-1} = \frac{\lambda(n-1)}{n}\phi_0^{2n/n-1}. \tag{3.53}$$

In Equation (3.53), the constant ϕ_0 indicates the value of $\phi(x)$ at a point where $\phi_x = 0$, if there is one, and if not it is just some constant. It is convenient to present the new dependent variable $\theta(x)$, to solve Equation (3.53), defined by

$$\phi(x) = \phi_0\left[\sin\theta(x)\right]^{\left|\frac{n-1}{n}\right|}. \tag{3.54}$$

Now Equation (3.53) becomes the following equation for $\theta(x)$:

$$\left\{\phi_0 \left|\frac{n-1}{n}\right| [\sin\theta(x)]^{\left|\frac{n-1}{n}\right|-1} \cos\theta(x).\frac{d\theta}{dx}\right\}^2 +$$

$$\frac{\lambda(n-1)}{n}\left[\phi_0^{\frac{2n}{n-1}}[\sin\theta(x)]^{\left|\frac{n-1}{n}\right|\frac{2n}{n-1}}\right] = \frac{\lambda(n-1)}{n}\phi_0^{\frac{2n}{n-1}}$$

$$\phi_0^2\left|\frac{n-1}{n}\right|^2 [\sin\theta(x)]^{2\left|\frac{n-1}{n}\right|-2} \cos^2\theta(x).(\frac{d\theta}{dx})^2 = \frac{\lambda(n-1)}{n}\phi_0^{\frac{2n}{n-1}}\left[1-[\sin\theta(x)]^{\left|\frac{n-1}{n}\right|\frac{2n}{n-1}}\right].$$

The term $\dfrac{n-1}{n}$ may be positive or negative value. It is investigated positive or

negative value of $\dfrac{n-1}{n}$ because of solving Equation (3.53):

a) If $\dfrac{n-1}{n}$ is positive value, it may be written following equations:

$$\phi_0^2(\frac{n-1}{n})^2 [\sin\theta(x)]^{\frac{-2}{n}} \cos^2\theta(x).(\frac{d\theta}{dx})^2 = \frac{\lambda(n-1)}{n}\phi_0^{\frac{2n}{n-1}}\left[1-[\sin\theta(x)]^2\right]$$

Because of $\sin^2\theta(x) + \cos^2\theta(x) = 1$, it is written $\left[\cos^2\theta(x)\right]$ instead of $\left[1-[\sin\theta(x)]^2\right]$.

$$\phi_0^2(\frac{n-1}{n})^2 [\sin\theta(x)]^{\frac{-2}{n}} \cos^2\theta(x).(\frac{d\theta}{dx})^2 = \frac{\lambda(n-1)}{n}\phi_0^{\frac{2n}{n-1}}\left[\cos^2\theta(x)\right]$$

$$\phi_0^2(\frac{n-1}{n})^2 [\sin\theta(x)]^{\frac{-2}{n}} (\frac{d\theta}{dx})^2 = \frac{\lambda(n-1)}{n}\phi_0^{\frac{2n}{n-1}}$$

If it is made necessary improvement, it is obtained following equations:

$$(\frac{n-1}{n})[\sin\theta(x)]^{\frac{-2}{n}}(\frac{d\theta}{dx})^2 = \lambda\phi_0^{\frac{2}{n-1}}$$

$$[\sin\theta(x)]^{\frac{-2}{n}}(\frac{d\theta}{dx})^2 = \lambda\frac{n}{n-1}\phi_0^{\frac{2}{n-1}}$$

$$[\sin\theta(x)]^{\frac{-1}{n}}(\frac{d\theta}{dx}) = (\lambda\frac{n}{n-1})^{\frac{1}{2}}\phi_0^{\frac{1}{n-1}}.$$

b) *If* $\dfrac{n-1}{n}$ *is negative value, it may be written following equations:*

$$\phi_0^2(\frac{n-1}{n})^2[\sin\theta(x)]^{\frac{2(1-n)}{n}-2}\cos^2\theta(x).(\frac{d\theta}{dx})^2 = \frac{\lambda(n-1)}{n}\phi_0^{\frac{2n}{n-1}}\left[1-[\sin\theta(x)]^{\frac{1-n}{n}\frac{2n}{n-1}}\right]$$

$$(\frac{1-n}{n})^2[\sin\theta(x)]^{\frac{2-4n}{n}}\cos^2\theta(x).(\frac{d\theta}{dx})^2 = \frac{\lambda(n-1)}{n}\phi_0^{\frac{2n}{n-1}-2}\left[1-[\sin^2\theta(x)]^{-1}\right]$$

$$(\frac{1-n}{n})^2[\sin\theta(x)]^{\frac{2-4n}{n}}\cos^2\theta(x).(\frac{d\theta}{dx})^2 = \frac{\lambda(n-1)}{n}\phi_0^{\frac{2}{n-1}}\left[\frac{\sin^2\theta(x)-1}{\sin^2\theta(x}\right]$$

$$(\frac{1-n}{n})[\sin\theta(x)]^{\frac{2-4n}{n}}(\frac{d\theta}{dx})^2 = \lambda\phi_0^{\frac{2}{n-1}}\left[\frac{1}{\sin^2\theta(x}\right]$$

$$[\sin\theta(x)]^{\frac{2-2n}{n}}(\frac{d\theta}{dx})^2 = \lambda\frac{n}{1-n}\phi_0^{\frac{2}{n-1}}$$

$$[\sin\theta(x)]^{\frac{1-n}{n}}(\frac{d\theta}{dx}) = (\lambda\frac{n}{1-n})^{\frac{1}{2}}\phi_0^{\frac{1}{n-1}}.$$

Consequently, Equation (3.54) becomes the following equation for $\theta(x)$ depending on β :

$$[\sin \theta]^{\beta} (\frac{d\theta}{dx}) = \left| \lambda \frac{n}{1-n} \right|^{1/2} \phi_0^{\frac{1}{n-1}} \Rightarrow \beta = \begin{cases} -\frac{1}{n}, (n-1)/ \ n \rangle 0 \\ \frac{(1-n)}{n}, (n-1)/n \langle 0 \end{cases} \qquad (3.55)$$

Let $\phi_0, \lambda_0, \rho_0$ denote a solution of Equation (3.41) and Equation (3.43) satisfying Equations (3.44) and (3.51). Then, λ_0 is stationary among all eigenvalue of Equations (3.41)-(3.43) with ρ satisfying Equation (3.44). It is now proving that there is at most one such value λ_0 and that is the maximum of the lowest eigenvalues of Equation (3.41) and Equation (3.43) when ρ satisfies Equation (3.44). The lowest eigenvalue λ is the minimum of a certain quotient of quadratic forms by the self-adjointsness of Equations (3.41)-(3.43) thus for any admissible v, (Tadjbaksh & Keller, 1962)

$$\lambda \leq \frac{\int_0^L v_x^2 dx + \psi[v(0), v(L)]}{\int_0^L \rho v^2 dx} . \qquad (3.56)$$

Here, ψ is defined following equations:

$$\psi = \frac{1}{\alpha_2} \left[\alpha_4 v^2(0) + 2\alpha_1 v(0)v(L) + \alpha_3 v^2(L) \right]. \qquad (3.57)$$

The admissible fuctions $v(x)$ are all fuctions satisfying Equation (3.42) and Equation (3.43) and having piecewise continuous first derivates.

If $\rho = \rho_0$ then equality in Equation (3.56) is acquire when $v = \phi_0$ and $\lambda = \lambda_0$. Upon inserting ϕ_0 and λ_0 into Equation (3.56) and making use of Equation (3.44) to calculate the denominator, it is obtained,

$$\lambda_0 = \frac{\int_0^L (\phi_{0_x})^2 \, dx + \psi\left[\phi_0(0), \phi_0(L)\right]}{k} \tag{3.58}$$

To relate λ to λ_0 it is followed the suggestion of H.F. Weinberger to employ the Hölder inequality (Tadjbaksh & Keller, 1962).

$$\left(\int_0^L fg \, dx\right)^p \leq \left(\int_0^L f^p \, dx\right)\left(\int_0^L g^{p'} \, dx\right)^{p/p'} \tag{3.59}$$

This inequality holds for any two functions *f(x)* and *g(x)* provided that $\frac{1}{p} + \frac{1}{p'} = 1$, $p' \rangle 0$.

Let us set,

$$f = (\rho v^2)^{1/p}, g = \rho^{n/p'}, p = 1 - \frac{1}{n}, p' = 1 - n.$$

Then if $n \langle 1$, Equation (3.59) is valid and yields,

$$\left(\int_0^L v^{2n/n-1} dx\right)^{1 - 1/n} \leq \left(\int_0^L \rho v^2 dx\right)\left(\int_0^L \rho^n dx\right)^{-1/n}, n \langle 1. \tag{3.60}$$

When Equation (3.60) is used in Equation (3.56), it yields,

$$\lambda \leq \frac{\int_0^L {v_x}^2 dx + \psi[v(0), v(L)]}{k^{1/n}(\int_0^L v^{2n/\,n-1} dx)^{1-\frac{1}{n}}} .$$

(3.61)

Upon chosing $v = \phi_0$ in Equation (3.61), it is obtained

$$\lambda \leq \frac{\int_0^L (\phi_{0x})^2 dx + \psi[\phi_0(0), \phi_0(L)]}{k}$$

(3.62)

From Equation (3.58), it is seen that the rigth side of Equation (3.59) is λ_0. Thus, Equation (3.62) can be written as,

$$\lambda \leq \lambda_0, n\langle 1$$

(3.63)

It is thus verified that for $n\langle 1$ the stationary value λ_0 is the maximum of the lowest eigenvalues Equations (3.41)-(3.43) when ρ satisfies Equation (3.42). When $\rho = A^{-2}$ is used in Equation (3.41) and $n = \frac{-1}{2}$ and $k=V$ used in Equation (3.44), from Equation (3.51), it yields,

$$\phi^2 = A^3$$

(3.64)

Thus, Equation (3.54) can be rewritten as,

$$[\sin\theta]^{-\frac{1}{n}}(\frac{d\theta}{dx}) = (\lambda \frac{n}{n-1})^{1/2} \phi_0^{\frac{1}{n-1}} \Rightarrow [\sin\theta]^2 d\theta = (\frac{\lambda}{3})^{1/2} \phi_0^{1/n-1}$$

(3.65)

Integrating Equation (3.65), it is obtained as *C1* and *C2* integration constants:

$$\int (\sin \theta)^2 \, d\theta = (\frac{\lambda}{3})^{1/2} \phi_0^{-2/3} \int d\varsigma$$

$$\frac{1}{2}\theta - \frac{1}{2}\sin \theta \cos \theta + C1 = (\frac{\lambda}{3})^{1/2} \phi_0^{-2/3}\varsigma + C2 \,.$$

It is also written as another constant *a=2C1-2C2*. Thus, it is obtained Equation (3.66) by using Equation (3.64):

$$\theta - \frac{1}{2}\sin 2\theta + a = 2(\frac{\lambda}{3})^{1/2} A_0^{-1}\varsigma \tag{3.66}$$

In these equations *a* ve A_0 are constants to be determined in each case so that ϕ satisfies the appropriate pair of boundary conditions. When it is taken $n = \frac{-1}{2}, k = V$ and $\rho = A^{-2}$ in equation (3.44), it yields followes equation:

$$\int_0^L \rho^n(x)dx = k \Rightarrow \int_0^L A(x)dx = V \Rightarrow \int_0^1 A(\varsigma)d\varsigma = \frac{V}{L} \,. \tag{3.67}$$

To detected ϕ, it is eliminated *A* from Equation (3.29) by means of (3.64) and obtain,

$$\phi_{\varsigma\varsigma} + \lambda\phi^{-1/2} = 0 \tag{3.68}$$

It is convenient to express to general solution $\phi(\varsigma)$ of (3.68), and the corresponding $A(\varsigma)$ determined with the aid of (3.64), in terms of a parameter $\theta(\varsigma)$.

The solutions are:

$$A(\varsigma) = A_0 \sin^2 \theta(\varsigma) \tag{3.69}$$

$$\phi(\varsigma) = A_0^{3/2} \sin^3 \theta(\varsigma) \tag{3.70}$$

$$\frac{d\phi}{d\varsigma} = 3.A_0.\frac{d\theta}{d\varsigma}.\sin^2 \theta(\varsigma).\cos \theta(\varsigma) \tag{3.71}$$

$$\frac{d\theta}{d\varsigma} = \left(\frac{\lambda}{3}\right)^{1/2} \phi_0^{-2/3} \sin^{-2} \theta(\varsigma)$$

$$\frac{d\phi(\varsigma)}{d\varsigma} = (3.A_0.\lambda)^{1/2}.\cos \theta(\varsigma) \Rightarrow \phi_\varsigma = (3.A_0.\lambda)^{1/2}.\cos \theta(\varsigma). \tag{3.72}$$

3.2.2   Analysed Cases and Boundary Conditions

In this section, it deals with the optimum design of Bernoulli-Euler's columns with variable, geometrically similar cross-sections of given shape (circular, quadratic and isosceles cross-sections) for six cases of boundary conditions shown in Figure 3.3 (Ozdamar, 1996). The optimum design and associated fundamental buckling modes for the clamped-clamped case are debatable case.
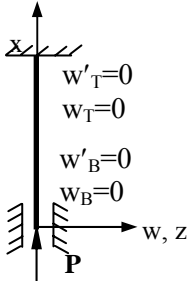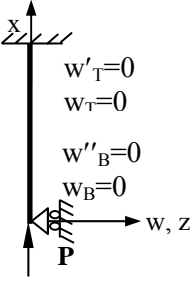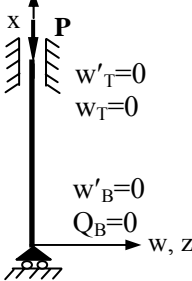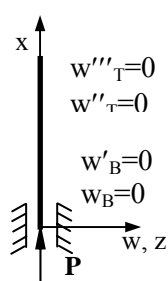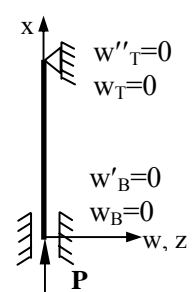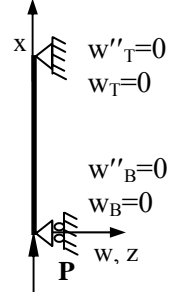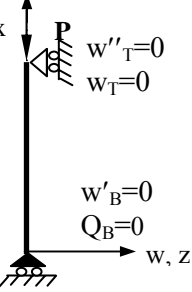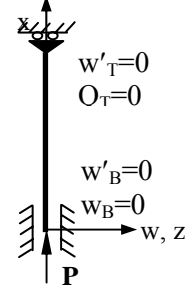
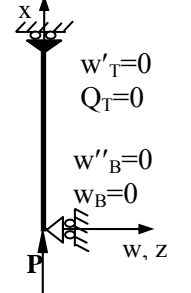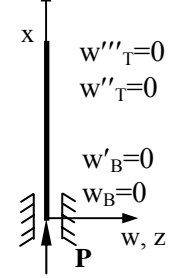| Top end \ Bottom End	Guide-clamped end	Pinned end	Guided-pinned end	Free end
Clamped or guide-clamped end	*CASE11* $w'_T=0$ $w_T=0$ $w'_B=0$ $w_B=0$ P w, z	*CASE12* $w'_T=0$ $w_T=0$ $w''_B=0$ $w_B=0$ P w, z	*CASE13* P $w'_T=0$ $w_T=0$ $w'_B=0$ $Q_B=0$ w, z	*CASE14* $w'''_T=0$ $w''_T=0$ $w'_B=0$ $w_B=0$ P w, z
Pinned or Guide-Pinned end	*CASE21=CASE12* $w''_T=0$ $w_T=0$ $w'_B=0$ $w_B=0$ P w, z	*CASE22* $w''_T=0$ $w_T=0$ $w''_B=0$ $w_B=0$ P w, z	*CASE23* P $w''_T=0$ $w_T=0$ $w'_B=0$ $Q_B=0$ w, z	*KINEMATIC*
Guided end	*CASE31=CASE1* $w'_T=0$ $O_T=0$ $w'_B=0$ $w_B=0$ P w, z	*CASE32=CASE23* $w'_T=0$ $Q_T=0$ $w''_B=0$ $w_B=0$ P w, z	*KINEMATIC*	*KINEMATIC*
Free end	*CASE41=CASE14* $w'''_T=0$ $w''_T=0$ $w'_B=0$ $w_B=0$ P w, z	*KINEMATIC*	*KINEMATIC*	*KINEMATIC*

Figure 3.3 Boundary conditions for column (Ozdamar, 1996)

3.2.2.1 Clamped-Clamped Case (Debatable Case)
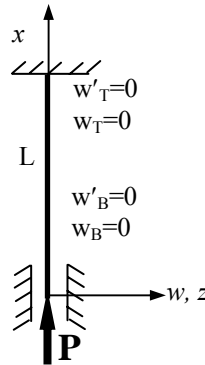
It is satisfied the two conditions at the end *x=0* and at the other end *x=L* for the clamped-clamped case.

$$x = 0 \Rightarrow w(0) = w_x(0) = 0$$

$$x = L \Rightarrow w(L) = w_x(L) = 0$$

It is suitable followed boundary conditions for clamped-clamped case for first derivative of the deflection function and lateral deflection *x=L*, respectively.

$$w_x(x = L) = (\lambda L)^{-1}\left[\phi_\varsigma(0) - \phi_\varsigma(1)\right] = 0 \Rightarrow \phi_\varsigma(0) - \phi_\varsigma(1) = 0$$

$$w(x = L) = (\lambda)^{-1}\left[\phi_\varsigma(0).1 - \phi(1) + \phi(0)\right] = 0 \Rightarrow \phi_\varsigma(0) - \phi(1) + \phi(0) = 0$$

Using Equation (3.70) and (3.72), it yields followed equations from boundary conditions of clamped-clamped case:

$$\cos\theta(0) - \cos\theta(1) = 0$$

$$(3\lambda)^{\frac{1}{2}} A_0^{-1} \cos\theta(0) - \sin^3\theta(1) + \sin^3\theta(0) = 0.$$

These equations are satisfied if it is set

$$\theta(0) = \frac{-\pi}{2}, \theta(1) = \frac{3\pi}{2}.$$

Any other solutions differs from this by the addition of an integer multiple of π to both $\theta(0)$ and $\theta(1)$, or by the addtion of an integer multiple of 2π to $\theta(1)$, or by both additions. Since A and ϕ given by Equation (3.69) and Equation (3.70) are periodic functions of θ with period π (ignoring the sign of ϕ, which is arbitrary), the addition of integer multiplies of π does not yield a different solution. However, the addition of an integer multiple of 2π to $\theta(1)$ does yield a different solution with ϕ having additional nodes. As it is searched the lowest eigenvalue, it is considered the eigenfuction ϕ. By using these values of $\theta(0)$ and $\theta(1)$ in Equation (3.66), it is obtained,

$$\theta(\varsigma = 0) = \frac{-\pi}{2} \Rightarrow \frac{-\pi}{2} - \frac{1}{2}\sin(2\frac{-\pi}{2}) + a = 2(\frac{\lambda}{3})^{\frac{1}{2}} A_0^{-1}.0 \Rightarrow a = \frac{\pi}{2}$$

$$\theta(\varsigma = 1) = \frac{3\pi}{2} \Rightarrow \frac{3\pi}{2} - \frac{1}{2}\sin(2\frac{3\pi}{2}) + a = 2(\frac{\lambda}{3})^{\frac{1}{2}} A_0^{-1}.1 \Rightarrow A_0 = \pi^{-1}(\frac{\lambda}{3})^{\frac{1}{2}}.$$

Finally, Equation (3.66) becomes,

$$\theta - \frac{1}{2}\sin 2\theta + \frac{\pi}{2} = 2\pi\varsigma .$$

Here $\theta(\varsigma)$ is given by above equation. ς and $d\varsigma$ are obtained from $\theta(\varsigma)$:

$$\varsigma = \frac{\theta}{2\pi} - \frac{1}{4\pi}\sin 2\theta + \frac{1}{4} \Rightarrow d\varsigma = \frac{1}{2\pi}d\theta - \frac{1}{4\pi}2\cos 2\theta d\theta$$

$$d\varsigma = (\frac{1-\cos 2\theta)}{2\pi}d\theta = \frac{1}{\pi}\sin^2\theta d\theta.$$

To determine λ, it is used Equation (3.69) and Equation (3.66) in Equation (3.40) which yields

$$\int_0^\theta A_0 \sin^2\theta(\varsigma)\frac{1}{\pi}\sin^2\theta(\varsigma)d\theta = \frac{V}{L} \Rightarrow \frac{A_0}{\pi}\int_{-\pi/2}^{3\pi/2}\sin^4\theta d\theta = \frac{V}{L} \Rightarrow V = \frac{3A_0L}{4}.$$

Thus $A_0 = 4V/3L$ and then using a and A_0 values yields for the eigenvalue λ,

$$\frac{4V}{3L} = \frac{1}{\pi}(\frac{\lambda}{3})^{1/2} \Rightarrow \lambda = \frac{16\pi^2}{3}(\frac{V}{L})^2$$

The cross-sectional area $A(\varsigma)$ given by Equation (3.69) can now be written as,

$$A(\varsigma) = \frac{4}{3}\frac{V}{L}\sin^2\theta(\varsigma).$$

This equation determines the shape of the strongest column in the clamped-clamped case and λ determines its buckling load. It is interesting to note that this buckling load is 4/3 as greater as that of a uniform column, for which the corresponding eigenvalue is $4\pi^2(V/L)^2$ (Tadjbaksh & Keller, 1962).

From this equation $A(\varsigma) = \frac{4}{3}\frac{V}{L}\sin^2\theta(\varsigma)$, it is found that

$$A(0) = A(\tfrac{1}{2}) = A(1) = \frac{4}{3}\frac{V}{L}$$

$$A(1/4) = A(3/4) = 0$$

It is shown that in Figure 3.4 a graph of $A(\varsigma)$. It is seen that the column consists of three parts. The middle part, from $\varsigma = \frac{1}{4}$ to $\varsigma = \frac{3}{4}$, contains one-half the total volume. Its shape is exactly that of the strongest column of the length $L/2$ and volume $V/2$, and each of the two end parts, from $\varsigma = 0$ to $\varsigma = 1/4$ and $\varsigma = 3/4$ to $\varsigma = 1$, coincides with one-half the middle part.
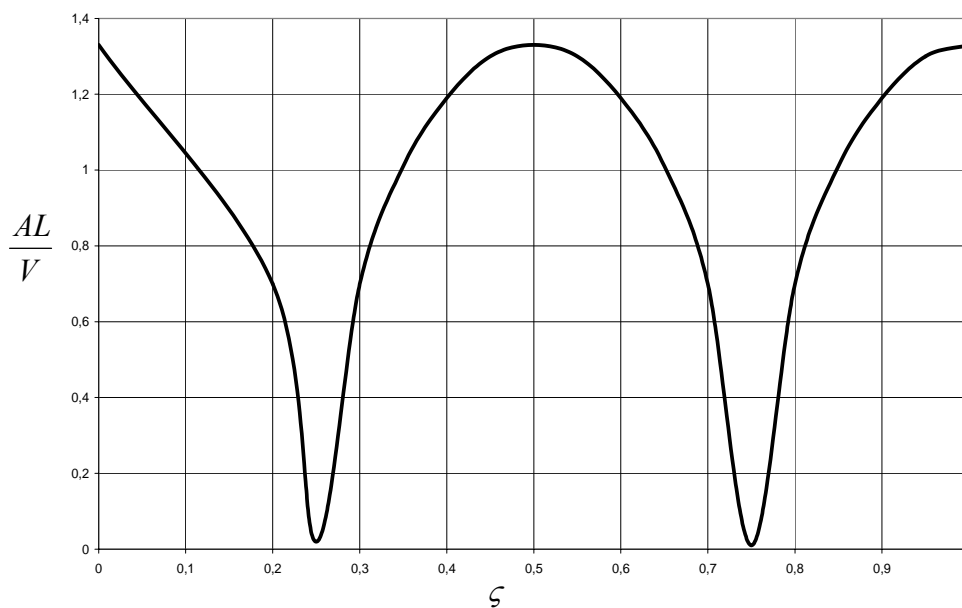

Figure 3.4 Cross-sectional area of strongest clamped-clamped column as a function of distance along column

Finally, the optimum (non-dimensional) eigenvalue and critical buckling load for clamped-clamped case are given by

$$\lambda = \frac{PL^2}{E\alpha} \Rightarrow P_{OPT} = \frac{\lambda \alpha E}{L^2} \Rightarrow P_{OPT} = \frac{16\pi^2}{3}(\frac{V}{L})^2 \frac{\alpha E}{L^2}$$

which gives:

(a) for cross-sectional of circular shape ($\alpha = \frac{1}{4\pi}$)

$$P_{OPT} = 4{,}1887902 \frac{EV^2}{L^4}$$

(b) for square shaped cross-sections ($\alpha = \frac{1}{12}$)

$$P_{OPT} = 4{,}3864908 \frac{EV^2}{L^4}$$

(c) for isosceles triangle cross-sections ($\alpha = \frac{\sqrt{3}}{18}$)

$$P_{OPT} = 5{,}0650833 \frac{EV^2}{L^4}$$

3.2.2.2 Clamped-Hinged Case
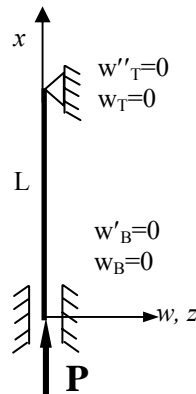
It is satisfied the two conditions at the end *x=0* and at the other end *x=L* for the clamped-hinged case.

$$x = 0 \Rightarrow w(0) = w_x(0) = 0$$

$$x = L \Rightarrow w(L) = w_{xx}(L) = 0$$

It is suitable followed boundary conditions for clamped-hinged case for lateral deflection and second derivative of the deflection function *x=L*, respectively.

$$w(x=L) = (\lambda)^{-1}\left[\phi_\varsigma(0).1 - \phi(1) + \phi(0)\right] = 0 \Rightarrow \phi_\varsigma(0) - \phi(1) + \phi(0) = 0$$

$$A^{-2}\phi = L^2 w_{xx}(\varsigma L) \Rightarrow w_{xx}(\varsigma L) = \frac{1}{L^2 A^2}\phi(\varsigma)$$

It is obtained following state from second derivative of the deflection function and deflection function for $x=L$:

$$w_{xx}(x=L) = \frac{1}{L^2 A^2}\phi(1) = 0 \Rightarrow \phi(1) = 0$$

$$\phi_\varsigma(0) - \phi(1) + \phi(0) = 0 \Rightarrow \phi_\varsigma(0) + \phi(0) = 0.$$

Using Equation (3.60) and (3.72), it is found:

$$\phi(1) = A_0^{3/2}\sin^3\theta(1) = 0 \Rightarrow \sin^3\theta(1) = 0 \Rightarrow \sin\theta(1) = 0$$

$$\phi_\varsigma(0) + \phi_\varsigma(1) = 0 \Rightarrow (3\lambda A_0)^{1/2}\cos\theta(0) + (A_0)^{3/2}\sin^3\theta(0) = 0$$

$$(3\lambda^{1/2}(A_0)^{-1}\cos\theta(0) + \sin^3\theta(0) = 0.$$

To satisfy $\sin\theta(1) = 0$, it may choose $\theta(1) = \pi$. Now Equation (3.63) becomes, for $\varsigma = 0$ and $\varsigma = 1$,

$$\theta(\varsigma=1) = \pi \Rightarrow \pi - \frac{1}{2}\sin(2\pi) + a = 2(\frac{\lambda}{3})^{1/2}A_0^{-1}.1 \Rightarrow a = 2(\frac{\lambda}{3})^{1/2}A_0^{-1} - \pi$$

$$\theta(0) - \frac{1}{2}\sin(2.\theta(0)) + 2(\frac{\lambda}{3})^{1/2}A_0^{-1} - \pi = 2(\frac{\lambda}{3})^{1/2}A_0^{-1}.0$$

$$A_0 = \frac{1}{2}(\frac{\lambda}{3})^{1/2}\left[\pi - \theta(0) + \frac{1}{2}\sin 2\theta(0)\right]$$

$$(3\lambda^{1/2}(A_0)^{-1}\cos\theta(0) + \sin^3\theta(0) = 0$$

$$\frac{3}{2}\cos\theta(0)\left[\pi + \frac{1}{2}\sin 2\theta(0) - \theta(0)\right] + \sin^3\theta(0) = 0.$$

It is found that for the lowest eigenvalue, to which corresponds the solution with the fewest nodes, $\theta(0)$ must lie in the range $-\frac{\pi}{2}\langle\theta(0)\langle 0$. Numerical solution of above equation, it yields,

$$\theta(0) = 1{,}4243$$

Finally, it is found following equations for a and A_0:

$$a = \frac{1}{2}\sin 2\theta(0) - \theta(0)$$

$$A_0 = 2(\frac{\lambda}{3})^{1/2}\frac{1}{\left[\pi + \frac{1}{2}\sin 2\theta(0) - \theta(0)\right]}$$

When the constants a and A_0 are written Equation (3.66) with obtained value from above equation, it yields following equation:

$$\theta - \frac{1}{2}\sin 2\theta + \left[\frac{1}{2}\sin 2\theta(0) - \theta(0)\right] = \left[\pi + \frac{1}{2}\sin 2\theta(0) - \theta(0)\right]\varsigma.$$

Here $\theta(\varsigma)$ is given by above equation. ς and $d\varsigma$ are obtained from $\theta(\varsigma)$:

$$\varsigma = \frac{\theta}{\left[\pi + \frac{1}{2}\sin 2\theta(0) - \theta(0)\right]} - \frac{1}{2}\sin 2\theta(0)\frac{1}{\left[\pi + \frac{1}{2}\sin 2\theta(0) - \theta(0)\right]} +$$

$$\frac{\left[\frac{1}{2}\sin 2\theta(0) - \theta(0)\right]}{\left[\pi + \frac{1}{2}\sin 2\theta(0) - \theta(0)\right]}$$

$$d\varsigma = \frac{2}{\left[\pi + \frac{1}{2}\sin 2\theta(0) - \theta(0)\right]}\sin^2 \theta(0)d\theta$$

To determine λ, it is used Equation (3.69) and Equation (3.66) in Equation (3.40) which yields:

$$\int_0^\theta A_0 \sin^2 \theta(\varsigma)\frac{2}{\left[\pi + \frac{1}{2}\sin 2\theta(0) - \theta(0)\right]}\sin^2 \theta(0)d\theta = \frac{V}{L} \Rightarrow A_0 = \frac{4}{3\sin^2 \theta(0)}\frac{V}{L}$$

$$\frac{4}{3\sin^2 \theta(0)}\frac{V}{L} = 2(\frac{\lambda}{3})^{\frac{1}{2}}\frac{1}{\left[\pi + \frac{1}{2}\sin 2\theta(0) - \theta(0)\right]}$$

$$\lambda = \frac{16}{27}\tan^2 \theta(0)(\frac{V}{L})^2 \Rightarrow \lambda \approx 27,22(\frac{V}{L})^2 .$$

It is obtained for the cross-sectional area of the strongest column for clamped-hinged case.

$$A(\varsigma) = \frac{4}{3}\frac{V}{L}\frac{\sin^2 \theta(\varsigma)}{\sin^2 \theta(0)}$$

It is shown that in Figure 3.5 a graph of $A(\varsigma)$.
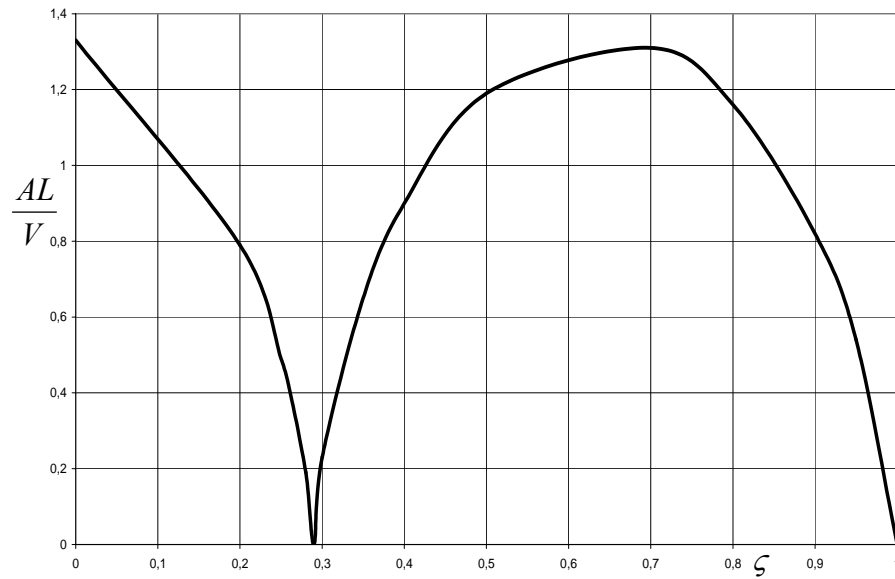
Figure 3.5 Cross-sectional area of strongest clamped-hinged column as a function of distance along column.

Finally, the optimum (nondimensional) eigenvalue and criticalbuckling load for clamped-hinged case are given by

$$\lambda = \frac{PL^2}{E\alpha} \Rightarrow P_{OPT} = \frac{\lambda \alpha E}{L^2} \Rightarrow P_{OPT} = 27{,}22(\frac{V}{L})^2 \frac{\alpha E}{L^2}$$

which gives:

(a) for cross-sectional of circular shape ($\alpha = \frac{1}{4\pi}$)

$$P_{OPT} = 2{,}1660988 \frac{EV^2}{L^4}$$

(b) for square shaped cross-sections ($\alpha = \frac{1}{12}$)

$$P_{OPT} = 2{,}2683333 \frac{EV^2}{L^4}$$

(c) for isosceles triangle cross-sections ($\alpha = \sqrt{3}/18$)

$$P_{OPT} = 2{,}6192457 \frac{EV^2}{L^4}$$

3.2.2.3 Clamped-Free Case
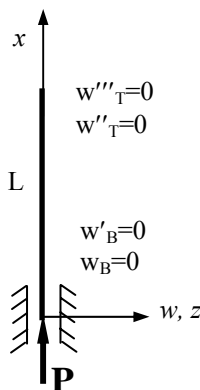
It is satisfied the two conditions at the end $x=0$ and at the other end $x=L$ for the clamped-free case.

$$x = 0 \Rightarrow w(0) = w_x(0) = 0$$

$$x = L \Rightarrow w_{xx}(L) = w_{xxx}(L) = 0$$

In the clamped-free case, the boundary conditions, for $x=L$, the bending moment and shear force must be expressed in point of $\phi(\varsigma)$.

$$M(x = L) = -E.I(x).\frac{1}{L^2 A^2}\phi(\varsigma) = 0 \Rightarrow \phi(1) = 0$$

Shear force is before obtained from Equation (3.32):

$$Q(x) = \frac{dM}{dx} - P\frac{dw}{dx}$$

It is obtained following equations from shear force:

$$Q = \frac{-E\alpha}{L^2}\frac{d\phi(\varsigma)}{d\varsigma}\frac{d\varsigma}{dx} - P(\lambda L)^{-1}\left[\phi_\varsigma(0) - \phi_\varsigma(\varsigma)\right] = 0 \Rightarrow \phi_\varsigma = 0.$$

Using Equations (3.70) and (3.72), it is obtained,

$$\phi(1) = A_0^{3/2}\sin^3\theta(1) = 0 \Rightarrow \sin^3\theta(1) = 0$$

$$\phi_\varsigma(0) = (3\lambda A_0)^{1/2}\cos\theta(0) = 0 \Rightarrow \cos\theta(0) = 0$$

These equations are satisfied if it is set $\theta(0) = \dfrac{-\pi}{2}, \theta(1) = 0$. To obtain a and A_0, it is used Equation (3.47) using $\theta(0)$ and $\theta(1)$:

$$\theta(\varsigma = 0) = \frac{-\pi}{2} \Rightarrow \frac{-\pi}{2} - \frac{1}{2}\sin(2\frac{-\pi}{2}) + a = 2(\frac{\lambda}{3})^{1/2}A_0^{-1}.0 \Rightarrow a = \frac{\pi}{2}$$

$$\theta(\varsigma = 1) = 0 \Rightarrow 0 - \frac{1}{2}\sin(2.0) + a = 2(\frac{\lambda}{3})^{1/2}A_0^{-1}.1 \Rightarrow A_0 = 4\pi^{-1}(\frac{\lambda}{3})^{1/2}$$

Finally, it is obtained Equation (3.66) following equation:

$$\theta - \frac{1}{2}\sin 2\theta + \frac{\pi}{2} = \frac{\pi}{2}\varsigma.$$

Here $\theta(\varsigma)$ is given by above equation. ς and $d\varsigma$ are obtained in $\theta(\varsigma)$:

$$\varsigma = \frac{2\theta}{\pi} - \frac{1}{\pi}\sin 2\theta + 1 \Rightarrow d\varsigma = \frac{2}{\pi}d\theta - \frac{1}{2\pi}2\cos 2\theta d\theta$$

$$d\varsigma = (\frac{1-\cos 2\theta}{\pi})2d\theta = \frac{4}{\pi}\sin^2\theta d\theta.$$

To determine λ, it is used Equation (3.69) and Equation (3.66) in Equation (3.40) which yields:

$$\int_0^\theta A_0 \sin^2 \theta(\varsigma) \frac{4}{\pi} \sin^2 \theta(\varsigma) d\theta = \frac{V}{L} \Rightarrow \frac{4A_0}{\pi} \int_{-\pi/2}^0 \sin^4 \theta d\theta = \frac{V}{L} \Rightarrow V = \frac{3A_0 L}{4}.$$

Thus $A_0 = \frac{4V}{3L}$ and then using a and A_0 values yields for the eigenvalue λ,

$$\frac{4V}{3L} = \frac{4}{\pi} (\frac{\lambda}{3})^{1/2} \Rightarrow \lambda = \frac{\pi^2}{3} (\frac{V}{L})^2$$

The cross-sectional area $A(\varsigma)$ given by Equation (3.69) can now be written as,

$$A(\varsigma) = \frac{4}{3} \frac{V}{L} \sin^2 \theta(\varsigma)$$

It is shown that in Figure 3.6 a graph of $A(\varsigma)$.
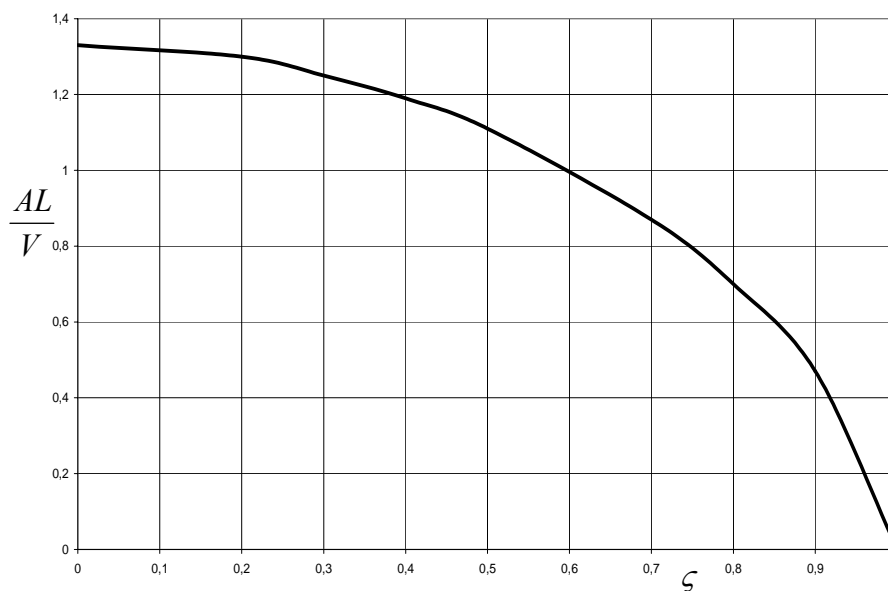
Figure 3.6 Cross-sectional area of strongest clamped-free column as a function of distance along column.

Finally, the optimum (nondimensional) eigenvalue and critical buckling load for clamped-free case are given by

$$\lambda = \frac{PL^2}{E\alpha} \Rightarrow P_{OPT} = \frac{\lambda \alpha E}{L^2} \Rightarrow P_{OPT} = \frac{\pi^2}{3}(\frac{V}{L})^2 \frac{\alpha E}{L^2}$$

which gives:

(a) for cross-sectional of circular shape ($\alpha = \frac{1}{4\pi}$)

$$P_{OPT} = 0,2617994\frac{EV^2}{L^4}$$

(b) for square shaped cross-sections ($\alpha = \frac{1}{12}$)

$$P_{OPT} = 0,2741557\frac{EV^2}{L^4}$$

(c) for isosceles triangle cross-sections ($\alpha = \frac{\sqrt{3}}{18}$)

$$P_{OPT} = 0,3165677\frac{EV^2}{L^4}$$

3.2.2.4 Hinged-Hinged Case

It is satisfied the two conditions at the end *x=0* and at the other end *x=L* for the hinged-hinged case.

$$x = 0 \Rightarrow w(0) = w_{xx}(0) = 0$$

$$x = L \Rightarrow w(L) = w_{xx}(L) = 0$$

To obtain necessary conditions, it is utilized Equation (3.36):

$$w_x(\varsigma L) - w_x(0) = \frac{-1}{\lambda L}\left[\phi_\varsigma(\varsigma) - \phi_\varsigma(0)\right]$$

If in this equation is integrated, it yields:

$$\int_0^\varsigma w_x(\varsigma L)d\varsigma = w_x(0)\cdot\varsigma + \frac{1}{\lambda L}\int_0^\varsigma \left[\phi_\varsigma(0) - \phi_\varsigma(\varsigma)\right]d\varsigma,$$
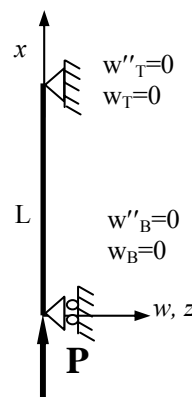
$$\frac{dw(\varsigma L)}{dx} = \frac{dw(\varsigma L)}{d\varsigma}\frac{d\varsigma}{dx}, d\varsigma = \frac{1}{L}dx$$

$$\frac{1}{L}w(\varsigma L)\Big|_0^\varsigma = w_x(0)\varsigma + \frac{1}{\lambda}\left[\phi_\varsigma(0)\varsigma - \phi(\varsigma)\Big|_0^\varsigma\right]$$

$$w(\varsigma L) - w(0) = w_x(0)\varsigma L + \frac{1}{\lambda}\left[\phi_\varsigma(0)\varsigma - \phi(\varsigma) + \phi(0)\right].$$

Now, it is applied boundary conditions for x=0 :

$$x = 0 \Rightarrow w(0) - w(0) = w_x(0)0L + \frac{1}{\lambda}\left[\phi_\varsigma(0)0 - \phi(0) + \phi(0)\right]$$

$$w_{xx}(\varsigma L) = \frac{-1}{\lambda L^2}\phi_{\varsigma\varsigma} = \frac{1}{L^2 A^2}\phi(\varsigma)$$

It is obtained following equation from second derivative of the deflection function for $x=0$:

$$w_{xx}(0) = \frac{1}{L^2 A^2} A_0^{3/2} \sin^3 \theta(0) = 0 \Rightarrow \sin^3 \theta(0) = 0, \phi(0) = 0$$

It is also applied boundary conditions for $x=L$:

$$w(L) - w(0) = w_x(0)L + \frac{1}{\lambda}\left[\phi_\varsigma(0)1 - \phi(1) + \phi(0)\right] \Rightarrow w_x(0) = \frac{-1}{\lambda L}\left[\phi_\varsigma(0) - \phi(1) + \phi(0)\right]$$

$$w''(L) = \frac{1}{L^2 A^2}\phi(1) = 0 \Rightarrow \phi(1) = 0$$

$$w_x(0) = \frac{-1}{\lambda L}\left[\phi_\varsigma(0) - \phi(1) + \phi(0)\right] \Rightarrow w_x(0) = \frac{-1}{\lambda L}\left[\phi_\varsigma(0) + \phi(0)\right]$$

$$w_x(0) = \frac{-1}{\lambda L}\left[(3\lambda A_0)^{1/2}\cos\theta(0) + A_0^{3/2}\sin^3\theta(0)\right]$$

$$\frac{-1}{\lambda L}\left[(3\lambda A_0)^{1/2}\cos\theta(0)\right] = \frac{-1}{L}(\frac{3A_0}{\lambda})^{1/2}\cos\theta(0).$$

Consequently, it is found following equations from boundary conditions for at the end $x=0$ and at the other end $x=L$:

$$\phi(0) = 0 \Rightarrow \sin^3\theta(0) = 0$$

$$\phi(1) = 0 \Rightarrow \sin^3\theta(1) = 0.$$

These equations are satisfied if it is set $\theta(0) = 0, \theta(1) = \pi$. To obtain a and A_0, it is used Equation (3.66) using $\theta(0)$ and $\theta(1)$:

$$\theta(\varsigma = 0) = 0 \Rightarrow 0 - \frac{1}{2}\sin(20) + a = 2(\frac{\lambda}{3})^{\frac{1}{2}} A_0^{-1}.0 \Rightarrow a = 0$$

$$\theta(\varsigma = 1) = \pi \Rightarrow \pi - \frac{1}{2}\sin(2.\pi) = 2(\frac{\lambda}{3})^{\frac{1}{2}} A_0^{-1}.1 \Rightarrow A_0 = 2\pi^{-1}(\frac{\lambda}{3})^{\frac{1}{2}}$$

Finally, it is obtained Equation (3.66) following equation:

$$\theta - \frac{1}{2}\sin 2\theta = \pi\varsigma .$$

Here $\theta(\varsigma)$ is given by above equation. ς and $d\varsigma$ are obtained in $\theta(\varsigma)$:

$$\varsigma = \frac{\theta}{\pi} - \frac{1}{2\pi}\sin 2\theta \Rightarrow d\varsigma = \frac{1}{\pi}d\theta - \frac{1}{2\pi}2\cos 2\theta d\theta$$

$$d\varsigma = (\frac{1-\cos 2\theta}{\pi})d\theta = \frac{2}{\pi}\sin^2 \theta d\theta$$

To determine λ, it is used Equation (3.69) and Equation (3.66) in Equation (3.40) which yields

$$\int_0^\theta A_0 \sin^2 \theta(\varsigma) \frac{2}{\pi}\sin^2 \theta(\varsigma)d\theta = \frac{V}{L} \Rightarrow \frac{2A_0}{\pi}\int_0^\pi \sin^4 \theta d\theta = \frac{V}{L} \Rightarrow V = \frac{3A_0 L}{4} .$$

Thus $A_0 = \frac{4V}{3L}$ and then using a and A_0 values yields for the eigenvalue λ,

$$\frac{4V}{3L} = \frac{2}{\pi}(\frac{\lambda}{3})^{\frac{1}{2}} \Rightarrow \lambda = \frac{4\pi^2}{3}(\frac{V}{L})^2$$

The cross-sectional area $A(\varsigma)$ given by Equation (3.69) can now be written as,

$$A(\varsigma) = \frac{4}{3}\frac{V}{L}\sin^2\theta(\varsigma)$$

It is shown that in Figure 3.7 a graph of $A(\varsigma)$.
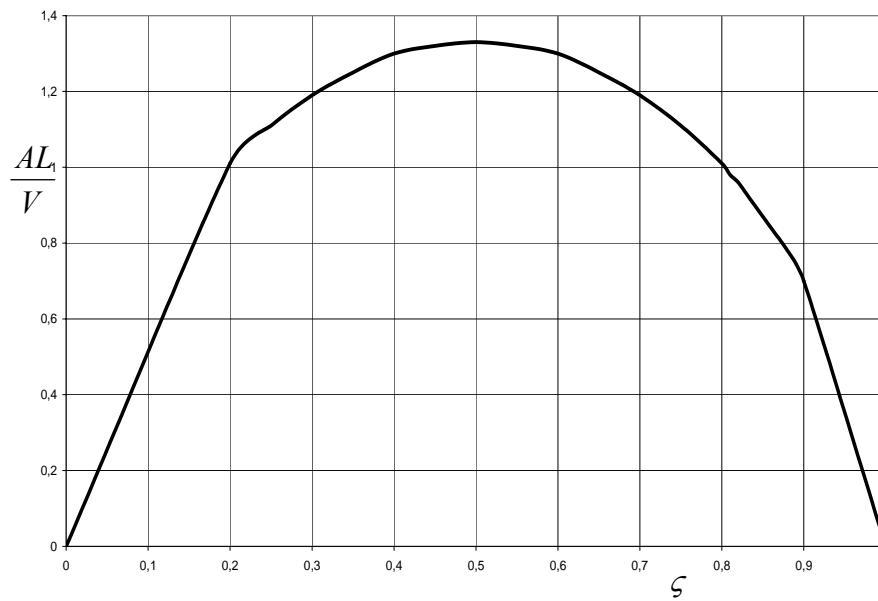

Figure 3.7 Cross-sectional area of strongest hinged-hinged column as a function of distance along column.

Finally, the optimum (nondimensional) eigenvalue and critical buckling load for hinged-hinged case are given by

$$\lambda = \frac{PL^2}{E\alpha} \Rightarrow P_{OPT} = \frac{\lambda\alpha E}{L^2} \Rightarrow P_{OPT} = \frac{4\pi^2}{3}(\frac{V}{L})^2\frac{\alpha E}{L^2}$$

which gives:

(a) for cross-sectional of circular shape ($\alpha = \frac{1}{4\pi}$)

$$P_{OPT} = 1,0471976 \frac{EV^2}{L^4}$$

(b) for square shaped cross-sections ($\alpha = \frac{1}{12}$)

$$P_{OPT} = 1,0966227 \frac{EV^2}{L^4}$$

(c) for isosceles triangle cross-sections ($\alpha = \frac{\sqrt{3}}{18}$)

$$P_{OPT} = 1,2662708 \frac{EV^2}{L^4}$$

3.2.2.5 Guided-Clamped Case
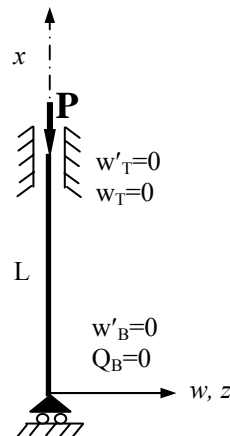
It is satisfied the two conditions at the end $x=0$ and at the other end $x=L$ for the guided-clamped case.

$$x = 0 \Rightarrow w_x(0) = Q(0) = 0$$

$$x = L \Rightarrow w(L) = w_x(L) = 0$$

It is suitable followed boundary conditions for guided-clamped case. It is written following equation Q for $x=0$:

$$Q = \frac{dM}{dx} - P\frac{dw}{dx}, M(x) = -E.I(x)w''(x)$$

$$Q(x) = -\left\{\frac{d}{dx}\left[EI(x)w''(x)\right] + P\frac{dw}{dx}\right\}$$

$$Q(x) = -\left\{E\left[I'(x)w''(x) + I(x)w'''(x)\right] + P\frac{dw}{dx}\right\}$$

Because, the area moment of inertia is dependent on x, the term $\frac{dI(x)}{dx}$ is written following equations:

$$I(x) = \alpha A^2(x) = \alpha A_0{}^2 \sin^4\theta(\varsigma) \Rightarrow \frac{dI(x)}{dx} = \alpha A_0{}^2 4\sin^3\theta(\varsigma)\cos\theta(\varsigma)\frac{d\theta(\varsigma)}{dx}$$

$$I'(x) = 4\alpha A_0{}^2 \sin^3\theta(\varsigma)\cos\theta(\varsigma)\theta'(\varsigma)$$

It yields second derivative of the deflection function:

$$w''(\varsigma) = \frac{1}{L^2 A^2(\varsigma)}\phi(\varsigma) \Rightarrow w''(\varsigma) = \frac{1}{L^2 A_0{}^2 \sin^4\theta(\varsigma)} A_0{}^{3/2} \sin^3\theta(\varsigma)$$

$$w''(\varsigma) = \frac{1}{L^2 A_0{}^{1/2} \sin\theta(\varsigma)}.$$

It is also obtained third derivation of the deflection function followed equation:

$$\frac{d}{dx}\left[w''(\varsigma)\right] = w'''(\varsigma) = \frac{1}{L^2 A_0^{1/2}} \frac{d}{dx}\left[\frac{1}{\sin\theta(\varsigma)}\right] = \frac{1}{L^2 A_0^{1/2}}\left[\frac{-\cos\theta(\varsigma)}{\sin^2\theta(\varsigma)}\theta'(\varsigma)\right]$$

$$w'''(\varsigma) = \frac{-1}{L^2 A_0^{1/2}}\frac{\cos\theta(\varsigma)}{\sin^2\theta(\varsigma)}\theta'(\varsigma).$$

It is applied boundary conditions for x=0:

$$x = 0 \Rightarrow w' = 0$$

$$w_x(\varsigma L) - w_x(0) = \frac{-1}{\lambda L}\left[\phi_\varsigma(0) - \phi_\varsigma(0)\right]$$

It is also written $Q = 0$ for *x=0* followed equation:

$$x = 0 \Rightarrow Q = 0 \Rightarrow -\left\{E\left[I'(0)w''(0) + I(0)w'''(0)\right] + Pw'(0)\right\} = 0$$

When it is placed first derivative of the area moment of inertia, second derivative of the deflection function and third derivation of the deflection function to this equation, Q is obtained as:

$$Q = -\left\{E\left[\frac{4\alpha A_0^2 \sin^3\theta(0)\cos\theta(0)}{L^2 A_0^{1/2}\sin\theta(0)}\frac{d\theta(0)}{dx} - \frac{\alpha A_0^2 \sin^4\theta(0)\cos\theta(0)}{L^2 A_0^{1/2}\sin^2\theta(0)}\frac{d\theta(0)}{dx}\right]\right\} = 0$$

$$Q = -\left\{E\left[\frac{4\alpha A_0^{3/2}\sin^2\theta(0)\cos\theta(0)}{L^2}\frac{d\theta(0)}{dx} - \frac{\alpha A_0^{3/2}\sin^2\theta(0)\cos\theta(0)}{L^2}\frac{d\theta(0)}{dx}\right]\right\} = 0.$$

If it is made necessary improvement, it yields,

$$Q = -\left\{ E\left[\frac{3\alpha A_0^{3/2} \sin^2 \theta(0) \cos\theta(0)}{L^2} \frac{d\theta(0)}{dx} \right] \right\} = 0$$

$$Q = -\left\{ E\left[\frac{3\alpha A_0^{3/2} \sin^2 \theta(0) \cos\theta(0)}{L^2} \frac{d\theta(\varsigma)}{d\varsigma} \frac{d\varsigma}{dx} \right] \right\} = 0$$

$$Q = \frac{3\alpha A_0^{3/2} \sin^2 \theta(0) \cos\theta(0)}{L^3} \frac{d\theta(0)}{d\varsigma} = 0 .$$

According to above equations, it is obtained following conditions:

$$\frac{3\alpha A_0^{3/2} \sin^2 \theta(0) \cos\theta(0)}{L^3} = 0 \Rightarrow \sin^2 \theta(0) \cos\theta(0) = 0$$

It is applied boundary conditions for x=L,

$$w(\varsigma L) - w(0) = w_x(0)\varsigma L + \frac{1}{\lambda}\left[\phi_\varsigma(0)\varsigma - \phi(\varsigma) + \phi(0) \right]$$

$$w(L) - w(0) = w_x(0)L + \frac{1}{\lambda}\left[\phi_\varsigma(0) - \phi(\varsigma) + \phi(0) \right]$$

In this equation, $w(0)$ is written as following equations:

$$-w(0) = w_x(0)L + \frac{1}{\lambda}\left[\phi_\varsigma(0) - \phi(\varsigma) + \phi(0) \right]$$

$$w_x(\varsigma L) - w_x(0) = -\frac{1}{\lambda L}\left[\phi_\varsigma(\varsigma) - \phi_\varsigma(0) \right] \Rightarrow -\frac{1}{\lambda L}\left[\phi_\varsigma(1) - \phi_\varsigma(0) \right] = 0$$

$$\frac{-1}{\lambda L}\left[(3\lambda A_0)^{1/2} \cos\theta(1) - (3\lambda A_0)^{1/2} \cos\theta(0) \right] \Rightarrow \cos\theta(1) - \cos\theta(0) = 0$$

$$-w(0) = \frac{1}{\lambda}\left[(3\lambda A_0)^{\frac{1}{2}}\cos\theta(0) - A_0^{\frac{3}{2}}\sin^3\theta(1) + A_0^{\frac{3}{2}}\sin^3\theta(0)\right]$$

Finally, it is obtained, lateral deflection function, $w(0)$, for $x=0$:

$$w(0) = \frac{-1}{\lambda}\left[(3\lambda A_0)^{\frac{1}{2}}\cos\theta(0) - A_0^{\frac{3}{2}}\sin^3\theta(1) + A_0^{\frac{3}{2}}\sin^3\theta(0)\right].$$

These equations are satisfied if it is set $\theta(0) = \frac{\pi}{2}, \theta(1) = \frac{3\pi}{2}$. To obtain a and A_0, it is used Equation (3.66) using $\theta(0)$ and $\theta(1)$:

$$\theta(\varsigma=0) = \frac{\pi}{2} \Rightarrow \frac{\pi}{2} - \frac{1}{2}\sin(2\frac{\pi}{2}) + a = 2(\frac{\lambda}{3})^{\frac{1}{2}}A_0^{-1}.0 \Rightarrow a = -\frac{\pi}{2}$$

$$\theta(\varsigma=1) = \frac{3\pi}{2} \Rightarrow \frac{3\pi}{2} - \frac{1}{2}\sin(2.\frac{3\pi}{2}) = 2(\frac{\lambda}{3})^{\frac{1}{2}}A_0^{-1}.1 \Rightarrow A_0 = 2\pi^{-1}(\frac{\lambda}{3})^{\frac{1}{2}}$$

It is obtained Equation (3.66) followed:

$$\theta - \frac{1}{2}\sin 2\theta - \frac{\pi}{2} = \pi\varsigma$$

Here $\theta(\varsigma)$ is given by above equation. ς and $d\varsigma$ are obtained in $\theta(\varsigma)$:

$$\varsigma = \frac{\theta}{\pi} - \frac{1}{2\pi}\sin 2\theta \Rightarrow d\varsigma = \frac{1}{\pi}d\theta - \frac{1}{2\pi}2\cos 2\theta d\theta$$

$$d\varsigma = (\frac{1-\cos 2\theta}{\pi})d\theta = \frac{2}{\pi}\sin^2\theta d\theta$$

To determine λ, it is used Equation (3.69) and Equation (3.66) in Equation (3.40) which yields:

$$\int_0^\theta A_0 \sin^2 \theta(\varsigma) \frac{2}{\pi} \sin^2 \theta(\varsigma) d\theta = \frac{V}{L} \Rightarrow \frac{2A_0}{\pi} \int_{\pi/2}^{3\pi/2} \sin^4 \theta d\theta = \frac{V}{L} \Rightarrow V = \frac{3A_0 L}{4}$$

Thus $A_0 = \dfrac{4V}{3L}$ and then using a and A_0 values yields for the eigenvalue λ,

$$\frac{4V}{3L} = \frac{2}{\pi} (\frac{\lambda}{3})^{1/2} \Rightarrow \lambda = \frac{4\pi^2}{3} (\frac{V}{L})^2$$

The cross-sectional area $A(\varsigma)$ given by Equation (3.69) can now be written as,

$$A(\varsigma) = \frac{4}{3} \frac{V}{L} \sin^2 \theta(\varsigma)$$

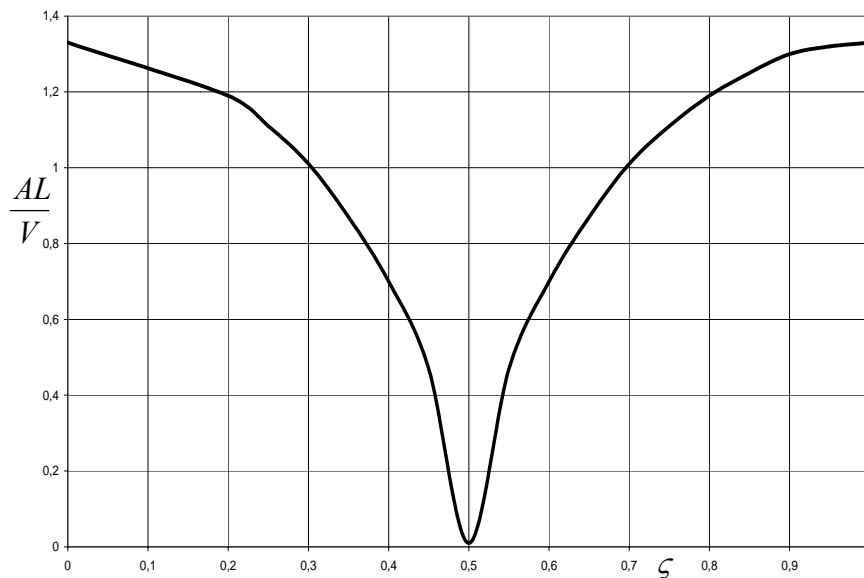It is shown that in Figure 3.8 a graph of $A(\varsigma)$.

Figure 3.8 Cross-sectional area of strongest guided-clamped column as a function of distance along column.

Finally, the optimum (nondimensional) eigenvalue and critical buckling load for guided-clamped case are given by

$$\lambda = \frac{PL^2}{E\alpha} \Rightarrow P_{OPT} = \frac{\lambda\alpha E}{L^2} \Rightarrow P_{OPT} = \frac{4\pi^2}{3}(\frac{V}{L})^2 \frac{\alpha E}{L^2}$$

which gives:

(d) for cross-sectional of circular shape ($\alpha = \frac{1}{4\pi}$)

$$P_{OPT} = 1{,}0471976\frac{EV^2}{L^4}$$

(e) for square shaped cross-sections ($\alpha = \frac{1}{12}$)

$$P_{OPT} = 1{,}0966227\frac{EV^2}{L^4}$$

(f) for isosceles triangle cross-sections ($\alpha = \frac{\sqrt{3}}{18}$)

$$P_{OPT} = 1{,}2662708\frac{EV^2}{L^4}$$

The optimum column design with the guided-clamped case boundary conditions is simply a scaled version (in the length direction) of half the column with both ends clamped and a symmetrical buckling mode (and two inner hinges placed at the quarter points). Due to the symmetry at the mid point, the upper half of the interval an optimum column and corresponding mode with guided-clamped boundary conditions. This optimum guided-clamped column also has the value P_{OPT} of its buckling load and the same values of E but only half of the and half the volume of the clamped-clamped column with the eigenvalue given above, so the optimum buckling eigenvalue for the optimum guided-clamped column of length L and volume V becomes:

$$P_{OPT} = \frac{4\pi^2}{3}(\frac{V}{L})^2\frac{\alpha E}{L^2} .$$

Finally, the optimal column for the case guided-clamped ends presents a half the optimal column clamped-clamped ends.

3.2.2.6 Guided-Pinned Case
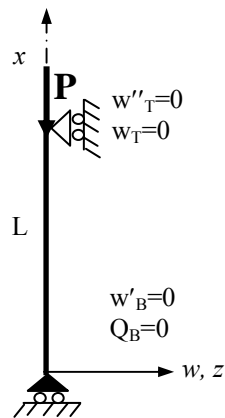
It is satisfied the two conditions at the end $x=0$ and at the other end $x=L$ for the guided-pinned case.

$$x = 0 \Rightarrow w_x(0) = Q(0) = 0$$

$$x = L \Rightarrow w(L) = w_{xx}(L) = 0$$

It is suitable followed boundary conditions for guided-pinned case. At the end $x=0$, it is also valid results obtained from guided-clamped case.

It is applied boundary conditions for x=L,

$$x = L \Rightarrow w(L) = 0 \Rightarrow w(L) - w(0) = w_x(0)L + \frac{1}{\lambda}\left[\phi_\varsigma(0) - \phi(1) + \phi(0)\right]$$

Deflection function and second derivative of the deflection function are written following equations, for x=0 and x=L, respectively:

$$w(0) = \frac{-1}{\lambda}\left[(3\lambda A_0)^{\frac{1}{2}} \cos\theta(0) - A_0^{\frac{3}{2}} \sin^3\theta(1) + A_0^{\frac{3}{2}} \sin^3\theta(0)\right]$$

$$w''(L) = \frac{1}{L^2 A_0^{\,2} \sin^4\theta(1)} A_0^{\frac{3}{2}} \sin^3\theta(1) \Rightarrow \phi(1) = 0 \Rightarrow \sin\theta(1) = 0$$

$$w(0) = \frac{-1}{\lambda}\left[\phi_\varsigma(0) - \phi(1) + \phi(0)\right]$$

$$w(0) = \frac{-1}{\lambda}\left[(3\lambda A_0)^{\frac{1}{2}} \cos\theta(0) + A_0^{\frac{3}{2}} \sin^3\theta(0)\right].$$

These equations are satisfied if it is set $\theta(0) = \frac{\pi}{2}, \theta(1) = \pi$. To obtain a and A0, it is used Equation (3.66) using $\theta(0)$ and $\theta(1)$:

$$\theta(\varsigma = 0) = \frac{\pi}{2} \Rightarrow \frac{\pi}{2} - \frac{1}{2}\sin(2\frac{\pi}{2}) + a = 2(\frac{\lambda}{3})^{\frac{1}{2}} A_0^{-1}.0 \Rightarrow a = -\frac{\pi}{2}$$

$$\theta(\varsigma = 1) = \pi \Rightarrow \pi - \frac{1}{2}\sin(2.\pi) = 2(\frac{\lambda}{3})^{\frac{1}{2}} A_0^{-1}.1 \Rightarrow A_0 = 4\pi^{-1}(\frac{\lambda}{3})^{\frac{1}{2}}$$

Finally, it is obtained Equation (3.66) followed:

$$\theta - \frac{1}{2}\sin 2\theta - \frac{\pi}{2} = \frac{\pi}{2}\varsigma$$

Here $\theta(\varsigma)$ is given by above equation. ς and $d\varsigma$ are obtained in $\theta(\varsigma)$:

$$\varsigma = \frac{2\theta}{\pi} - \frac{2}{2\pi}\sin 2\theta - 1 \Rightarrow d\varsigma = \frac{2}{\pi}d\theta - \frac{2}{2\pi}2\cos 2\theta d\theta$$

$$d\varsigma = 2(\frac{1 - \cos 2\theta}{\pi})d\theta = \frac{4}{\pi}\sin^2 \theta d\theta$$

To determine λ, it is used Equation (3.69) and Equation (3.66) in Equation (3.40) which yields:

$$\int_0^\theta A_0 \sin^2 \theta(\varsigma)\frac{4}{\pi}\sin^2 \theta(\varsigma)d\theta = \frac{V}{L} \Rightarrow \frac{4A_0}{\pi}\int_{\pi/2}^\pi \sin^4 \theta d\theta = \frac{V}{L} \Rightarrow V = \frac{3A_0L}{4}$$

Thus $A_0 = \frac{4V}{3L}$ and then using a and A_0 values yields for the eigenvalue λ,

$$\frac{4V}{3L} = \frac{4}{\pi}(\frac{\lambda}{3})^{1/2} \Rightarrow \lambda = \frac{\pi^2}{3}(\frac{V}{L})^2$$

The cross-sectional area $A(\varsigma)$ given by Equation (3.69) can now be written as,

$$A(\varsigma) = \frac{4}{3}\frac{V}{L}\sin^2 \theta(\varsigma)$$

It is shown that in Figure 3.9 a graph of $A(\varsigma)$.
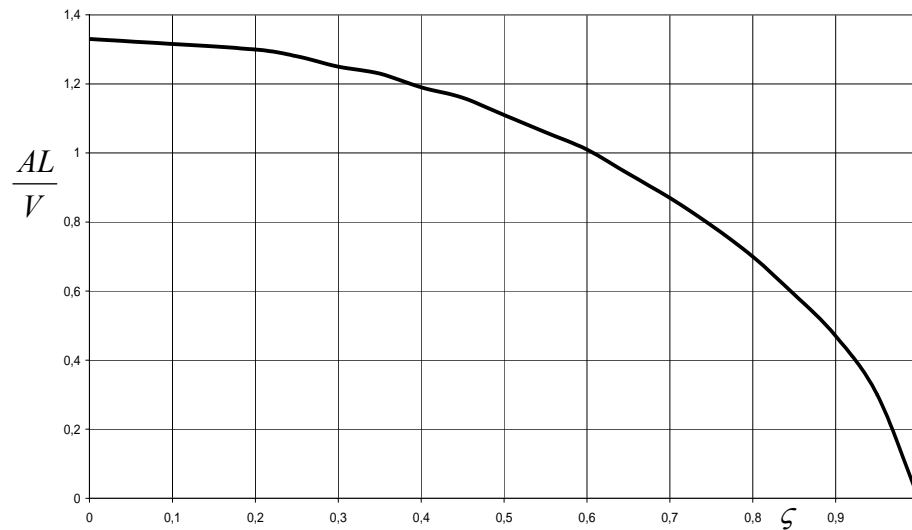
Figure 3.9 Cross-sectional area of strongest guided-pinned column as a function of distance along column

Finally, the optimum (nondimensional) eigenvalue and critical uckling load for guided-pinned case are given by

$$\lambda = \frac{PL^2}{E\alpha} \Rightarrow P_{OPT} = \frac{\lambda \alpha E}{L^2} \Rightarrow P_{OPT} = \frac{\pi^2}{3}(\frac{V}{L})^2 \frac{\alpha E}{L^2}$$

which gives:

(a) for cross-sectional of circular shape ($\alpha = \frac{1}{4\pi}$)

$$P_{OPT} = 0{,}2617994 \frac{EV^2}{L^4}$$

(b) for square shaped cross-sections ($\alpha = \frac{1}{12}$)

$$P_{OPT} = 0{,}2741557 \frac{EV^2}{L^4}$$

(c) for isosceles triangle cross-sections ($\alpha = \frac{\sqrt{3}}{18}$)

$$P_{OPT} = 0{,}3165677 \frac{EV^2}{L^4}$$

Let us consider the optimum column with both ends simply supported and the corresponding buckling mode. The optimum (nondimensional) buckling eigenvalue for both ends simply supported is given by,

$$\lambda = \frac{4\pi^2}{3}(\frac{V}{L})^2 .$$

Cut through at the mid point of the column axis the buckling mode and this optimum column with simply supported ends. Due to the symmetry at the mid point, the upper half of the interval an optimum column and corresponding mode with guided-pinned boundary conditions. This optimum guided-pinned column also has the value P_{OPT} of its buckling load and the same values of E but only half of the and half the volume of the simply supported column with the eigenvalue given above, so the optimum buckling eigenvalue for the optimum guided-pinned column of length L and volume V becomes,

$$\lambda = \frac{\pi^2}{3}(\frac{V}{L})^2$$

$$P_{OPT} = \frac{\pi^2}{3}(\frac{V}{L})^2 \frac{\alpha E}{L^2}$$

The optimal column for the case guided-pinned ends presents a half the optimal column simply supported at both ends.

The solution offered by Tadjbaksh & Keller with six different sets of boundary conditions is together displayed in Figure 3.10.

As shown in Figure 3.10, the cross-section area shows theoretically in points of *0,25 L* and *0,75 L* of column to zero *clamped-clamped* case. This area in the middle of the column decreases towards ends. *Hinged-hinged* column, the cross-section area is the maximum in the middle of the column and its becomes to zero hinged ends. The column in *guided-pinned* case has the maximum cross-section area at the guided end and this area decreases towards the hinged end, where it becomes zero. In this form, it is valid also optimum *clamped-free* column. It is reported that the optimal column for the case *guided-pinned* ends presents a half the optimal column simply supported at both ends. *Guided-clamped* ends, the cross-section area yields theoretically in the middle of column to zero. The area increases towards both ends, where they take the maximum value. It is also obvious that the optimal column for the case *guided-clamped* ends presents a half the optimal column clamped-clamped ends.
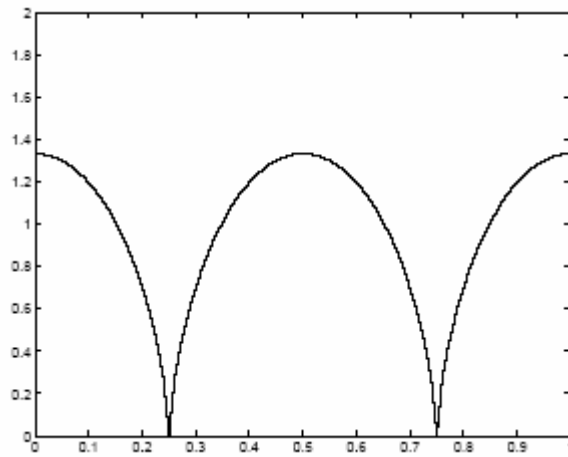
a) Optimum clamped-clamped column
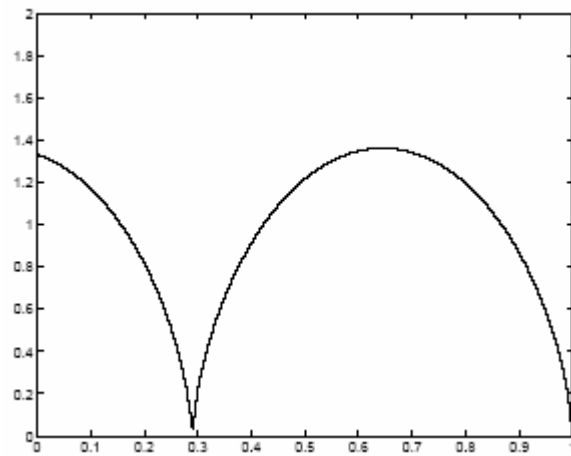
b) Optimum clamped-hinged column
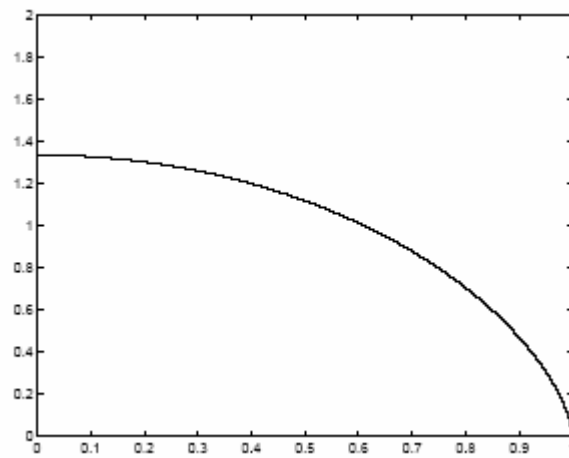
c) Optimum clamped-free column

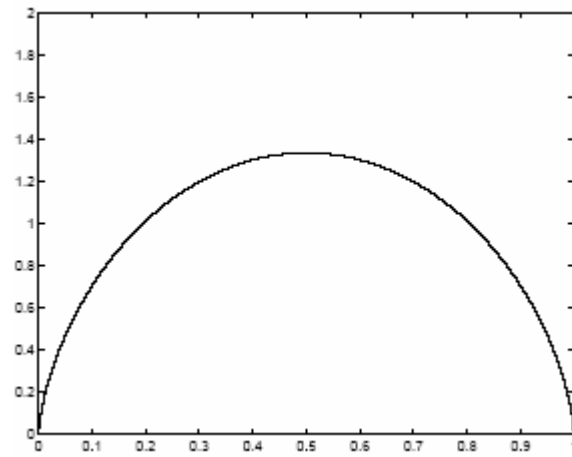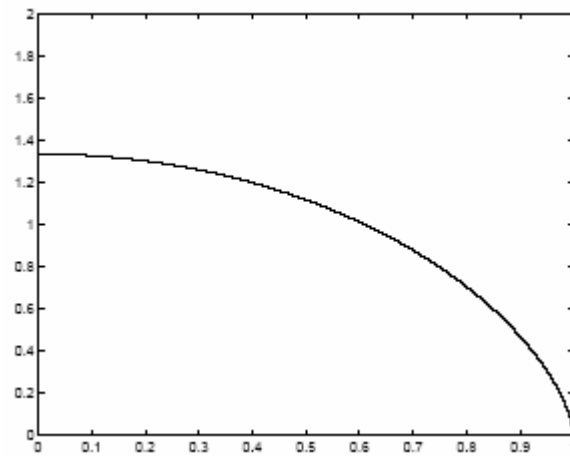Figure 3.10 The optimum solution offered by Tadjbaksh & Keller with different ends

d) Optimum hinged-hinged column

e) Optimum guided-pinned column
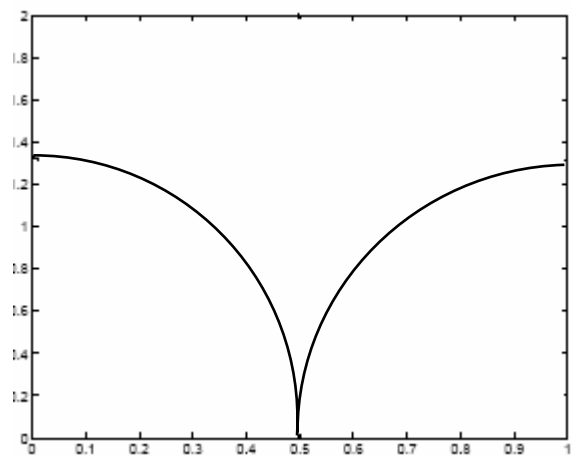
f) Optimum guided-clamped column

Figure 3.10 The optimum solution offered by Tadjbaksh & Keller with different ends (Continue)

The critical buckling load is also given in Table 3.2 and 3.3 for optimum columns with six different sets of boundary conditions and three different variable cross sections.

Table 3.2 Results obtained with respect to different supported types

Supported Types	$\theta(0)$	$\theta(1)$	a	A_0	λ
Clamped–Clamped	$-\pi/2$	$3\pi/2$	$\pi/2$	$\dfrac{1}{\pi}\left(\dfrac{\lambda}{3}\right)^{1/2}$	$\dfrac{16\pi^2}{3}\left(\dfrac{V}{L}\right)^2$
Clamped-Free	$-\pi/2$	0	$\pi/2$	$\dfrac{4}{\pi}\left(\dfrac{\lambda}{3}\right)^{1/2}$	$\dfrac{\pi^2}{3}\left(\dfrac{V}{L}\right)^2$
Clamped-Hinged	-1,4243	π	1,28	$0,452\left(\dfrac{\lambda}{3}\right)^{1/2}$	$2,76\pi^2\left(\dfrac{V}{L}\right)^2$
Hinged-Hinged	0	π	0	$\dfrac{2}{\pi}\left(\dfrac{\lambda}{3}\right)^{1/2}$	$\dfrac{4\pi^2}{3}\left(\dfrac{V}{L}\right)^2$
Guided–Pinned	$-\pi/2$	π	$-\pi/2$	$\dfrac{4}{\pi}\left(\dfrac{\lambda}{3}\right)^{1/2}$	$\dfrac{\pi^2}{3}\left(\dfrac{V}{L}\right)^2$
Guided-Clamped	$\pi/2$	$3\pi/2$	$-\pi/2$	$\dfrac{2}{\pi}\left(\dfrac{\lambda}{3}\right)^{1/2}$	$\dfrac{4\pi^2}{3}\left(\dfrac{V}{L}\right)^2$

Table 3.3 The critical buckling load for three variable cross-sections for different supported types

Supported types	Uniform Cross-sections	Cross-sectional of Circular shape	Square shaped Cross-sections	Isosceles triangle Cross-sections
Clamped-Clamped	$\dfrac{4\pi^2 EI}{L^2}$	$4{,}18879\dfrac{EV^2}{L^4}$	$4{,}38649\dfrac{EV^2}{L^4}$	$5{,}06508\dfrac{EV^2}{L^4}$
Clamped-Free	$\dfrac{\pi^2 EI}{4L^2}$	$0{,}26179\dfrac{EV^2}{L^4}$	$0{,}274155\dfrac{EV^2}{L^4}$	$0{,}31657\dfrac{EV^2}{L^4}$
Clamped-Hinged	$\dfrac{2{,}05\pi^2 EI}{L^2}$	$2{,}16609\dfrac{EV^2}{L^4}$	$2{,}26833\dfrac{EV^2}{L^4}$	$2{,}61925\dfrac{EV^2}{L^4}$
Hinged-Hinged	$\dfrac{\pi^2 EI}{L^2}$	$1{,}04719\dfrac{EV^2}{L^4}$	$1{,}09662\dfrac{EV^2}{L^4}$	$1{,}26627\dfrac{EV^2}{L^4}$
Guided–Pinned	$\dfrac{\pi^2 EI}{4L^2}$	$0{,}26179\dfrac{EV^2}{L^4}$	$0{,}274155\dfrac{EV^2}{L^4}$	$0{,}31657\dfrac{EV^2}{L^4}$
Guided-Clamped	$\dfrac{\pi^2 EI}{L^2}$	$1{,}04719\dfrac{EV^2}{L^4}$	$1{,}09662\dfrac{EV^2}{L^4}$	$1{,}26627\dfrac{EV^2}{L^4}$

In order to determine the achieved savings of material volume through the longitudinal optimal variation of the cross-section of the column, the respective critical buckling loads affecting columns with constant cross-section and with variable cross-sections as given in Table 3.3 must be equated to each other. In two cases treated in present study, a column having a uniform cross-section is additionally compared with another column of the same length that has a variable cross-section as well as the same buckling load. It is found that the volume relationship of the column with constant cross-section to the column with variable cross-section amounts to about 1.15, which is independent of the cross-section form

and of support type of the column; (i.e. up to 15 percent of the material in construction can be spared, if the longitudinal optimal cross-section of a column under a critical buckling load is determined).

3.2.3 Tadjbaksh-Keller's Results for Composite Specimens Specimens for Clamped-Clamped Case

In this Ph. D thesis, both natural and manufactured composite materials were examined for clamped-clamped case. In this section, it is calculated the critical buckling laod obtained by Tadjbaksh & Keller for clamped-clamped ends.

Tadjbaksh & Keller found optimum crtical buckling load following equation for clamped-clamped case:

$$\lambda = \frac{PL^2}{E\alpha} \Rightarrow P_{OPT} = \frac{\lambda \alpha E}{L^2} \Rightarrow P_{OPT} = \frac{16\pi^2}{3}(\frac{V}{L})^2 \frac{\alpha E}{L^2}.$$

To calculate of critical buckling load for various composite materials, it is needed young modulus for each material according to above equation obtained by Tadjbaksh & Keller. Properties of these materials were detailed found in the experimental section. Table 3.4 shows young modulus of cedar, oak, sapele and glass-epoxy, glass-vinylester, glass-polyester with different fiber orientation angle.

Table 3.4 Young modulus (E) of natural and manufactured composite materials for different fiber orientation angle (**MPa**)

a)

Natural Composite Materials	Modulus of Elasticity
CEDAR	2228,68
OAK	3426,41
SAPELE	4257,30

b)

Manufactured Composite Materials	0-degree Modulus of Elasticity (E)	45-degree Modulus of Elasticity (E)	90-degree Modulus of Elasticity (E)
GLASS-EPOXY	9943,86	7938,30	7242,98
GLASS-VINYLESTER	8123,04	7641,10	6942,40
GLASS-POLYESTER	7590,10	7254,10	6558,90

In calculations, the diameter length of oak and sapele is taken as 25 mm and 750 mm, respectively, for uniform cross-section, while the diameter of cedar is as 20 mm. It is found volume for uniform cross-section followed equation:

$$V = \frac{\pi(25)^2}{4}(750) = 368155,39 mm^3$$

$$V_{CEDAR} = \frac{\pi(20)^2}{4}(750) = 235619,45 mm^3$$

Due to $\frac{AL}{V} = 1,33$ for $\varsigma = 0$, it is obtained the cross-sectional area $A(\varsigma)$ and diameter for sapele, oak and cedar respectively:

For sapele and oak wood composite materials:

$$\frac{A(\varsigma)L}{V} = 1,33 \Rightarrow A(\varsigma) = 1,33\frac{V}{L} = 1,33\frac{(368155,39)}{750} = 652,87 mm^2$$

$$A(\varsigma) = \frac{\pi D_{Variable}^2}{4} = 652,87 \Rightarrow D_{Variable} = 28,83 mm$$

For cedar wood composite materials:

$$\frac{A(\varsigma)L}{V} = 1,33 \Rightarrow A_{cedar}(\varsigma) = 1,33\frac{V}{L} = 1,33\frac{(235619,45)}{750} = 417,83mm^2$$

$$A_{cedar}(\varsigma) = \frac{\pi D_{Variable}^2}{4} = 417,83 \Rightarrow D_{Variable} = 23,1mm$$

Consequently, it is calculated critical buckling load for natural and manufactured composite materials according to Tadjbaksh & Keller. Results are given in Tables 3.5 and 3.6 for three variable cross-sections.

Table 3.5 The analytic critical buckling load according to **<u>Tadjbaksh & Keller</u>** for wood composite materials with *variable cross-sections* ($D_{uniform}$=**25 mm and $D_{variable}$=28,83 mm for sapele and cedar, $D_{uniform}$=20 mm and $D_{variable}$=23,1 mm for cedar materials**)

Natural Composite Materials	Cross-section form		
	Circular Shape	Square Shape	Isosceles triangle cross-sections
OAK	6148,1618	6438,3401	7434,3547
SAPELE	7639,0652	7999,6104	9237,1544
CEDAR	1637,9990	1715,3085	1980,6677

It is obtained similarly equations for manufactured composite materials. In this case, the diameter of manufacture composited materials is taken as 22 mm.

For manufactured composite materials

$$V = \frac{\pi(22)^2}{4}(750) = 285099,53mm^3$$

$$\frac{A(\varsigma)L}{V} = 1,33 \Rightarrow A(\varsigma) = 1,33\frac{V}{L} = 1,33\frac{(285099,53)}{750} = 505,57 mm^2$$

$$A(\varsigma) = \frac{\pi D_{Variable}^{\;2}}{4} = 505,57 \Rightarrow D_{Variable} = 25,37 mm$$

Table 3.6 The analytic critical buckling load according to **Tadjbaksh & Keller** for composite materials with *variable cross-sections* for 0, 45 and 90 degree of fiber orientation angle (**$D_{uniform}$=22 mm and $D_{variable}$=25,37 mm**)

a) Fiber Orientation Angle=0 degree

Manufacture Composite Materials	Cross-section form		
	Circular Shape	Square Shape	Isosceles triangle cross-sections
GLASS-EPOXY	10700,1937	11205,2167	12938,6697
GLASS-VINYLESTER	8740,8815	9153,4297	10659,4702
GLASS-POLYESTER	8167,4059	8552,8874	9876,0237

b) Fiber Orientation Angle=45 degree

Composite specimens	Cross-section form		
	Circular Shape	Square Shape	Isosceles triangle cross-sections
GLASS-EPOXY	8542,0901	8945,2558	10329,0917
GLASS-VINYLESTER	8222,2849	8610,3567	9942,3835
GLASS-POLYESTER	7805,8496	8174,2666	9438,8300

c) Fiber Orientation Angle=90 degree

Composite specimens	Cross-section form		
	Circular Shape	Square Shape	Isosceles triangle cross-sections
GLASS-EPOXY	7793,8838	8161,7360	9424,3609
GLASS-VINYLESTER	7470,4416	7823,0281	9033,2548
GLASS-POLYESTER	7057,78	7390,8820	8534,2554

3.3 Olhoff & Rasmussen's Solution for Clamped-Clamped Case

Olhoff & Rasmussen (1977) showed that the optimal solution of buckling problem for columns with clamped ends should be bimodal, namely, possessing two linearly independent buckling modes, and they determined this optimal solution by a numerical method. They claimed that the column possesses a buckling mode that becomes critical at a lower value of the axial load than the mode considered in the analytical class of deflection functions than Tadjbaksh & Keller's solution. Note that the solution found by Olhoff & Rasmussen exhibits no hinges.

The optimal design problem has expressed by finding a structure of minimum volume for given lowest eigenvalue constraint. They reconsidered that the optimum fundamental buckling load λ^*, thus the optimum solution, should be a double eigenvalue. The governing equations for solving the problem were presented by variational analysis. In Olhoff & Rasmussen, a dimensionless cross-sectional area $\alpha^*(x)$ and a buckling load λ^* were introduced as follows:

$$\alpha^*(x) = A(x)L/V \tag{3.73}$$

$$\lambda^* = \frac{PL^4}{EcV^2} \tag{3.74}$$

Due to the consideration of the fundamental buckling load of the optimum column, which is a double eigenvalue, it follows:

$$\lambda^* = \int_0^1 \alpha^{*2} w_i''^2 dx \Rightarrow i = 1,2 \tag{3.75}$$

where w_1 (x) and w_2 (x) indicate the two buckling modes related to the optimum λ^*. It is also stated with the clamped end boundary conditions followed for unimodal and bimodal solution, respectively:

$$\left. \begin{array}{l} (\alpha^{*2} w'')'' = -\lambda^* w'' \\[2ex] w\ (0) = w'\ (0) = w(1) = w'\ (1) = 0 \end{array} \right\} \Rightarrow Eigenvalue \ \ problem \ \ of \ \ Unimodal \ \ solution$$

$$\tag{3.76}$$

$$\left. \begin{array}{l} (\alpha^{*2} w_i'')'' = -\lambda^* w_i'' \\[2ex] w_i(0) = w_i'\ (0) = w_i(1) = w_i'\ (1) = 0 \end{array} \right\} i = 1,2 \Rightarrow \ Bimodal \ solution \tag{3.77}$$

where the column ends $x=0$ and $x=1$. It is also expressed the fixed volume condition by,

$$\int_0^1 \alpha dx = 1 \tag{3.78}$$

In addition, it was expressed an additional constraint for the design variable $\alpha^*(x)$, i.e. $\alpha^*(x) \geq \bar{\alpha}$ throughout, assuming the minimum allowable value $\bar{\alpha}(0 \leq \bar{\alpha} \leq 1)$ to be given. The real slack variable g(x) gives the minimum constraint by means of:

$$g^2(x) = \alpha^*(x) - \overline{\alpha} \qquad (3.79)$$

In Equation (3.79), $\overline{\alpha}$ that is to be given denotes geometric minimum constraint. Olhoff & Rasmussen applied a variational formulation of optimization problem and they expressed by,

$$\lambda^{**} = \int_0^1 \alpha^{*2} w_1^{''2} dx - \gamma \left\{ \int_0^1 \alpha^{*2} w_1^{''2} dx - \int_0^1 \alpha^{*2} w_2^{''2} dx \right\} -$$

$$\sum_{i=1}^2 \eta_i \left\{ \int_0^1 w_1^{'2} dx - 1 \right\} - 2\beta \left\{ \int_0^1 \alpha^* dx - 2\int_0^1 \mu(x) \{ g^2 - \alpha^* + \overline{\alpha} \} dx 1 \right\} \qquad (3.80)$$

where Lagrangian multipliers $\gamma, \eta_i (i = 1,2), \beta$ and $\mu(x)$. The governing equations of the optimization problem were achieved as Euler-Lagrange equations following from the stationarity of the functional λ^{**} with respect to variation of $\alpha^*(x)$, $g(x)$ and $w_1(x)$ and $w_2(x)$. Variation of $\alpha^*(x)$ and $g(x)$ leads to the bimodal optimality condition, respectively, which may present the optimum cross-sectional area function $\alpha^*(x)$:

$$\alpha^* \left\{ (1-\gamma) w_1^{''2} + \gamma w_2^{''2} \right\} - \beta + \mu(x) = 0$$

$$\qquad (3.81)$$

$$\mu(x) g(x) = 0$$

The stationary of λ^* for arbitrary admissible variations of w_i (i=1, 2) gives the buckling differential equations for w_i after identifying the Lagrangian multipliers η_i by means of Equation (3.75). The unknowns to be obtained were the optimum double buckling eigenvalue λ^*, the optimum column cross-sectional area function $\alpha^*(x)$, the eigenfunctions w_1 and w_2 and the Lagrangian multipliers. The method used for solving equations of the bimodal eigenvalue optimization problem were consisted of a numerical procedure of successive iterations based on a finite difference

formulation of equations, in consideration of this geometric minimum constraint $\overline{\alpha}$. Figure 3.11 and 3.12 show the optimum column shapes for selected values of $\overline{\alpha}$.

It is shown in Figure 3.11, optimum column shapes, represented through $\pm\sqrt{\alpha^*}$, with associated fundamental modes w_1 (and w_2 when optimum λ^* is a double eigenvalue) for selected values of $\overline{\alpha}$. It is shown in Figure 3.11(c) and (d) the fundamental modes w_1 (x) and w_2 (x) for the double optimum eigenvalue solutions, which found out along with the optimum area function $\alpha^*(x)$, eigenvalue λ^* and Lagrangian multipliers from the non-linear optimality equations. The modes w_1 (x) and w_2 (x) belonging together were also non-symmetrical. For value of $\overline{\alpha}$ 0,7 and 0,4 respectively, it was found that the optimum buckling load was a simple eigenvalue.

The buckling loads were as 48,690 and 51,775 for $\overline{\alpha} = 0,7$ and $\overline{\alpha} = 0,4$ respectively. As shown in Figures 3.11(a) and (b), the column parts were mutually rigidly connected at the points $x = \dfrac{1}{4}$ and $x = \dfrac{3}{4}$, respectively, where the bending moment of the symmetrical mode vanishes, and where the geometric minimum constraint was active. For $\overline{\alpha} = 0,25$, it was detected that the optimum buckling load was a double eigenvalue. The buckling load was as 52,349. Optimum design was obtained for $0 \le \overline{\alpha} \le 0,226$, and the buckling load was as 52,3563 (Olhoff & Rasmussen, 1977).

As shown in Figure 3.12, it is displayed by curve ABCD the dimensionless buckling eigenvalue λ^* of the optimum solutions as a function of the minimum constraint $\overline{\alpha}$ in the interval $0 \le \overline{\alpha} \le 1$, where the end point values correspond to geometrically unconstrained and uniform column, respectively. It had been determined the second eigenvalues λ^*_2 of the optimum solutions subject to $0,280 \le \overline{\alpha} \le 1$ by means of a common procedure of calculating eigenvalues and

modes. It is displayed obtained results by curve CE in Figure 3.12. The second eigenvalue λ^*_2 combined with the fundamental eigenvalue λ^* of the optimum column for $\bar{\alpha} = 0,280$. The optimum buckling load λ^* was associated with two modes w_1 and w_2, by the curve ABC in Figure 3.12. This case was also shown in Figures 1(c) and (d). Optimum λ^* increases with decreasing geometric constraint for $0,226 \leq \bar{\alpha} \leq 1$, by the curve BCD in Figure 3.12. In addition, it found that the constraint $\bar{\alpha}$ was active in corresponding design. For any value $\bar{\alpha}$ in the interval $0 \leq \bar{\alpha} \leq 0,226$, it was obtained the same optimum design and double buckling load. Point A was denoted the optimum bimodal buckling load. The points H and G described the overestimated and the actual fundamental buckling load, respectively. This case is specified solution obtained by Tadjbaksh & Keller (Olhoff & Rasmussen, 1977).
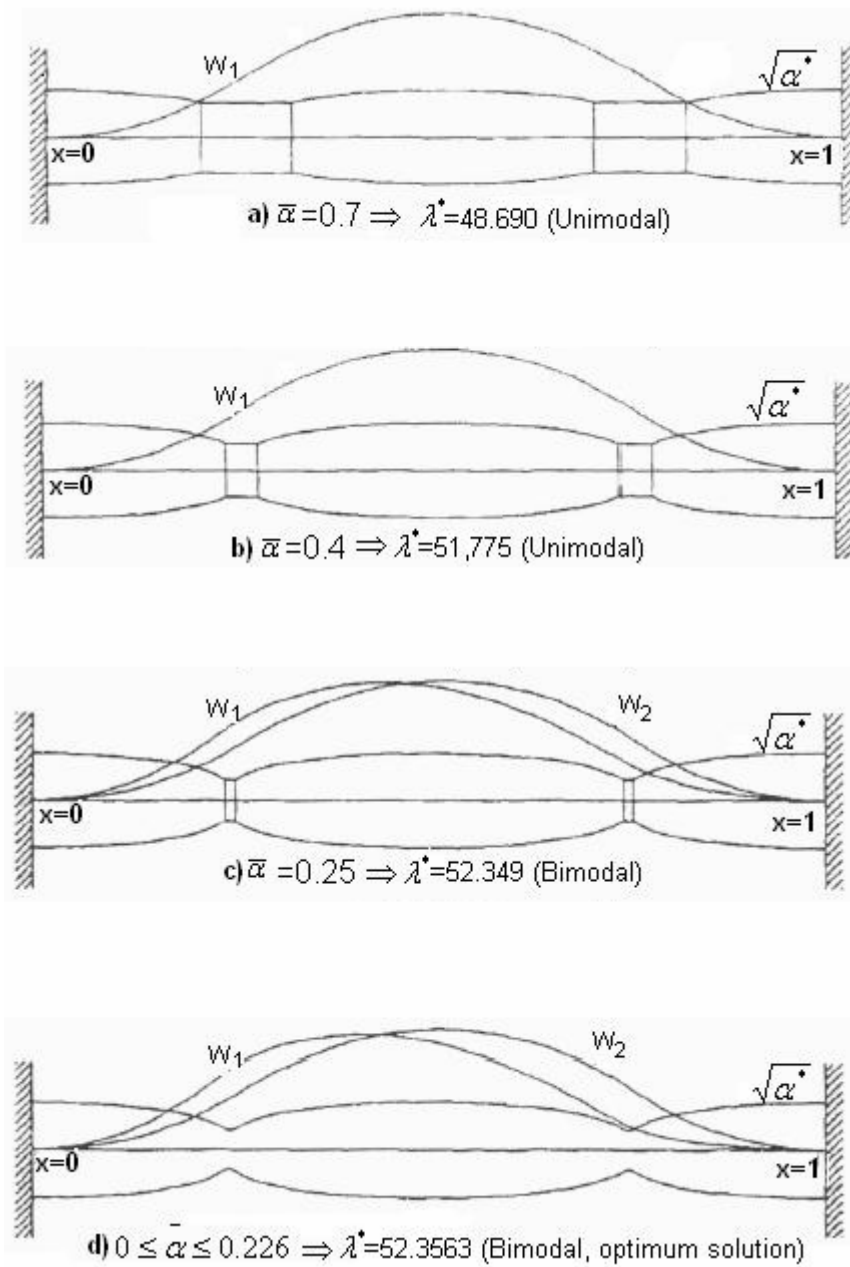
Figure 3.11 Optimum column shapes and associated fundamental modes according to Olhoff & Rasmussen (1977)
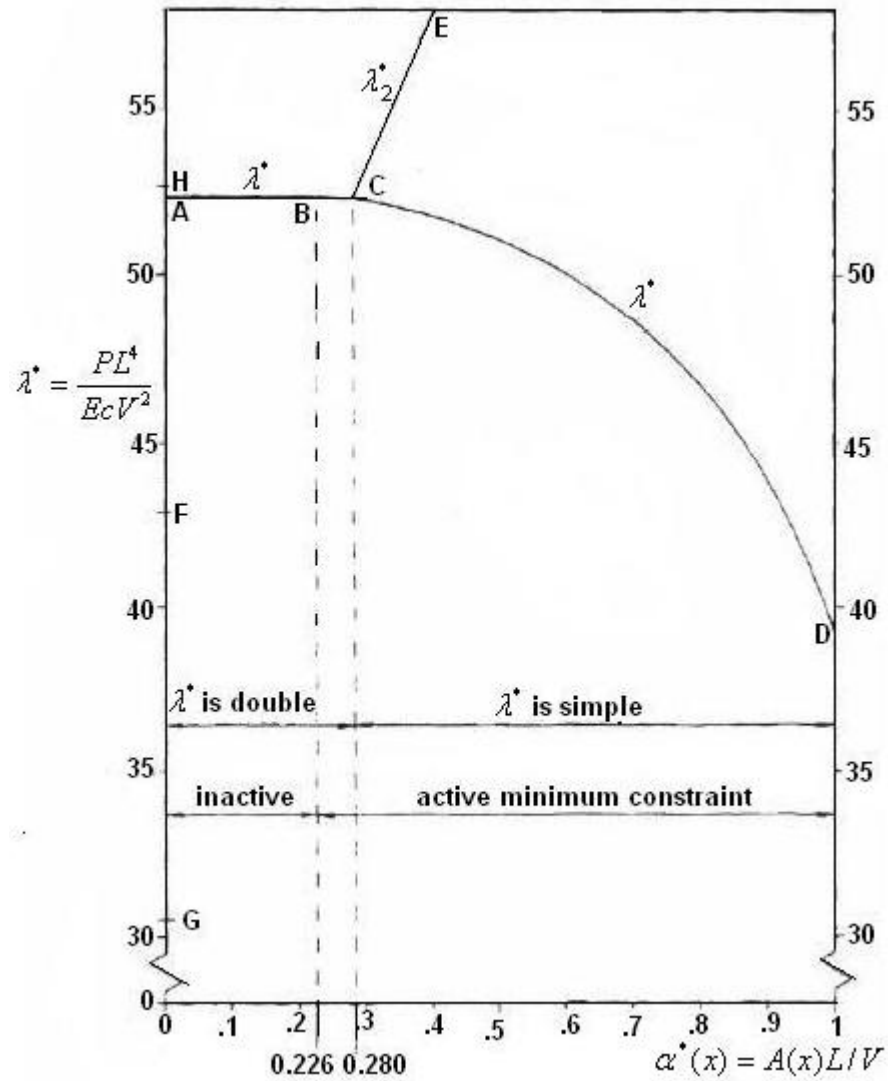
Figure 3.12 Optimum buckling loads vs. minimum constraint for column cross-sectional area according to Olhoff & Rasmussen (1977)
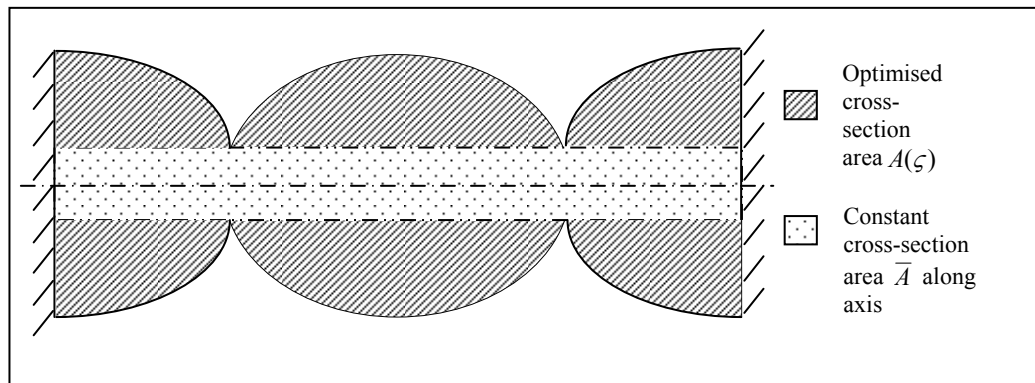
Figure 3.13 Optimised cross-sections of column with clamped ends according to the solution of Olhoff & Rasmussen

Olhoff & Rasmussen have assumed $\overline{\alpha}$ as a constant in their study. This means that the variable cross section consists of a certain constant and a variable term as seen in Equation 3.57. Thus, in Olhoff & Rasmussen's equation, a constant cross section assumption *prevails* at each point of the column, which cannot be equal to zero. Hence, the remaining volume is optimized as seen in Figure 3.13.

For this reason, when this constant volume denoted by $\overline{\alpha}$ is taken as zero, the constant volume requirement vanishes at every point of the column. In this case, both solutions of the optimization problems of Tadjbakhsh & Keller (1962) and Olhoff & Rasmussen (1977) are identical. Tadjbakhsh & Keller had not investigated the case, in which $\overline{\alpha}$ is unequal to zero, and therefore, the results of two studies cannot be compared with each other. For $\overline{\alpha}=0$, the buckling load obtained by Olhoff & Rasmussen (1977) with a numeric method was found to be as $\lambda^*=52{,}3563$ as bimodal buckling load of the optimum column. This result is quite close to the analytic solution value as $\lambda=52{,}638$ of Tadjbakhsh & Keller.

3.3.1 Olhoff-Rasmussen's Solution for Composite Specimens for Clamped-Clamped Case

The critical buckling load is calculated following equation acoording to Olhoff & Rasmussen's for clamped-clamped case:

$$\lambda = \frac{P_{Optimum}L^4}{E\alpha V^2} = 52,3563 \Rightarrow P_{Optimum} = 52,3563\frac{E\alpha V^2}{L^4}$$

which gives:

(a) for cross-sectional of circular shape ($\alpha = \frac{1}{4\pi}$)

$$P_{OPT} = 4,16639\frac{EV^2}{L^4}$$

(b) for square shaped cross-sections ($\alpha = \frac{1}{12}$)

$$P_{OPT} = 4,36302\frac{EV^2}{L^4}$$

(c) for isosceles triangle cross-sections ($\alpha = \frac{\sqrt{3}}{18}$)

$$P_{OPT} = 5,03799\frac{EV^2}{L^4}$$

It is given critical buckling load for natural and manufactured composite materials according to Olhoff & Rasmussen in Tables 3.7 and 3.8 for natural and manufactured composite materials, respectively, for three variable cross-sections.

Table 3.7 The analytic critical buckling load according to **Olhoff & Rasmussen** for wood composite materials with *variable cross-sections* ($D_{uniform}$=25 mm and $D_{variable}$=28,83 mm for sapele and cedar, $D_{uniform}$=20 mm and $D_{variable}$=23,1 mm for cedar materials)

Natural Composite Materials	Cross-section form		
	Circular Shape	Square Shape	Isosceles triangle cross-sections
OAK	6115,2707	6403,8965	7394,5827
SAPELE	7598,1981	7956,8144	9187,7379
CEDAR	1629,2360	1706,1320	1970,0716

Table 3.8 The analytic critical buckling load according to **Olhoff & Rasmussen** for composite materials with *variable cross-sections* for 0, 45 and 90 degree of fiber orientation angle ($D_{uniform}$=22 mm and $D_{variable}$=25,37 mm)

a) Fiber Orientation Angle=0 degree

Manufactured Composite Materials	Cross-section form		
	Circular Shape	Square Shape	Isosceles triangle cross-sections
GLASS-EPOXY	10642,9503	11145,2715	12869,4510
GLASS-VINYLESTER	8694,1199	9104,4611	10512,9261
GLASS-POLYESTER	8123,7122	8507,1315	9823,1894

b) Fiber Orientation Angle=45 degree

Manufactured Composite Materials	Cross-section form		
	Circular Shape	Square Shape	Isosceles triangle cross-sections
GLASS-EPOXY	8496,3920	8897,4009	10273,8336
GLASS-VINYLESTER	8178,2977	8564,2933	9889,1841
GLASS-POLYESTER	7764,0902	8130,5362	9388,3345

c) Fiber Orientation Angle=90 degree

Manufactured Composite Materials	Cross-section form		
	Circular Shape	Square Shape	Isosceles triangle cross-sections
GLASS-EPOXY	7752,1884	8118,0727	9373,9429
GLASS-VINYLESTER	7430,4765	7781,1768	8984,9290
GLASS-POLYESTER	7020,0150	7351,3426	8488,5992

3.4 Masur's Solution for Clamped-Clamped Case

Tadjbaksh & Keller (1962) obtained an optimal design that displayed hinges at the quarter points and symetric-buckling mode. Olhoff & Rasmussen (1977) showed that the solution was based on the double eigenvalue and exhibited no hinges and antisymetric-buckling mode. Masur (1984) has been reinvestigated for the case of a double eigenvalue in the light of singularity conditions. Masur (1984) derived the bimodal optimality conditions for the clamped-clamped case and stated an extension to multiple eigenvalues. Optimality was reached with the double eigevalue solution. In addition, previously established by Olhoff & Rasmussen double eigenvalue a solution was reinvestigated in the ligth of singularity conditions. It was derived specific necessary and sufficient conditions for local and global optimality and explicit optimality criteria were created for double eigenvalues, including a geometric interpretation. It was also developed an analytical closed solution for the case of the optimal design of clamped-clamped column.the results obtained by Masur were in good agreement with obtained by Olhoff & Rasmussen. Masur's solution is show followed:

The two buckling modes w_i (i=1, 2) are expressed by

$$(EIw_{ixx})_{xx} + Pw_{ixx} = 0, \ x \in [0, L]$$

(3.82)

$$w_i(0) = w_{ix}(0) = w_i(L) = w_{ix}(L) = 0$$

(3.83)

Let us assume the moment of inertia I is proportional to the square of the cross-section A and the introduce the non-dimensional variables ς and η and buckling load parameter λ through

$$I = \alpha.A^2$$

(3.84)

$$A(\varsigma) = \frac{V}{L} h(\varsigma) = \frac{V}{L} \sqrt{\lambda} \eta(\varsigma), x = \varsigma L$$

(3.85)

$$P = \frac{E\alpha V^2 \lambda}{L^4}$$

(3.86)

Then Equation (3.82) reduces to:

$$(EIw_{ixx})_{xx} + Pw_{ixx} = 0$$

$$\left[E\alpha A^2(x)w_{ixx} \right]_{xx} + P.\frac{d}{dx}\left\{ \frac{d}{dx} w_i \right\} = 0$$

$$\frac{d}{dx}\left\{ \frac{d}{dx}(E\alpha A^2(x)w_{ixx}) \right\} + P\frac{d}{dx}\left\{ \frac{d\varsigma}{dx} \frac{d}{d\varsigma} u_i \right\} = 0$$

$$\frac{d}{dx}\left\{ \frac{d\varsigma}{dx} \frac{d}{d\varsigma}(E\alpha A^2(x)w_{ixx}) \right\} + P\frac{d}{dx}(\frac{1}{L} w_i') = 0$$

$$\frac{d}{dx}\left\{ \frac{d}{d\varsigma}(E\alpha \frac{A^2(x)}{L} w_{ixx}) \right\} + P\frac{d\varsigma}{dx} \frac{d}{d\varsigma}(\frac{1}{L} w_i') = 0$$

$$\frac{d\varsigma}{dx}\frac{d}{d\varsigma}\left\{\frac{d}{d\varsigma}(E\alpha\frac{A^2(x)}{L}w_{ixx})\right\} + P\frac{d}{d\varsigma}(\frac{1}{L^2}w_i{}') = 0$$

$$\frac{d}{d\varsigma}\left\{\frac{d}{d\varsigma}(E\alpha\frac{A^2(x)}{L}w_{ixx})\right\} + P(\frac{1}{L^2}w_i{}'') = 0$$

$$\frac{d}{d\varsigma}\left\{\frac{d}{d\varsigma}(E\alpha\frac{A^2(x)}{P}w_{ixx})\right\} + w_i{}'' = 0$$

$$\frac{d}{d\varsigma}\left\{\frac{d}{d\varsigma}(E\alpha\frac{A^2(x)}{P}\frac{d}{dx}(\frac{d}{dx}w_i))\right\} + w_i{}'' = 0$$

$$\frac{d}{d\varsigma}\left\{\frac{d}{d\varsigma}(E\alpha\frac{A^2(x)}{P}\frac{d}{dx}(\frac{d\varsigma}{dx}\frac{d}{d\varsigma}w_i))\right\} + w_i{}'' = 0$$

$$\frac{d}{d\varsigma}\left\{\frac{d}{d\varsigma}(E\alpha\frac{A^2(x)}{P}\frac{d}{dx}(\frac{1}{L}w_i{}'))\right\} + w_i{}'' = 0$$

$$\frac{d}{d\varsigma}\left\{\frac{d}{d\varsigma}(E\alpha\frac{A^2(x)}{P}\frac{d\varsigma}{dx}\frac{d}{d\varsigma}(\frac{1}{L}w_i{}'))\right\} + w_i{}'' = 0$$

$$\frac{d}{d\varsigma}\left\{\frac{d}{d\varsigma}(E\alpha\frac{A^2(x)}{P}\frac{1}{L^2}w_i{}'')\right\} + w_i{}'' = 0$$

$$\frac{d^2}{d\varsigma^2}\left\{E\alpha\frac{\eta^2(\varsigma)V^2\lambda}{P}\frac{1}{L^4}w_i{}''\right\} + w_i{}'' = 0$$

$$P = \frac{E\alpha V^2\lambda}{L^4} \Rightarrow \left[\eta^2(\varsigma)w_i{}''\right]'' + w_i{}'' = 0, \varsigma \in [0,1]$$

$$\left[\eta^2(\varsigma)w_i{}''\right]'' + w_i{}'' = 0, \varsigma \in [0,1] \tag{3.87}$$

with boundary conditions,

$$w_i(0) = w_i'(0) = w_i(1) = w_i'(1) = 0, i = 1,2 \qquad (3.88)$$

The design variable $\eta(\varsigma)$ being symetric with respect to the center of the column and with the assumption that w_1 is symetric and w_2 is antisymetric, optimality condition with the introduction of Lagrangian multipliers γ_{ij}, becomes (Masur, 1984),

$$\sum_{i=1}^{n}\sum_{j=1}^{n}\gamma_{ij\Omega_{ij}} = k^2 \qquad (3.89)$$

$$\gamma_{11}\Omega_{11} + 2\gamma_{12}\Omega_{12} + \gamma_{22}\Omega_{22} = k^2 \Rightarrow c_1^{\,2}\eta w_1''^2 + c_2^{\,2}\eta w_2''^2 = 1, \varsigma \in [0,1] \qquad (3.90)$$

where Ω_{ij} is the surface energy densities, and the column buckles into a symetric mode of constant curvature $w_1'' = \pm k$, in the central half and in the quarter points.

Masur stated that Equation (3.89) were necessary for local optimality and represented a generalization and extension of the conditions first introduced by Olhoff & Rasmussen. Additionally, global optimality established restrictions on the value of the Lagrangian multipliers γ_{ij}. This condition is stated for the case, $n = 2$ by Masur.

The volume constraint is written as,

$$\int_0^1 \eta d\varsigma = \frac{1}{\sqrt{\lambda}}. \qquad (3.91)$$

It is satisfied Equation (3.90) by letting,

$$w_1'' = \frac{\sin\theta}{c_1\sqrt{\eta}}, w_2'' = \frac{\cos\theta}{c_2\sqrt{\eta}}, \theta \equiv \theta(\varsigma). \tag{3.92}$$

When Equation (3.92) inserted in Equation (3.87), it is obtained,

$$(\eta^{3/2}\sin\theta)'' + \eta^{-1/2}\sin\theta = 0$$
$$. \tag{3.93}$$
$$(\eta^{3/2}\cos\theta)'' + \eta^{-1/2}\cos\theta = 0$$

By multiplying the first these by $\cos\theta$ and the second by $\sin\theta$ and by taking difference, and after integration:

$$3\eta^{1/2}\eta'\theta' + \eta^{3/2}\theta'' \equiv \eta^{-3/2}(\eta^3\theta')' = 0 \Rightarrow \theta' = \frac{a}{\eta^3} \tag{3.94}$$

which a is the integration constant. Similarly, by multiplying the first of Equation (3.93) by $\sin\theta$ and the second by $\cos\theta$ and by adding two, and after integration:

$$\eta'' + \frac{1}{2}\frac{\eta'^2}{\eta} - \frac{2}{3}\frac{a^2}{\eta^5} + \frac{2}{3\eta} = 0$$

$$\eta'^2 = \frac{4}{3}\frac{q(\eta)}{\eta^4} \Rightarrow q(\eta) = -\eta^4 + \frac{3}{2}b\eta^3 - \frac{1}{3}a^2 \tag{3.95}$$

where b is the another integration constant. These constants are determined from the boundary conditions. When Equation (3.87) is integrating, it is showed following equations:

$$w_1'' = \frac{-1}{c_1}(\eta^{3/2}\sin\theta)'',\ w_2'' = \frac{-1}{c_2}(\eta^{3/2}\cos\theta)'' \tag{3.93}$$

$$w_1 = \frac{-1}{c_1}\left[\eta^{3/2}\sin\theta - \eta_0^{3/2}\sin\theta_0\right]$$

$$w_2 = \frac{-1}{c_2}\left[\eta^{3/2}\cos\theta + (2\varsigma-1)\eta_0^{3/2}\cos\theta_0\right] \tag{3.94}$$

in which $\eta_0 \equiv \eta(0) = \eta(1)$ and $\theta_0 \equiv \theta(0)$. It is obtained the final form of Equations (3.75) and (3.76), respectively,

$$d\varsigma = \pm\frac{\sqrt{3}}{2}\frac{\eta^2 d\eta}{\sqrt{q(\eta)}} \tag{3.95}$$

$$d\theta = \pm\frac{\sqrt{3}}{2}\eta_0^3\sin 2\theta_0\frac{d\eta}{\eta\sqrt{q(\eta)}} \tag{3.96}$$

where

$$q(\eta) = -\eta^4 + \eta^3\left[\eta_0 + \frac{2}{3}\eta_0^3(1+\cos 2\theta_0)\right] - \frac{1}{3}\eta_0^6\sin^2 2\theta_0$$

$$\equiv (\eta_1 - \eta)(\eta - \eta_2)(\eta - \eta_3)(\eta - \eta_4)$$

If ς_2 is described by $\eta(\varsigma_2) = \eta_2$, it follows from Equation (3.95) that

$$\varsigma_2 = \frac{\sqrt{3}}{2}\int_{\eta_2}^{\eta_0}\frac{\eta^2 d\eta}{\sqrt{q}}. \tag{3.97}$$

Similarly again from Equation (3.96),

$$\varsigma(\eta) = \varsigma_2 - \frac{\sqrt{3}}{2} \int_{\eta_2}^{\eta} \frac{\eta^2 d\eta}{\sqrt{q}}, \varsigma \in \left[0, \varsigma_2\right] \tag{3.98}$$

$$\varsigma(\eta) = \varsigma_2 + \frac{\sqrt{3}}{2} \int_{\eta_2}^{\eta} \frac{\eta^2 d\eta}{\sqrt{q}}, \varsigma \in \left[\varsigma_2, \frac{1}{2}\right] \tag{3.99}$$

It is noted that $\varsigma(\eta_1) = (\frac{1}{2})$ from Equation (3.99) with the substitution of Equation (3.98), to determine the remaining constants η_0 and θ_0, this means that,

$$\frac{1}{2} = \frac{\sqrt{3}}{2} (\int_{\eta_2}^{\eta_0} \frac{\eta^2 d\eta}{\sqrt{q}} + \int_{\eta_2}^{\eta_1} \frac{\eta^2 d\eta}{\sqrt{q}}) \tag{3.100}$$

It is also $\theta(0) = \theta_0$ and $\theta(\frac{1}{2}) = \frac{3\pi}{2}$. And integration of Equations (3.96) is followed,

$$\frac{3\pi}{2} - \theta_0 = \frac{\sqrt{3}}{2} \eta_0^{\,3} \sin 2\theta_0 (\int_{\eta_2}^{\eta_0} \frac{d\eta}{\eta\sqrt{q}} + \int_{\eta_2}^{\eta_1} \frac{d\eta}{\eta\sqrt{q}}) \tag{3.101}$$

which involves elliptic integrals of the first, second and third kind. It is jointly solved Equation (3.100) and (3.101) to determine the remaining constants η_0 and θ_0. It is also expressed the colume constraint Equation (3.91),

$$\frac{1}{\lambda} = 3 \left\{ \int_{\eta_2}^{\eta_0} \frac{\eta^2 d\eta}{\sqrt{q}} + \int_{\eta_2}^{\eta_1} \frac{\eta^2 d\eta}{\sqrt{q}} \right\}^2 . \tag{3.102}$$

Obtained results are shown below (Masur, 1984):

$$\lambda = 52{,}3565$$

$$\theta_0 = 1{,}24984$$

$$\eta_0 = 0{,}18427 \Rightarrow h_0 = 1{,}33334$$

$$\eta_1 = 0{,}18435 \Rightarrow h_0 = 1{,}33392$$

$$\eta_2 = 0{,}03121 \Rightarrow h_2 = 0{,}22583$$

$$\eta_{3,4} = -0{,}01523 \pm 0{,}02411i$$

The buckling load was 52,3565 by Masur from the bimodal optimum solution.Consequently, Masur (1984) showed that the solution was based on the a double eigenvalue and exhibited no hinges and antisymetric buckling mode.

3.4.1 Masur's Solution for Composite Specimens for Clamped-Clamped Case

The critical buckling load is calculated following equation acoording to Masur's for clamped-clamped case:

$$\lambda = \frac{P_{Optimum}L^4}{E\alpha V^2} = 52{,}3565 \Rightarrow P_{Optimum} = 52{,}3565\frac{E\alpha V^2}{L^4}$$

which gives:

(a) for cross-sectional of circular shape ($\alpha = \frac{1}{4\pi}$)

$$P_{OPT} = 4{,}166398788\frac{EV^2}{L^4}$$

(b) for square shaped cross-sections ($\alpha = \frac{1}{12}$)

$$P_{OPT} = 4{,}36304166\frac{EV^2}{L^4}$$

(c) for isosceles triangle cross-sections ($\alpha = \frac{\sqrt{3}}{18}$)

$$P_{OPT} = 5{,}03780066\frac{EV^2}{L^4}$$

It is given critical buckling load for natural and manufactured composite materials according to Masur in Tables 3.9 and 3.10 for natural and manufactured composite materials, respectively, for three variable cross-sections.

Table 3.9 The analytic critical buckling load according to **Masur** for wood composite materials with *variable cross-sections* ($D_{uniform}$=25 mm and $D_{variable}$=28,83 mm for sapele and cedar, $D_{uniform}$=20 mm and $D_{variable}$=23,1 mm for cedar materials)

Natural Composite Materials	Cross-section form		
	Circular Shape	Square Shape	Isosceles triangle cross-sections
OAK	6115,2940	6403,9209	7394,6109
SAPELE	7598,2271	7956,8448	9187,7730
CEDAR	1629,2423	1706,1386	1970,0791

Table 3.10 The analytic critical buckling load according to **Masur** for composite materials with *variable cross-sections* for 0, 45 and 90 degree of fiber orientation angle ($D_{uniform}$=22 mm and $D_{variable}$=25,37 mm)

a) Fiber Orientation Angle=0 degree

Manufactured Composite Materials	Cross-section form		
	Circular Shape	Square Shape	Isosceles triangle cross-sections
GLASS-EPOXY	10642,9910	11145,3140	12869,5001
GLASS-VINYLESTER	8694,1531	9104,4958	10512,9662
GLASS-POLYESTER	8123,7433	8507,1641	9823,2269

b) Fiber Orientation Angle=45 degree

Manufactured Composite Materials	Cross-section form		
	Circular Shape	Square Shape	Isosceles triangle cross-sections
GLASS-EPOXY	8496,4244	8897,4349	10273,8728
GLASS-VINYLESTER	8178,3289	8564,3260	9889,2319
GLASS-POLYESTER	7764,1198	8130,5673	9388,3704

c) Fiber Orientation Angle=90 degree

Manufactured Composite Materials	Cross-section form		
	Circular Shape	Square Shape	Isosceles triangle cross-sections
GLASS-EPOXY	7752,2180	8118,1037	9373,9787
GLASS-VINYLESTER	7430,5049	7781,2065	8984,9634
GLASS-POLYESTER	7020,0419	7351,3706	8488,6316

3.5 Proposed Optimum Solution for Clamped-Clamped Case

The purpose of this Ph. D. thesis, optimum design of composite structures against buckling is achieved by finding the minimum weight structure that satisfies a buckling load constraint. In another words, it is thought about determining what shape of column has the largest possible buckling load of composite column of a given length and volume. The optimization problem is formulated as the maximization of the smallest eigenvalue given total volume of material of the structure. Alternatively, it may be to maximise the fundamental buckling load for a structure with a given volume or weight. For this case, both natural and man-made composite materials with different fiber orientation angle were studied for clamped-clamped ends.

Tadjbakhsh & Keller (1962) examined analytically the optimal longitudinal cross-sections of column under critical buckling loads for different support ends "clamped/clamped, clamped/free and clamped/slide-hinged case". For clamped-clamped ends, it was found that points of zero thickness, and consequently of infinite stress exist at the columns ends, as shown in Figure 3.14.
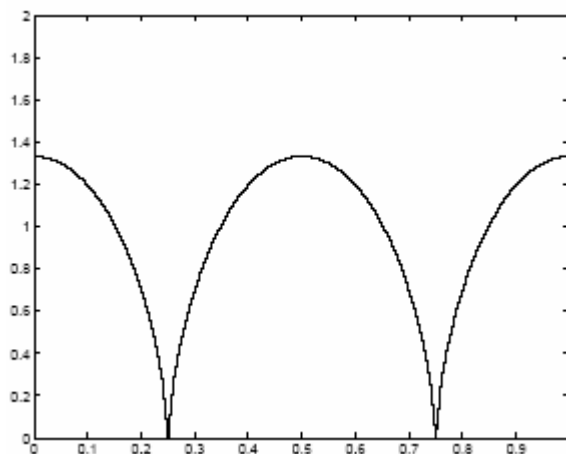

Figure 3.14 Optimal clamped-clamped column according to Tadjbaksh & Keller

Olhoff & Rasmussen (1977) displayed that the bimodality of the optimum eigenvalue must be taken into account in the mathematical formulation of the problem in order to obtain the correct optimum solution and determined numerically the optimal solution to the problem.
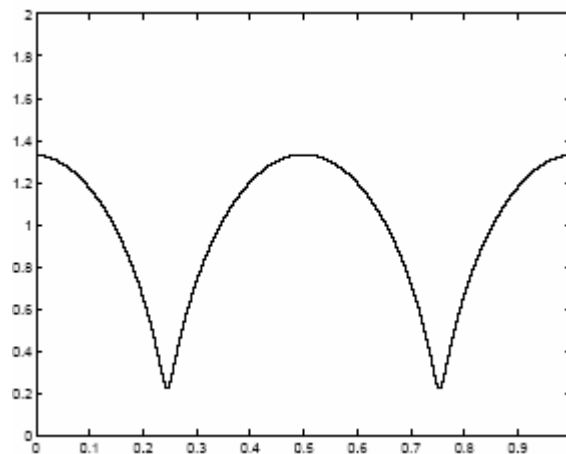

Figure 3.15 Optimal clamped-clamped column according to Olhoff & Rasmussen

The solution given by Olhoff & Rasmussen (1977) displayed in Figure 3.15 has a double eigenvalue. The optimum bimodal buckling load was later given in Masur (1984). Considering clamped-clamped ends, Masur's solution was allowed bimodal optimum condition. Masur's solution was good agreement with Olhoff & Rasmussen's solution.

There have followed a sequence of alternative designs which have come closer and closer in both shape and buckling load to the original Tadjbakhsh & Keller's (1962) solution. Non dimensional buckling load obtained by Tadjbaksh & Keller, Olhoff & Rasmussen and Masur was shown in Table 3.11.

Table 3.11 Comparison of non dimensional buckling load of given for optimum columns

Prescribed Buckling Load	Tadjbaksh & Keller (1962)	Olhoff & Rasmussen (1977)	Masur (1984)
$\lambda = \dfrac{NL^4}{E\alpha V^2}$	52,6379	52,3563	52,3565

However, in these solutions, it is only considered stability criterion in structure. Especially in points of minimum thickness which was found with bimodal optimum solution is crush occurred but not buckling. Consequently, bimodal solution is not practical and optimal since in points of minimum thickness crush occurred but not buckling. This leads to the necessity of both stability and crush criterion formulation of the optimization problem.

The present contribution of this Ph. D. thesis is that crush is taken into account in the formulation of column optimization problem allowing for bimodal optimum solution. The criteria will be developed here with the use of both the analytical closed solution found by Masur (1984) for clamped-clamped ends and crush criterion in points of minimum thickness. True solution that is applicaple to practise was obtained that was taken into account crushing criteria to Masur's analytic bimodal solution for clamped-clamped case.

New proposed optimum solution obtained by taking into accounts both stability and crush criterion will be verified with numerical analysis and experimental data for columns with clamped ends.

In new proposed optimum solution column design given length and volume will be resisted both buckling and crush, especially, in points of minimum thickness. To understand the verification of the new proposed optimum solution, natural and manufactured composite specimens including i.e. cedar (cedrela), sapele (entandrophragma cylindricum) oak (quercus spp.), glass-epoxy, glass-vinylester and

glass-polyester with 0, 45 and 90 degree of fiber orientation angle were tested experimentally and numerically and (Sayman & Pekbey 2004).

In this Ph. D. thesis, it is rearranged in points of minimum thickness in our solution obtained by taking into consideration both stability and crush criterion. At first, the crushing criterion is considered in points of minimum thickness for an assumed initial shape of a column obtained by Masur bimodal solution. In the model by Masur, in points of minimum thickness crush occurred but not buckling. For this reason, the bimodal solution which obtained by Masur is not optimal and practical. An example is shown for this case belowed. The present contribution of this Ph. D. thesis is that crush is taken into account in the formulation of column optimization problem allowing for bimodal optimum solution. For this reason, it is firstly chosen the volume, which satisfied bimodal optimality conditions given by Masur for endure buckling and crushing in columns. The chosen volume value is smaller than the initial volume that is equal to the uniform column's volume. Next, it is added volume, ΔV, in the points of minimum thickness. The volume that is added, ΔV is formulated in MATLAB that is mathematical programe. Such a procedure is repeated until the difference between assumed volume and initial volume is zero. Flow scheme of new optimum proposed solution is showed in Figure 3.16.
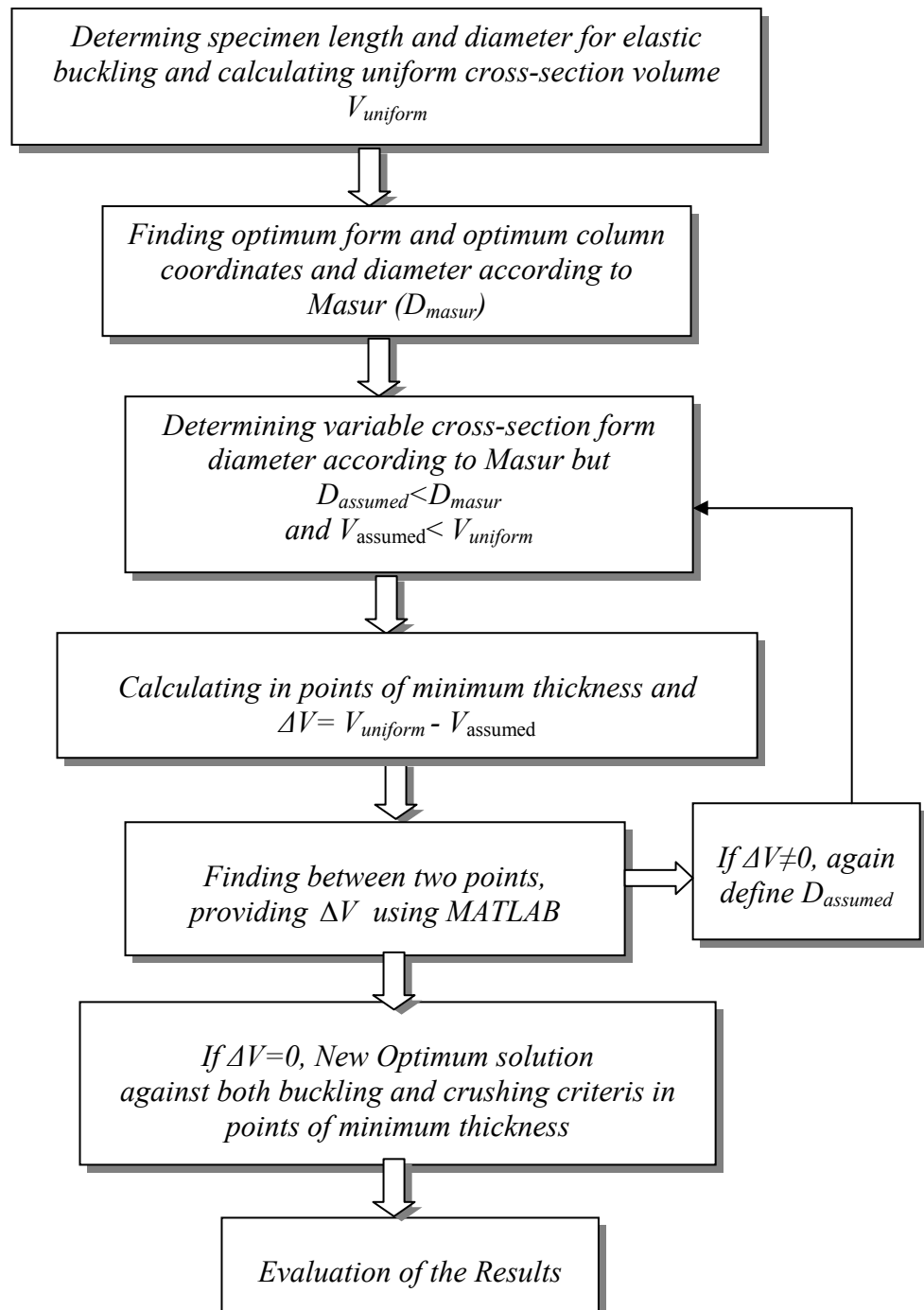
Figure 3.16 Flow scheme of new optimum proposed solution

The criteria will be developed here with the use of both the analytical closed solution found by Masur (1984) for clamped-clamped ends and crush criterion in points of minimum thickness. For this reason, the cross-sections at $\varsigma = \dfrac{1}{4}$ and $\varsigma = \dfrac{3}{4}$ have been increased to make it safe against crushing according to the following equation:

$$A \geq \frac{N_{cr}}{\sigma_{yield}} \tag{3.103}$$

In our new optimum column design given length and volume is resisted both buckling and crush, especially, in points of minimum thickness. It is also given an example following section depending on new optimum solution.

As a result of this P.h. D. thesis, it was shown that results obtained in the previous studies of variation optimum cross-sectional area for columns under compressive forces clamped-clamped ends were erroneous. The corrected optimum form was obtained, as shown in Figure 3.17, and results were checked by numerical calculations and experimental tests of natural and manufactured composite columns.
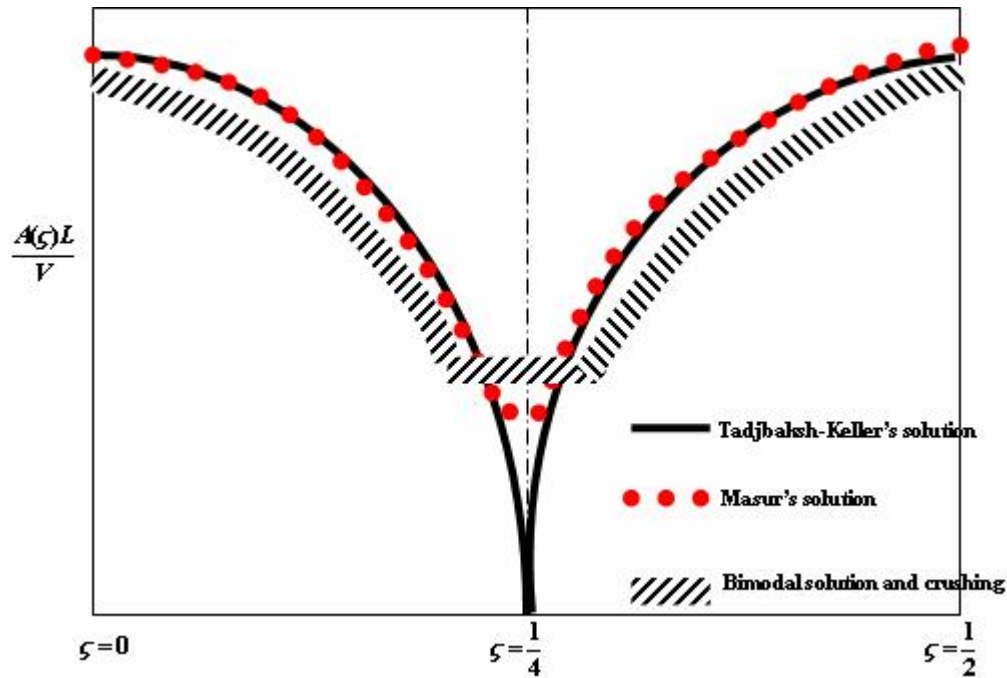
Figure 3.17 Comparisions of optimum shape of clamped-clamped column obtained by Tadjbaksh & Keller, Masur and New Proposed Optimum Solution

3.5.1 An Examined Case for Clamped-Clamped ends

Let us define glass-epoxy uniform composite column with circular shape which diameter and length of the column is as 22 mm and 750 mm respectively. The critical Euler buckling load is obtained followed equation for clamped-clamped case:

$$P_{EULER} = \frac{4\pi^2 EI}{L^2} = \frac{4\pi^2(9943,86)\left[\frac{\pi(22)^4}{64}\right]}{(750)^2} = 8025,14N$$

Mechanical properties for glass-epoxy are obtained from experiments as follows:

$$E = 9943,86 MPa; \sigma_{yield} = 106,8 MPa$$

Now, it is purposed to maximise the fundamental buckling load for the composite column with a given volume, i.e. $V = \dfrac{\pi(22)^2}{4}(750) = 285099,53mm^3$.

The optimum form was specified in following diameter according to Tadjbaksh & Keller and Masur as representing $\varsigma = \dfrac{x}{L}$:

Maximum diameter:

$$\varsigma = 0 = 0,5 = 1 \Rightarrow \frac{AL}{V} = 1,33 \Rightarrow \frac{\pi D_{max.}^{2}}{4}\frac{750}{285099,53} = 1,33 \Rightarrow D_{max.} = 25,37mm$$

Table 3.12 The optimum column coordinates according to Tadjbaksh & Keller for diameter of 25,37 mm with variable circle cross-sections (**D$_{maximum}$=25,37 mm, V=285099,53 mm^3**)

ς	x (mm)	$\dfrac{AL}{V}$	Radius, mm Tadjbaksh & Keller's solution
0	0	1,33	12,685
0,1	75	1,20	12,05
0,2	150	0,7	9,20
0,25	187,5	0	0
0,3	225	0,7	9,20
0,4	300	1,2	12,05
0,5	375	1,33	12,685
0,6	450	1,2	12,05
0,7	525	0,7	9,20
0,75	562,5	0	0
0,8	600	0,7	9,20
0,9	675	1,2	12,05
1	750	1,33	12,685

Masur gave it following equation in points of minimum thickness:

$$A(\varsigma) = \frac{V}{L}(0,22583) = \frac{285099,53}{750}(0,22583) = 85,845$$

$$\frac{\pi D_{min}{}^2}{4} = 85,845 \Rightarrow D_{min} = 10,454 mm$$

The critical buckling load is written followed:

$$P_{TADJBAKSH-KELLER} = 4,188\frac{EV^2}{L^4} = 4,188\frac{(9943,86)(285099,53)^2}{(750)^4} = 10698,173N$$

$$P_{MASUR} = 4,16639\frac{EV^2}{L^4} = 4,16639\frac{(9943,86)(285099,53)^2}{(750)^4} = 10642,97N$$

Table 3.13 The optimum column coordinates according to Masur for diameter of 25,37and 23,64 mm mm with variable circle cross-sections

ς	x (mm)	$\dfrac{AL}{V}$	Masur's solution	
			Radius, mm $D_{maximum}=25,37$ mm, $V=285099,53$ mm³	Radius, mm $D_{maximum}=23,64$ mm $V=247510,968$ mm³
0	0	1,33	12,685	11,82
0,1	75	1,20	12,05	11,23
0,2	150	0,7	9,20	8,58
0,25	187,5	0,22583	5,227	4,871
0,3	225	0,7	9,20	8,58
0,4	300	1,2	12,05	11,23
0,5	375	1,33	12,685	11,82
0,6	450	1,2	12,05	11,23
0,7	525	0,7	9,20	8,58
0,75	562,5	0,22583	5,227	4,871
0,8	600	0,7	9,20	8,58
0,9	675	1,2	12,05	11,23
1	750	1,33	12,685	11,82

The force was calculated in points of minimum thickness as follows:

$$P = \sigma_{YIELD} A = (106,8)(85,845) = 9168,25N \ .$$

This optimum column modeled by Masur does not occur buckling, but crush occur in points of minimum thickness because of $P \langle P_{MASUR}$. Now, our new optimum solution will be devoleped.

Let us take the column modeled by Masur, but it is defined as $D_{maximum}$=23,64 mm in the beginning. The chosen volume value must be smaller than the initial volume that is equal to the uniform column's volume.

$$\frac{AL}{V} = 1,33 \Rightarrow \frac{\pi(23,64)^2}{4} \frac{750}{\overline{V}} = 1,33 \Rightarrow \overline{V} = 247510,968 mm^3$$

Next, it is added volume, ΔV, in the points of minimum thickness because of aiming at a given volume, i.e. $V = \frac{\pi(22)^2}{4}(750) = 285099,53 mm^3$.

The volume that is added, ΔV namely

$\Delta V = V - \overline{V} = 285099,53 - 247510,968 = 37588,562 mm^3$ is formulated in MATLAB that is mathematical programe. Such a procedure is repeated until the difference between assumed volume and initial volume is zero. The MATLAB program is given ends of this section.

Table 3.14 The optimum column coordinates according to our new optimum solution

x (mm)	Proposed Optimum Solution ($D_{maximum}$=23,64 mm,V=285099,53 mm^3) Radius, mm
0	11,82
75	11,23
150	8,58
168,75	5,225
206,25	5,225
225	8,58
300	11,23
375	11,82
450	11,23
525	8,58
543,75	5,225
581,25	5,225
600	8,58
675	11,23
750	11,82

Consequently, the volume obtained with our new solution is equal to the initial volume, but this optimal shape endures both buckling and crushing and in points of minimum thickness crush does not occurred. To understand the verification of the new optimum solution, composite specimens were tested. The results obtained experiments will be shown Experimental section.

```matlab
1   x=zeros(6,1);
2   %Aralık olarak 168,75 ten başlayıp 206,25 noktalarında hacim farkını
3   %yakalayabildik.
4   x(1,1)=0;
5   x(2,1)=9.375;
6   x(3,1)=18.75;
7   Y=5.225;
8   y=zeros(6,1);
9   y(1,1)=Y;
10  y(2,1)=0.612*Y;
11  y(3,1)=0;
12  M=zeros(3,3);
13  for i=1:3
14      for j=1:3
15          sum=0;
16          a=i+j-2;
17          for k=1:3
18              sum=sum+(x(k,1)^a);
19          end
20          M(i,j)=sum;
21      end
22  end
23  F=zeros(3,1);
24  for j=1:3
25      sum=0;
26      for i=1:3
27          sum=sum+(y(i,1)*x(i,1)^(j-1));
28      end
29      F(j)=sum;
30  end
31  F
32  M
33  KK=M;
34  VV=F;
```

deneme.m   deneme2.m

script   Ln 14   Col 14   OVR

170

File   Edit   Text   Desktop   Window   Help

```matlab
31   F
32   M
33   KK=M;
34   VV=F;
35   mm=3
36   for i=1:mm-1
37       for j=i+1:mm
38           if KK(j,i)~=0
39               factor=KK(i,i)/KK(j,i);
40               for ii=1:mm
41                   KK(j,ii)=KK(j,ii)*factor-KK(i,ii);
42               end
43               VV(j)=VV(j)*factor-VV(i);
44           end
45       end
46   end
47   T=zeros(mm,1);
48   T(mm,1)=VV(mm,1)/KK(mm,mm);
49   for i=mm-1:-1:1
50       for j=mm:-1:i+1
51           VV(i,1)=VV(i,1)-KK(i,j)*T(j,1);
52       end
53       T(i,1)=VV(i,1)/KK(i,i);
54   end
55   T
56   A=T
57   syms z t z2
58   P=[A(3) A(2) A(1)]
59   P=conv(P,P);
60   res1=polyval(polyint (P),0);
61   res2=polyval(polyint (P),18.75)
62   res1=pi*(res2-res1)
63   A1=pi*Y^2*18.75;
64   4*(A1-res1)
65
66
```

script   Ln 1   Col 1   OVR

CHAPTER FOUR
EXPERIMENTAL INVESTIGATION FOR CLAMPED-CLAMPED CASE

4. Introduction

This Ph. D. thesis studied was focused on new proposed optimum model solution of column which given length and volume were resisted to both buckling and crush, especially, in points of minimum thickness. To understand the verification of the new optimum solution, natural composite and manufactured composite specimens were sapele (entandrophragma cylindricum) cedar (cedrela), oak (quercus spp.), glass-epoxy, glass-vinylester and glass-polyester.

Two types of specimens were used to compare buckling load of composite column with both uniform and variable cross-sections. It is obtained by taking into accounts both stability and crush criterion has been proved with numerical analysis and experimental data for columns with clamped ends (Ozdamar & Pekbey 2004, Sayman & Pekbey, 2004). Fiber orientation angle which describes the orientation of fiber with respect to the loading direction is important parameters. In this thesis, fiber orientation angle is changed as 0, 45 and 90 degrees.

In this chapter, the properties of materials used, configuration of specimens, fabrication and processing of composites, test setup, and testing details are presented.

4.1 Fabrication and Processing of Composite Columns

All manufacturing methods provide the structural shape for the composite material. In the fabrication phase, the fiber reinforcement and matrix material are placed into structural form. It is used to heat and pressure to density and consolidate the structure during the process phase. In all manufacturing methods, it is required to apply temperature and pressure after the fiber and matrix are brought together into the desired structural form. While fabrication techniques are independent on the type

of the matrix material, it is completely processing condition on the type of the matrix material used. For example, thermosets are desired for long processing times, whereas thermoplastics need relatively high pressures and temperatures (Hyer, 1998).

The fibers and matrix material can be commercially obtained in a variety of forms. Manufacturing process of composites is varied according to cost, size of production, machines and product quality. One of used commercial manufacturing processes is the hand lay-up method. The hand lay-up is the oldest and most common fabrication method for composite structures although the method has been replaced with automated techniques. In this method, its process depends on many factors, such as part size and shape, cost and schedule. Because of it's a reliable process, it is by nature very slow and labor intensive. This method depends on the individual skill of the operator.

This type of fabrication is the most-time consuming but it results in high quality parts. A description of these steps is given in Figure 4.1. The first ply in oriented and subsequent plies are placed one upon another, a roller is used to compact the plies and remove entrapped air that could later lead to voids or layer separations. Once the composite plies are combined with desired shape and orientation, it is necessary to apply the temperature and pressure for periods of time to produce composite materials. The pressure can be applied on the product while being cured in order to consolidate the fiber interaction and reduce the content of voids.

In this Ph. D. Thesis, the composite plies were cured at 180°C for 2 h under a pressure of 12 MPa using a pressing machine. The fabrication and processing phases of glass fiber-epoxy, glass fiber-vinylester, and glass fiber-polyester are shown in Figure 4.1.
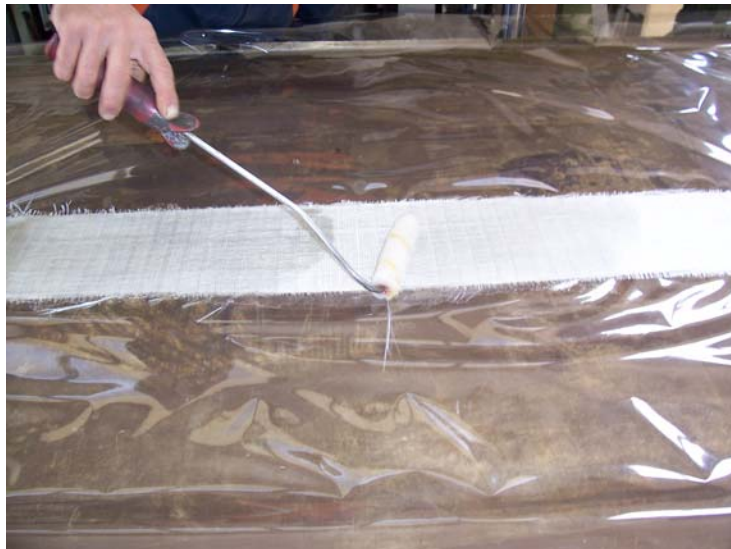
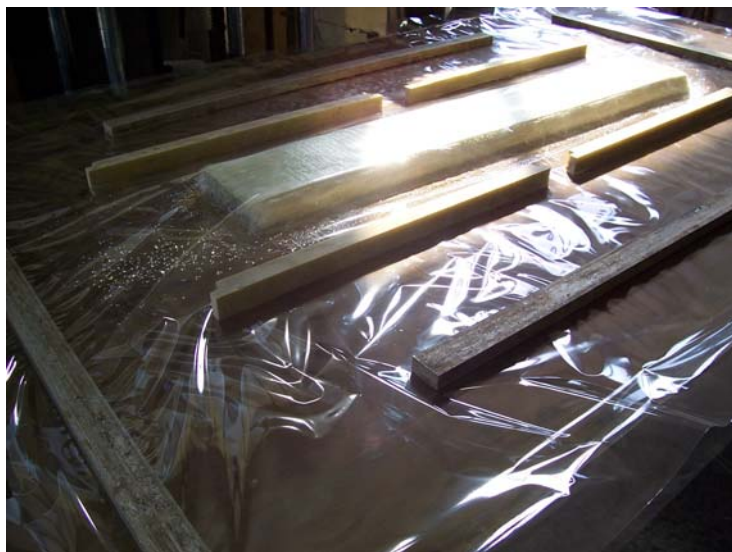Figure 4.1 Fabricating and processing of composite materials

Figure 4.1 Fabricating and processing of composite materials (Continue)

Figure 4.1 Fabricating and processing of composite materials (Continue)

Figure 4.1 Fabricating and processing of composite materials (Continue)

4.2 Details of Specimens

All specimens were manufactured both uniform and variable cross-sections. The length was defined as 750 mm. The diameter of wood composite specimens was 25 mm for sapele, oak and cedar for circle-cross-sections while the diameter of glass-epoxy, glass-vinylester and glass-polyester was 22 mm with 0, 45 and 90 degree of fiber orientation angle. Every specimen was operated in lathe because of obtaining requested diameter. In this way, it was manufactured all natural and manufactured composite materials for uniform cross-sections. Other specimens, in other words the composite columns with variable cross-sections processed in CNC workbench. This procedure was the most-time consuming. Because it was changed thickness every points of composite column. Especially, it was very difficult to form the minimum thickness of points of composite columns. It was able to manufactured glass-epoxy with 0 and 45 degree of fiber orientation angle, glass-vinylester and glass-polyester with 90 degree of fiber orientation angle. Numbers of three specimens each of materials were fabricated. Three specimens were tested in longitudinal compression because of obtaining mechanical properties of composite materials.

Finally, the specimens used in this study were as follows:

- Sapele, cedar and oak wood composite materials with uniform cross-sections (Figure 4.2)
- Sapele, cedar and oak wood composite materials with variable cross-sections (Figure 4.2)
- Glass-epoxy, Glass-vinylester and Glass-polyester composite materials with uniform cross-section and with 0, 45 and 90 degree of fiber orientation angle (Figure 4.3)
- Glass-epoxy composite materials with variable cross-section and with 0, 45 degree of fiber orientation angle (Figure 4.4)
- Glass-vinylester and glass-polyester composite materials with variable cross-section and with 90 degree of fiber orientation angle (Figure 4.4).

The compressive stiffness and critical buckling load were determined using these specimens. The specimens were tested in the Laboratory of the University of Ege Department of Mechanical Engineering.

Figure 4.2 Buckling test specimens with uniform and variable cross-sections for wood composite materials

Figure 4.3 Buckling test specimens with uniform cross-sections for 0, 45 and 90 degree of fiber orientation angle for composite materials

Figure 4.4 Buckling test specimens with uniform and variable cross-sections for composite materials with different fiber orientation angle

4.3 Material Properties and Test Set-up

Experimental studies are performed to verify the validity of the present model. The tensile and compressive strength of composites are different, and therefore have to be determined separately. Because of the difficulty in avoiding coupon buckling during the test, compression testing is a lot more problematic than the tension tests. It is interested in determining the compression modulus, yield strength in the compression tests. Compression modulus was obtained from a typical stress-strain diagram. The stress-strain curve in compression is not perfectly linear to failure, but for the purposes of obtaining the properties. Another interesting characterization of composites is their behavior under compressive loads. Most often the critical buckling loads are determined through an eigenvalue analysis. In this thesis, compression tests were carried out on wood composite materials (sapele, oak, and cedar), glass-epoxy, and glass-polyester and glass-vinylester composites in order to evaluate the critical buckling load.

Mechanical properties of composites depend on the shape and the dimension of the reinforcement. The highest stiffness is obtained along the direction of the fibers.

Traditionally, wood characteristic strength values in compression are determined using small clear specimens. ASTM (1994) specifies a clear straight-grained specimen 203 mm long, 51x51 mm cross sectional area, tested to failure, to obtain the compression strength parallel to the grain. Compression strengths of clear wood of various species and grades are published in the Wood Engineering Handbook (1990) (Lau 2000). The compression strength of lumber with defects is generally less than that of clear material of the same species. To address this issue, the traditional method of predicting the strength of lumber with defects is to reduce the clear wood strength using modification factors to account for the defects. The test method refers to the ASTM standard D198-94 (1995), and procedures to establish the allowable properties are given in ASTM standard D 1990-91. On the other hand, long members

and short members perform differently under compression load. While short members will attain the ultimate compression strength, long members will fail in buckling. Thus, a lateral instability failure is a characteristic of slender compression members. The capacity of long columns depends on the stiffness of the member. For this reason, the design codes typically classify compression members into three categories short, intermediate and long members, according to the slender ratios, C_c, defined by

$$C_C = \frac{L}{d}$$
(4.1)

where

L= length of the member, or effective length in case of different boundary conditions

d= dimension of cross-section of the member in the direction of buckling

Cedar, sapele and oak were chosen for this thesis because they are locally available and commercially important species. Compression tests were conducted on the wood specimens. For compression testing, three specimens each (which were averaged after testing to give a characteristic value), with a length of 40 mm, were cut from cedar sapele and oak stick to give a compressive specimen. The low length-to-width ratio prevented failure of the specimen by Euler buckling (Gindl & Teischinger 2002). The specimen consists of a straight piece of cedar, sapele and oak wood which is sufficiently short to ensure that failure will occur first in crushing (rather than in buckling).

The wood and manufactured composite materials under testing consist of uniform and variable cross-sections. It was sized optimized column with variable cross-section which considered together both bimodal solution and crushing. The dimensions of composite columns were also selected different fiber orientation angle.

The critical buckling load measurements were made using long, slender circle composite columns with uniform and variable cross-sections. The length of the column is as L=750 mm. The column is subjected to concentrated compressive force at the centroid of the cross-section at the end of the column. The force is increased until the column buckles; the corresponding force is called the buckling load. In the analysis, it is assumed that the column behaves in a linearly elastic manner and the deformations are small. The shear deformations in the plane of the walls are not taken into account.

The experiments were designed to provide information on the load deformation response and stress-strain characteristics. The experiments were also designed to study the effect of fiber orientation angle of composite columns.

Firstly, for these specimens, it was determined modulus of elasticity and yield stress. Three specimens were tested in longitudinal compression. Average values from each test were recorded and presented in Tables 4.1 for natural and manufactured composite materials.

And then, a diameter was calculated for elastic buckling in the uniform column for wood and manufactured composite materials. In this diameter value was 25 mm and 20 mm for sapele-oak and cedar materials, respectively. It was 22 mm for glass-epoxy, glass-vinylester and glass-polyester.

Table 4.1 Average values of Young modulus (E) and yield stress of natural and manufactured composite materials for different fiber orientation angle **(MPa)**

a) For Natural Composite Materials

Natural Composite Materials	E	σ_{Yield}
CEDAR	2228,68	21,30
OAK	3426,41	42,48
SAPELE	4257,30	42,88

b) For Manufactured Composite Materials

Manufacture Composite Materials	Fiber Orientation Angle					
	0 degree		45 degree		90 degree	
	E	σ_{Yield}	E	σ_{Yield}	E	σ_{Yield}
GLASS-EPOXY	9943,86	106,80	7938,30	83,92	7242,98	77,2
GLASS-VINYLESTER	8123,04	86,70	7641,10	78,88	6942,40	74,75
GLASS-POLYESTER	7590,10	78,50	7254,10	72,52	6558,90	70,70

The composite column specimens were tested by applying compression in a hydraulic testing machine. Compression strength was determined on a Shimadzu AG 100 kN universal testing machine. A typical specimen mounted in the test fixture is shown in Figure 4.5. The columns were placed between the moving jaws. The specimens were checked for verticality to avoid any initial inclination. The load was applied at a constant rate of 0,5 mm/min and load, strains and deformations were recorded by universal test machine.

Figure 4.5 Test apparatus for buckling and compressive tests

Secondly, compressive tests for wood and man-made composite materials were performed to obtain the critical buckling load. A total of two different tests were performed to study the behavior of the under compressive loads for uniform cross- and variable cross-section. The specimens were tested as clamped-clamped ends columns in vertical position loaded with axial compressive load. All specimens were loaded slowly until buckling. Buckling modes were also observed. The buckling form for wood and man-made composite materials with uniform and variable cross-section is shown in Figures 4.6 and 4.10.

The applied load and the measured strains were recorded using a data-acquisition system. The data-acquisition system saves the recorded data as a file. And then this file was imported into Microsoft Excel. In this way, the critical buckling load was determined both uniform and variable cross-sections for clamped-clamped ends.

Figure 4.6 Buckling of natural composite materials for uniform cross-sections
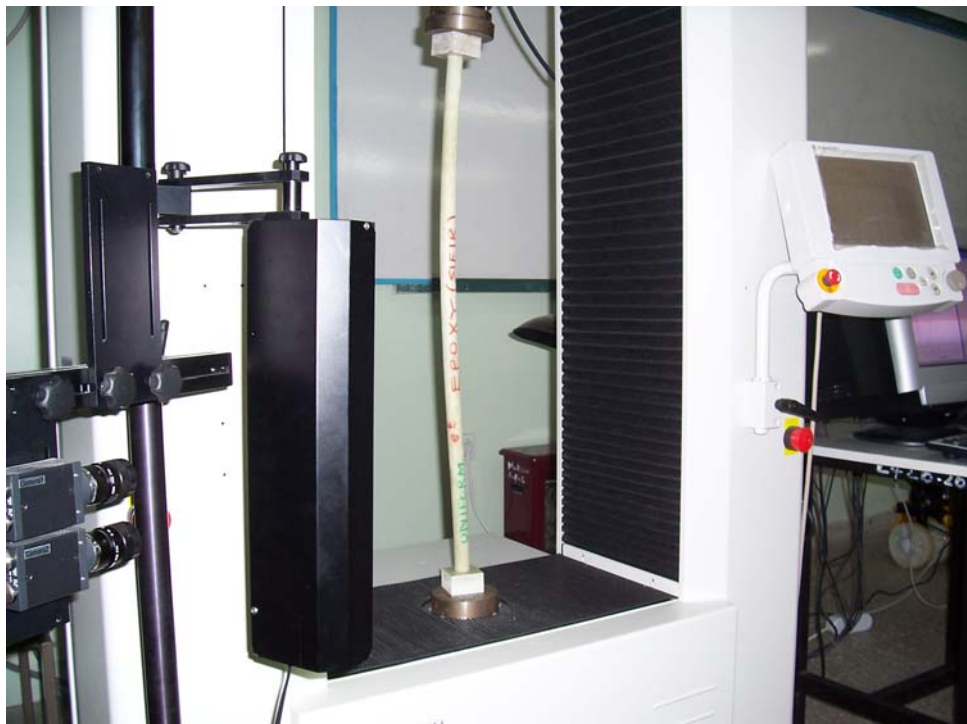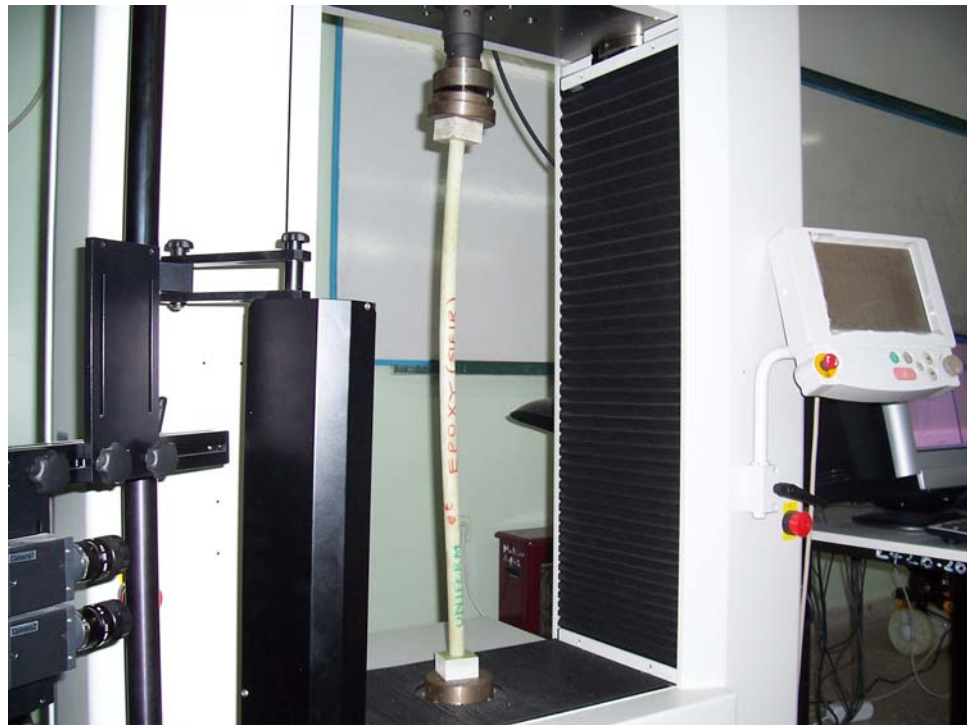
Figure 4.7 Buckling form of glass-epoxy composite materials for uniform cross-sections with 0 degree fiber orientation angle

Figure 4.8 Buckling of glass-epoxy composite materials for variable cross-sections with 0 degree fiber orientation angle
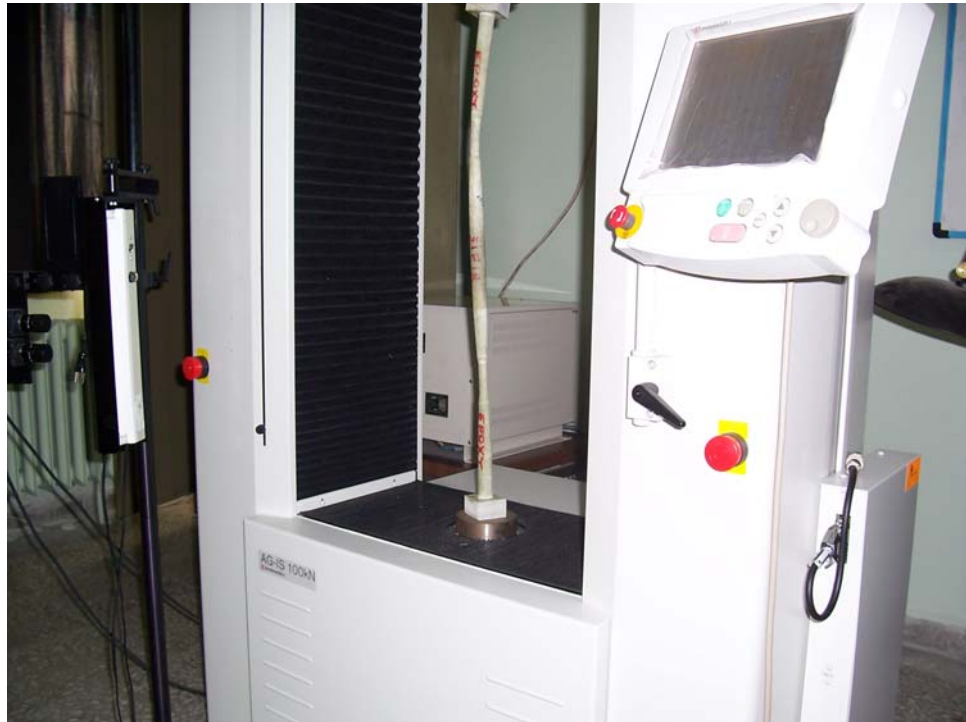
Figure 4.9 Buckling form of glass-epoxy composite materials for variable cross-sections with 0 degree fiber orientation angle (Continue)

From the measured load-strain data, it was calculated the critical buckling load for uniform and variable cross-section for sapele, oak, cedar; glass-epoxy, glass-vinylester and glass-polyester with 0, 45 and 90 degree of fiber orientation angle. One of result of an experimental measurement was shown in Figure 4.10. The load which the initial part of the curve deviated linearity, was taken as the critical buckling load. The calculated values are shown in Tables 4.5 and 4.7.
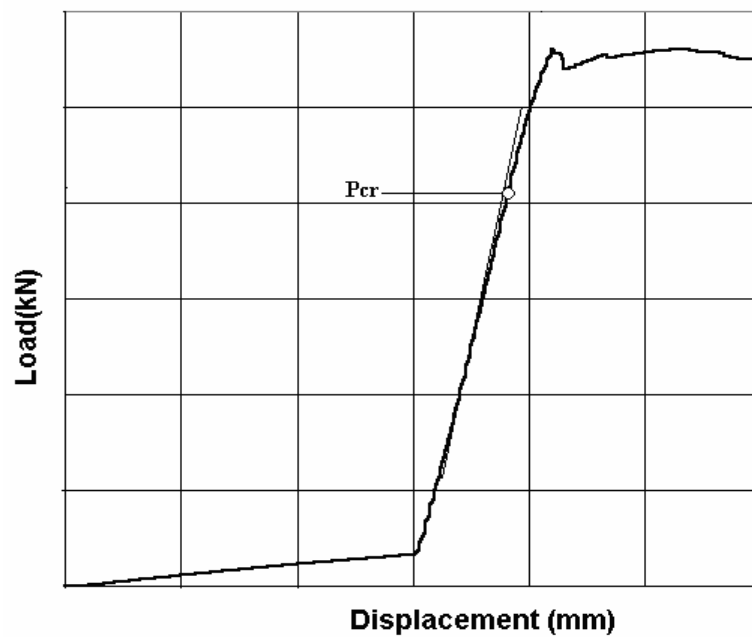
Figure 4.10 The critical buckling load obtained from experimental measurements

In the following subsections, experimental results will be compared in the form of load-displacement curves, with the theoretical and numerical calculations.

Table 4.5 The critical buckling load (N) results obtained experiments for wood composite materials with uniform cross-sections

Natural Composite Materials	Uniform Cross-Section	Variable Cross-section (New Proposed Optimum Model)
CEDAR	1200	1400
OAK	4650	5990
SAPELE	5730	6850

Table 4.6 The critical buckling load (N) results obtained experiments for manufactured composite materials with uniform cross-sections

Composite specimens	Fiber Orientation Angle		
	0°	45°	90°
GLASS-EPOXY	8074,25	6350,75	5766,50
GLASS-VINYLESTER	6615,50	6100,00	5475,75
GLASS-POLYESTER	6227,85	5770,25	5245,50

Table 4.7 The critical buckling load (N) results obtained experiments for manufactured composite materials with variable cross-sections

Composite Specimens and Fiber Orientation Angle	The Critical Buckling Load (N) (New Proposed Optimum Model)
GLASS/EPOXY (0 degree)	8750
GLASS/EPOXY (45 degree)	7000
GLASS/VİNYLESTER (90 degree)	6250
GLASS/POLYESTER (90 degree)	5850

CHAPTER FIVE
FINITE ELEMENT ANALYSIS OF THE EXPERIMENTAL
METHOD FOR CLAMPED-CLAMPED CASE

5. General

It is always preferable to confirm the experimental program. Therefore, the experimental and theoretical results can be compared using a numerical method. If good agreement between the results, the numerical model can be used broadly to conduct a comprehensive study. It is true that numerical modeling is faster and cheaper approach of collecting data about a certain problem than depending completely on an extensive and expensive, experimental investigation. The finite element method (FEM) is most powerful and flexible method because of providing a complete solution for elastic and inelastic problems. The goal behind using the finite element method is first to simulate the experimental work described in the previous chapter.

The finite element method is a numerical procedure intended to provide approximate solutions for a broad range of problems which do not admit closed form solutions. It originated in the aircraft industry where a reliable tool for both static and dynamic analyses required. The method quickly acquired popularity and began to be applied in many areas of engineering.

The finite element method has rapidly become a very popular technique for the computer solution of complex problems in engineering. This method is used practically all fields of engineering analysis. It can be regarded in structures as an extension of earlier established analysis techniques, in which a structure is represented as an assemblage of discrete elements interconnected a finite number of nodal points (Xi, 1998).

Today a solid mathematical foundation supports the finite element method. Its convergence characteristics and accuracy have been thoroughly studied and known

to be intrinsically associated with the choice of the basis functions and element types. In general, the method considers a continuous domain as composed of finite regions (finite element) and describes the properties of each region by a finite number of parameters. Then, applying the conditions of compatibility between regions, a system of simultaneous equations is formed with the parameters. Solution of this system of equations along with boundary conditions provides the unknown parameters. The finite element method strongly relies on numerical solutions of equations. That postponed its usefulness until the sixties when digital computers began to develop. Many steps of the finite element solution procedures are repeated and systematic, thereby, well suited for computers. Furthermore, it is often the case that the volume of data to be handled is large and practically intractable without the aid of computers. One of the limiting factors is computation complexity, which requires high speed and high capacity computers. With the advance of computer systems, the use of this method on highly variable materials

5.1 Fundamentals of Finite Element Method

The finite element method has been widely used in engineering and science in the approximate solution of boundary-value problems that cannot be solved analytically for a very long time. Over the last decade or so, the finite element method has been used and developed as a powerful and standard computational method for the solution of structural problems due to mechanical advantages and manifold features. It is one of the most effective numerical analysis tools in the engineering and efficient computational method for the numerical solution of engineering problems. There are several references about finite element and its application. The most important advantage of this method is its capability to model various arrangements of structural elements, material properties and boundary conditions.

The finite element method is an analytical procedure. The fundamental idea underlying this method is that the total structure can be modeled analytically by its subdivision into the finite elements in each of which the behavior is explained by a separate set of assumed functions illustrating the stresses of displacements in that

region, when applied to problems of structural analysis. It is often chosen these sets of functions in a form that confirms continuity of the expressed behavior throughout the complete continuum. If the behavior of the structure is characterized by a single differential equation, then the finite element method, in common with the series and finite difference schemes, describes an approach to the approximate solution of that equation. If the total structure is heterogeneous, being composed of many separate structural forms in each of which the behavior is described by a distinct differential equation, the finite element approach continues to be directly applicable (Anonymous, 2005k).

This method becomes a powerful tool for the numerical solution of a wide range of engineering problems. The finite element method of applications such as deformation and stress analysis of automotive, aircraft, building, and bridge structures to field analysis of heat flux, fluid flow, magnetic flux, seepage, and other flow problems. It can be modeled complex problems with the advances in computer technology and CAD systems. It can be tested on a computer several alternative configurations before the first prototype is constructed. In this reason, it is important understanding the basic theory, modeling techniques, and computational aspects of the finite element method. In the finite elements method, it is discredited a complex region simple geometric shapes called finite elements. It is regarded as material properties and the governing relationships over these elements. The assembly of these elements to for the whole structure is physically equivalent to superimposing these element equations mathematically. The result is composed of a large set of simultaneous equations that can be solved using computers. It is obtained the approximate behavior of the continuum by solution of these equations (Anonymous, 2005k).

The finite element method desires the formation and solution of systems of algebraic equations. It is the special advantages of the method in its suitability for automation of the equation formation process and in the ability to show highly irregular and complex structures and loading situations (Anonymous, 2005k).

It is well known that the core aspects of finite element method are: first to divide the structure in question into finite small elements, second to establish the relationship of forces and displacements in tem of stiffness matrix for each element, third to assemble these individual relations to form one relation for the whole structure with proper force or displacement boundary conditions and finally to find the internal forces (stresses) and strains or displacements of any point within the structure from the established relations hip.

The first step in a finite element analysis is to discretize the problem into sets of structural components. Each finite element is interconnected with the adjacent elements by the nodal points. Nodal forces act at each nodal point which, in turn, is subjected to displacements and rotations. A standard set of simultaneous equations can be written to relate these physical quantities. Assembling these elements to form the whole structure is equivalent physically to superimposing these elements equations mathematically. The result is a huge set of simultaneous equations that can be solved using computers. From the potential energy formulation, the following equation in a matrix form is obtained:

$$\Pi_P = \frac{1}{2}\{U\}^T[K_e]\{U\} + \frac{1}{2}\{U\}^T[K_G]\{U\} - \{U\}^T\{P\} \tag{5.1}$$

where, Π_P is the potential energy of the system; $\{U\}$ is the global displacement vector, $\{P\}$ is the global load vector: $[K_e]$ is the global elastic stiffness matrix; and $[K_G]$ is the global geometric stiffness matrix. The geometric stiffness matrix is included in the analysis to account for the deformed geometry of the elements in the equilibrium equations since the problem of angle members under a compressive load is a large deflection problem (Shani, 1998).

Differentiating with respect to the displacement and equating the result to zero to determine the minimum potential energy of the system results in the following:

$$[K_e]\{U\} + [K_G]\{U\} = \{P\} \tag{5.2}$$

which can be simplified to the following basic finite element equation relating the global displacements and the global loads

$$[K]\{U\} = \{P\} \tag{5.3}$$

where, $[K] = [K_e] + [K_G]$.

The finite element method can be requested to the evaluation of the elastic critical load. This method is based on the use of local functions. Each member of structure is subdivided into a series of fairly short elements. It may be defined the deformation over each element by a simple polynomial function. If the displacement of each node is known, the coefficients of these polynomial functions may be determined. As a result, the individual displacements of the structure may be calculated. It may be described the behavior of the structure in terms of the displacements of the nodes. It must be stationary for equilibrium the increment in total potential energy with respect to these nodal displacements (Anonymous, 2005e). This guides to a set of linear homogeneous equations, namely, the following eigenvalue problem:

$$\lambda^f [K_E]\{\psi\} = [K_G]\{\psi\} \tag{5.4}$$

where, ψ are nodal displacements, λ^f is the load factor, K_E is the global elastic stiffness matrix corresponding to the nodes, K_G is the geometric stiffness matrix. The smallest value of λ^f is known both the first eigenvalue and the critical load factor $\lambda_{cr}{}^f$. The structure becomes unstable at $\lambda_{cr}{}^f$.

The eigenvalue and the eigenfuction are called as buckling load and buckling mode, respectively. The eigenvalues and the eigenvectors can be get by applying several techniques, such as inverse iteration, forward iteration and Rayleigh quotient iteration, transformation methods, likely Jacobi method and generalized Jacobi method and the subspace iteration method.

Finally, the problem of buckling can be solved in two ways;

- By forming a geometric stiffness matrix of the entire structure under a fraction of the loading pattern and extracting eigenvalues and mode shapes. This is useful only when the structure remain elastic until buckling.
- By conducting a nonlinear analysis. In this case, buckling is indicated by excessive deformations and consequent reduction in load carrying capacity.

5.1.1 Types of Elements Used in the Finite Element Method

It is *the simple framework element* member of the total family of finite elements. It expresses truss and space frame structures, when used in combination with elements of exclusively the same type (Anonymous, 2005k).

It is *the basic elements* in finite element analysis the thin plates loaded by forces in their own plane. This case is also described the condition of plane stress. Plane stress elements may be triangular and quadrilateral. It is feasible many other geometric shapes in this class of element, although such other forms generally serve very specialized purposes (Anonymous, 2005k).

It is *the solid elements* three-dimensional generalizations of the plane stress elements. The most common shapes of three-dimensional elements are the tetrahedron and hexahedron. It is essential to analytical models of soil and rock mechanics problems and of structures for nuclear power (Anonymous, 2005k).

It is *the axisymmetric solid elements* one of the most important fields of application of the finite element method. It is fall a great variety of engineering

problems in this category such as concrete and steel tanks, nuclear containment vessels, rotors, pistons, shafts, and rocket nozzles (Anonymous, 2005k).

It is the *axisymmetric thin shell structures* the same range of significance in practical application as the axisymmetric solids. Axisymmetric thin shell formulations bridge the gap between flat plate bending and stretching and general thin shell elements (Anonymous, 2005k).

5.2 ANSYS Program

The finite element can deal with structural engineering which cannot be effectively solved using classical methods. The procedure uses the finite element method and makes use of the ANSYS program to solve eigenvalue problem. The finite element method is very often used as a numerical experiment in order to confirm the results obtained in the analytical way. In the finite element method model assumed in the analysis with the ANSYS 9.0 package, the composite column with uniform and variable cross-sections were modeled.

ANSYS is designed as a general finite element package for numeric modeling of structural response in linear and non-linear static and dynamic analysis. This computer program runs as a batch application to assemble a data deck that describes a problem so that it can be analyzed the structure. A data deck is described finite element model, the elements element properties, material definition, nodal constraints.

In this thesis, finite element modeling is used to gain further understanding of the critical buckling load. ANSYS are used to analyze the critical buckling load of various composites natural and man-made composite materials in order to see how changes the fiber orientation angle of composite column would affect the buckling load.

Eigenvalue buckling analysis predicts the theoretical buckling strength of an ideal linear elastic structure. It is showed ANSYS program procedure for eigenvalue buckling analysis below:

- Build the model.
- Obtain the static solution.
- Obtain the eigenvalue buckling solution.
- Expand the solution.
- Review the results.

5.2.1 ANSYS Eigenvalue Analysis Options

5.2.1.1 Subspace Method

The eigenvalue and eigenvector problem which needs to be solved for mode-frequency and buckling analyses has the form of (from ANSYS Help Section):

$$[K]\{\varphi_i\} = \lambda_i [M]\{\varphi_i\} \tag{5.5}$$

where

$[K]$ = *structure stiffness matrix*

$\{\varphi_i\}$ = *eigenvector*

λ_i = *ith eigenvalue*

$[M]$ = *structure mass matrix.*

For prestressed modal analyses, the *[K]* matrix includes the stress stiffness matrix *[S]*. For eigenvalue buckling analyses, the *[M]* matrix is replaced with the stress stiffness matrix *[S]*. It is formulated the buckling problem as an eigenvalue problem:

$$([K] + \lambda_i[S])\{\psi_i\} = \{0\} \tag{5.6}$$

where

ψ_i = *ith eigenvector of displacements.*

The eigenvectors are evaluated using inverse iteration with shifting. The eigenvectors associated with multiple eigenvalues are evaluated using initial vector deflation by Gram-Schmidt orthogonalization in the inverse iteration procedure.

The subspace iteration method algorithm consists of the following steps:

1. Define the initial shifts:

The Sturm sequence check computes the number of negative pivots encountered during the triangularization of the shifted matrix [K*]. This number will match the number of converged eigenvalues unless some eigenvalues have been missed. In that case, more iteration vectors must be used or the initial shift (see step 1) was past the first mode. For the final Sturm sequence check, the shift used is defined as:

$$s = \lambda_p + 0{,}1(\lambda_{p+1} - \lambda_p) \tag{5.7}$$

where:

λ_p = eigenvalue of the last requested mode
λ_{p+1} = eigenvalue of the next computed mode.

2. Initialize the starting vectors $[X_0]$

The number of starting (iteration) vectors used is determined from:

$$q = p + d \tag{5.8}$$

where

  p = requested number of modes to extract

  d = number of extra iteration vectors to use.

The q starting vectors *[X₀]* are initialized as follows. For each predefined rigid-body motion, define a rigid-body vector:

1. If a translational rigid-body motion, set the DOF (Degrees of Freedom) slot in $\{X_0\}$ to 1.0 ($\{X_0\}$ is a column of *[X₀]*).
2. If a rotational rigid-body motion, set the DOF (Degrees of Freedom) slot in $\{X_0\}$ corresponding to a unit rotation about the global origin corresponding to the *Dof* label.

The rigid-body vectors are M-orthogonalized (Gram-Schmidt orthogonalization). The remainder of the vectors is initialized to random vectors.

3. Triangularize the shifted matrix

$$\left[K^*\right] = \left[K\right] + s\left[M\right] \tag{5.9}$$

where:
[K] = assembled stiffness matrix
[M] = stress stiffness matrix.

4. For each subspace iteration n (1 to N_M), do steps 5 to 14:

where:

N_M = maximum number of subspace iterations

5. Form [F] = [M][X_{n-1}] and scale [F] by $\{\lambda_{n-1}\}$

where:

$\{\lambda_{n-1}\}$ = previously estimated eigenvalues

6. Solve for $[\overline{X}_n]$

$$[K^*][\overline{X}_n] = [F] \tag{5.10}$$

7. Scale the vectors $[\overline{X}_n]$ by $\{(\lambda_{n-1} - s)/\lambda_{n-1}\}$

8. M-orthogonalize the vectors to the previously converged vectors (Gram-Schmidt orthogonalization).

9. Define the subspace matrices $[\overline{K}]$ and $[\overline{M}]$:

$$[\overline{K}] = [\overline{X}_n]^T [K][\overline{X}_n] \tag{5.11}$$

$$[\overline{M}] = [\overline{X}_n]^T [M][\overline{X}_n] \tag{5.12}$$

10. Adjust for the shift, $[\overline{K}^*] = [\overline{K}] + s[\overline{M}]$

11. Compute the eigenvalues and vectors of the subspace using a generalized Jacobi iteration:

$$[K^*][Q] = [\overline{M}][Q]\{\lambda_n\} \tag{5.13}$$

where:
[Q] = subspace eigenvectors
$\{\lambda_n\}$ = updated eigenvalues.

12. Update the approximation to the eigenvectors:

$$[X_n] = [\bar{X}_n][Q] \tag{5.14}$$

13. *If any negative or redundant modes are found, remove them and create a new random vector.*

14. *Check for convergence* (described below):

- All requested modes converged? If yes, go to step 15.
- If a new shift is required (described below), go to step 3
- Go to the next iteration, step 4

In order to improve the rate of convergence during the iteration process, a shifting strategy is adopted as follows:

1. If the current converged mode(s) is zero(s) and the next mode $i+1$ is nonzero, shift to just below the nonzero mode:

$$s = \lambda_{i+1} - \begin{cases} .05\lambda_{i+1} \Rightarrow & \text{if } \lambda_{i+1} \text{ is close to being converged} \\ .5(\lambda_{i+1} - \lambda_i) & \text{if not} \end{cases}$$

2. If the number of iterations since the last shift exceeds N_S(minimum number of subspace iterations completed before a shift is performed), then shift to just below the next unconverged mode i+1

$$s = \lambda_{i+1} - \begin{cases} .05(\lambda_{i+1} - \lambda_i) \Rightarrow \text{if } \lambda_{i+1} \text{ is close to being converged} \\ .5(\lambda_{i+1} - \lambda_i) \quad \text{if not} \end{cases}$$

The convergence check requires that all of the requested eigenvalues satisfy the convergence ratio:

$$e_i = \frac{(\lambda_i)_n - (\lambda_i)_{n-1}}{B} \tag{5.15}$$

where:

$(\lambda_i)_n$ = value of ith eigenvalue as computed in iteration n

$(\lambda i)_{n-1}$ = value of ith eigenvalue as computed in iteration n-1

$$B = \begin{cases} 1 \\ (\lambda_i)_n \end{cases} \text{ whichever is greater } tol = tolerance\ value, \text{ set to } 1.0E\text{-}5$$

15. Perform a final Sturm sequence check if requested

5.2.1.2 Block Lanczos

The Block Lanczos eigenvalue extraction method is available for large symmetric eigenvalue problems. Typically, this solver is applicable to the type of problems solved using the subspace eigenvalue method, however, at a faster convergence rate (From ANSYS Help Section).

The method used by the modal analysis employs an automated shift strategy, combined with Sturm sequence checks, to extract the number of eigenvalues requested. The Sturm sequence check also ensures that the requested number of eigenfrequencies beyond the user supplied shift frequency is found without missing any modes.

The Block Lanczos algorithm is a variation of the classical Lanczos algorithm, where the Lanczos recursions are performed using a block of vectors, as opposed to a single vector.

Use of the Block Lanczos method for solving large models (100,000 DOF: Degrees of Fredom, for example) with many constraint equations (CE) can require a significant amount of computer memory. This occurs when certain constraint equations lead to a huge wave front size. For this reason, the Lagrange Multiplier approach is implemented to treat constraint equations in the block Lanczos eigensolver, rather than explicitly eliminating them prior to writing.

5.3 Finite Element Model of the Problem for Clamped-Clamped Case

The Finite Element Analysis was conducted to investigate the behavior of wood materials (sapele, cedar and oak) and man-made composite materials (glass-epoxy, glass-polyester, glass-vinylester) under compressive loads. A model of each experimental specimen was analyzed using finite element method. The purpose of this analysis is to model the behavior of a built-up column under axial load, hence, verify the analysis by the experimental results. A three-dimensional finite element model was developed to predict the mechanical behavior of composite materials.

Two different finite element models were obtained. These were uniform and variable cross-sections for wood and man-made composite materials. In other words, uniform column was formed and optimized column using ANSYS for composite materials. The specimen length of the all composites both uniform and variable cross-sections were taken as 750 mm.

a) For uniform cross-sections:

The diameters of the wood composites were as 25 mm and 20 mm for sapele-oak and cedar wood materials, respectively. In this value for man-made composite materials was taken as 22 mm for uniform cross-sections. Fiber orientation angle was also changed as 0, 45 and 90 degree for glass-epoxy, glass-polyester, and glass-vinylester.

b) For Variable cross-sections:

The maximum diameter were as 23,64 mm for glass-epoxy, glass-polyester, glass-vinylester, while it was taken as 27,5 mm and 22,5 mm for sapele-cedar and oak materials, respectively . It was also modeled Masur'solution which the maximum and minimum diameter was as 23,64 mm and 10,454 mm for composite materials. Additionally, the new our optimum solution was modeled, which minimum thickness

of points had not been crush occur. Furthermore, all cases were investigated for different fiber orientation angle: 0, 45 and 90 degree.

The columns with uniform cross-sections were modeled with the beam elements (Ozdamar & Pekbey 2004). But other columns which have variable cross-sections were modeled with the solid elements. In the finite element model, the optimum element sizes used to obtain accurate results when the models were meshed. It is also assumed that the materials are to be isotropic and linearly elastic.

The composite columns were analyzed under clamped-clamped end conditions. The boundary conditions were applied to the edge nodes of the columns. A pressure of a unit value was applied on the upper areas. The rotations in the xy-, yz- and xy-planes are taken zero at the nodes through clamped edges. The boundary and load conditions of the column are shown in Figures 5.1 and 5.5.
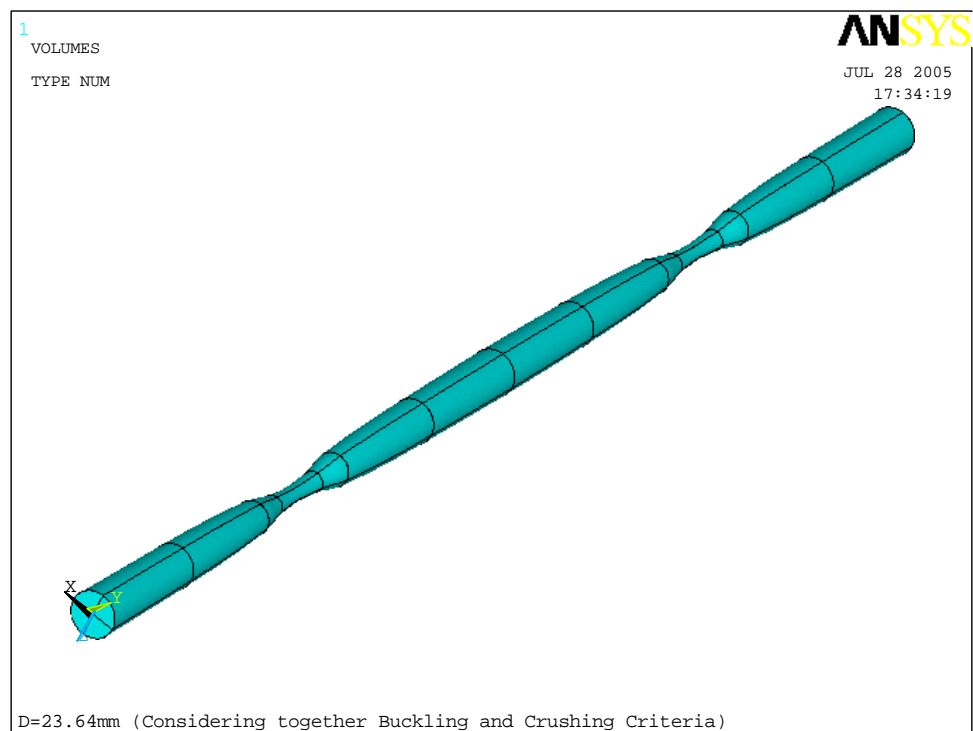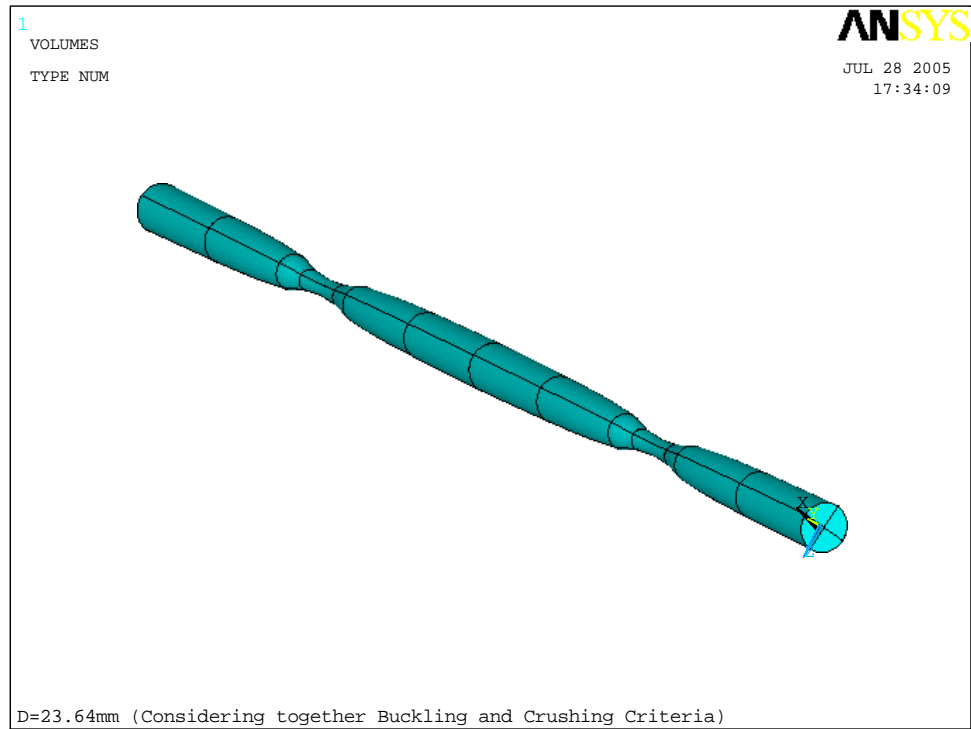
Figure 5.1 The Finite Element Modeling according to considering together buckling and crushing criteria
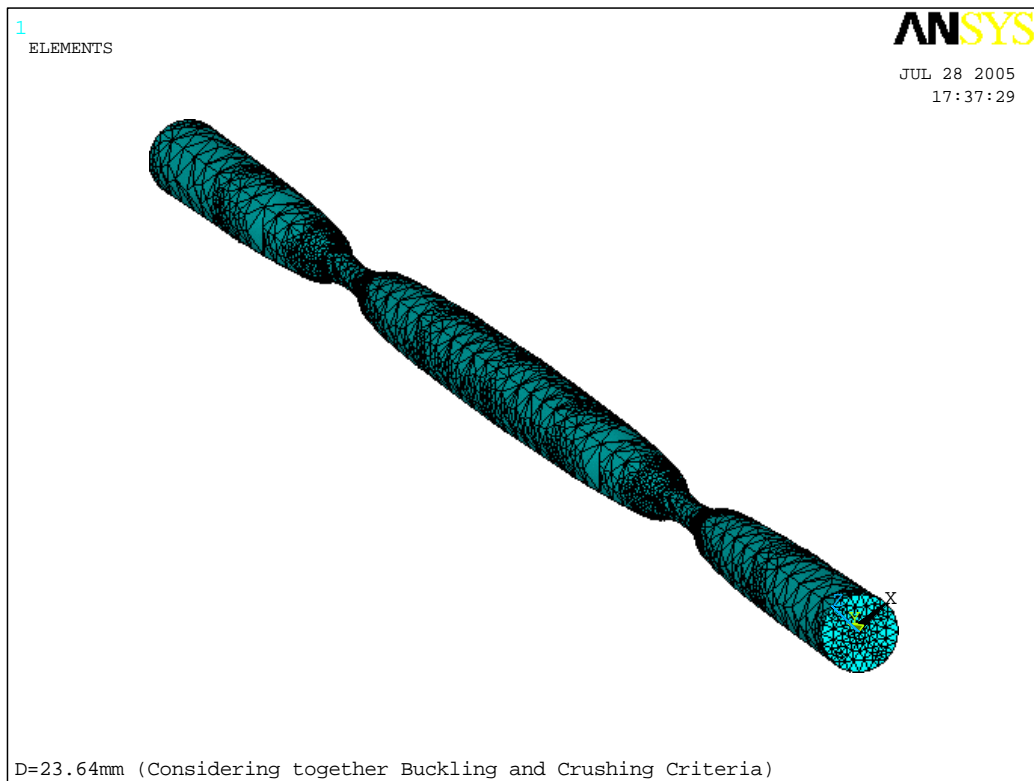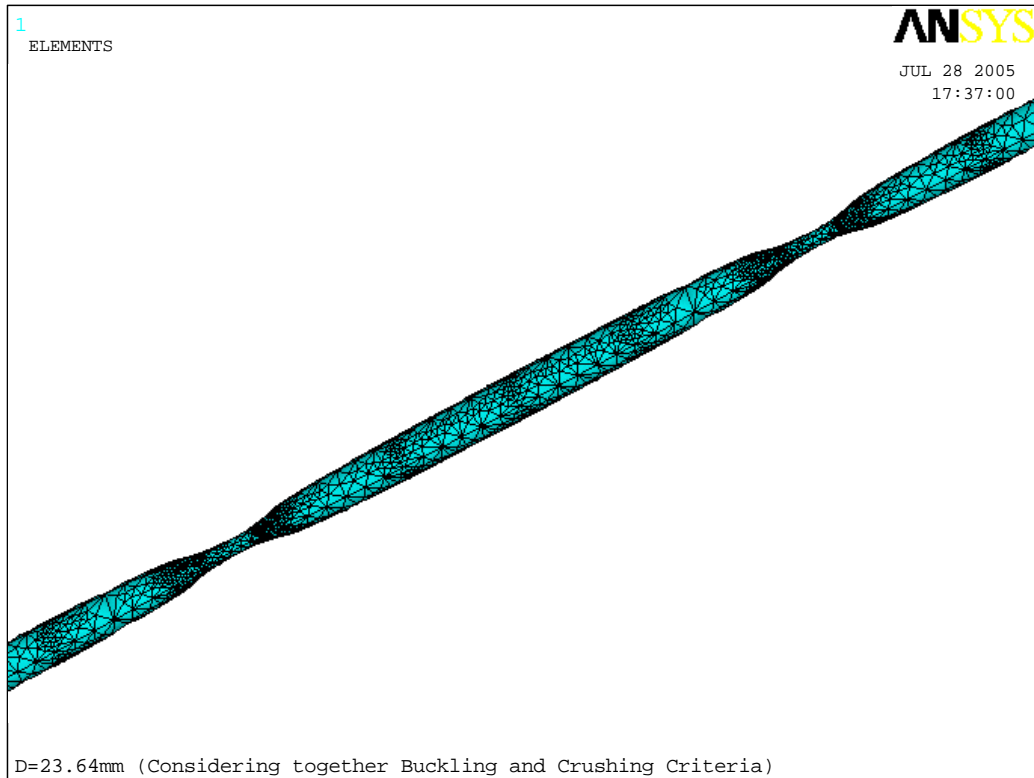
Figure 5.2 The finite element mesh model for new proposed optimum solution

D=23.64mm (Considering together Buckling and Crushing Criteria)

D=23.64mm (Considering together Buckling and Crushing Criteria)
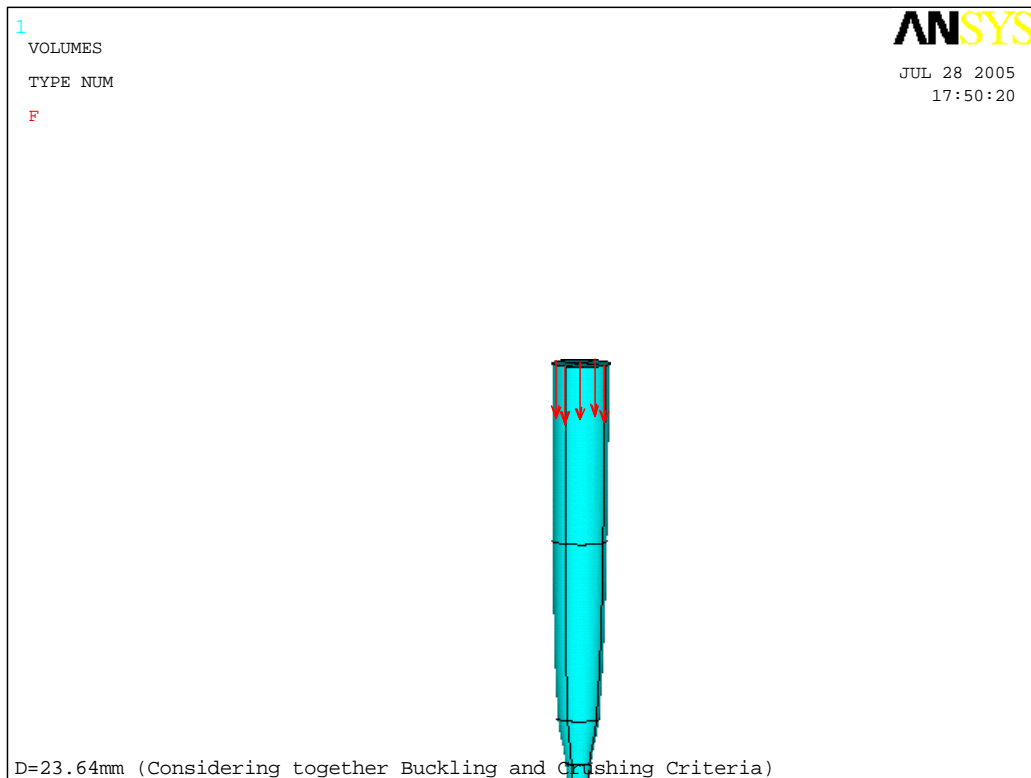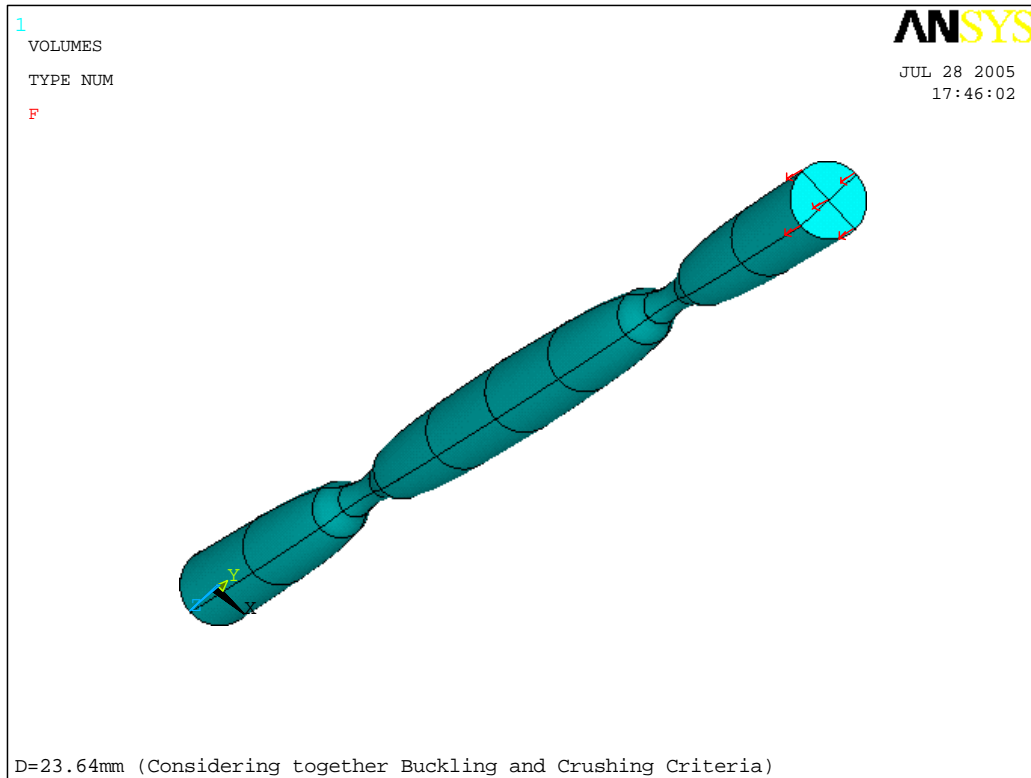
Figure 5.3 The loading conditions for new proposed optimum model solution
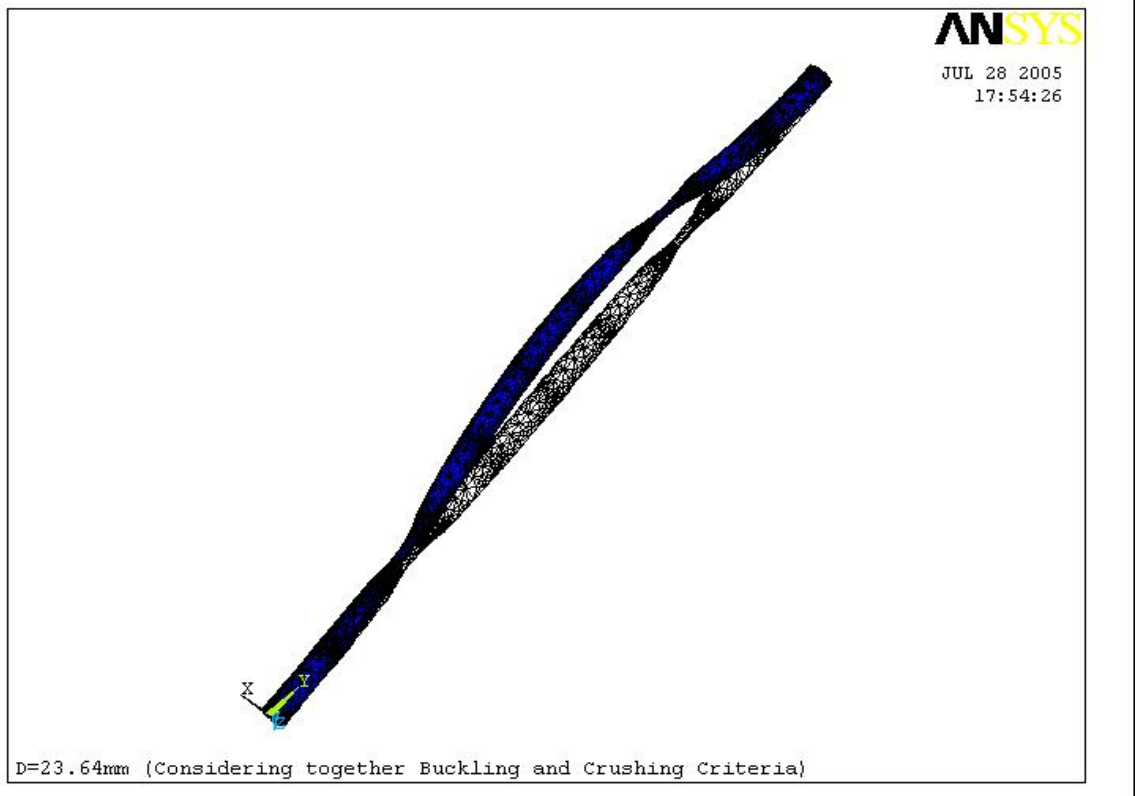
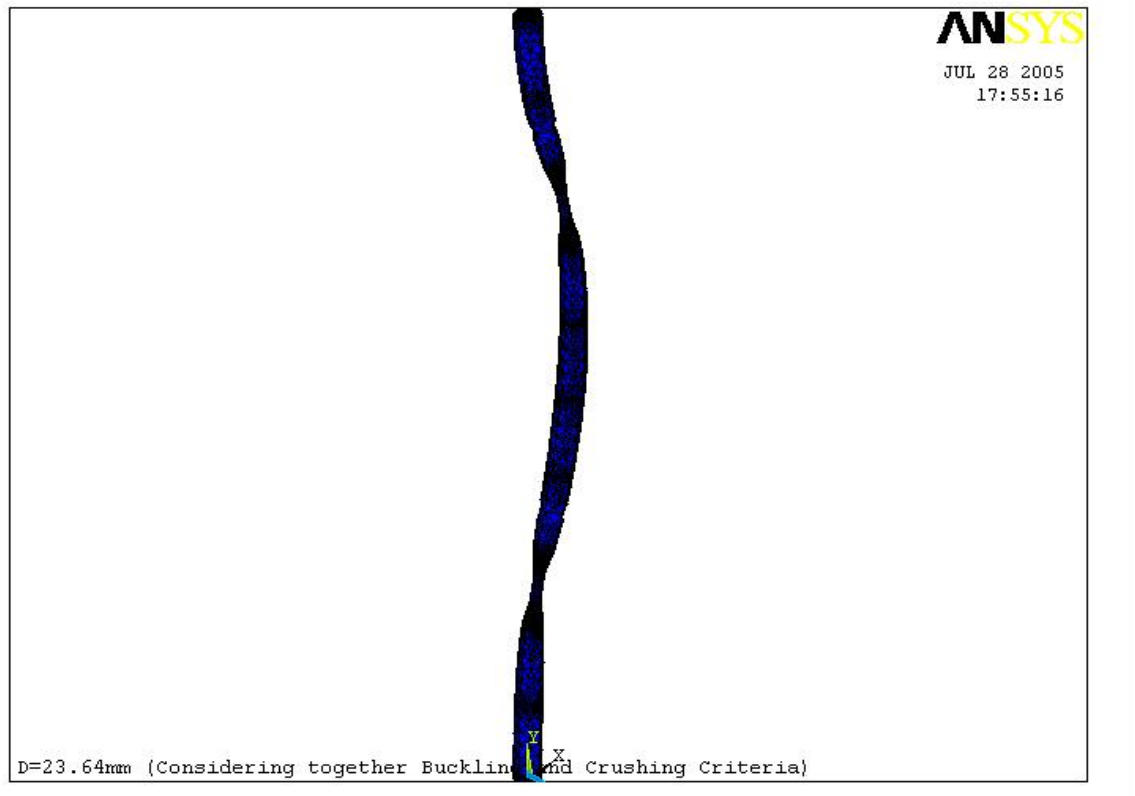Figure5. 4 The buckling mode for new proposed optimum solution

5.4 ANSYS Results for Clamped-Clamped Case

Table 5.1 shows the finite element results obtained by ANSYS for uniform and the variable cross-sections for natural composite materials.

Table 5.1 The critical buckling load results obtained from numerical method for wood composite materials with uniform and variable cross-sections (new proposed optimum model solution)

Natural Composite Materials	Uniform Cross-Section	Variable cross-section
CEDAR	1228,49	1402,10
OAK	4611,20	5829,20
SAPELE	5729,40	6831,90

In addition, optimum shape of the column found by Masur was modeled in ANSYS for 25,37 mm maximum diameter of variable cross-section of column. ANSYS results are shown in Table 5.2.

Table 5.2 The critical buckling load results obtained from numerical method and analytic method obtained by Masur for composite materials with variable cross-sections (new proposed optimum model solution)

Manufactured Composite Materials	0°		45°		90°	
	Analytic	Finite Element result	Analytic	Finite Element result	Analytic	Finite Element result
GLASS-EPOXY	10642,99	10672,00	8496,42	8519,70	7752,22	7773,40
GLASS-VINYLESTER	8694,15	8717,90	8178,32	8200,70	7430,50	7450,80
GLASS-POLYESTER	8123,74	8146,00	7764,1198	7813,50	7020,0419	7039,20

Results in Table 5.2 are good agreement with each other; however, the optimum solution obtained by Masur is not valid because crush occurs in points of minimum thickness. Consequently, it is considered both buckling and crush criteria for optimum columns. It is taken into account stability and crush criteria for new proposed optimum solution. The critical buckling load is numerically obtained for uniform and variable cross-sections for manufactured composite materials. Results given in Table 5.3 are new proposed optimum model's results.

Table 5.3 The critical buckling load results obtained from numerical method for composite materials with uniform cross-sections and variable cross-sections (new proposed optimum model solution)

Manufactured Composite Materials	0°		45°		90°	
	Uniform	Variable	Uniform	Variable	Uniform	Variable
GLASS-EPOXY	8025,30	8692,40	6406,70	6939,30	5845,50	6331,50
GLASS-VINYLESTER	6555,70	7100,80	6166,80	6679,50	5602,90	6068,70
GLASS-POLYESTER	6125,70	6634,90	5854,50	5893,20	5293,40	5802,40

CHAPTER SIX
RESULTS AND CONCLUSIONS

6.1 Results

In 1744, Euler treated critical buckling forces for columns with constant cross-section supported with four different bearing types. If an economical and lighter design of these columns is required, their cross-sections must vary longitudinally. In 1962, Tadjbaksh & Keller examined the optimal longitudinal cross-sections of columns under critical buckling loads for different support ends, and they determined the optimal solution analytically, which was unimodal, namely, possessing a single buckling mode.

Olhoff & Rasmussen also displayed in 1977 that the optimal solution obtained by Tadjbaksh & Keller was to be incorrect for columns with clamped ends. They developed the bimodal optimal solution for columns with clamped ends, which was obtained through application of a numeric method in solving the differential equation. These differences depend on the minimal cross-sectional area. Further, the optimization problem of columns has been studied by many different authors such as one of them Masur (1984). Masur demonstrated the formulation of column optimization problems in respect of bimodal solution for columns with clamped ends.

The critical buckling load results of Tadjbaksh & Keller, Olhoff & Rasmussen (1977)-Masur (1984) is closer with each other for clamped-clamped ends. However, the difference is originated from optimum shape of the column, especially in points of minimum thickness. Tadjbaksh & Keller found the points of vanishing cross-section to be placed at $x=0,25$ and $x=0,75$ where the column ends $x=0$ and $x=L$ are assumed to be clamped-clamped ends while Olhoff & Rasmussen (1977)-Masur (1984) obtained nonzero cross-section in these points with bimodal optimum solution.

However, in these solutions, it is only considered stability criterion in structure. Especially in points of minimum thickness which was found with bimodal optimum solution is crush occurred but not buckling. Consequently, bimodal solution is not practical and optimal since in points of minimum thickness crush occurred but not buckling. This leads to the necessity of both stability and crush criterion formulation of the optimization problem. Thus, in order to determine the optimum column with clamped ends, it is necessary to take into consideration the possibility that in points of minimum thickness is crush occurred.

The present contribution of this Ph. D. thesis is that crush is taken into account in the formulation of column optimization problem allowing for bimodal optimum solution. The new proposed optimum model solution in this Ph. D. thesis is based on taking into account stability and crush criterion in points of minimum thickness. It is emphasized that in the bimodal case, the stress in points of minimum thickness is lower than the than critical buckling stress. Thus, the optimum column is crushed in the axial force not buckled. The criteria will be developed here with the use of both the analytical closed solution found by Masur for clamped-clamped ends and crush criterion in points of minimum thickness. And then optimal solution which is applicable to practise will be obtained.

The new proposed optimum model solution has been verified with numerical analysis and experimental data for columns with clamped-clamped ends.

It is shown the critical buckling loads for natural and manufactured composite materials for uniform cross-sections between Tables 6.1 and 6.3. As shown in Tables 6.2 and 6.4, the difference between analytical results and experimental data is very small for uniform cross-sections. Similar results are valid analytical results and numerical results.

Table 6.1 Comparing to critical buckling load obtained from results analytically, experimentally and numerically for uniform cross-sections for wood materials

Natural Composite Materials	Analytical	Experimental	Numerical
CEDAR	1228,49899	1200	1228,49
OAK	4611,12051	4650	4611,20
SAPELE	5729,29782	5730	5729,40

Table 6.2 Error (%) between analytical solution, experimental data and numeric results for wood materials for uniform cross-sections

Natural Composite Materials	ERROR (%)	
	Between Analytical solution and Experimental data	Between Analytical solution and Numerical results
CEDAR	-2,3199	-0,00081
OAK	0,8436	0,0021
SAPELE	0,0104	0,00178

Table 6.3 Comparing to critical buckling load obtained from results analytically, experimentally and numerically for uniform cross-sections for manufactured composite materials for 0, 45 and 90 degree of fiber orientation angle

a) Fiber Orientation Angle=0°

Manufactured Composite Materials	Analytical	Experimental	Numerical
GLASS-EPOXY	8025,14	8074,25	8025,30
GLASS-VINYLESTER	6555,66	6615,50	6555,70
GLASS-POLYESTER	6125,55	6227,85	6125,70

b) Fiber Orientation Angle=45°

Manufactured Composite Materials	Analytical	Experimental	Numerical
GLASS-EPOXY	6406,57	6350,75	6406,70
GLASS-VINYLESTER	6166,71	6100,00	6166,80
GLASS-POLYESTER	5854,39	5770,25	5854,50

c) Fiber Orientation Angle=90°

Manufactured Composite Materials	Analytic	Experimental	Numeric
GLASS-EPOXY	5845,41	5766,50	5845,50
GLASS-VINYLESTER	5602,83	5475,75	5602,90
GLASS-POLYESTER	5293,33	5245,50	5293,40

Table 6.4 Error (%) between analytical solution, experimental data and numeric results for uniform cross-sections for manufactured composite materials for 0, 45 and 90 degree of fiber orientation angle

Composite Specimens	ERROR (%)					
	Between Analytical solution and Experimental data			Between Analytical solution and Numerical results		
	0°	45°	90°	0°	45°	90°
GLASS-EPOXY	0,61	-0,87	-1,35	$1,99^{-03}$	$2,03^{-03}$	$1,54^{-03}$
GLASS-VINYLESTER	0,91	-1,08	-2,27	$6,10^{-04}$	$1,46^{-03}$	$1,25^{-03}$
GLASS-POLYESTER	1,67	-1,44	-0,90	$2,25^{-03}$	$1,88^{-03}$	$1,32^{-03}$

It is shown in Table 6.5 critical buckling load obtained by Tadjbaksh & Keller, Olhoff & Rasmussen and Masur for natural composite materials with variable circle-cross-section. As shown in Table 6.5, the critical buckling load results are closer with each other. However, these solutions only become different in cross-sectional area especiallay, in the points of minimum thickness. According to Tadjbaksh & Keller, cross-sectional area in the points of minimum thickness is zero whereas cross-sectional area in the points of minimum thickness is different from zero according to Olhoff & Rasmussen and Masur. When these critical buckling load are examined, it is seen that highest critical buckling load is obtained for sapele within natural composite materials.

In Table 6.5, maximum diameter of variable cross-section is 28,83 mm and 23,1 mm for sapele, oak and cedar natural composite materials, respectively. Minimum diameter of variable cross-section is also calculated as 11,88 mm and 9,504 mm for sapele, oak and cedar natural composite materials, respectively, according to Masur's

bimodal optimum solution. In this diamater value is zero according to Tadjbaksh & Keller. As shown in Table 6.5, crushing force in points of minimum thickness is smaller than buckling force of column designed according to Tadjbaksh & Keller, Olhoff & Rasmussen and Masur. For this reason, it occurs crush not buckling in points of minimum thickness. Consequently, these designs acquired by Tadjbaksh & Keller, Olhoff & Rasmussen and Masur are not practical and optimal.

Table 6.5 The Analytical critical buckling load and crushing force (N) in points of minimum thickness for wood composite materials with *variable circle cross-section*

Natural Composite Materials	Tadbaksh & Keller	Olhoff & Rasmussen	Masur	Crushing Force
CEDAR	1637,9990	1629,2360	1629,2423	1511,2350
OAK	6148,1618	6115,2707	6115,2940	4709,0779
SAPELE	7639,0652	7598,1981	7598,2271	4753,3752

The critical buckling load obtained by Tadjbaksh & Keller, Olhoff & Rasmussen and Masur is shown in Table 6.6 for manufactured composite materials depending on fiber orientation angle for circle-cross-section. When these critical buckling loads are examined, it is seen that highest critical buckling load is acquired glass-epoxy within manufactured composite materials. It is also seen that highest critical buckling load is occured 0 degree of fiber orientation angle after 45 degree and 90 degree of fiber orientation angle. Fibers are most effective when the fiber orientation angle is 0 degree when they are oriented parallel to the loading direction.

In Table 6.6 maximum diameter of variable cross-section is 25,37 mm for manufactured composite materials. Minimum diameter of variable cross-section is also calculated as 10,454 mm for manufactured composite materials according to Masur's bimodal optimum solution, while minimum diameter of columns is obtained as zero according to Tadjbaksh & Keller.

Table 6.6 The analytic critical buckling load and crushing force (N) in points of minimum thickness for *variable circle cross-section* for manufactured composite materials for 0, 45 and 90 degree of fiber orientation angle

a) Fiber Orientation Angle= 0 degree

Manufactured Composite Materials	Tadbaksh & Keller	Olhoff & Rasmussen	Masur	Crushing Force
GLASS-EPOXY	10700,1937	10642,9503	10642,9910	9166,9766
GLASS-VINYLESTER	8740,8815	8694,1199	8694,1531	7441,7311
GLASS-POLYESTER	8167,4059	8123,7122	8123,7433	6737,8995

b) Fiber Orientation Angle= 45 degree

Manufactured Composite Materials	Tadbaksh & Keller	Olhoff & Rasmussen	Masur	Crushing Force
GLASS-EPOXY	8542,0901	8496,3920	8496,4244	7203,1150
GLASS-VINYLESTER	8222,2849	8178,2977	8178,3289	6770,5161
GLASS-POLYESTER	7805,8496	7764,0902	7764,1198	6224,6175

c) Fiber Orientation Angle= 90 degree

Manufactured Composite Materials	Tadbaksh & Keller	Olhoff & Rasmussen	Masur	Crushing Force
GLASS-EPOXY	7793,8838	7752,1884	7752,2180	6626,3165
GLASS-VINYLESTER	7470,4416	7430,4765	7430,5049	6416,0253
GLASS-POLYESTER	7057,7800	7020,0150	7020,0419	6068,4012

In this Ph. D. thesis, true optimum solution was obtained that was taken into account crushing criteria to Masur's analytic bimodal solution for clamped-clamped case. The new proposed optimum model solution obtained by taking into accounts both stability and crush criterion has been verified with numerical analysis and

experimental data for columns with clamped ends. Analytical results, experimental data and numerical results are shown in Table 6.7 and Figure 6.1 for new proposed optimum model solution.

Table 6.7 Comparing to analytic, experimental and numeric critical buckling load according to new proposed optimum model for circle-cross-sections

a) Natural Composite Materials

The Critical Buckling Load (New Proposed Optimum Model)				
Natural Composite Specimens	Uniform cross-section Pcr (N)	Variable cross-section		
		Experimental Data Pcr (N)	Finite Element Results (ANSYS) Pcr (N)	Crushing Force in minimum cross-section
CEDAR	1228,5	1400	1402,1	1415,9
OAK	4611,12	5990	5829,2	6918,3
SAPELE	5729,4	6850	6831,9	6983,4

b) Manufactured Composite Materials

The Critical Buckling Load (New Proposed Optimum Model)				
Composite specimens and fiber orientation angle	Uniform cross-section Pcr (N)	Variable cross-section		
		Experimental Data Pcr (N)	Finite Element Results (ANSYS) Pcr (N)	Crushing Force in minimum cross-section
Glass-Epoxy (0 degree)	8025,14	8750	8692,40	9159,96
Glass-Epoxy (45 degree)	6406,57	7000	6939,30	7197,60
Glass-Vinylester (90 degree)	5602,83	6250	6068,70	6411,12
Glass-Polyester (90 degree)	5293,33	5850	5802,40	6063,76

Table 6.8 Error (%) Between, Experimental data and Numeric results for new proposed optimum model for circle-cross-sections

Composite specimens and fiber orientation angle	% ERROR (Experimental data- Finite Element results)
Glass-Epoxy(0 degree)	-0,66
Glass-Epoxy(45 degree)	-0,87
Glass-Vinylester (90 degree)	-2,9
Glass-Polyester (90 degree)	-0,81
Cedar	0,15
Oak	-2,68
Sapele	-0,26
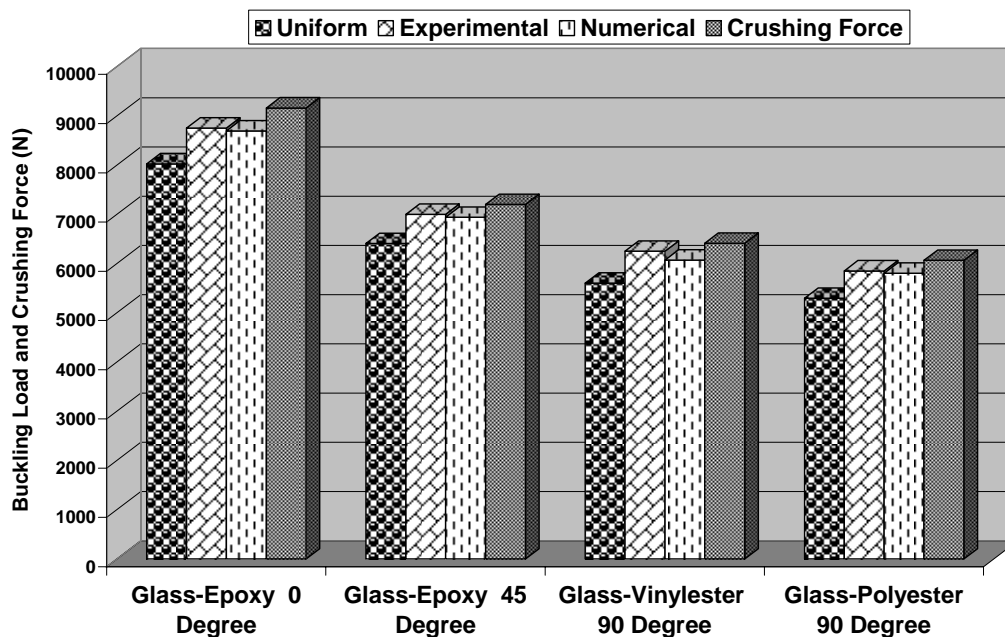
Figure 6. 1 Comparing to critical buckling load for uniform and variable cross-sections with circle cross-sections form for **new proposed optimum model** ($D_{uniform}$=22 mm, $D_{maximum}$=23,64 mm)

As shown in Table 6.8, the difference between experimental data and finite element results for new proposed optimum solution is very small. Another words, it is good agreement between finite element model and experimental data for proposed optimum solution which takes into account both stability and crush criterion. Consequently, the accuracy of new optimized composite column is proved for clamped ends.

For other composite columns which have different fiber orientation angle, it is only compared with results obtained by finite element and analytic method (Table 6.9 and Figure 6.2).

Table 6.9 Comparing to numeric critical buckling load according to new proposed optimum model for circle-cross-sections

The Critical Buckling Load (New Proposed Optimum Model) (N)			
Composite specimens and fiber orientation angle	Uniform cross-section Pcr	Variable cross-section	
		Finite Element Results (ANSYS) Pcr	Crushing Force in minimum cross-section
Glass-Vinylester (0 degree)	6555,66	7100,80	7436,04
Glass-Polyester (0 degree)	6125,55	6634,90	6732,74
Glass-Vinylester (45 degree)	6166,71	6679,50	6765,34
Glass- Polyester (45 degree)	5854,39	5893,20	6219,85
Glass- Epoxy (90 degree)	5845,41	6331,50	6621,25
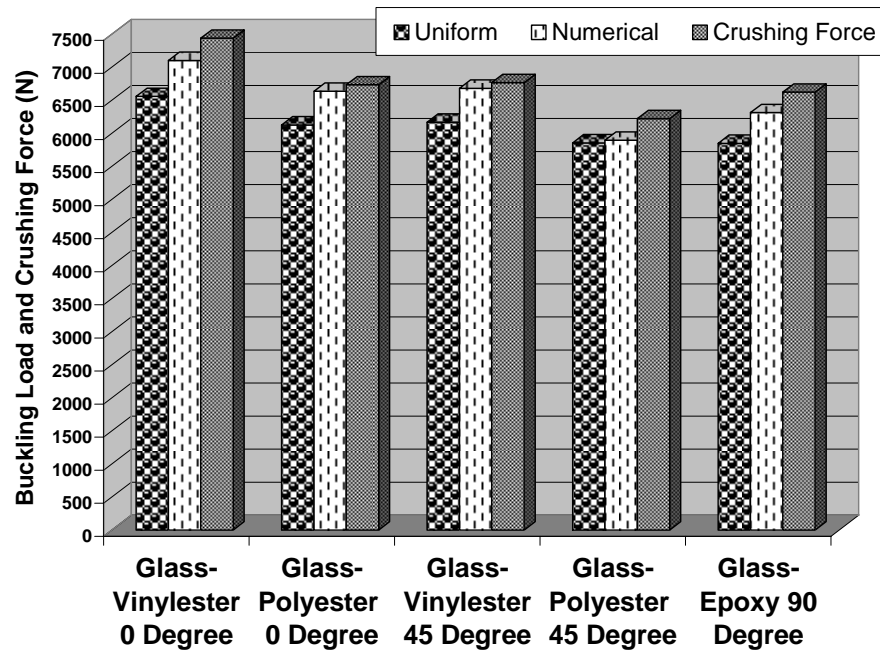
Figure 6.2 Comparing to critical buckling load for uniform and variable circle cross-sections for **new proposed optimum model** ($D_{uniform}$=22 mm, $D_{maximum}$=23,64 mm)

It is also noted that there are discrepancies between the experimental results and those calculated by the theoretical relations. This is attributed to the manufacturing related anomalies such as fiber misalignment, void content and residual stresses in the composite that were not accounted for in the theoretical equations, which were developed based on some idealized assumptions. Improving the manufacturing process would significantly reduce these defects and produce composites of higher properties.

In this Ph. D. thesis, it is also compared to critical buckling load for cross-sectional of circular shape, square shaped cross-section and isosceles triangle cross-section. These comparisons are given between Figures 6.3 and 6.17 for natural composite materials and manufactured composite materials.

It is shown that the highest critical buckling load is obtained for isosceles triangle cross-sections. The column with isosceles triangle cross-section can be loaded with the maximum buckling force in clamped-clamped case where all columns have the same length as well as the same volume. The highest critical buckling load is occurred sapele and glass-epoxy among natural manufactured composite materials, respectively. It is acquired the lowest critical buckling load for cross-section of circular shape. If the maximum buckling load for the column with circle cross-section is assumed to be 100 percent any supported types maximum buckling loads yield for the column with square cross-section and with isosceles triangle cross-section to 104,27 percent and to 121 percent, respectively.
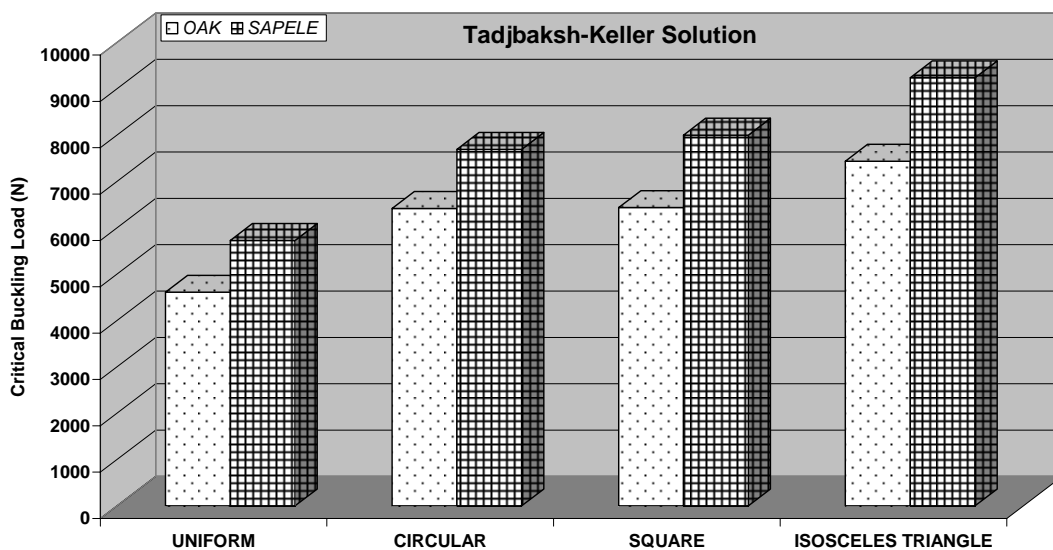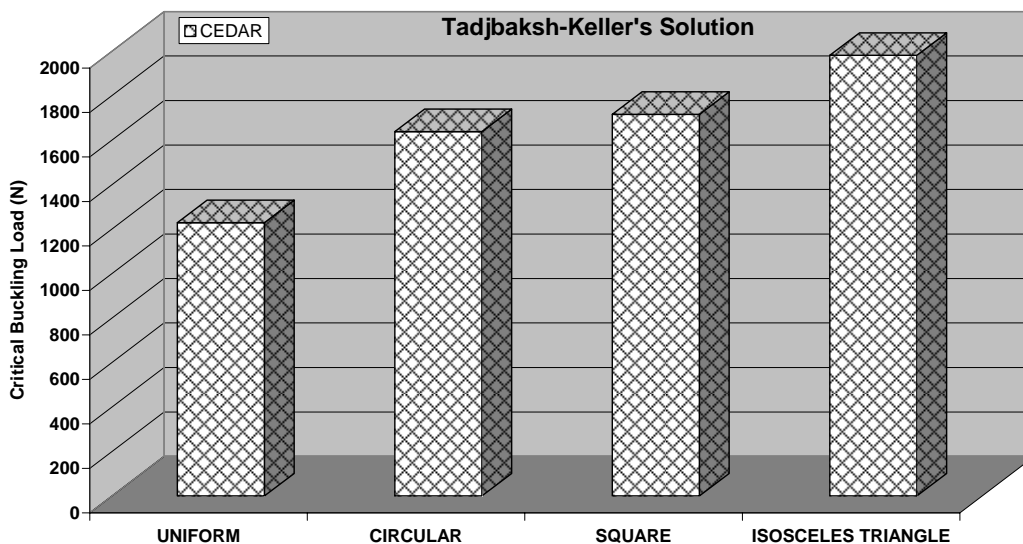
Figure 6.3 Comparing to critical buckling load according to **Tadjbaksh & Keller** for uniform with circle cross-section and variable cross-sections with different cross-sections form for sapele and oak wood composite materials ($D_{uniform}$=25 mm, $D_{maximum}$=28,83 mm)
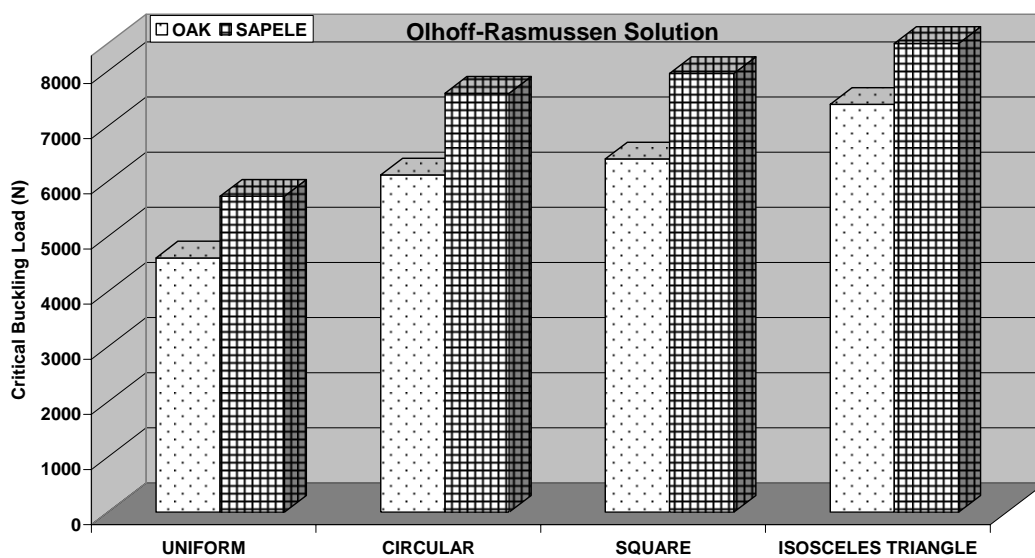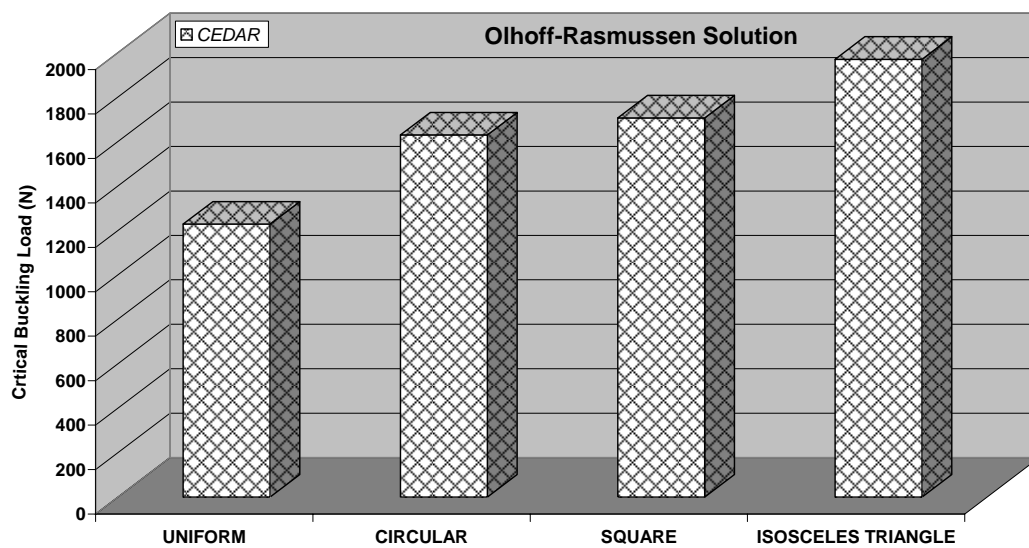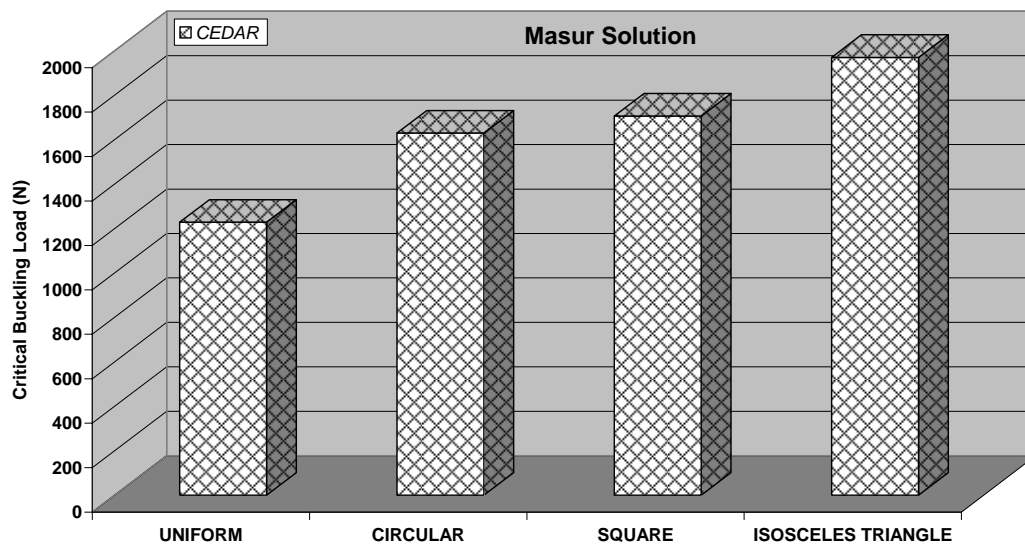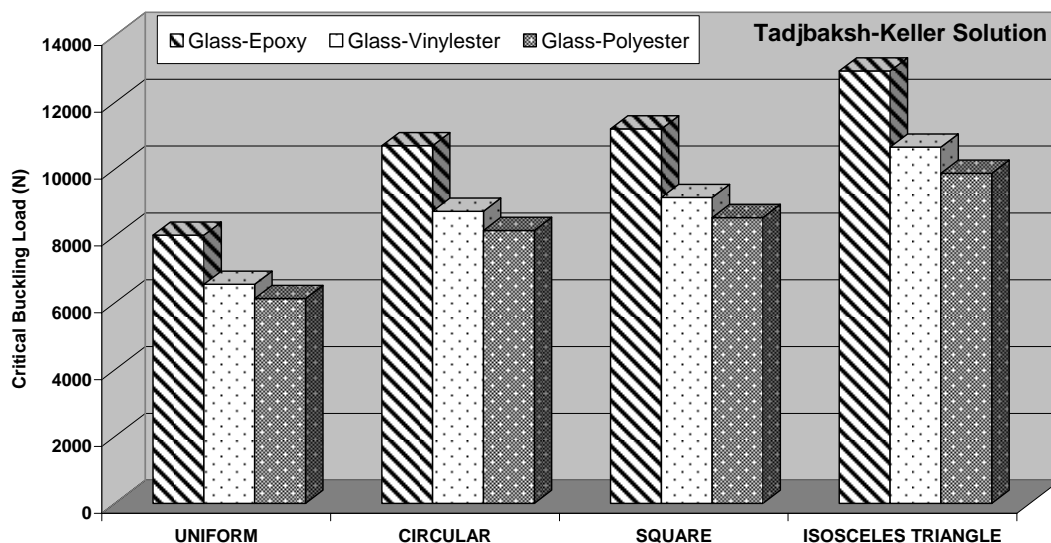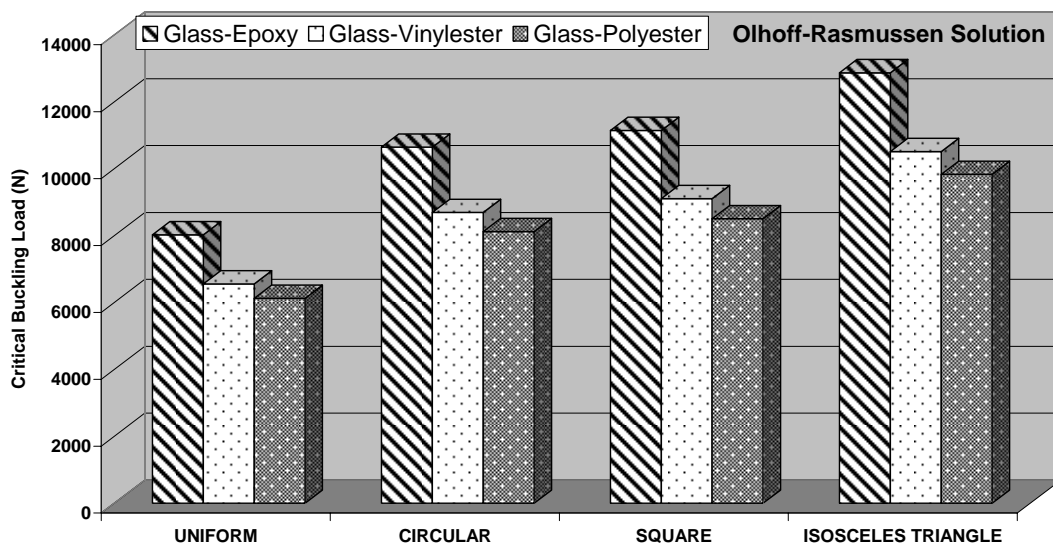

Figure 6.4 Comparing to critical buckling load according to **Olhoff & Rasmussen** for uniform with circle cross-section and variable cross-sections with different cross-sections form for sapele and oak wood composite materials ($D_{uniform}$=25 mm, $D_{maximum}$=28,83 mm)
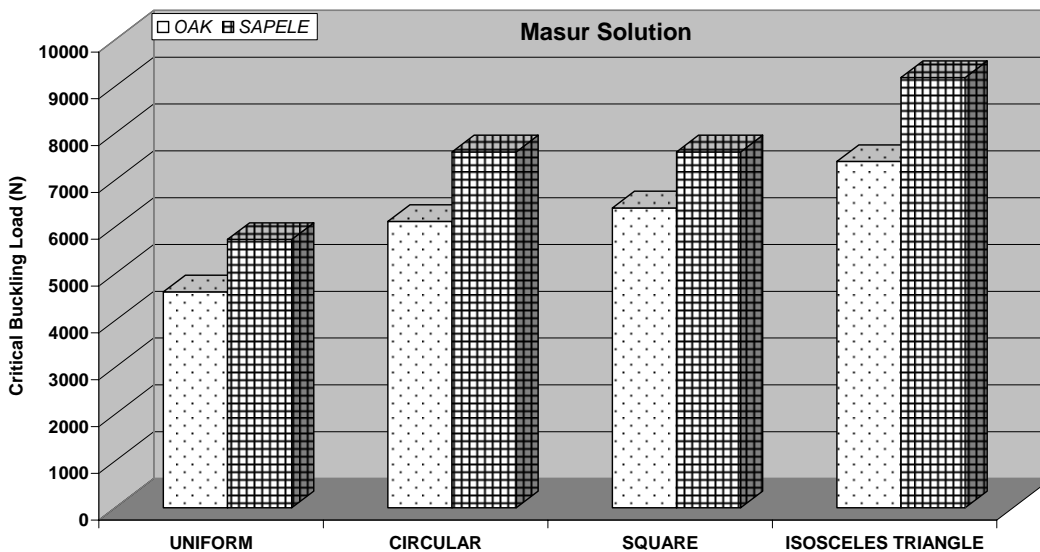
Figure 6.5 Comparing to critical buckling load according to **Masur** for uniform with circle cross-section and variable cross-sections with different cross-sections form for sapele and oak wood composite materials ($D_{uniform}$=25 mm, $D_{maximum}$=28,83 mm)

Figure 6.6 Comparing to critical buckling load according to **Tadjbaksh & Keller** for uniform with circle cross-section and variable cross-sections with different cross-sections form for cedar wood composite materials ($D_{uniform}$=20 mm, $D_{maximum}$=23,1 mm)

Figure 6.7 Comparing to critical buckling load according to **Olhoff & Rasmussen** for uniform with circle cross-section and variable cross-sections with different cross-sections form for cedar wood composite materials ($D_{uniform}$=20 mm, $D_{maximum}$=23,1 mm)
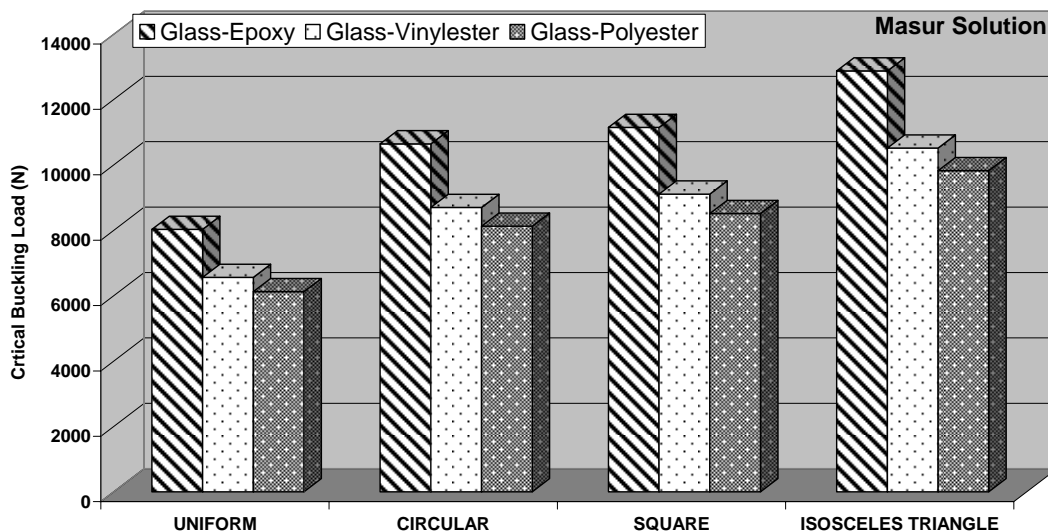

Figure 6.8 Comparing to critical buckling load according to **Masur** for uniform with circle cross-section and variable cross-sections with different cross-sections form for cedar wood composite materials ($D_{uniform}$=20 mm, $D_{maximum}$=23,1 mm)
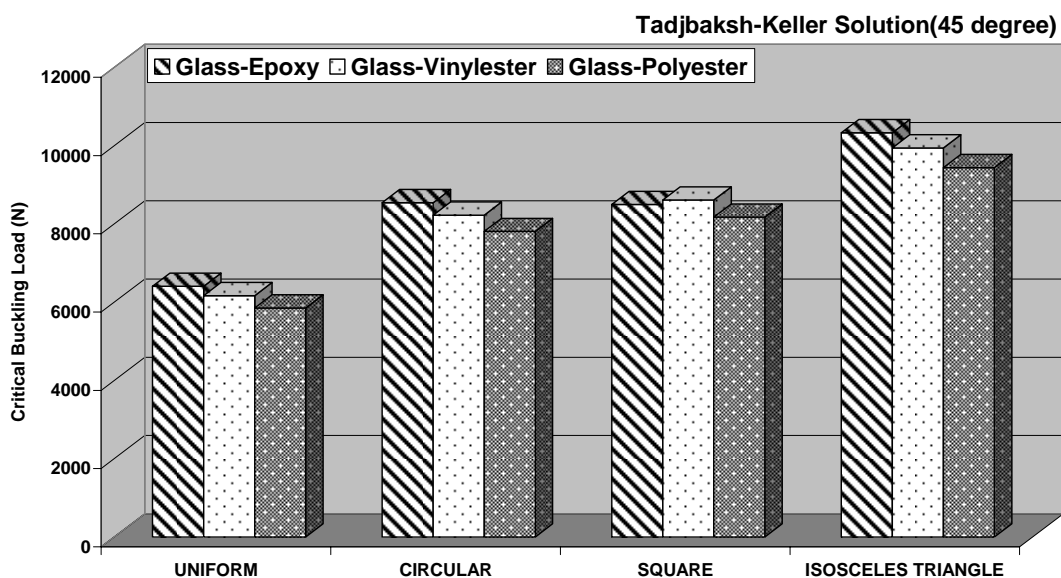
Figure 6.9 Comparing to critical buckling load according to **Tadjbaksh & Keller** for uniform with circle cross-section and variable cross-sections with different cross-sections form for **0-degree of fiber orientation angle** for glass-epoxy, glass-vinylester and glass-polyester ($D_{uniform}$=22 mm, $D_{maximum}$=25,37 mm)
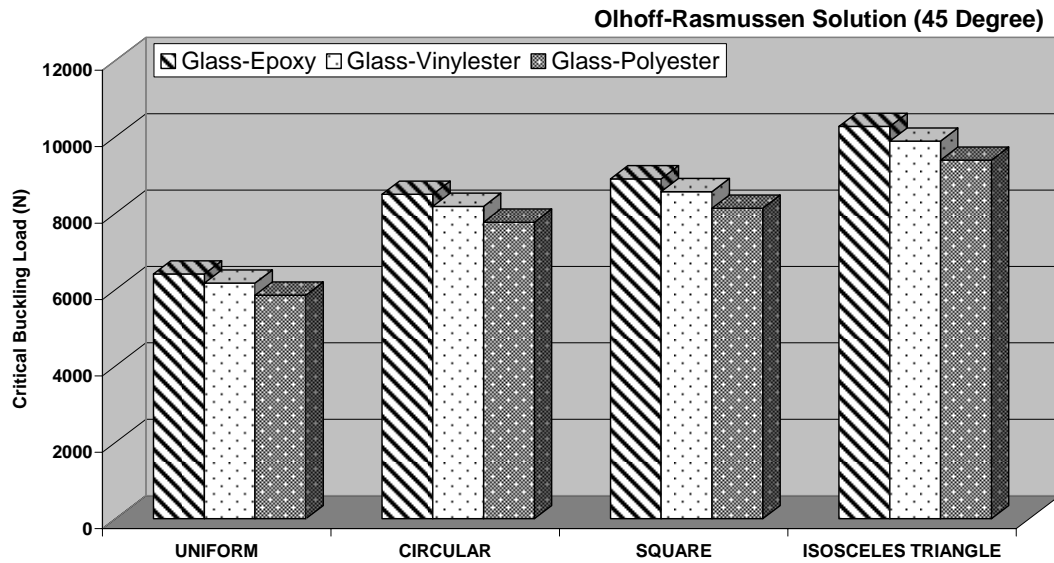

Figure 6.10 Comparing to critical buckling load according to **Olhoff & Rasmussen** for uniform with circle cross-section and variable cross-sections with different cross-sections form for **0-degree of fiber orientation angle** for glass-epoxy, glass-vinylester and glass-polyester ($D_{uniform}$=22 mm, $D_{maximum}$=25,37 mm)
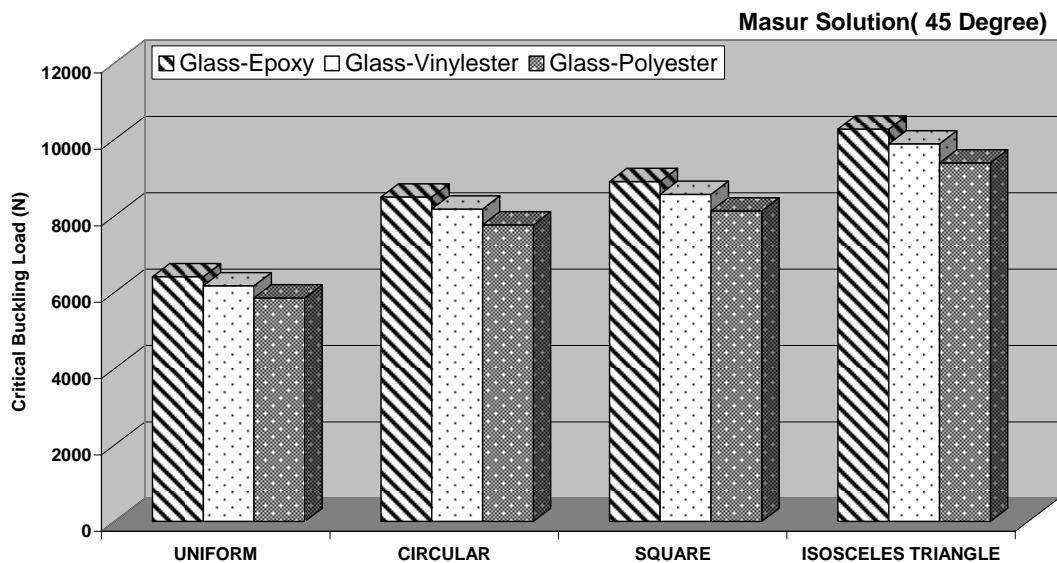
Figure 6.11 Comparing to critical buckling load according to **Masur** for uniform with circle cross-section and variable cross-sections with different cross-sections form for **0-degree of fiber orientation angle** for glass-epoxy, glass-vinylester and glass-polyester ($D_{uniform}$=22 mm, $D_{maximum}$=25,37 mm)

Figure 6.12 Comparing to critical buckling load according to **Tadjbaksh & Keller** for uniform with circle cross-section and variable cross-sections with different cross-sections form for **45-degree of fiber orientation angle** for glass-epoxy, glass-vinylester and glass-polyester ($D_{uniform}$=22 mm, $D_{maximum}$=25,37 mm)

Figure 6.13 Comparing to critical buckling load according to **Olhoff & Rasmussen** for uniform with circle cross-section and variable cross-sections with different cross-sections form for **45-degree of fiber orientation angle** for glass-epoxy, glass-vinylester and glass-polyester ($D_{uniform}$=22 mm, $D_{maximum}$=25,37 mm)

Figure 6.14 Comparing to critical buckling load according to **Masur** for uniform with circle cross-section and variable cross-sections with different cross-sections form for **45 degree of fiber orientation angle** for glass-epoxy, glass-vinylester and glass-polyester ($D_{uniform}$=22 mm, $D_{maximum}$=25,37 mm)
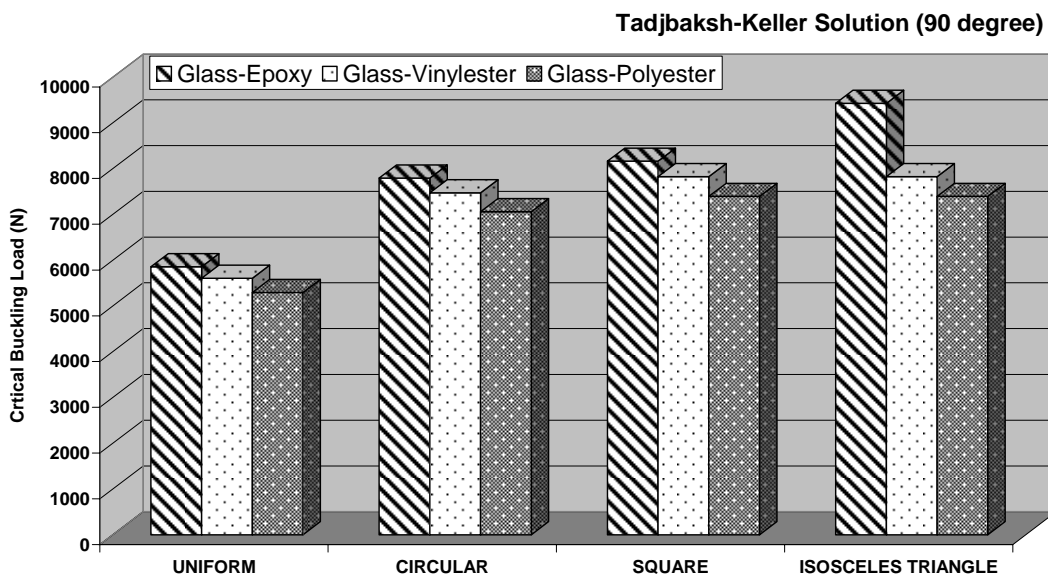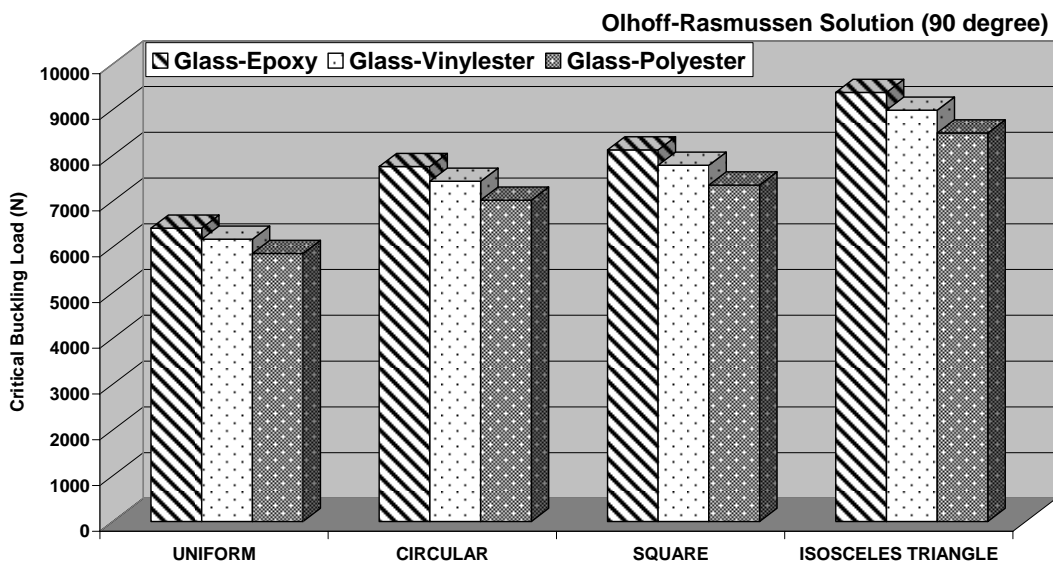
Figure 6.15 Comparing to critical buckling load according to **Tadjbaksh & Keller** for uniform with circle cross-section and variable cross-sections with different cross-sections form for **90 degree of fiber orientation angle** for glass-epoxy, glass-vinylester and glass-polyester ($D_{uniform}$=22 mm, $D_{maximum}$=25,37 mm)

Figure 6.16 Comparing to critical buckling load according to **Olhoff & Rasmussen** for uniform with circle cross-section and variable cross-sections with different cross-sections form for **90-degree of fiber orientation angle** for glass-epoxy, glass-vinylester and glass-polyester ($D_{uniform}$=22 mm, $D_{maximum}$=25,37 mm)
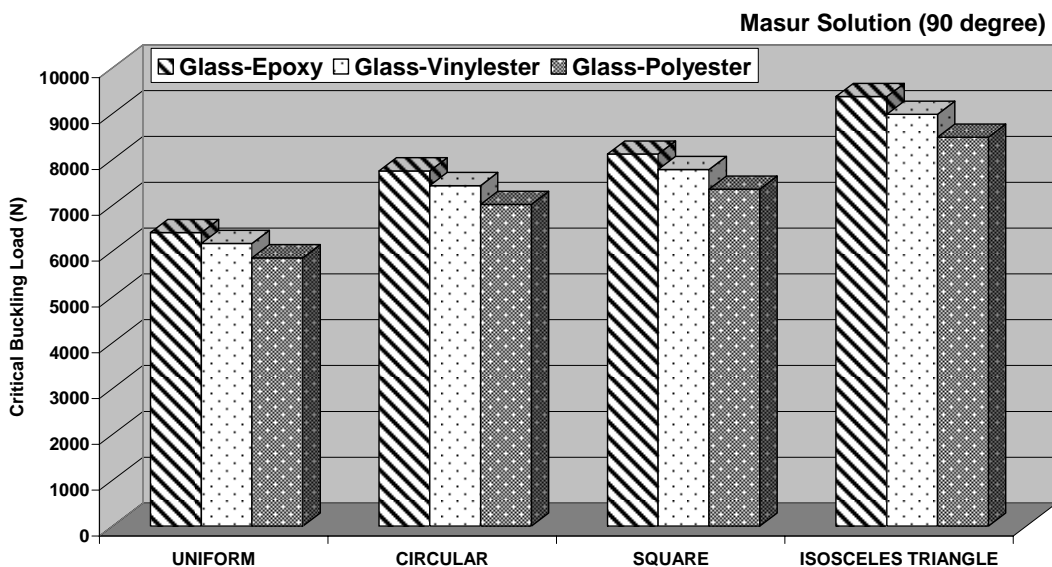
Figure 6.17 Comparing to critical buckling load according to **Masur** for uniform with circle cross-section and variable cross-sections with different cross-sections form for **90-degree of fiber orientation angle** for glass-epoxy, glass-vinylester and glass-polyester ($D_{uniform}$=22 mm, $D_{maximum}$=25,37 mm)

In this Ph. D. thesis, comparisons are made according to Tadjbaksh & Keller, Olhoff & Rasmussen and Masur for natural and manufactured composite materials with 0, 45 and 90 degree of fiber orientation angle. It is given comparison of buckling loads obtained by Tadjbaksh & Keller, Olhoff & Rasmussen and Masur between Figures 6.16 and 6.20. Highest critical buckling load is occurred along the direction of the fibers. The lowest critical buckling load is obtained 90 degree of fiber orientation angle. As shown between Figures 6.18 and 6.22, it is especially seen that Olhoff & Rasmussen solution is much closed Masur's solution.
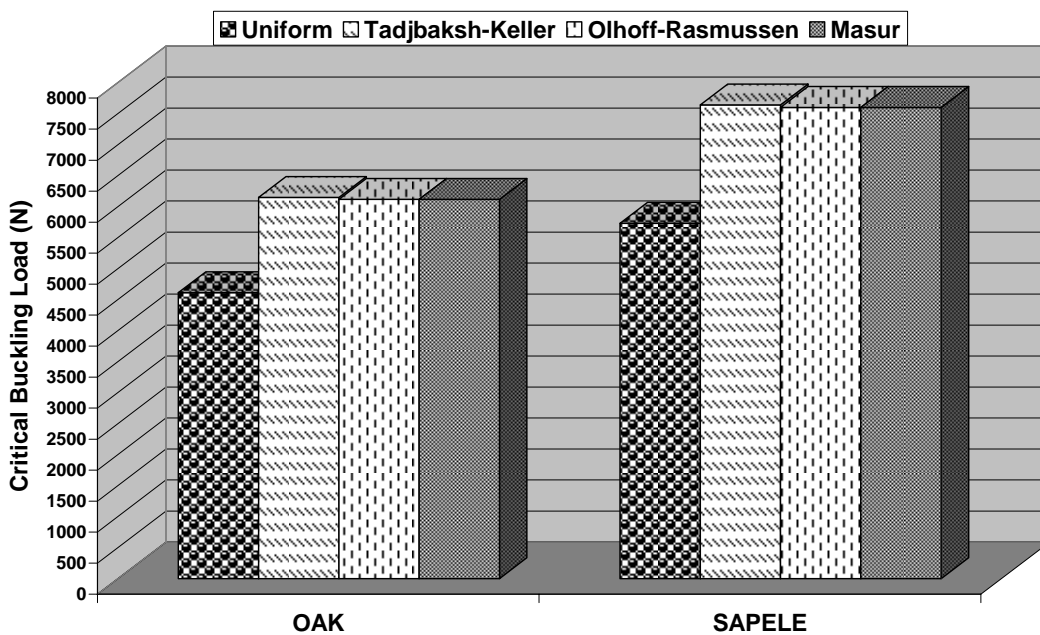
Figure 6.18 Comparing to critical buckling load for uniform and variable cross-sections with circle cross-sections form for sapele and oak wood composite materials ($D_{uniform}$=25 mm, $D_{maximum}$=27,50 mm)
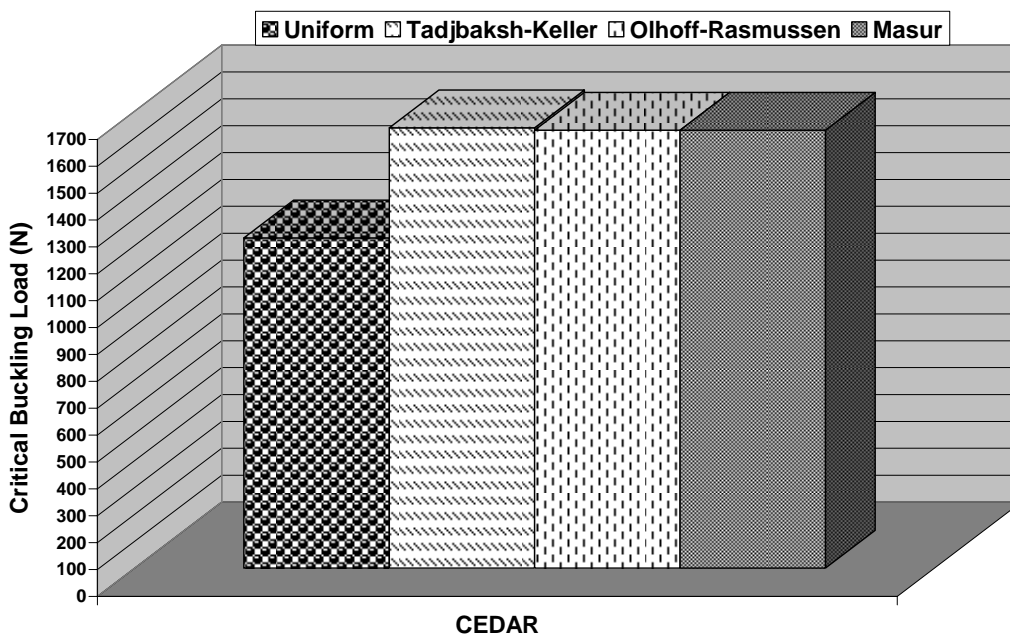

Figure 6.19 Comparing to critical buckling load for uniform and variable cross-sections with circle cross-sections form for cedar wood composite materials ($D_{uniform}$=20 mm, $D_{maximum}$=22,50 mm)
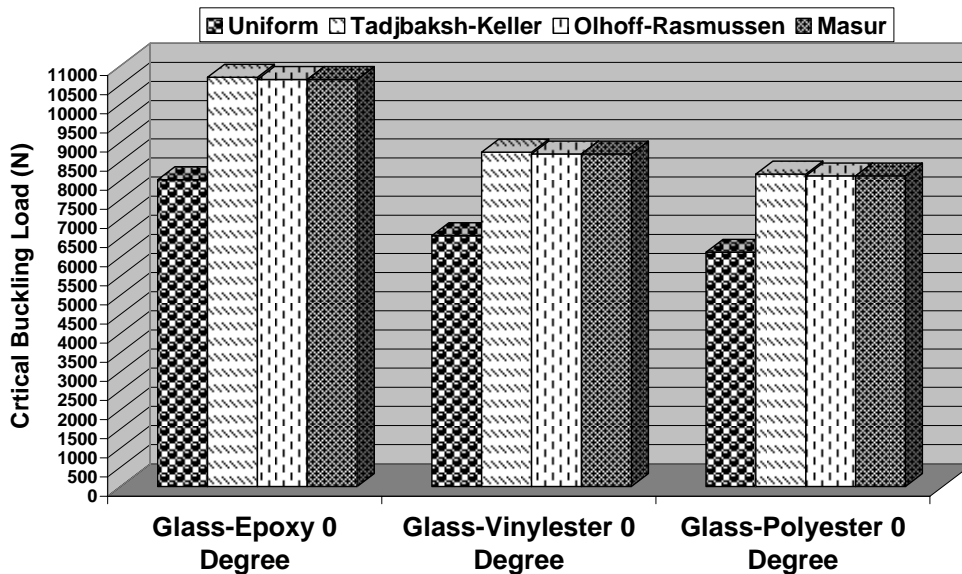
Figure 6.20 Comparing to critical buckling load for uniform and variable cross-sections with circle cross-sections form **for 0 degree of fiber orientation angle** for glass-epoxy, glass-vinylester and glass-polyester ($D_{uniform}$=22 mm, $D_{maximum}$=25,37 mm)

Figure 6.21 Comparing to critical buckling load for uniform and variable cross-sections with circle cross-sections form **for 45 degree of fiber orientation angle** for glass-epoxy, glass-vinylester and glass-polyester ($D_{uniform}$=22 mm, $D_{maximum}$=25,37 mm)
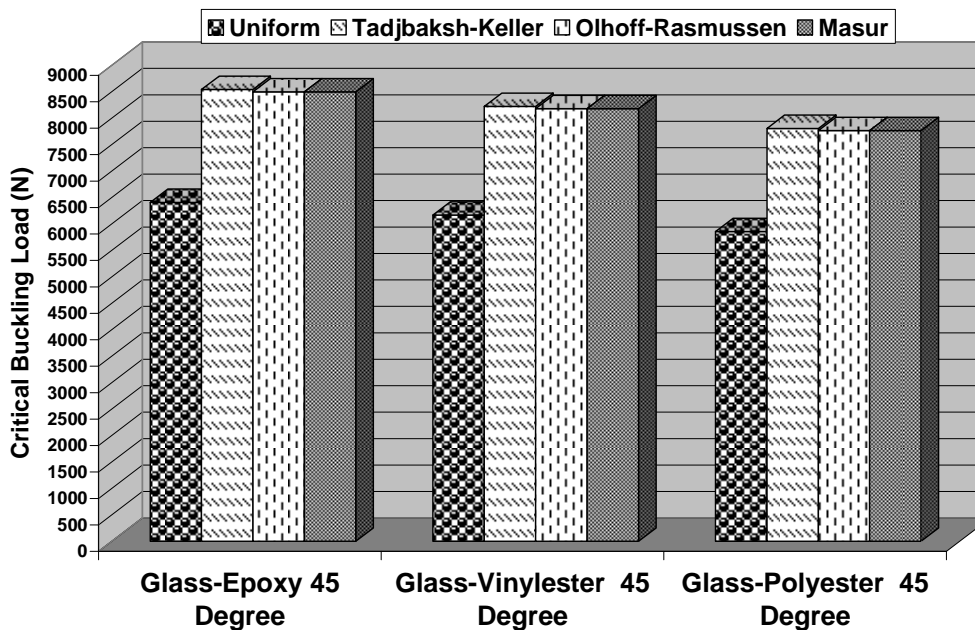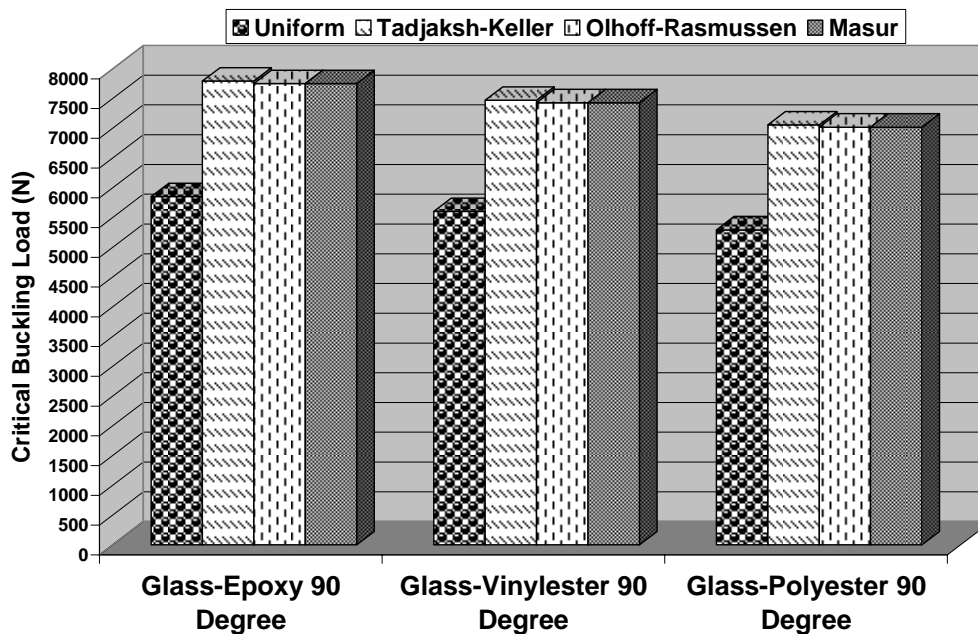
Figure 6.22 Comparing to critical buckling load for uniform and variable cross-sections with circle cross-sections form **for 90 degree of fiber orientation angle** for glass-epoxy, glass-vinylester and glass-polyester ($D_{uniform}$=22 mm, $D_{maximum}$=25,37 mm)

6.2 Conclusions

The objective of this Ph. D. thesis was to develop and design optimized composite column against buckling. It is thought about determining what shape of column has the largest possible buckling load of composite column of a given length and volume. The optimization problem was formulated as the maximization of the smallest eigenvalue given total volume of material of the structure.

It was also proved that the solution of Tadjbakhsh & Keller, Olhoff & Rasmussen and Masur was not optimum for columns with clamped ends. It was showed that the new proposed optimum model was given the optimum solution for clamped-clamped case. The present contribution of this paper is that crush is taken into account in the formulation of column optimization problem allowing for bimodal optimum solution.

True solution is obtained that was taken into account crushing criteria to Masur's analytic bimodal solution for clamped-clamped case. The cross-sectional area is changed through column. This area in the middle of the column decreases towards ends. The cross-sectional area which is different from zero in points of minimum thickness must be buckled according to new proposed optimum form of column.

It is firstly chosen the volume, which satisfied bimodal optimality conditions given by Masur for clamped-clamped ends. The chosen volume value is smaller than the initial volume that is equal to the uniform column's volume. Next, it is added volume, ΔV, in the points of minimum thickness. Consequently, new proposed optimum column buckles in highest critical buckling load in comparison with uniform cross-section given length and volume

In this Ph. D. thesis, it is rearranged in points of minimum thickness in new proposed optimum model solution obtained by taking into consideration both stability and crush criterion. It is shown in Figure 6.23 optimum clamped-clamped column shape obtained by Tadjbaksh & Keller, Masur and new proposed optimum solution for half of the column.
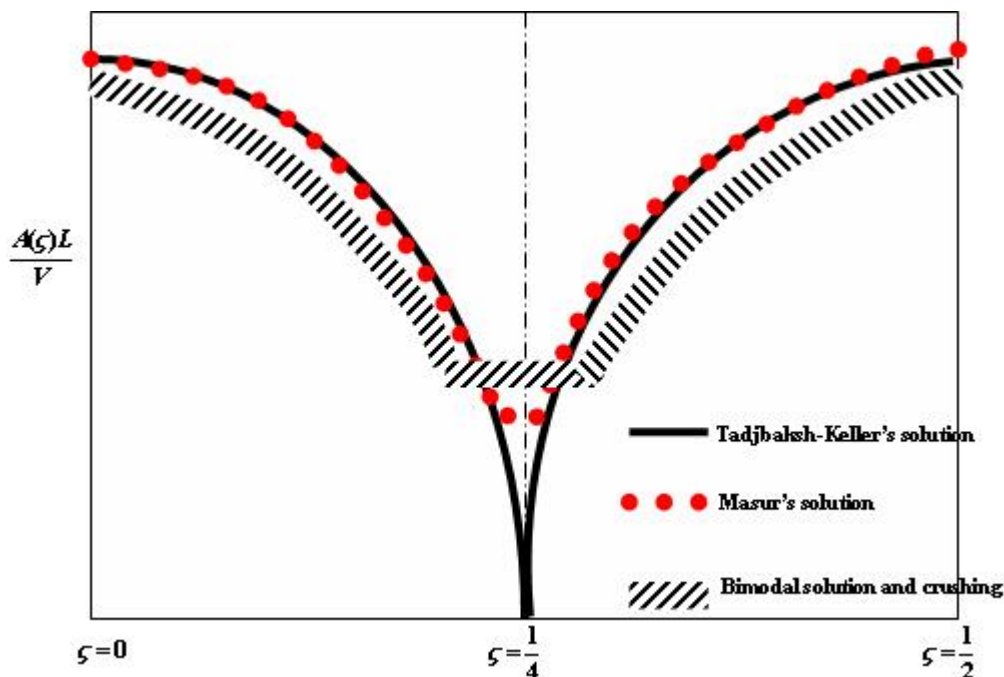
Figure 6.23 Comparisons of optimum shape of clamped-clamped column obtained by Tadjbaksh & Keller, Masur and New Proposed Optimum Solution

To test the accuracy of our new optimized composite column with clamped ends, experimental data were compared to numerical analysis using ANSYS. Both necessary and sufficient optimality conditions were derived. In this study, it was used both natural and manufactured composite materials. New proposed optimum model's results are in agreement with results obtained by numerical analysis and by experiments.

It was obtained natural and manufactured composite columns, which has largest possible buckling load and was stronger against crush in the points of minimum thickness, given volume and length in this Ph. D. thesis.

As a result of this Ph. D. thesis, it was shown that results obtained in the previous studies of variation optimum cross-sectional area for columns under compressive forces clamped-clamped ends was erroneous. The corrected optimum form was obtained and results checked by numerical calculations and experimental tests of natural and manufactured composite columns.

REFERENCES

Adali, S., Lene, F., Duvaut, G., & Chiaruttini, V. (2003). Optimization of laminated composites subject to uncertain buckling loads. *Composite & Structures, 62*, 261-269.

Anonymous (2005a). *Combined Compression and Bending: Columns.* University of Maryland College Park Department of Civil and Environmental Engineering Retrieved September 8, 2005, from http://ctsm.umd.edu/assakkaf/Courses/ENCE454/Lectures/CHAPTER9a.pdf

Anonymous (2005b). *Lecturer in Structural Mechanics by Ahmer Wadee.*Department of Civil and Environmental Engineering the University of Imperial College of Sceince, Technology and Medicine Retrieved September 8, 2005, from http://structures-www.cv.imperial.ac.uk/staff/wadee/

Anonymous (2005c). *Notes on Design and Analysis of Machine Elements by Douglas Rigth.* Department of Mechanical and Materials Engineering the University of Western Australia Retrieved September 8, 2005, from http://www.mech.uwa.edu.au/DANotes/intro/contents.html#top

Anonymous (2005d). *Lecturer in Structural Mechanics by Ahmer Wadee.* Department of Civil and Environmental Engineering the University of Imperial College of Sceince, Technology and Medicine Retrieved September 8, 2005, from http://structures-www.cv.imperial.ac.uk/staff/wadee/

Anonymous (2005e). *Laboratory Experiments and Interactive Demos, Downloadable Experiments For Teachers and Students,* American Institue of Aeronautics and Astronautics (AIAA) Retrieved September 8, 2005, from http://www.aiaa.org/tc/sd/Education/physics_of_sd/

Anonymous (2005f). *Lecture Notes Structural Steel Design,* The Citadel Civil and Environmental Engineering Department Retrieved September 8, 2005, from http://cee.citadel.edu/civl406/.

Anonymous (2005g). *Lecture Notes Mechanical Design Applications,* Rice University Department Mechanical Engineering Retrieved September 8, 2005, from http://www.owlnet.rice.edu/~mech401/.

Anonymous (2005h). *Lecture Notes Structural Stability,* Virginia Tech Department of Aerospace and Ocean Engineering Retrieved September 8, 2005, from http://www.aoe.vt.edu/~johnson/.

Anonymous (2005i). *Lecture Notes,* George Mason University Civil, Environmental and Infrastructure Engineering Retrieved September 8, 2005, from http://www.civil.gmu.edu/Course%20outlines/ENGR310.8ppt.

Anonymous (2005j). *Solid Mechanics Lecture Notes, Buckling of Columns* (April 19, 2004). University of Manitoba Department of Civil Engineering, Retrieved September 8, 2005, from http://www.ce.umanitoba.ca/.

Anonymous (2005k). *Composite Material.* Rai Foundation Colleges Retrieved August 27, 2005, from http: //rcw.raifoundation.org/course-mech-btech-me-notes- commtrl.htm.

Anonymous (1996l). Theory and Design of Structural Systems Lecture Notes of University of Oregon, Retrieved September 8, 2005, from http://darkwing.uoregon.edu/~struct/courseware/461/461_lectures/461_lecture29/461_lecture29.html.

Arpakcı, M. (2000). A study on selection of optimal cross-sections and savings of material for buckling of columns. Thesis of M.Sc. at Institute of Natural and Technological Science of Ege University. (In Turkish; Supervisor: A. Ozdamar)

Atanackovic, T. M. (2004). On the optimal shape of a compressed rotating rod. *Meccanica 39*, 147-157.

Barnes, D. C. (1988). The shape of the strongest column is arbitrary close the shape of the weakest column. *Quarterly of Applied Mathematics, 4*, 605-609.

Bauld, N. R., & Tzeng, L. S. (1984). A Vlasov theory for fiber-reinforced beams with thin walled open cross sections. *International Journal of Solids and Structures*, *20* (3), 277-297.

Chase, J. G., Yim, M. (1999). Optimal stabilization of column buckling. *Journal of Engineering Mechanics, 125* (9), 987-993.

Chawla, K. K. (Ed.). (2001). *Composite Materials Science and Engineering* (Second edition). Springer-Verlag Press.

Clausen, T. (1851). Uber die Form architektonischer Saulen. *Bulletin physico mathematiques et Astronumiques, 1*, 279-294.

Coello, C. A. C., Christiansen, A. D., & Farrera, F. A. (1996). A genetic algorithm for the optimal design of axially loaded non-prismatic columns. *Civil Engineering System, 14* (2), 111-146.

Cox, S. J., & Overton, M. L. (1992). On the optimal design of columns against buckling. *SIAM Journal on Mathematical Analysis, 23*, 287-325.

Drazumeric, R., & Kosel, F. (2003).Optimizing the geometry for the buckling of a bar. *Strojniski Vestnik- Journal of Mechanical Engineering 49* (7-8), 385-397.

Egorov Y. V. (2004). On the optimizaiton of higher eigenvalues. *C.R. Mecanique*, *332*, 673-678.

Elishakoff, I. (2001). Euler's problem revisited: 222 Years later. *Meccanica, 36* , 265-272.

Euler, L. (1744). De curvis elasticis. In Methodus inveniendi leneas curva maximi minimive proprietate gaudentes, sive solutio problematis isoperimetrici lattisimo sensu accepti, Lausannae, E65A. O. O. Ser.I., 24, 231-297.

Faria, A. R. (2000). Buckling optimization of composite plates and cylindrical shells: Uncertain Loading-Combinations. University of Toronto Department of Aerospace Science and Engineering degree of Doctor of Philosophy.

Filho, M. K. (1997). Optimization of nonhomogeneous face sheets in composite sandwich Plates. University of Toronto Department of Aerospace Science and Engineering degree of Doctor of Philosophy.

Fridman, M., & Zyczkowski, M. (2001). Structural optimization of elastic columns under stress corrosion conditions. *Structural and Multidisciplinary Optimization, 21* (3), 218-228.

Gea, H. C., & Luo, J. (2001). Topology optimization of structures with geometrical nonlinearities. *Computers and Structures, 79*, 1977-1985.

Gibson, R. F. (Ed.). (1994). *Principles of composite material mechanics* (International editions). Mc Graw-Hill.

Gindl, W., & Teischinger, A. (2002). Axial compression strength of Norway spruce related to structural variability and lignin content. *Composites Part A, 33*, 1623-1628.

Green, D. W., Winandy, J. E., & Kretschmann, D.E. (1999). Wood Handbook, Wood as an Enginnering Material, United States Department of Agriculture Forest Service, Forest Products Laboratory, General Technical Report, 463p, FPL-GTR-113, Madison, Wisconsin.

Hassan, M. (1998). Optimum design and development of a cost-effective pultruded hybrid composite mast. Dalhousie University Faculty of Engineering Department of Civil Engineering, Degree of Master of Applied Science.

Homam, S. M. (2000) Durability of fibre reinforced polymers (FRP) used in concrete structures. University of Toronto Department of Civil Engineering, Degree of Master of Applied Science.

Hyer, M. W. (Ed.). (1998). *Stress analysis of Fiber –Reinforced Composite Materials* (International editions). Mc Graw-Hill.

Ishida, R., & Sugiyama, Y. (1995). Propasal of constructive algorithm and discrete shape design of the strongest column. *AIAA Journal*, *33* (3), 401-406.

Jones, R. M. (Ed.). (1999). *Mechanics of composite materials* (Second edition). Taylor&Francis Press.

Jung, C. M., & Feeny B. F. (2002). On the discretization of an elastic rod with distributed sliding friction. *Journal of Sound and Vibration, 252* (3), 409-428.

Kanno, Y., & Ohsaki, M. (2001). Necessary and sufficient conditions for global optimality of eigenvalue optimization problems, *Structural and Multidisciplinary Optimization, 22*, 228-252.

Karaa, S. (2003). Properties of the first eigenfunctions of the clamped column equation, *Theoretical Applied Mechanics*, *30* (4), 265-276.

Keller, J. B. (1960). The shape of the strongest column. *Arch Ration Mechanical Analysis, 5,* 275-285.

Khong, P. W. (1999). Optimal design of laminates for maximum buckling resistance and minimum weight. *Journal of Composites Technology & Research, 21* (1), 25-32.

Kruzelecki, J., & Smas P. (2004). Optimal design of simply supported columns for buckling under loading controlled by displacements. *Engineering Optimization, 36* (6), 645-658.

Lagrange, J. L. (1773). Sur la figure des colonnes. *Miscellanea Taurinensia*, 123.

Langthjem, M. A., & Sugiyama, Y. (1999). Optimum design of Beck's column with a constrainton the static buckling load. *Structural and Multidisciplinary Optimization, 18* (4), 228-235.

Lau, W. W. S. (2000). Strength model and finite element analysis wood beam columns in truss applications. University of British Columbia Department of Wood Science Degree of Doctor of Philosophy.

Lee, B. K., Oh, S. J., & Li, G. (2002). Buckling loads of columns of regular polygon cross section with constant volume and clamped ends. *Electronic Journal of Structural Engineering, 2*, 76-84.

Lewis, A., & Overton, M. (1996). Eigenvalue optimization. *Acta Numerica*, 149-190.

Lin, Z. M., Polyzois, D., & Shah, A. (1996). Stability of thin-walled pultruded structural members by the finite element method. *Thin Walled Structures, 24*, 1-18.

Maalawi, K. Y. (2002). Buckling optimization of flexible columns. *International Journal of Solids and Structures, 39*, 5865-5876.

Mahfouz, S. Y. (1999). Design optimization of steel frame structures according to he British codes of practice using a genetic algorithm. Department of Civil and Environmental Engineering University of Bradford, Degree of Doctor of Philosophy.

Mallick P. K. (Ed.). (1993). *Fiber-Reinforced Composites* (Second edition, Revised and Expanded). Marcel Dekker Inc.

Mallick P. K. (Ed.). (1997). *Composites Engineering Handbook, Einband 1* (Second edition, Revised and Expanded). Marcel Dekker Inc.

Manickarajah, D., Xie, Y. M., & Steven, G. P. (2000). Optimisation of columns and frames against buckling. *Computers & Structures 75*, 45-54.

Masur, E. (1984). Optimal structural design under multiple eigenvalue constraints. *International Journal of Solids and Structures, 20*, 211-231.

Myers, M. K. & Spillers, W. R. (1986). A note on the strongest fixed-fixed column. *Quarterly of Applied Mathematics*, *3*, 583-588.

Olhoff, N., & Rasmussen, S.H. (1977). On the single and bimodal optimum buckling loads of clamped columns. *International Journal of Solids and Structures, 13*, 605-614.

Overton, M. L. (1991). Large-scale optimization of eigenvalues. *SIAM Journal on Optimization, 2,* 88-120.

Ozdamar, A. (1996). Das Knicken schwerer Gestaenge, Technical University of Berlin Verlag fuer Wissenschaft und Forschung, Berlin, Thesis of Ph. D. (in German, Supervisor: E. Wolf).

Ozdamar, A., & Pekbey Y. Numeric and experimental investigation of buckling optimization of different composite columns with variable cross-sectional area. Ege University Scientific Research Project Report (04/MUH/035), Izmir, 2004. (In Turkish) (Not finished).

Pekbey, Y., & Ozdamar, A. (2002). Optimum cross-section determination against buckling of bars under compressive loading. *The Journal of Graduate School of Natural and Aplied Sciences of Dokuz Eylul University*, *4* (3), 103-112.

Poulsen, J. S., Moran P. M., Shilr C. F., & Byskov E. (1997). Kink band initation and band broadening in clear wood under compressive loading. *Mechanics of Materials, 25*, 67-77.

Qiusheng, L., Hong, C., & Guiqing, L. (1994). Stability analysis of a bar with multi-segments of varying cross-section. *Computers & Structures, 53* (5), 1085-1089.

Qiusheng, L., Hong, C., & Guiqing, L. (1995). Stability analysis of bars with varying cross-section. *International Journal of Solids and Structures, 32* (21), 3217-3228.

Ratzersdorfer, J. (Ed.). (1936). Die Knickfestigkeit von Staeben und Stabwerken. Springer Verlag, Wien, 103-106, (in German).

Reddy, J. N. (Ed.). (1997). *Mechanics of laminated composite plates* (International editions). CRC Press.

Reiterer, A., Stefanie, E., & Tschegg, S. (2001). Compressive behaviour of softwood under axial loading at different orientations to the grain. *Mechanics of Materials*, *33*, 705-715.

Reiterer, A., Burgert, I., Sinn, G., & Tschegg, S. (2002). The radial reinforcement of the wood structure and its implication on mechanical and fracture mechanical properties-A comparison between two tree species. *Journal of Materials Science*, *37*, 935-940.

Rong, J. H., Xie, Y. M., & Yang, X. Y. (2001). An improved method for evolutionary structural optimisation against buckling. *Computers & Structures, 79*, 253-263.

Sayman, O., & Pekbey Y. Analytical and experimental investigation of buckling optimization of different composite columns with variable cross-sectional area. Dokuz Eylul University Scientific Research Project Report (04/KB.FEN/044), Izmir, 2004. (In Turkish) (Not finished).

Seyranian, A., Lund, E., & Olhoff, N. (1994). Multiple eigenvalues in structural optimization problems. *Structural Optimization, 8*, 207-227.

Seyranian, A. P., & Privalova, O. G. (2003). The Lagrange problem on an optimal column: old and new results. *Structural and Multidisciplinary Optimization, 25*, 393-410.

Shani, M. A. (1998). Compressive strength of eccentrically loaded steel angles. University of Windsor Department of Civil Engineering Degree of Master of Applied Science.

Smitses, G. J., Kamat, M.P., & Smith, C. V. (1973). Strongest column by the finite element displacement method. *AIAA Journal, 11* (9), 1231, 1973.

Simitses, G. J. (Ed.). (1976). *An introduction to the elastic stability of structures*. New Jersey, Prentice-Hall.

Szyszkowski, W., Watson, L. G., & Fietkiewicz, B. (1989). Bimodal optimization of frames for maximum stability. *Computers & Structures, 32* (5), 1093-1104.

Szyazkowski, W. (1992). Multimodal optimality criterion for maximum stability. *International Journal of Non-Linear Mechanics, 27* (4), 623-633.

Szyszkowski, W. S., & Watson, L. G. (1998). Optimization of the buckling load of columns and frames. *Engineering Structures, 10* (4),249-256.

Tabarsa, T. (1999). Compression perpendicular to grain behaviour of wood. The University of New Brunswick in the Graduate Academic Unit of Forestry and Environmental Management Degree of Doctor of Philosophy.

Tabiei, A., & Wu J. (2000). Three dimensional nonlinear orthotropic finite element material model for wood. *Composite Structures*, *50*, 143-149.

Tada, Y., & Wang, L. (1995). Reinvestigation on optimization of clamped-clamped columns and symmetry of corresponding eigenfunctions. *JSME International Journal of Series Mechanical and Material Engineering, 38* (1), 38-43.

Tadjbakhsh, I., & Keller, J. B. (1962). Strongest columns and isoperimetric inequalities for eigenvalues. *Journal of Applied Mechanics, 29,* 159-164.

Taylor, J. E. (1967). The strongest column an energy approach. *Journal of Applied Mechanics, 34* (2), 486-487.

Timoshenko, S. P., & Gere, J. M. (Eds.). 1961: *Theory of elastic stability*, McGraw-Hill (2nd ed.) New York.

Vaziri, H. H., & Xie, J. (1992). Buckling of columns under variably distributed axial loads. *Computers & Structures, 45* (3), 505-509.

Vinogradov, A. M., & Derrick, W. R. (2000). Structure-material relations in the buckling problem of asymmetric composite column. *International Journal of Non-Linear Mechanic, 35*, 167-175.

Wadee, M. A. (October 19, 2004). Struc 24: Structural Stability. Retrieved September 8, 2005, from http://structures-www.cv.imperial.ac.uk/staff/wadee/pdf/st/.

Winandy, J. E. (1994). Wood Properties. Arntzen, Charles J., ed. Encyclopedia of Agricultural Science, Orlando, FL: Academic Press: 549-561. Vol. 4.

Xi, G. Q. (1998). Experimental investigation and finite element nonlinear analysis of continuous composite curved multi-cell box-girder bridges. Ottawa-Carleton Institute Department of Civil Engineering Degree of Doctor of Philosophy.

Ying, W., Li, S. R., & Teng, Z. C. (2003). Post buckling of a cantilever rod with variable cross-sections under combined load. *Applied Mathematics and Mechanics, 24* (9), 1111-1118.